Communications
Research
Centre

BEVERAGE ANTENNAS FOR HF COMMUNICATIONS, DIRECTION FINDING AND OVER-THE-HORIZON RADARS

by

J. litva and B.J. Rook

DEPARTMENT OF COMMUNICATIONS
MINISTERE DES COMMUNICATIONS

CRC REPORT NO. 1282

CANADA

OTTAWA, AUGUST 1976

COMMUNICATIONS RESEARCH CENTRE

BEVERAGE ANTENNAS FOR HF COMMUNICATIONS, DIRECTION FINDING AND OVER-THE-HORIZON RADARS

by

J. **Litva** and **B.J.** Rook

(Radio and Radar Branch)

76-106

TABLE OF CONTENTS

v

BEVERAGE ANTENNAS FOR HF COMMUNICATIONS, DIRECTION FINDING AND

OVER-THE-HORIZON RADARS

by

J. Litva **and** B.J. **Rook**

ABSTRACT

A detailed description is given of the exper-
imental and theoretical results obtained from a
study of the Beverage antenna. The results show
that this antenna is useful as a receiving
antenna in the high frequency range because it is
highly directive largely frequency independent,
has a low take-off angle and is relatively inex-
pensive to construct. Since the electrical
properties of the ground over which HF antennas
may be situated will affect their performance, a
novel technique is described, which utilizes a
single Beverage element to determine these
properties. Comprehensive Beverage antenna
engineering-design-data have been calculated and
tabulated in a readily accessible format for the
communications engineer. Beverage antennas are
shown to be effective elements or "building
blocks" for HF antenna systems, such as rosette
and linear antenna arrays. These have application
to HF direction finding, over-the-horizon radar
and point-to-point communication systems. It is
shown that a Beverage linear array system has
sufficient gain at high frequency that it may be
used in the transmitting as well as the receiving
mode. A listing of a computer program is included
which can be used to calculate all necessary design
parameters of either single Beverage antennas or
arrays of Beverage antennas.

1. INTRODUCTION

1.1 DESCRIPTION OF THE BEVERAGE ANTENNA

A Beverage antenna is a non-resonant broadband antenna which has been used and tested over the frequency range 3 to 30 MHz. It consists of a long wire (Figure 1) stretched horizontally above the ground and is, in essence, a lossy transmission line with the ground acting as the conductor for the return current. Its characteristic impedance is approximately *400-600* ohms. The antenna is terminated in its characteristic impedance at one end, via a ground screen, and the received signal is taken from the other end through a transformer, one side of which is connected to ground via another ground screen. The transformer is used to match the 400-600 ohm impedance of the antenna to a standard 50-ohm coaxial cable. The direction of the beam, or maximum sensitivity of the antenna to radio signals, is toward the terminated end. The dimensions of HF Beverage antennas are as follows; their lengths vary from 50 to 150 m and their heights above ground vary from **0.3** to **3** m. Typically though, their length and height are respectively about 110 m and 1.5 m.

The behaviour of the Beverage antenna can most easily be described in the role of a receiving antenna. One imagines the antenna subdivided into elements of equal length, each of which is affected by a direct and indirect ray emanating from a radio transmitter. The resulting horizontal component of the electrical field outside each element is the vector sum of the horizontal components associated with the two rays. The resultant electric-field component for each element will induce an alternating voltage in that element. The elements can now be thought of as containing RF generators, which cause RF currents to flow that are attenuated at the receiver terminals in proportion to the distance of the antenna element from the receiver. The energy arriving at the terminated end is absorbed and dissipated by the terminating resistor; the magnitude of the current at the receiving end is the vector sum of the currents generated by each imaginary generator, delayed in phase and attenuated in amplitude in proportion to the distance of the generator from the receiving end of the antenna.

1.2 PREVIOUS WORK

The initial developmental work performed with the Beverage antenna was carried out by H.H. Beverage prior to 1923. He tested the antenna on a transoceanic circuit using long waves in the frequency range 12 to 42 KHz and found that with antenna lengths of approximately one wavelength (7 to 25 km) the antenna was effective in reducing interference and static because of its directive nature. This work was first reported in a near classical paper by Beverage, et. al (1923).

Travers et al. did extensive theoretical and experimental research with the Beverage antenna from 1961 to 1967. Their work is documented in a series of reports, with limited distribution, submitted to the U.S. Navy. A brief unclassified summary of their work appeared in Martin et al. (1965).

The work of Travers et al. consisted of the first extensive applica ion of the antenna for reception at HF frequencies. In the course of their work they concluded that the antenna was an effective low cost element with high directivity that worked over good *as* well as poor soil throughout the complete band from **1** to **30** MHz. They found **it** to be non−resonant over at least a five octave frequency range when its length was greater than one−half wavelength, and impedance to be primarily resistive and flat over the HF band. Numerous theoretical antenna radiation patterns were calculated for various antenna lengths, heights, soil conditions, radio wave polarizations and elevation angles−of−arrival. They also concluded that due to its directive nature, the antenna was not only useful for reception but also for transmission either singly or arrayed.

Extensive developmental work was also performed by Travers et al. in HF direction finding using large numbers of Beverage antenna configured in rosette arrays of various dimensions. In one 360" rosette array, for example, the elements were 120 m in length and separated by 10". The standard deviation in angle−of−arrival of *402* bearings taken on sky−wave signals "of chance" was reported to be **3.8".** In another installation, a 72" rosette array with elements 300 m in length separated by 2° yielded a standard deviation for *408* bearings of 1.04".

Some developmental work has been performed by the staff of Rome Air Development Center (RADC) at their Dexter, N.Y. antenna site. This has been directed towards developing an effective over−the−horizon (OTH) radar antenna. A number of linear phased arrays have been constructed and tested in both the radar receive and transmit modes. A two−dimensional array is currently being evaluated and is being used to develop and test adaptive array techniques. Their initial work pre−dates that performed by CRC. Discussions between CRC and RADC personnel were held prior to CRC's embarking on the HF antenna program described in this report.

1.3 MOTIVATION FOR CRC WORK

Originally, the motivation for conducting developmental work on Beverage antennas came from a CRC requirement for a highly directional OTH radar receive antenna with a 360" azimuthal capability. This antenna was to be sited at Cambridge Bay, **N.W.T.** and was therefore required to withstand extreme climatic conditions. A thorough search of commercially available HF antennas revealed the following general shortcomings:

- they were prohibitively expensive;

- their installation was expensive because it required specialized personnel and equipment;

- they had large moving structures which could prove to be troublesome in low Arctic temperatures;

- their directivity gains were limited to about 10 dB and their azimuthal beamwidths were at least 60 degrees;

- they required extensive ground screens;

- their maintenance requirements were quite substantial and therefore expensive.

It was decided, on the basis of the encouraging results of early radiation pattern measurements of Beverage antennas, that a rosette array of *24* Beverage antennas (elements) be installed at Cambridge Bay, N.W.T. The elements of the rosette array were phased in pairs, giving 12 fixed beams, which could be selected with a remotely operated electrical switch located at the centre of the array. This configuration of Beverage elements resulted in an inexpensive highly directional HF antenna which had a low physical profile, and in addition, contained no moving parts. The Cambridge Bay rosette array was, needless to say, found to be an effective OTH radar receiving antenna. The success realized in this application pointed to the use of Beverage antennas as "building blocks" for wide-aperture inexpensive HF antennas. These would find use in HF communications, OTH radars and HF direction finding systems. The Beverage antenna's attractiveness stems from its high direct- ivity and wide bandwidth characteristics, and of utmost importance, its simplicity and low cost.

It was decided that a thorough knowledge of its parameters was required to allow for optimization of its performance in various configurations. The motivation then for the antenna work that has taken place at CRC since 1971 has been, simply, to derive a complete description of the technical parameters of the antenna and to determine, by testing, its potential as an HF antenna. With this in mind tests and evaluations have been performed in three distinct areas: namely, communications, direction finding and radar. Extensive measurements have been performed on individual Beverage elements and compared with results derived by using theoretical developments that have been publish- ed elsewhere. Comprehensive engineering data have been calculated and tabulated in a readily accessible and usable format. These can be used by the communications engineer to effectively design HF Beverage antenna systems. Techniques have been developed which permit comprehensive assessments of antenna sites. Finally, a computer program was developed, based in large measure on the theoretical work performed at the South West Research Institute (SWRI). This gives CRC a capability for calculating parameters for either single Beverage elements or arrays of Beverage elements.

1.4 PREVIEW

This report gives a summary of the experimental and theoretical data that have been accumulated and developed, respectively, at the Communications Research Centre since July 1971 at which time some exploratory measurements were performed on a Beverage antenna erected at Hall Beach, N.W.T.

Because of the large wavelengths exhibited by HF radio waves, the ground on which HF antennas are erected must be considered an integral part of these antennas. Therefore, properties of the ground must be taken into consideration when attempting to determine the performance of HF antennas. With this in mind techniques are outlined in Section 2 for measuring ground parameters for siting of Beverage or other HF antennas, by the erection of a single Beverage element and measurement of its electrical parameters. The effect of the electrical properties of the ground on the antenna's impedance, gain, current-wave velocity, current-wave attenuation, take-off angle, etc., is discussed in considerable detail. It is shown that any one of these readily-measured parameters can be used to derive the electrical parameters of the ground.

Once the electrical parameters of the ground to be used are known, precise engineering of Beverage antennas can be accomplished by referring to data given in Appendix II. It consists of theoretical curves which give the following Beverage antenna parameters; azimuthal beamwidth, vertical beam-width, power gain and vertical take-off angle. These are given for a wide range of antenna geometries (length and height) and ground parameters. An extensive comparison is also made of theoretically derived and measured antenna parameters to define the precision and confidence levels that can be assigned to the theoretical curves.

It is shown that the performance of a single Beverage element, as a receive antenna in the HF band, is not degraded by its low efficiency (− 2%). This is due to the presence of atmospheric and galactic noise at HF frequencies making the HF environment inherently noisy.

Section 4 deals with rosette and linear phased arrays using Beverage antennas as basic building blocks. Results are given of evaluations performed on a number of prototype Beverage arrays used as direction finding and communications antennas. These have been developed and constructed by CRC during the course of the work described in this report. Both their theoret-ical and measured electrical parameters are given in this section.

It is also shown in Section 4 that a linear phased array of Beverage antennas can be effectively used not only as a point–to–point communications receive antenna, but also as a transmi antenna. Although the efficiency of a single element is only about 1.5%, resulting in an antenna with a power gain of 0 dBi, an increase in efficiency aue to a reduction in ground losses can be realized by phasing a number of antenna elements together. It is expected that an efficiency of 25% can be realized in practice, which then permits fabrication of communications antennas with power gains of about 15–18 dBi. The performance of these antennas surpasses in many instances, that of classical antennas. Furthermore they can be installed and maintained at an antenna site at a fraction of the cost of classical antennas.

The majority of the theoretical development used in this report is given in Appendix IV. Equations are derived which permit the calculation of all pertinent electrical parameters for Beverage elements. A later section of Appendix IV gives equations which can be used to calculate radiation patterns of linear phased arrays. Finally, a listing is given of the computer program used to calculate the electrical parameters of both single Beverage elements and also linear phased arrays of Beverage antennas.

2. SITING OF **BEVERAGE** ANTENNAS

2.1 SITING

The electrical properties of the ground over which a Beverage antenna or any HF antenna is erected affect its electrical parameters and thereby its performance. It is of particular importance that the ground surrounding Beverage antenna arrays be chosen to be as isotropic and homogeneous as possible to ensure that the radiation patterns of the individual antennas are

6

symmetrical, similar and not skewed in azimuth. Variations in the electrical
properties of the ground will tend to degrade the radiation patterns of
antenna arrays and in particular Beverage arrays.

The electrical parameters of the ground at Cambridge Bay, N.W.T., are
deduced from a number of independent Beverage antenna parameter measurements.
These are described in detail in Section 2.3. A topographical map of the site
showing the location of both the rosette and linear Beverage antenna arrays
is given in Figures 2 and 3. The numerous lakes in the vicinity of these
antennas suggests that the ground at this site is not likely to be either
isotropic or homogeneous. In general, the terrain, although relatively flat,
is interspersed with hills. The elevation of the rosette and linear Beverage
antenna arrays above sea level respectively was approximately 100 and 50 ft.
The rosette antenna array was sited near the crest of a hill whereas the
linear antenna array was sited in an adjacent low-lying area.

2.2 HOMOGENEITY OF THE GROUND

Two types of measurements were performed at Cambridge Bay to detect any
heterogeneity in the ground surrounding the Beverage rosette antenna array.
The position of the rosette array is shown in the topographical map given in
Figure 2. The first consisted of field intensity measurements in the vicinity
of a $\lambda/4$ monopole. They were made on the ground with a field intensity meter.
The range of the meter from the monopole was 610 m throughout, and its azimuth
was incremented in 15° steps. The monopole was excited by a 9.5 MHz one-watt
source and was located at the geometrical centre of the array. Results are
given in Figure 4 of the measurements which were made on 26 July 1972 and
26 September 1972. The first measurement was made prior to the installation
of the rosette antenna array, while the latter was made following its
installation. They both indicate that the ground within a 610 m radius of
the rosette antenna array is relatively homogeneous in azimuth, although there
are small perturbations probably caused by the small lakes and hills in the
vicinity of the array. For example, peaks in signal level in Figure 4 occur
at azimuths of 120°, 240" and 300". Figure 2 indicates that these correspond
closely to azimuths where at least part of the ground between the monopole
and detector is covered with water. It is of some interest to note that the
irregularities appearing on the curve for 26 July also appear on the curve
for 26 September. The field intensity level measured on 26 September was
roughly 5 dB greater than that measured on 26 July, which was contrary to
expectations since the electrical parameters of the ground in the Arctic are
usually considered to deteriorate during the winter season. However, the
increase is easily explained if it is attributed to a decrease in the effect-
ive distance of propagation due to an enhancement of the conductivity of that
portion of the path covered with Beverage antennas and their copper ground
screens.

The second type of measurement was performed in the air with an air-
craft. An airborne measurement of the field intensity emitted by a dipole
was made on 19 August 1974. The monopole was located slightly northeast of
the rosette array for this measurement. Its location is given in Figure 3.
An improved XELEDOP technique (Barnes, 1965) was employed to make the
measurements.

A XELEDOP is a short dipole antenna with an HF transmitter located at its terminals. Antenna pattern measurenents are made by towing this package behind an aircraft. Since the package used at Cambridge Bay consisted of a short dipole antenna and an HF receiver at its terminals rather than a transmitter it was called a RELEDOP.

The amplitude of the fields radiated by the monopole antenna was measured with an aircraft and the RELEDOP package and the data were relayed to a chart recorder located in the aircraft. The aircraft towing the RELEDOP flew at an altitude of 10,000 ft. (3.05 km) and a constant range of 8 nm (14.8 km) from a ground based radar situated near the monopole. The elevation angle-of-arrival of a ray joining the detector and the monopole was 11.6'. The results of a measurement made at 9.75 MHz are shown in Figure 5 together with the measured pattern of a Beverage pair antenna. More will be said of the Beverage pair antenna measurement at a later time.

The accuracy of these field intensity measurements was determined primarily by the accuracy to which the aircraft could be kept at a range of 8 nm from the tracking radar. This value was 20.1 nm. Since the relative change in field intensity E at the aircraft due to this variation in range r is given by

$$\frac{E + \Delta E}{E} = 1 + \frac{\Delta r}{r} = 1 + \frac{0.1}{8}$$

it follows that the accuracy of the measurement was 20.1 dB. The physical separation of the monopole and the tracking radar caused a systematic error in the measurements. This error is easily corrected by using the inverse relationship between field intensity and range.

An example of the accuracy of the measurements is provided in Figure 5 by the variation in the level of the background signal. The level was approximately 0.8 dB greater at an azimuth of 125' than at an azimuth of 305". The radar used to track the aircraft with the RELEDOP was not collocated with the monopole, as mentioned before, but rather, was located in "D" train which was a distance of 0.41 nm from the monopole, on a radial whose azimuth was 125". Therefore, at an azimuth of 125° the aircraft was 0.82 nm further from the monopole than when its azimuth was 305°. This would be expected to produce a variation of 0.85 dB in the measured field intensity, which is in close agreement with what was measured.

It is of interest to note that the variation in the field radiated by the monopole antenna and which is attributable to variations in the topography of the land in the vicinity of the antenna is less than 0.5 dB. This result is surprising because the terrain slopes down from the monopole for azimuths between 20 and 200°, whereas for azimuths between 240 and 20° the terrain not only is rougher, but the monopole is somewhat obscured by the crest of the hill on which it is situated. At these azimuths one would expect, both scattering of the electromagnetic energy and some obscuration of the monopole by the crest of the hill.

The second-is the superior of the two techniques used at Cambridge Bay for determining the homogeneity of the ground. This stems from its close simulation of a skywave configuration. The first technique measures the effect of the ground on the electromagnetic wave which propagates from the vertical monopole directly to the detector. The strength of the signal is proportional primarily to the conductivity of the ground over which the wave propagates. Variations in the strength of the signal can be attributed to variations in the electrical conductivity of the ground. In the second technique, the signal at the detector consists of a direct ray not affected by the ground and a reflected wave whose amplitude and phase is a function of the electrical parameters of the ground. This dependence can be observed in Figures 6 and 7 where 10 MHz reflection coefficients are given for seven types of ground. This latter technique allows one, in principle, to deduce the ground reflection coefficient in the vicinity of the source–monopole antenna and therefore the electrical ground parameters. It in effect integrates the properties of the ground over a region approximately the size of one fresnel zone, which for a 10 MHz monopole antenna receiving electromagnetic energy at an elevation angle of say 11.6°, is an ellipse whose dimensions are 780 by 160 meters. The total area contained within this ellipse is 23.6 acres, approximately twice the area covered by the rosette antenna array shown in Figure 3. Clearly, the second technique is superior to the first for probing ground homogeneity, simply because it employs a geometry which is a closer approximation to that used when HF skywaves are used for communications, direction finding or OTH radars.

In Figure 3 a compass rose has been drawn concentric with the location of the monopole used for the airborne tests. The dashed circle defines the outer edge of the first Fresnel zone at 10 MHz. The bottom curve (binary curve) in Figure 5 is intended to indicate the location of the lakes within the area described by the circle in Figure 3. It was derived from Figure 3, firstly, by drawing radials, at appropriate azimuthal increments, from the centre of the circle to its circumference. If the radial was found to pass over a lake contained within this circle it was assigned the number "one". On the other hand, if it did not it was assigned the number zero. In the bottom graph in Figure 5 these numbers are plotted against their azimuths. The dashed lines in Figure 5 attempt to show that there is a correlation between the measured variation in the monopole's terminal voltage and the location of the lakes contained within the circle in Figure 3. The correlation is particularly good for azimuths between 234 and 286" where a substantial portion of a relatively large lake is in the first Fresnel region of the monopole antenna. The correlation at other azimuths is not as well defined due to the difficulty of deciding where, in terms of their effect on the reflected ray, the lakes effectively start and stop and also the difficulty of matching the perturbations in terminal voltage to the correct lake. Nevertheless, the good agreement in Figure 5 between the azimuths at which perturbation occur on the field intensity curve and the azimuths at which the binary curve has a value of 1 suggests a high degree of correlation between the perturbations and the presence of lakes. Figure 5 provides an example therefore of the characteristics exhibited by pertrubations caused by ground which is not homogeneous and in particular it demonstrates their relative magnitudes.

2.3   MEASUREMENT OF GROUND CONSTANTS

The ground parameters at Cambridge Bay were derived independently from
five measurements which are described in detail and are as follows:

- measurement of the amplitude of the field radiated by a monopole as a
  function of radial distance from the monopole;

- measurement of the input impedance of a Beverage antenna as a function
  of frequency;

- measurement of the phase velocity of a current-wave on a Beverage
  antenna as a function of frequency;

- measurement of the attenuation of a current-wave on a Beverage
  antenna as a function of frequency;

- measurement of the gain of a Beverage antenna at 9 MHz.

Four of the five methods involve measurements of Beverage antenna
parameters. The first was included to serve as a check on the accuracy of
the remaining four. They will be discussed individually, and in particular,
it will be shown that Beverage antenna parameters can be used to find the
electrical constants of the ground beneath the antenna. The ground parameters
can then be used to derive certain other essential electrical parameters of
the Beverage antenna using a computer program developed at CRC and which is
based in part on theoretical work described by Travers et al (1964). This
program and the theoretical development on which it is based are described in
complete detail in Appendix IV. The program can be used to calibrate gain
and azimuthal radiation patterns of arrays of Beverage antennas for a given
elevation angle.

2.3.1   Field Intensity Versus Radial Distance

A measurement of field intensity versus distance from *a* monopole antenna
excited with a 9.75 MHz transmitter was made on 18 August 1974. The location
of the monopole is shown in Figure 3. The radial along which the measure-
ments were made coincided with a road which ran to the north-west of the
monopole. The results are shown plotted in Figure 8 with two theoretical
curves derived from a Sommerfeld analysis of ground-wave propagation (Terman,
Electronic and Radio Engineering, p. 804, 1955) for average ground (wet) and
poor ground. Their conductivities and dielectric constants are given in
Table I, which lists the electrical parameters of nine distinct and identi-
fiable types of earth. There is good agreement between the theoretical curve
for poor ground and the experimental results of 18 August 1974. The field
intensity measurements made on 26 September 1972 and 26 July 1972 are also
included. These were previously given in greater detail in Figure 4. Average
values are plotted with error bars showing the range of the variation in the
measurements due to inhomogeneities in the ground.

TABLE I

Eorth Conductivity Converstion Table
(With Typical Dielectric Constants) (After Travers et al, 1964)

| Type of Earth | Conductivity (σ) | | | Resistivity $\frac{1}{\sigma}$ | Dielectric constant (Typical) |
	emu (Abmho cm)	esu (statmho cm)	MKS (mho-meter)	MKS (ohm-meter)	(Relative Units)
Sea Water	5×10^{-11}	4.5×10^{10}	5	.2	81
Sea Water	3×10^{-11}	2.7×10^{10}	3	.33	81
Wet Rich Soil	3×10^{13}	2.7×10^{8}	.03	33	15 – 16
Average Soil (Wet)	1×10^{-13}	9×10^{7}	.01	100	10 – 25
Average Soil (Dry)	3×10^{-14}	2.7×10^{7}	3×10^{-3}	333	10 – 15
Poor Soil	1×10^{-14}	9×10^{6}	1×10^{-3}	10^{3}	10
Poor Soil (Dry)	3×10^{-15}	2.7×10^{6}	3×10^{-4}	3.3×10^{3}	8
Dry Sand	1×10^{-15}	9×10^{5}	1×10^{-4}	10^{4}	5
Dry Granite (Subsurface)	1×10^{-18}	900	10^{-7}	10^{7}	Probably < 5

The average value of field intensity measured on 26 July 1972 is consistent with a ground wave which has propagated a distance of 0.610 km over dry average soil ($\sigma = 3 \times 10^{-3}$ mho/m, $\varepsilon \approx 12$). This is best seen in Figure 9, which gives theoretically derived values of field intensity at a distance of 0.610 km from a short vertical antenna excited with 1 kw of RF power. Since the radiation pattern of a $\lambda/4$ monopole is similar to a short vertical antenna these results also apply to the field radiated by a monopole. The calculated values which were derived from Figure 22–2 and Equation 22–1 in Terman (1955) are a function of the electrical constants of the earth over which the wave has propagated.

In Figure 9 they have been calculated for seven of the types of earth listed in Table I, ranging from dry sand to sea water. The dashed line is a best fit to the theoretically derived values. The length of the vertical sides of the rectangle are proportional to the variation in field intensity measured at Cambridge Bay. The horizontal extent of the rectangle defines the range in the ground conductivity. It varies between 2×10^{-3} and 8×10^{-3} or as defined in Table I the ground type varies between about poor soil and average soil (wet). On the average though the ground type might be best classified as being average soil (dry).

The soil at Cambridge Bay is not homogenous because it was found to vary between poor soil and average soil (wet). Lakes were observed to have a

higher conductivity than the surrounding terrain because their presence enhanced the average conductivity of the region that contained them.

The value of field intensity shown in Figure 8 for 26 September 1972 is also consistent with the conclusion that the ground type is average soil (dry). It must be remembered that these measurements were made with the rosette array in place. It is surmised that the copper wire associated with the rosette array increased the conductivity of the ground over the first 0.152 km of the 0.610 km path between the monopole and the field intensity meter.

To demonstrate the effect of the ground screen, first the field intensity at a distance of 0.152 km from a monopole is calculated for average ground (dry). Using the material quoted in Terman (1955) it is found to be 112.6 dB > 1 μv/m. If the rosette array were to improve the conductivity of the ground *so* that it was equivalent to that of wet rich soil with the dielectric constant remaining unaltered the field strength of 0.152 km would increase to 119.8 dB > 1 μv/m. Thus an improvement in conductivity of the first 0.152 km of a 0.610 km path of this magnitude is sufficient to increase the signal level measured at a distance of 0.152 km and also 0.610 km from the monopole by 7.2 dB. This is sufficient to account for the discrepancy between the measurements made on 26 September and 26 July 1972.

It may be concluded that the ground in the vicinity of the rosette array corresponds on the average to average ground (dry). Measurements show in addition that it varies between poor ground and average ground (wet).

2.3.2 Beverage Antenna Parameters

(a) *Impedance Measurements:* Impedance measurements were made as a function of frequency on seven of the twenty–four Beverage antennas contained in the Cambridge Bay rosette antenna array. The average of these seven measurements is plotted as a dashed curve in each of the four diagrams given in Figure 10. The quasi–periodic nature of the experimental curve indicates a standing wave condition on the Beverage antennas which suggests that the antennas were not terminated in their characteristic impedances.

Two theoretical curves of input impedance are also included in each of the diagrams of Figure 10, one for a Beverage antenna terminated in 390 ohms and the other for a Beverage antenna terminated in its characteristic impedance. The graphs are for four different types of soil consisting of poor soil, average soil (dry), average soil (wet) and wet rich soil. In all cases the antenna's height above ground is 1 meter.

A comparison of the amplitude and phases of the perturbations on the experimental curve and the theoretical curve for a 390 Ω termination, suggests closest agreement occurs for average soil (dry) and average soil (wet). From these input impedance measurements one concludes that the soil type at Cambridge Bay, in terms of its electrical parameters is located between, $\sigma_1 = 3 \times 10^{-3}$, $\epsilon_1 = 12$ and $\sigma_2 = 10^{-2}$, $\epsilon_2 = 17$, where the values of ϵ are medians of those listed in Table I.

(b) *Attenuation Measurements:* One of the Beverage antenna pairs in the rosette array was excited with an RF generator at a number of frequencies between 5.8 and 23.7 MHz. The resulting amplitude of the current–wave on one

12

of the wires was measured with a current probe, as a function of distance from the feed point. In Figure 11 the relative amplitude of the current versus the distance from the feed point is shown for the various test frequencies. The attenuation constant for the Beverage element was derived from these curves and is also plotted as a function of frequency in Figure 11. The attenuation constant increases monotonically with increasing frequency.

Theoretical values of current-wave attenuation on a Beverage antenna whose height above ground is one meter are given in Figure 12 for average soil (dry), average soil (wet) and wet rich soil. The experimental curve for Cambridge Bay is superimposed in each graph so that a comparison can be readily made between the experimental and theoretical curves. The best agreement occurs for ground parameters for average soil (wet); namely, $\sigma = 10^{-2}$ mho/m and $\varepsilon = 17.0$.

(c) *Measurement of Phase Velocity:* The termination of one of the Beverage antennas in the Cambridge Bay rosette array was replaced with a "short". The antenna was then excited with an RF generator at frequencies of 5, 10, 15 and 20 MHz. The short circuit caused an RF current standing wave condition on the antenna. A current probe was used to locate current-wave nodes which were numbered consecutively, starting from the terminated end. The measurements are plotted in Figure 13 in terms of distance of the nulls from the terminated end as a function of their assigned numbers. The wavelength of the current-wave is readily derived from the slopes of the straight lines. The velocity of the wave is then calculated and the ratios of the current-wave velocities and the speed of light are plotted in Figure 14. Theoretical values of current-wave velocity ratios are given for antenna heights between 0.3 and 3.0 meters and for average soil (dry), average soil (wet) and wet rich soil.

The agreement in Figure 14 between the experimental and theoretical curves is not sufficiently close to allow for an unambiguous selection of the ground types. Further measurements need to be made to resolve the discrepancy between the theoretical and experimental values of current-wave velocity.

(d) *Measurement of Beverage Pair Gain:* A derivation of the Beverage pair gain, based for the most part, on the data in Figure 5 is as follows:

- gain of Beverage pair antenna with respect to (w.r.t.) the
  monopole antenna at an elevation angle of 11°   6 dB

- Beverage pair cable losses   5 dB

- monopple antenna cable losses   7.5 dB

- net gain of Beverage pair w.r.t. monopole antenna   3.5 dB

- gain of monopole antenna w.r.t. isotropic (assuming
  average soil wet) at 11° elevation angle   −1 dB

- gain of monopole antenna w.r.t. isotropic (assuming
  poor soil) at 11° elevation angle   −5 dB

- gain of Beverage pair w.r.t. isotropic (assuming average
  soil wet) at elevation angle of 11°   2.5 dBi

- gain of Beverage pair w.r.t. isotropic (assuming poor **soil)** at elevation angle of **11"**   −1.5 dBi

- gain of Beverage pair antenna at nose w.r.t. gain at **11"**   No dB

- gain of Beverage antenna w.r.t. Beverage pair antenna   **−3** dB

- gain of Beverage antenna w.r.t. isotropic (assuming average soil − wet)   −0.5 dBi

- gain of Beverage antenna w.r.t. isotropic (assuming poor soil)   −4.5 dBi

The theoretical gain of a Beverage antenna whose height above ground is 1 meter and length is 100 meters is given in Figure **21.** Its value at 10 MHz is −3.4 dBi and is essentially constant for ground types between poor soil (dry) and wet rich soil. The gain of a monopole, on the other hand, varies from +5 dBi for perfect ground to −1 dBi for average soil (wet) and finally −5 dBi for poor soil. Agreement between the theoretical gain of a Beverage antenna and that deduced from the Cambridge Bay measurements occurs only if it is assumed that the monopole at Cambridge Bay was situated on soil which fell between average soil wet and poor soil. From the Beverage pair gain measurements, therefore, it can be concluded that the ground type at Cambridge Bay is roughly average soil (dry).

The gain of a Cambridge Bay Beverage pair was measured previously using a 9 MHz dipole suspended from a balloon at a distance of *0.488* km from the centre of the rosette array (Litva and Stevens, 1973). The field at the centre of the array was measured with a field intensity meter and in addition a measurement was made of the voltage at the terminals of a Beverage pair antenna. From these it was concluded that the gain of the Beverage pair was 0 dBi, suggesting the gain of an individual element to be −3 dBi, which is in close agreement with the theoretical gain. This result tends to lend support to the argument made above for deducing ground parameters at Cambridge Bay from a measurement of the gain of a Beverage pair antenna with respect to the gain of a $\lambda/4$ monopole antenna.

2.3.3 Listing of Soil Types Deduced from Field Intensity and Antenna Measurements

Table II gives a listing of soil types deduced from two distinct types of measurements performed at Cambridge Bay. The first consist of measurements of the field intensity of ground waves radiated by $\lambda/4$ monopole antennas. The second consisted of measurements of those electrical parameters of Beverage antennas which are a function of the soil type beneath the antenna.

The soil type at Cambridge Bay is seen in Table II to vary between poor soil and average soil (wet). It is not homogeneous, but, if it is to be classified with one label, the one that best describes it is average **soil** (dry), with the following electrical parameters, $\sigma = 3 \times 10^{-3}$ mho/m and $\epsilon = 12$.

The agreement shown in Table II between the soil types deduced from the various measurements listed in Table II is reasonably good. This tends to corroborate the effectiveness of the CRC Beverage computer program in correctly predicting Beverage antenna parameters, when the ground parameters are known.

<div align="center">

TABLE II

Listing** of **Soil Types Derived from Measurements at Cambridge Bay

</div>

Technique	Type of Soil	σ (mho/m)	ϵ (Air = 1)
I Field Intensity	poor soil − average soil (wet)	$10^{-3} - 10^{-2}$	10 − 17
II Antenna Measurements			
(a) Impedance	average soil (dry)	3×10^{-3}	12
	average soil (wet)	10^{-2}	17
(b) Attenuation	average soil (wet)	10^{-2}	17
(c) Phase Velocity	Inconclusive	Inconclusive	Inconclusive
(d) Gain	average soil (dry)	3×10^{-3}	12
Average	average soil (dry)	3×10^{3}	12

Only the current-wave phase velocity was found to be problematic in that the evidence it provided regarding the soil type at Cambridge Bay was inconclusive. Further work is required to resolve the discrepancy between the measured and theoretical values.

2.4 THEORETICAL ATTENUATION, IMPEDANCE AND PHASE VELOCITY

Theoretical values are given in Appendix I of attenuation, characteristic impedance and phase velocity of Beverage antennas with heights above ground varying between **0.3** and **3.0** meters and for seven types of soil. The ground constants vary from $\sigma = 10^{-7}$, $\epsilon = 2$ (Dry Granite, substrate) to $\sigma = 10^{-2}$, $\epsilon = 17$ (Average soil, wet). These data can be used in the design and engineering of Beverage antenna systems. Once an antenna site is selected, the ground parameters need first to be determined, either by a measurement of signal strength as a function of distance from a monopole, or by a measurement of the attenuation of a current-wave on a temporary Beverage antenna. The value of the terminating resistor can be obtained from the curves of characteristic impedance given in these figures. The attenuation curves can be used to determine the power dissipation requirements of the terminating resistor for Beverage antennas used for transmitting.

In Chapter **3** it will be seen that following a determination of the ground constants at the chosen antenna site the theoretical radiation patterns can be derived. The antenna can then be engineered to optimize the take-off angle, beamwidth, directivity and power gain within the constraints imposed by the type and quantity of the available real estate.

2.5 DEBERT MEASUREMENTS

The procedures given in Section 2.4 for determining ground parameters to facilitate derivation of antenna parameters will be demonstrated by means

of an example. The antenna in this example is an eight–element Beverage array currently being used as a communication antenna at Debert, N.S. These results presented here will also provide a further test of the CRC Beverage antenna computer program.

The Beverage array at Debert consists of Beverage elements whose lengths are 110 m and whose height above ground vary between 0.73 and **2.9** m because of variations in topography. The average height of the elements in the array is 1.8 **m.** Most of the measurements reported here were made on element #1 whose height varies between 0.73 and 1.55 m with an average value of 1.13 m.

A composite measurement of the input impedances of the eight–elements of the Debert array is given in Figure 15(a). Each element was terminated in its characteristic impedance (Z_0). The magnitude of Z, was obtained by measuring the input impedance of each antenna, at certain frequencies, and varying the value of its terminating resistor until the antenna's input impedance was equal to the value of the resistor. The value of the input impedance at which this agreement occurred was taken **as** the characteristic impedance of the element. The measured values in Figure 15(a) are fairly constant over the frequency range 2 – 17 MHz, suggesting that this procedure for determining the characteristic impedance is valid. Above 17 MHz a "fall–off" in impedance is evident on all the elements.

The measured data is compared with a theoretical curve derived for **a** Beverage element situated on average soil (wet) with a height above ground of **2** m. The soil type was obtained from a consideration of Figure 16(d) and will be discussed in more detail later. There is reasonably good agreement between the theoretical and experimental values in Figure 15(a). The measured input impedance of element #1 terminated in its characteristic impedance is given in Figure 15(b). The experimental curve is compared here with theoretical curves for average soil (dry), average soil (wet) and wet rich soil. Although reasonably good agreement exists, the input impedance of the Beverage antenna is a weak function of the soil type and therefore does not allow for a unique selection of soil type.

* Open circuit and short circuit input impedance measurements of element #1 are given in Figure 15(c) and (d). These measurements were made at frequencies for which the input impedance of the element was real when short circuited. The curve for characteristic impedance in Figure 16(a) was derived from the data contained in Figures 15(c) and (d) with the expression

$$Z_0 = \sqrt{Z_{OC} Z_{SC}} \qquad (1)$$

where Z_{OC} = open circuit impedance

Z_{SC} = closed circuit impedance

Z_0 = characteristic impedance

The average value of characteristic impedance determined in this manner and shown in Figure 16(a) is *480* Ω.

A plot of short circuit resonance number for element #1 is given as a function of frequency in Figure 16(b). These curves were obtained by consecutive numbering of the data points in Figure 15(c) and then plotting the number associated with each resonance point against the frequency at which the resonance occurred. The phase velocity ratio (n) of the current-wave on the antenna can be determined from this graph using **(2).** This expression was derived by using the fact that the number of half-wavelengths of the current-wave on the antenna increases by one when the frequency is increased from one resonance point to the next

$$n = \frac{2\ell}{mc} \tag{2}$$

where n = phase velocity ratio

              ℓ = length of the antenna

              m = slope of the curve in Figure 16(b)

              c = velocity of light

Derived values of the phase velocity ratio for element #1 are plotted in Figure 16(c) with theoretical curves for wet rich soil and average soil (wet). Although the agreement is reasonably good, the experimental values are somewhat greater than the theoretical values.

Finally, the attenuation of the current-wave on element #1 was derived from the closed circuit impedance measurements given in Figure 15(c) and Equation (6).

The input impedance of a transmission line is given by (Ramo et al, 1967)

$$Z_i = Z_r \frac{1 + \rho \ e^{-2\gamma R}}{1 - \rho \ e^{-2\gamma \ell}} \tag{3}$$

where Z_r = characteristic impedance

              Z_i = input impedance

$$\rho_L = \frac{Z_L - Z_0}{Z_L + Z_0}$$

where Z_L = load impedance

              $\gamma = \alpha + j\beta$ (propagation constant)

where α = attenuation constant (nepers/m)

              β = phase constant

If the line is sh rt circuited, $\rho = -1$ and it follows from (3)

$$e^{-2\gamma\ell} = \frac{Z_0 - Z_i}{Z_i + Z_0} = A + jB \qquad (4)$$

(handwritten: real↑ imag↑)

If the characteristic impedance of the element is assumed to be r al then,

$$Z_0 = R_0$$

(handwritten: $\dfrac{\ell_r - (R_i + jX_i)}{(R_i + jX_i) + R_o}$)

and

$$Z_i = R_i + jX_i$$

where R_i and X_i are the real and imaginary parts respectively of the input impedance,

then *(handwritten: should be not =)*

(handwritten: $\dfrac{R_o^2 - R_i - (R_i + jX_i)^2}{(R_0 + R_i) + (R_i + jX_i)}$)

$$A = \frac{(R_0 - R_i)(R_0 + R_i) = |X_i|^2}{(R_0 + R_i) + X_i^2}$$

(handwritten: (real part))

and

$$B = \frac{-2 R_0 X_i}{(R_0 + R_i)^2 + X_i^2}$$

Now, if $X_i = 0$ *(handwritten: real part)* then B = 0

(handwritten: $Z_0 = R_0$ = Characteristic)

$$A = \frac{R_0 - R_i}{R_0 + R_i}$$

(handwritten: $Z_i = R_i$ = R input)

(handwritten: constant ↓)

$$(5)$$

From $e^{-2\gamma\ell} = A + jB$ it follows that

(handwritten: $\left(\dfrac{\ln A^2}{4 L}\right) = $ XGAMMA, XGAM(1))

$$\alpha = -\frac{1}{4\ell} \ln(A^2 + B^2) \quad \text{neper/m}$$

$$\alpha_1 = -\frac{8.686}{4\ell} \ln A^2$$

(handwritten: ℓ = length of antenna)

(handwritten: $A = $)

$$(6)$$

where α_1 = attenuation constant in dB/m

(handwritten: "DB" in the pgm)

(handwritten: Expected values: 1 MHz = .01 dB/m, 2 MHz = .02 dB/m)

The attenuation of the current-wave on the Beverage antenna can be obtained from (6) and a measurement of Z_i at the antenna's resonant frequencies where $X_i = 0$. This technique was tested on a Beverage element at CRC whose length and height above ground was 110 m and 1 m, respectively. The results are given in Figure 17 where a comparison is made between the attenuation determined from the current amplitude measurements along the wire and the

values determined from measurement of Z_i. The results derived from the impedance measurements show a greater degree of scatter because of interfering signals on the wire at the time of the measurements. Theoretical curves are also shown in Figure 17, from which it can be concluded that the ground at CRC can be classified as being between average soil (dry) and average soil (wet).

The curve giving α_1 versus frequency for Beverage element #1 at Debert is shown in Figure 16(d) with some superimposed theoretical curves. The theoretical curve for average soil (wet) shows the best agreement with the measurements, suggesting this to be the soil type at Debert. This conclusion is not in disagreement with the visual appearance and texture of the ground at Debert .

From the measurement of the open and closed circuit impedances of Beverage element #1 at Debert, one now knows the characteristic impedance of the antenna and the soil type at Debert. This information then permits correct termination of the antenna and in addition a derivation of all the antenna's electrical properties, in particular, its gain and two dimensional radiation pattern.

3.   BEVERAGE ANTENNA PARAMETERS

3.1   DESIGN PARAMETERS

This section gives theoretically derived design parameters for Beverage antennas. It is intended that the material will be of sufficient scope to allow the antenna engineer to design antenna system using Beverage elements, which will meet his requirements within constraints set by available real estate. In other words, if the antennas are to be installed on ground whose electrical parameters can be defined by the range between poor soil (dry) to wet rich soil, and to have specified values of gain and take-off angles, the data in this section will allow for selection of the optimum antenna length and height.

The following parameters are given in some detail:

- gain of the antenna at the nose of its radiation pattern (G_N) relative to an isotropic antenna;

- 3 dB vertical beamwidth (BW_V);

- 3 dB azimuthal beamdwidth (BW_A);

- take-off angle of the nose of the radiation pattern (ψ_N).

These parameters are defined in detail in Figure 18 where theoretical vertical and azimuthal radiation patterns are given for a typical Beverage element. In this example the antenna is situated over average soil (dry) and its length and height are respectively 110 m and 1 m.

Figures II-1 to 11-48 give theoretical values of G_N, BW_V, BW_A and ψ_N for Beverage antennas with lengths of 100, 200, 300 and 400 meters, heights of 0.3, 1.0, 2.0 and 3.0 meters, situated over poor soil (dry), average soil (dry), and wet rich soil (see Table I). Generally, it is seen that the gain G_N in each case tends to increase with increasing frequency, whereas the vertical beamwidth BW_V, azimuthal beamwidth BW_A and take-off angle ψ_N tend to decrease with increasing frequency. As an example consider the Beverage antenna defined in Figure 18 and cited previously as being typical. Its parameters are given in Figure 11-21. The magnitude *of* their variations in the frequency range 3 to 25 MHz is as follows:

G_N, -8.5 to -0.5 dBi

BW_A, 65 to 28°

BW_V, 46 to 16"

ψ_N, 24 to 14"

The discontinuities that appear in the graphs are caused by the amplitude of the secondary lobe increasing monotonically as the frequency is increased and surpassing the magnitude of the main lobe at these discontinuities. The side lobe then assumes the role of the main beam and the curves for BW_V, BW_A and G_N undergo discrete changes in level. It should be noticed that these discontinuities become more closely crowded towards the low frequency end of the spectrum as the length of the antenna is increased. Also, the graphs have been smoothed so that the discontinuities do not appear to be as abrupt as they actually are.

An example of this effect can be seen in Figure 19, which gives portions of some vertical radiation patterns for a Beverage antenna with the parameters listed for Figure 11-36. These patterns are given for the frequencies 4, 4.5, 5 and 5.5 MHz which encompass the frequency in Figure 11-36 (approximately 4.15 MHz) at which discontinuities occur in BW_A, BW_V and ψ_N. At a frequency of 4.0 MHz the vertical pattern has a main beam at 8.5" and a side lobe at 29". As the frequency is raised the side lobe grows in magnitude with respect to the main beam. Its magnitude is greater than that of the main beam at 4.5 MHz and thus it assumes the role of the main beam at a frequency between 4.0 and 4.5 MHz. The switching of the roles of these beams at roughly 4.25 MHz accounts in Figure 11-36 for the discontinuous jump from 9 to 25" in the curve for ψ_N. Since the discontinuities in the curves for BW_A and BW_V occur at the same frequency as that for ψ_N, it follows that these discontinuities can be attributed to the same mechanism.

A brief summary of the 10 MHz information contained in the theoretical curves for ψ_N, G_N, BW_A and BW_V in Figures II-1 to 11-48 is given in Figures 20 to 22. These are intended only to show the general trends in the electrical parameters of Beverage antennas as a function of their length and of the ground constants of the earth over which they are situated. All curves are strictly applicable to only one RF frequency, namely, 10 MHz. This frequency was chosen because it is located at the approximate middle of the active HF band.

Figure 20(a) gives the gain of a Beverage element as a function of its length for average soil (dry). It varies from −16 dBi for an element height of 0.3 m to −2 dBi for an element height of 3.0 m. There is little or no variation in gain as the length of the element is varied from 100 to 400 m.

Curves giving the variation of azimuthal beamwidth BW_A of a Beverage antenna with length are shown in Figure 20(b). Roughly speaking for heights between 1 and 3 m, BW_A decreases from a value of 40° for an element length of 100 m to about 30° for an element length of 400 m. On the other hand, this parameter shows little or no variation with length for an element whose height above ground is 0.3 m. In this latter example BW_A has a constant value of about 60".

Figure 20(c) gives vertical beamwidths versus element lengths, for elements heights between 0.3 to 3 m. For an element length of 100 m it is about 25" and decreases to a value of about 17" at an element length of 400 m. Once again, for an element height of 0.3 m, there is little or no variation of this parameter with length. The vertical beamwidth remains virtually constant with a magnitude of 34".

The take−off angle of the beam of a Beverage element is given as a function of length and height in Figure 20(d). It is about 26" for an element height of 0.3 and varies little as the length of the antenna is changed. For element heights between 1 and 3 m it is roughly 20" for element lengths of 100 m and decreases to approximately 15" for element lengths of 400 m.

The gain of Beverage elements for heights above ground between 0.3 to 3 m, lengths between 100 to 300 m and soil types between poor soil (dry) and wet rich soil is given in Figure 21(a). Usually, the gain of the antenna increases as the soil type is varied from poor to good but the magnitude of this increase is at most 6 dB. For most antenna geometries this variation in gain is less than 2 or 3 dB.

The azimuthal beamwidth BW_A of a Beverage antenna as a function of height, length and soil type is given in Figure 21(b). Most of the values shown in this figure for this parameter lie between 25 and 45°. The vertical beamwidth BW_V is given in Figure 22(a), and its values are contained in the interval from 15 to 30" with a median value of about 22".

Figure 22(b) gives the take−off angle ψ_N of the beam of the Beverage antenna as a function of ground type, height and length. For most of the configurations shown the magnitude of ψ_N is within the interval 14 to 25". The take−offbangle is seen to be rather insensitive to the type of ground beneath the antenna except for the case of an element whose length and height are respectively 200 and 0.3 m. In this instance the take−off angle varies from about 20 to 10" as the soil type is varied from poor to good.

Figure 23 gives some comparisons of theoretical and measured values of gain and azimuthal beamwidths as a function of height of the element above the ground and frequency of the radio energy received by the antenna. The measurements were made at Shirley Bay using a transmitter towed by an aircraft (XELEDOP, see p. 7). There is reasonably good agreement between the experimental and theoretical curves in Figures 23(a) to 23(c) which give the gain of a Beverage element, both as a function of height of the element above

ground and also frequency of the radio wave impinging on the antenna. Figures 23(e) and 23(f) show reasonable agreement between the experimental and theoretical curves for azimuthal beamwidth as a function of frequency of elements with heights above ground of 1.0 m and 1.7 m. Poor agreement, on the other hand, exists between the theoretical and experimental curves in Figures 23(d) of BW_A versus frequency for an element whose height is **0.3** m.

3.2 EFFICIENCY OF BEVERAGE ANTENNAS

Most of the measurements nade by CRC have been on Beverage elements which typically are 110 meters long and have a height above ground of 1 meter. They have been, for the most part, erected over soil which according to Table I would be classified as averag soil (dry). It was shown in Section 3.1 that the gain of a Beverage antenna with these parameters is insensitive to the soil type on which it is placed. Further, the dimensions of this Beverage element are compatible with those of classical HF antennas. It follows that its parameters are probably airly representative of those which are likely to be used for Beverage antenna systems. Typically, it has been found that these Beverage elements have the following parameters:

- power gain, 0 dBi;

- directivity gain, 18 dB;

- azimuthal beamwidth, 40°;

- vertical beamwidth, 2 ,

- side lobes down 15-25 d ith respect to main beam;

- take-off angle = 15".

The discrepancy shown above betw the antenna's directivity gain and power gain is caused by its low effic v which is usually less than 2 per cent. As has been pointed out in the l rature the major disadvantage of this type of antenna is its low efficiency

It will be demonstratec I that the inefficiency of the Beverage antenna does not limit its usefulness as a receiving antenna in the HF band because of the inherently noi ectromagnetic environment present within this band. It will also be shown in Section *4.4* that an "overfilled" linear phased array (spacing less th.: 4λ at the highest frequency) of Beverage antennas has greater efficiency t an that of a single antenna because of decreased ground losses. Finally it will be demonstrated that a communications antenna can be constructed with Beverage elements having a gain at 10 MHz of 23 dB as a receiving an enna and a gain of up to 15 dB as a transmitting antenna. The real estate requirements would be similar to those of the larger classical HF anteinas, roughly a site whose dimensions were 150 by 150 m.

Minimum and maximum ex ecte values of atmospheric and galactic noise for a Beverage antenna situa ed i. the northern hemisphere are given in Figure *24.* These curves wer obt ined from those given in CCIR Report 322 for a short vertical antenna assuming the distribution of noise to be iso-tropic. If the Beverage antnna vere 100 percent efficient, it would receive

the same noise power as the dipole. The curves in Figure *24* are displaced downwards from those in CCIR Report **322** to account for the low efficiency of the antenna. At 10 MHz, for example, the displacement is 18 dB because this is the difference between the directivity and power gains of the antenna. If the antenna is followed by a preamplifier with a noise figure of say, *4.0* dB the antenna is limited by external noise, just as a more efficient antenna would be, between **2.3** and 18 MHz. Therefore, it appears that in many cases the performance of the Beverage antenna as a receiving antenna will not be seriously degraded as a result of its low efficiency. In Section *4.4* it will be shown that this is particularly true for overfilled linear phased arrays of Beverage antennas because of the increase in efficiency that is expected to be realized.

Atmospheric and galactic noise are not the only types of noise encountered in the HF band. Man–made or site noise can in many cases be the predominant source of noise near industrialized areas. The numerous coherent man–made signals present in the HF band can also be a source of noise. They can cause relatively high levels of intermodulation (IM) products to be generated in HF receivers because of non–linearities in their various stages of amplification. Since the HF band is congested, this source of noise can only be reduced by using receivers which are very linear and therefore expensive and by using highly directional antennas. The SNR of a signal received with a Beverage antenna may in many cases be greater than that received with a more efficient antenna simply because it has greater directivity than many conventional antennas and therefore greater ability to attenuate signals not arriving from the direction of the wanted transmitter, thereby reducing the level of IM products in associated receiving equipment.

3.3   RADIATION PATTERNS

3.3.1   Individual Beverage Element

An extensive computer program has been developed at CRC which is capable of calculating all of the important electrical parameters for Beverage antennas. The inputs to the program consist of ground parameters (conductivity and dielectric constant), height and length of the antenna. It can be used to calculate antenna gain, attenuation, phase velocity of the current-wave on the wire and two dimensional antenna radiation patterns.

Some measured Beverage element radiation patterns for 12 and 18 MHz are given in Figure 25 for antenna heights between *0.3* and 1.7 m. The measurements were performed at Shirley Bay on a Beverage antenna whose length was 110 m. A transmitting dipole (XELEDOP) was ued to make the measurements (see p. 7).

The side and back lobe levels for the patterns shown in Figure 25 decrease quite drastically with respect to the main beam when the height of the antenna is lowered from 1.7 m to 0.3 m. Dramatic evidence of this is seen from the patterns in Figure 25(a) to Figure 25(c). Initially the maximum front to side lobe ratio is –7.5 dB. This value decreases to –15 dB as the height of the antenna is lowered from 1.7 to 0.3 m. **On** the other hand the gain of the antenna increases almost linearly with height, the gain being roughly 10 dB greater at 1.7 m than at 0.3 m. The antenna has good side and

back lobe rejection when H = **0.3** m, f = 12 MHz, and goo back lobe rejec ion when H = 1.7 m, f = 18 MHz.

A comparison is made in Figures 26 and 27 of theoretical radiation patterns and the experimental patterns shown in polar **form** in Figure 25. In most instances the agreement between the two curves is reasonably good for azimuths within ±60° of the boresight. The exception to this occurs in the two examples shown for a Beverage antenna whose height is 0.3 m. In these instances there is some disagreement between the Beverage antenna's theoret-ical and experimental main beam patterns. In general there is also a discrepancy between the theoretical and experimental side lobe levels. In many of these, though, there is fairly good agreement between the fine structure of the theoretical and experimental side lobes.

Measured vertical patterns for a Beverage antenna located at Shirley Bay with dimensions H = 1.7 m and L = 110 m are given in Figure 28. The measurements were again made with an aircraft towing a transmitting dipole (XELEDOP). While it flew along a straight line at a constant altitude of 300 m over the Beverage antenna the amplitude of the signal at the terminals of the Beverage was recorded. The recorded signal level was corrected for variations caused by the changing range and radiation pattern of the towed dipole, as the aircraft flew over the Beverage antenna.

As **a** check on the accuracy of the technique the pattern of a monopole was measured and compared with **a** theoretical curve for a monopole antenna situated on average ground. Good agreement is seen to exist between the two up to an elevation angle of 50°. Beyond this point the Xeledop data appears to become unreliable.

Figure 28(a) gives the vertical pattern of a Beverage element measured with a horizontally polarized Xeledop package. Figure 28(b) gives a comparison between the pattern given in Figure 28(a) and that measured with a vertically polarized Xeledop package (dashed lines). There is reasonably good agreement between the *two* patterns up to an elevation angle of 30°. Beyond this angle agreement exists only between the levels of the two sets of side lobes. There is disagreement in their locations. Figure 28(c) gives **a** comparison between the measured pattern of Figure 28(a) and a theoretical pattern. There is reasonably good agreement between the two patterns. **Two** exceptions to this, are the location, once again, of the nulls and the level **of** the back lobes of the antenna.

Agreement between theoretical and experimental Beverage antenna radiation patterns have proved in general to be good except that the level of the side and back lobes is usually greater for the measured patterns than for the theoretical ones. Typically the side lobes of theoretical patterns are 25 dB lower than the main beam whereas measured values are normally only about 15 dB below the level of the main beam.

It is believed that the discrepancy between the levels of theoretical and experimental side lobes for Beverage antennas is largely due to the component of horizontal polarization possessed by the radio waves used in making the measurements. Although considerable effort was extended towards ensuring that the Xeledop antenna was vertical when it was being towed by the aircraft, it is likely that the antenna possessed sufficient tilt to introduce

a significant horizontal polarization to th   radio waves it em
theoretical patterns have been derived only for vertically pol
waves. For example, the maximum deviation between the experime
theoretical patterns in Figures *26* and 27 occurs for azimuths o
At these azimuths the sensitivity of the antenna to the horizon
of polarization of the radio waves impinging on it is a maximum,
hand the closest agreement between the experimental and theoreti
occurs for azimuths near the boresite and anti-boresite directio
antenna is least sensitive to the horizontal component of the ra
which it is being illuminated.   Since skywaves, being elliptical:
inherently have a component of horizontal polarization the respor
antenna to the horizontal component of polarization of radio wave
that should be investigated in the future.

3.3.2   Beverage Pair Antenna

The rosette array consisted of 24 Beverage elements separate
azimuth. A segment of the array is shown in Figure *29.*   Each elem
m long with a height above ground of approximately 1 m.   The elemen
phased together in pairs with power adders to form 12 fixed beams s
in azimuth by 30°. A plan view of the overall array is shown in Fi
where each element pair or Beverage pair in Figure 29 is shown as o
This diagram shows the azimuths of the fixed beams and gives an indi
the area occupied by the array.

The distance between the two elements in each Beverage pair wa
to give the apparent phase centres of the elements a separation of ap
mately $\lambda/2$ at 10 MHz. *On* solely intuitive grounds, the apparent phas
of Beverage antennas was taken to be the point on the antenna where t
amplitude of a current-wave, excited by a transmitter at the feed poir
the antenna, was 3 dB less than its amplitude at the feed point (See §
3.5).   This configuration was chosen to increase the discrimination ga
the element pairs by causing cancellation of the radio-wave energy arr
from the sides because of the $\lambda/2$ spatial separation.   Each element pa
connected, to a switch box at the centre of the array via an RF cable.
switch was operated remotely to connect a receiver located in a buildin
from the rosette array to any one of the array's twelve element-pairs.

The azimuthal pattern of one of the Beverage pair antennas is giv
Figure 31(a). This was measured at *9.75* MHz using the towed transmitter
technique (XELEDOP). It is the same pattern as that shown in Figure 5,
except that here it has been transformed into polar form. Figure 31(b)
the pattern given in Figure 31(a) with some super-imposed skywave measure
ments. These were measured with the rosette array on signals-of-opportun
Part of the data was obtained by monitoring the signal on each Beverage p
antenna for a duration of *6* seconds, determining an average value of its
amplitude and then plotting this value in Figure 31(b). The azimuth of ea
point corresponds to the azimuth of the signal with respect to the boresig
of the Beverage pair antenna on which it was received. The remainder were
obtained from quasi-instantaneous measurements of the signal at each antenn
and plotted in the same way. For the latter, a diode switch at the centre
the array was programmed to connect the receiver to the individual array
members in rapid succession. The dwell time on each antenna position was
approximately *1.4* msc. Pictures of oscilloscope displays of the signal

It follows fi
extends to a range
ments made with th
pair they are, at

A complete
This was measured
(RELEDOP) and fly
height of 3.1 km
MHz and the sign
ments made previ
(Litva and Steve
the main lobe ar
two. There is
the main beam.
accurate of the
Beverage pair,
On the other h
likely to be l
the radio wave
during each t

3.4   ISOLATIO

One Be
an RF genera
voltage indu
measured.
voltage ind
applied to
antennas wa

3.5   PHASE

Sin
of the Be
grounds a
into the
the anter
the curr
on a gra
moves aw
that if
are sep
Beverag
frequen
As the
estima
spatia
freque
the fe
placi
of th
frequ

ampli ude were ob ained as the swi ch stepped sequentially through the various antenna positions. This technique allowed for measurement of the relative amplitudes of the voltages, induced by skywave signals at the antenna termi- nals, in a recording time that was short compared to the normal fading rate for HF signals.

There is reasonably good agreement between the two sets of measurements in Figure 31(b). The azimuthal beamwidths and side lobe levels are essential- ly the same in both cases suggesting that the measurements made with the towed transmitter and vertically polarized antenna gave a good approximation to the radiation pattern of the Beverage antenna appropriate for skywaves.

In Figure 31(c) a comparison is given between the XELEDOP pattern of Figure 31(a) and a measurement made with a balloon. The latter was performed at 9 MHz with a transmitter and a vertically polarized half-wave dipole suspended from a balloon, of the type normally used to collect meteorological data. There is good agreement between the main beams of the two patterns but a fairly large discrepancy in the side and back lobe levels. These levels are considerably lower on the balloon measurements. This may result from the balloon-suspended-dipole being more closely vertically polarized than was the case for the Xeledop antenna towed by the aircraft.

Some measurements of the vertical pattern of a Beverage pair are given in Figure *32*. The solid curve was deduced from the theoretical curve for a single element with ground parameters appropriate to average soil (dry). The theoretical results were augmented by 3 dB because there are two Beverage elements in each Beverage pair. Balloon and aircraft measurements are super- imposed. The measurements show good agreement with one another and with the theoretical curve. The balloon measurements do depart, however, from the theoretical curve at low elevation angles, below, say 4° and in addition above about *24"*. The former discrepancy is due, as will be discussed in Section 3.6, to contamination by a ground wave component. This was radiated by the balloon suspended transmitter at these low elevation angles because its close proximity to the ground. Since the balloon measurements were made at a radius of ply *0.488* **km** the balloon suspended dipole came to within $\lambda/4$ of the ground at the lower elevation angles indicated in Figure *32*. The low eleva- tion angle aircraft measurements on the other hand were made with the test antenna at a much greater height and range and therefore were not affected by a surface wave component.

Furthermore, the balloon measurements will also be somewhat in error because they were not made in the far field of the Beverage pair antenna. The near field of an antenna following Kraus (1950) is given by the following relation,

$$R = 2L^2/\lambda$$

where   R = range from antenna to its near field – far field boundary

L = largest physical dimension of the antenna

λ = wavelength

26

It follows from this expression that the Beverage pair near field extends to a range of 0.81 km at 10 MHz. Since the radiation pattern measurements made with the balloon were made within the near field of the Beverage pair they are, at best, an approximation to its far field pattern.

A complete vertical pattern for the Beverage pair is given in Figure 33. This was measured with an aircraft towing a short dipole antenna and receiver (RELEDOP) and flying directly over the Beverage pair antenna at a constant height of 3.1 km. For this measurement the Beverage pair was excited at 9.75 MHz and the signal received by the towed dipole was recorded. Balloon measurements made previously at 9.0 MHz are superimposed for purposes of comparison (Litva and Stevens, 1973). Although there is disagreement in the detail of the main lobe and back lobe there is agreement in the relative levels of the two. There is also some disagreement in the location and the beamwidths of the main beam. It is expected that the aircraft measurements are the more accurate of the two because the former were made in the far field of the Beverage pair, whereas the latter were made in the near field of the antenna. On the other hand it must be remembered that the balloon measurements are likely to be less contaminated by a horizontal component of polarization of the radio waves either transmitted or received by the dipole antennas aloft during each type of measurement.

3.4   ISOLATION BETWEEN BEVERAGE ELEMENTS

One Beverage pair of the Cambridge Bay rosette array was excited with an RF generator at a number of frequencies between 5.8 and 23.7 MHz and the voltage induced at the terminals of each of the remaining eleven antennas was measured. The results of these measurements are given in Figure 34. The voltage induced in the two adjacent antennas was at least 30 dB below that applied to the antenna being excited. The voltage induced in the non-adjacent antennas was at least 50 dB below the excitation level.

3.5   PHASE CENTRE OF BEVERAGE ELEMENTS

Since no concrete evidence exists as to the location of the phase centre of the Beverage element, an estimated phase centre was chosen, on intuitive grounds alone, to be the point at which the amplitude of a current-wave fed into the antenna by a transmitter was attenuated by 3 dB from its value at the antenna's input terminal. Contours for 3-, 10-, and 20-dB reductions in the current were derived from Figure 11(b) and are shown in Figure 35 plotted on a graph whose coordinates are frequency and distance. The 3-dB point moves away from the feed point as the frequency is decreased. This suggests that if the estimated phase centres of the two elements of an element pair are separated by $\lambda/2$ at a particular frequency (10 MHz for the Cambridge Bay Beverage pairs), this separation of $\lambda/2$ can be maintained over a range of frequencies if the antennas are on radials such as shown in Figures 29 and 30. As the frequency, for example, is increased and the wavelength decreased, the estimated phase centres of an element moves toward the feed point, where the spatial separation of elements is also less. In the case of decreasing frequency and increasing wavelength the estimated phase centre moves away from the feed point to a region where separation of the elements is greater. By placing the two element in each pair on appropriate radials, this $\lambda/2$ separation of the estimated phase centres may be maintained over a fairly broad range of frequencies.

3.6 LOW FREQUENCY BEVERAGE ANTENNA

The original development work on the Beverage antenna was directed toward developing an antenna for reception of trans-Atlantic low frequency radio waves. Although tests have not been carried out in this frequency band at CRC, it is felt that the antenna could, in some cases, replace the large vertical monopole antennas used currently for both transmitting and receiving skywaves at these frequencies. This applies to point-to-point application where a considerable saving might be realized in the cost of antennas.

Figure 36 gives the theoretical radiation patterns at 125 kHz for a Beverage antenna situated over poor ground with the following dimensions, H = 7.62 m, L = 7.4 km. It is to be noted that the gain at the nose of the patterns is -15 dBi which compares very favourably with antenna gains achieved presently with large towers. The cost of this type of Beverage antenna would be only about 1/10 that of a large LF tower which is a predominant antenna type at these frequencies. It should be emphasized that the antenna gain at these frequencies has not yet been validated by measurements. It is presented here as an area that deserves further investigation.

3.7 SURFACE WAVE GAIN OF BEVERAGE ANTENNAS

3.7.1 Theoretical Expression

An expression for the gain of a Beverage antenna for surface or ground waves can be obtained from Equation 33 in Travers et al (1964). It follows from this equation that the magnitude of the voltage at the terminals of a Beverage antenna illuminated with a surface wave is given by

$$V_T = \frac{|\overline{E}|}{2} \left| \frac{1 - e^{j\beta_0 L \cos 6 - \gamma \ell}}{Y - j\beta_0 \cos \delta} \right| \sin \delta$$

and ,

$$\gamma = \alpha + j\beta$$

where

V_T = RMS amplitude of the terminal voltage

$|\overline{E}|$ = RMS amplitude of surface wave field inte sity

$\beta_0 = 2\pi/\lambda$

λ = free space wavelength

ℓ = length of antenna

δ = tilt angle of surface wave

α = current-wave attenuation on antenna (nepers/metre)

$8 = \beta_0/n$

n = antenna current-wave propagation factor

The wave tilt angle is given as Equation 41 in Travers et al (1964).

$$\delta = \tan^{-1} \left\{ \frac{\left[(\epsilon_g - 1)^2 + \left(\frac{\sigma_g}{\epsilon_0 \omega}\right)^2 \right]^{\frac{1}{4}}}{\left[\epsilon_g^2 + \left(\frac{\sigma_g}{\epsilon_0 \omega}\right)^2 \right]^2} \right\}$$

where

$\omega = 2\pi f$

ϵ_0 = permittivity of free space

ϵ_g = relative dielectric constant of the earth

σ_g = conductivity of the earth

With the substitution

$$\Gamma = \gamma - j\beta_0 \cos \delta$$

the expression for the terminal voltages becomes

$$V_T = \frac{|\overline{E}|}{2} \sin \delta \left| \frac{1 - e^{-\Gamma \ell}}{\Gamma} \right|$$

The power P_r that the antenna extracts from a passing surface wave is given by

$$Pr = P_d \times A = \frac{|\overline{E}|^2}{\eta} \times \frac{g\lambda^2}{4\pi}$$

where

P_d = power density

g = gain of antenna w.r.t. isotropic

η = characteristic impedance of free space (377 ohm)

A = effective aperture of antenna

The power delivered to the terminals of the antenna is also given by

$$P_r = \frac{V_T^2}{Z_0}$$

or groundwaves. Th field int nsities in Figure 38 for vertical angles less ,
than about 4° appear to be greater than might be expected, since the coeffi-
cient of reflection for the indirect ray approaches -1, and a large null
should occur at these low elevation angles. For ground coefficients of
$\sigma = 10^{-3}$ mho/m $\in = 10$, for example, the reflection coefficients at 4°, 2°, and
0.5" are respectively $0.63 | -178°$, $0.8 | -179°$ and $0.951 | - 179.50°$, (see Figure 7).
Accordingly, the field intensity shown in Figure 38 at these angles should be
reduced by 9, 14, and 25 dB, respectively, from its peak value at 15". Since
no deep null is apparent, it appears that a surface wave has been generated
by the balloon-suspended transmitter and its dipole antenna, and that the
field intensity measured, especially at very low vertical angles, is due
essentially to this wave.

It might be argued that the reason the null did not appear in the
vertical radiation pattern of the Beverage pair antenna, at low elevation
angles, was because the source was within the antenna's near field or Fesnel
region. This argument is readily dispelled by the realization that at low
elevation angles the direct and indirect space waves from the balloon trans-
mitter cancel because the ground reflection coefficient is near -1. Therefore
the wave that propagated from the source to the Beverage pair antenna at these
low elevation angles can only have been a surface wave.

The Beverage antenna is sensitive to surface waves because they travel
with a forward tilt and therefore have a horizontal component of polarization
which is able to induce a current in the horizontal Beverage antennas. For
angles less than 4" the actual values of field intensity at each angle, rather
than its value at a vertical angle of 15" were used to calculate the cross
section and gain of the element pair. A value of about 0 dBi was derived
from these measurements for the gain of a Beverage pair antenna. Recalling
that the gain of a Beverage element is 3 dB less than a Beverage pair it
follows then that gain of a Beverage element is -3 dBi which is in reasonably
good agreement with the theoretical results in Figure 37.

The second of the two types of measurements mentioned at the start of
this section was performed at Area 9 (near Richmond, Ontario). The ground,
as can be seen from Figure 32, is much better than that found at Cambridge
Bay. A comparison was made of the surface wave field intensities generated
by a reference monopole antenna and a Beverage antenna at a distance of about
1 mile. It was found that the gain of the Beverage antenna was about 2 dB
relative to the monopole antenna. Since the theoretical gain of a monopole
antenna is 5.16 dBi (Smith, 1946) it appears to follow that the gain of a
Beverage is 7.16 dB. This results in a discrepancy of about 14 dB with the
theoretical curve in Figure 32.

Careful measurements were made of the monopole antenna's gain by
illuminating it with a surface wave and measuring both field intensity and the
antenna's terminal voltage. It was found that the monopole's average gain
was -3 dBi, from which it follows that the gain of the Beverage is approxi-
mately -1 dBi.

A further measurement was made at Area 9 with a Beverage antenna
intercepting a surface wave generated by a transmitter at a distance of 7
miles. The frequency of the signal was 8.172 MHz. Both the field intensity
near the Beverage antenna and the terminal voltage of the antenna were

measured. From this measurement it was deduced that the surface wave gain of the Beverage antenna was −9.5 dBi which is in close agreement with the theoretical results in Figure **37.**

It is concluded from the limited surface wave data presented here that there is agreement, within experimental error, between theory and measurements. Further measurenents need to be made to confirm the dependence of the gain of the antenna on frequency.

3.8 THEORETICALLY DERIVED VALUES OF SURFACE WAVE GAIN

Theoretical curves giving the surface wave gain of Beverage antennas are shown in Figure III-1 and III-2. The antennas are sited on poor soil (dry) and rich soil (wet). Their heights and lengths are varied respectively between 0.3 to **3** m and 100 to 300 m.

It should be noted that the gain of the Beverage antenna tends to be higher when sited on poor soil (dry) than when it is sited on rich soil . (wet). For the most part this effect is due to the tilt of the surface wave being greater and therefore its electrical vector having a larger horizontal component parallel to the Beverage antenna, when propagating over poor soil than when propagating over good soil. In most instances the gain of the antenna is independent of its height above ground for frequencies below about 5 MHz. Further, for frequencies above 5 MHz the gain of the antenna appears to change little as its length is increased from 100 to 300 m. Below 5 MHz, on the other hand, the gain does tend to increase monotonically as the length of the Beverage element is increased from 100 to 300 m.

4. BEVERAGE ANTENNA SYSTEMS

4.1 INTRODUCTION

Beverage antennas used as elements or building blocks for HF antenna systems with large apertures are covered in this section. HF antenna systems are currently being used for direction finding, over−the−horizon radars and point−to−point communications. It will be shown that the efficiency of a linear array of Beverage antennas can be considerably greater than the efficiency of a single Beverage antenna. If a sufficient number of elements are phased together, not only will the resulting array be effective as a receiving antenna, but it will also be effective as a transmitting antenna.

Two types *of* arrays will be discussed in detail; firstly, the rosette array and secondly, the linear array. Both of these have been evaluated by CRC at Ottawa and at Cambridge Bay, N.W.T., as communications, direction finding and radar antennas. The first is recommended for use on point−to−point communication circuits, and the latter for communications terminals requiring azimuthal dexterity. The latter is also recommended **as a** relative−ly inexpensive antenna system with applications in HF direction finding. All of these antenna systems have a relatively low physical profile because of the low profile of the Beverage antenna which serves as the basic element for these systems.

4.2   ROSETTE ARRAYS

4.2.1   **Cambridge Bay Rosette Array**

One of the first Beverage arrays developed at CRC was a rosette array installed at Cambridge Bay, N.W.T., which was described in some detail in Section 3.5.   It might be reiterated that the elements were phased together in pairs with power adders to form 12 fixed beams separated in azimuth by 30". The azimuths of these 12 beams are given in Figure 30.   Each Beverage pair was connected to a switch box at the centre of the array via an RF cable.   The switch box consisted of twelve diode switches which facilitated selection of the output of any one of the Beverage pairs from the building housing the receiver.   The rosette array of Beverage antennas and electrical switch constituted a receiving antenna with a **3** dB azimuthal beamwidth of 30" which was steerable in 360" of azimuth.

No further results of the electrical parameters of the Beverage elements of the Cambridge Bay rosette array will be given since these were covered in some detail in Sections 2 and **3.**   Rather, results of evaluations of the effectiveness of the Cambridge Bay rosette array as an HF direction finding and communications antenna will be given here.   It should be stated in passing that this antenna was primarily used as an OTH radar receiving antenna at Cambridge Bay.   Data showing its effectiveness in this capacity are not included here because of its classified nature (Jenkins and Hagg, 1975).

4.2.2   **Rosette Array as a Communications Antenna**

Figure 40 gives pictures of the CRT display of a Hewlett Packard spectrum analyzer connected alternately to a rosette Beverage pair and a monopole antenna resonant at 9.748 MHz.   Both of these antennas were monitoring an HF signal whose frequency was 9.748 MHz and emanated from a transmitter at Alert. The pictures show signals in **a** 2 MHz portion of the HF spectrum centred on the frequency of the Alert signal.

The SNR of the Alert signal with respect to interference levels in a ±0.2 MHz band centred on the frequency of the Alert signal is indicated for 12 consecutive time intervals.   The duration of time between measurements was a random variable but, on the average, it probably was 15 minutes.   These values were obtained from the pictures of the spectrum analyzer display. This ratio indicates the effectiveness of an antenna in discriminating against interference.   It was found to be considerably larger on the Beverage member than on the monopole antenna.   The median **SNR** measured for the Beverage member was +20 dB and that for the monopole antenna was +5 dB.   Therefore, the difference in SNR is +15 dB, which closely corresponds to the difference in directivity gains of the two antennas.   For example, the directivity gain of the Beverage member is 18 dB and that of the monopole antenna 6 dB at 10 MHz which gives a difference of 12 dB in the gains of the two antennas.   If the distribution of the interference were isotropic the difference in signal-to-interference ratios measured on the two antennas would tend to approximate the difference in their directivity gains.

4.2.3   Rosette Array **as** *a* DF Antenna

The electronic switch located at the centre of the Cambridge Bay rosette array facilitated rapid azimuthal steering or switching of the antenna beam. This permitted the terminal voltages of the 12 members of the rosette array to be sampled in a time that was short compared to the normal fading period of HF signals. The amplitude of the signals at the terminals of the rosette array was found to vary in magnitude, as was expected, with the largest signal appearing on the array member most closely aligned with the azimuthal direction of arrival of the signal. It was found that the direction of arrival of the signal could be interpolated between two array members from the ratio of amplitudes of the signals on these two members. These initial tests suggested that this configuration of Beverage antennas and electronic switch could be the basis for an inexpensive direction finding system with an accuracy of about 1 to 2 degrees (J. Litva and E.E. Stevens, patent pending, 1973).

Results of some initial tests performed to determine the feasibility of direction finding with the Cambridge Bay rosette array are given in Figure 41. These consist of pictures of the CRT display of an oscilliscope monitoring the audio output of a receiver tuned to accept WWV skywave signals received by the rosette array. Each trace consists of the terminal voltages of the 12 rosette antennas monitored consecutively in time, each for a duration of 1.2 msec. Although a wide range of sampling times were possible only on: was actually used in these preliminary results. Each complete trace consis ing of samples of the 12 antenna terminal voltages provided by the rosette array required 14.4 msec. Figure 41(a), for example, shows quite dramatically the manner in which the antenna terminal voltages vary as the terminals of the 12 antennas are sampled sequentially. The strongest signal appeared on antenna 6 whose azimuth was 143" (see Figure 30). This suggests that the approximate azimuth of the signal was 143" ±15°. It will be shown that the accuracy of this bearing can be improved by considering the ratio of the amplitudes of the signals on the two antennas adjacent to antenna 6.

Direction finding traces obtained with a 15 MHz signal emitted by the WWV transmitter located at Boulder, Colorado are given in Figures 41(b) to 41(c). Although the azimuth of this transmitter with respect to Cambridge Bay is 179.5°, this need not be the azimuthal angle of arrival of HF signals emanating from this transmitter. Bearings of HF signals are observed to vary with time, principally because of tilts in the ionosphere. Therefore the azimuthal angle of arrival of HF signals can deviate quite markedly from its great circle bearing. In Figure 41(b) the signal of largest amplitude appears on antenna 7 whose azimuth was 173". The signal amplitudes are almost equal on the two antennas adjacent to antenna 7. This suggests that the azimuth of the signal is in close agreement with the azimuth of antenna 7 or 173". In Figure 41(c), on the other hand, the amplitude of the signal on antenna 8 is almost equal to the amplitude of the signal on antenna 7. If the amplitude was the same on both, the azimuth of the signal would be 188°, which is half way between the two antennas. Since the amplitude is somewhat less on antenna 8 than on 7, it follows that the azimuth of the signal is somewhat less than 188" or approximately 185". On the other hand in Figure 41(d) the signal is strongest on antenna 6 with a slight bias towards antenna 5, since the amplitude of the signal is greater on 5 than on 7, This suggests that the azimuth of the signal in this instance is about 135". This simple example outlines the mode of operation for an inexpensive **HFDF** system using a rosette

array of 24–Beverage antennas. The technique for determining a correction to the initial approximation of the signal's azimuth can be greatly refined by the use of calibration curves. These curves give the ratio of signal level on each adjacent antenna with respect to the signal level on the central antenna for azimuths of ±7.5° centred on the azimuth of the central antenna. A small computer could then be programmed to select the antenna with the largest signal, calculate a bearing correction and compute the correct bearing by applying the bearing correction to the azimuth of the antenna on which the largest terminal voltage was recorded.

Further results obtained with the Cambridge Bay rosette array are given in Figures 42 and 43. These were obtained on skywave signals from known transmitters and were obtained from the patterns in Figures 42 and 43 by deducing the azimuth that bi–sected the patterns rather than using the maxima of the patterns. The great–circle azimuths of the transmitters are indicated. As mentioned earlier these need not be the true bearings of the signals because tilts and irregularities in the ionosphere can cause the signal to deviate from the great circle path. Furthermore, signals that arrive at a receiving station via a side scatter mode can be deviated by up to 30–40° from the great circle path. It is seen, though, that these crude bearings agree to within about 8° of azimuth with the great circle bearings of the signals.

4.3 CAMBRIDGE BAY LINEAR ARRAY

4.3.1 Description of the Array

In August 1973 a wide–aperture antenna was installed at Cambridge Bay, N.W.T. The antenna was a linear phased array of 32 Beverage elements. A list of pertinent parameters is given in Table 111.

TABLE III

Parameters of Cambridge Bay Wide Aperture Antenna

Aperture	1.26 km (4,134 ft.)
Inter-Element Spacing	40.65 m (133.4 ft.)
Boresight Direction	18.63" East of North (Alert direction)
Steer Capability	±6°, in 10 steps
Vertical Beamwidth	12°, at 3 dB points (10 MHz)
Elevation Angle of Maximum	15° (10 MHz)
Azimuthal Beamwidth	1.2° (10 MHz)

A scematic illustration of the linear array and its phasing network is given in Figure 44. The outputs were summed in groups of 4, in 4:1 power combiners, to give 8 sub–array outputs which were then fed into a switch box with appropriate lengths of phasing cables.

The calculated beamwidth and directivity gain of the linear array are given in Figures 45(a) and (b). At 10 MHz these are respectively 1.2' and 34.6 dB. This directivity gain is near the upper limit achieved to date for HF antennas. The solid curves in Figure 45(c) give the positions of the primary grating lobes with respect to the main beam. These lobes result from

the int r-element spacing being greater than 3/4λ (Terman, 1955). Sin e each Beverage element has directive properties, the grating lobes are reduced in gain from the main beam. Curve B in Figure 45(c) gives the angular displace-' ment beyond which the amplitude of these lobes is reduced by at least 13 dB.

The dashed curves in Figure 45(c) give the location of the secondary lobes which are present when the array is steered off boresight. These appear because the array is steered by adjusting the phase of groups of four elements rather than single elements. Therefore when the array is steered it behaves like an array of 8 antennas whose inter-element spacing is 4 times as great as when the antenna beam is on boresight. The amplitude of these lobes is determined by the pattern of four Beverage antennas phased together, in the same way that the primary grating lobe amplitudes are determined by the patterns of the individual elements. Figure 46 gives some computed array patterns at 10 MHz for azimuths adjacent to the main beam. It can be seen that the amplitude of the side lobes adjacent to the main beam are 13 dB less than the amplitude of the main beam for the example showing a 1" steer. The amplitudes of the secondary lobes on the other hand grow with steer angle and become greater than that of the main beam at a steer angle of 6°.

The measured pattern of the array with aperture weighting is given in Figure 47(b). To illustrate the degree of aperture weighting used here, the results of measurement of the relative current amplitudes at the terminated ends of the individual Beverage elements are given in Figure 47(a). Array weighting is evident, with the centre elements given more weight than the outer elements. A theoretical array pattern derived from the measured current distribution is shown as a dashed curve in Figure 47(b). Reasonably good agreement exists between the location of the theoretical and measured grating lobes and some side lobes. The lack of agreement between the grating lobe levels on the two patterns results from the use of a single-element theoretical pattern whose side lobe level, with respect to the main beam is lower than are the measured side lobe levels of single Beverage elements. The measured 3 dB beamwidth of the array is 2.3". Theoretically, the beamwidth of an unweighted array with an aperture of 4000 ft. is 1.28". The array weighting used should cause beam broadening by a factor of 1.5, which gives a beamwidth of 1.9°, in reasonable agreement with the measured value.

4.4 LINEAR PHASED BEVERAGE ARRAYS FOR COMMUNICATIONS

4.4.1 Initial Considerations

It has been demonstrated in Section 4.2.1 that the SNR of the radio energy received by an antenna in a point-to-point communications circuit is roughly proportional to its directivity gain. Considerable improvement was shown to be realized from using a Beverage member with a directivity gain of 18 dB rather than a monopole with a directivity gain of 6 dB.

The theoretical directivity gain of the Cambridge Bay linear array is given, as a function of frequency, in Figure 45(b) and is seen to have been approximately 34 dB for frequencies between 4 and 24 MHz. Although an antenna of this size is not practical as a communications antenna, it is worthwhile to consider the use of antennas with 8 or 16 elements and apertures of 150 m for communications applications. They would have azimuthal beamwidths of 10°,

elevation beamwidths of 20° and "take-off" angles of 15" at 10 MHz. The directivity gain would be **23** dB at this frequency. Such antennas likely to be highly effective on long range point–to–point circuits because of their high directivity gain and low "take-off angles". The beamwidths are still sufficiently broad to prevent attenuation of the HF signal due to variations in azimuthal angle of arrival caused by ionospheric tilts and irregularities.

The pattern of an unweighted 8–element Beverage array with an aperture of 150 m is given in Figure 48(a). The beamwidth at 10 MHz is 9" and the adjacent side lobes are down from the main beam by **13** dB, **as** is to be expect- ed, since their level is determined by the function $\sin x/x$. The side lobes can be reduced by weighting of the aperture of the array. Figure 48(b) shows the pattern that results from applying $\cos^2$ weighting to the aperture of the array. The side lobes are reduced by 20 dB from the unweighted case. The price that is paid in using this technique is broadening of the main beam, in this case by a factor of 1.6, and a reduction in the gain of the antenna by approximately 6 dB.

Figures **49** to 51 show the effect of increasing the number of elements from 2 to **32** in an array with an aperture of 150 m. It can be seen that the grating lobes can be made to disappear by increasing the number of elements in the array and thereby reducing the inter–element spacing. For example, increasing the number to 8 results in a pattern with no grating lobes at a frequency of 10 MHz. The patterns are all calculated for a frequency of 10 MHz. The directivity gain of the array ceases to increase appreciably once there are 4–elements in the array aperture. It ceases to increase entirely when the array aperture contains 8–elements. At this point the array is filled in; in other words, the inter–element spacing is less than or equal to $3/4\lambda$.

The theoretical efficiency and power gain of an array with the follow- ing parameters, assuming non–interacting Beverage elements, are given in Figure 52;

- array aperture = 150 m;
- element length = 110 m;
- element height = **2** m;
- array azimuthal beamwidth = 10" (at 10 MHz);
- number of elements = **1** to 64.

The power gain in Figure 52 increases monotonically with the number of elements provided the elements are independent (De Santis et al, 1973). It increases by **3** dB each time the number of elements is doubled, This one to one relationship between power gain and the number of elements in the aperture of the array starts to break down when the elements are no longer independent because of high mutual coupling resulting from their proximity. Although efficient antennas must be separated by at least about $\lambda/2$ to prevent inter- action by their induction fields, inefficient antennas can be brought closer together before there is appreciable interaction. Travers et al (1964) indicated that the interaction between individual Beverage elements does not become appreciable until the elements are spaced closer than their heights above ground. For Beverage elements **2** meters in height, for example, this

suggests that an array aperture can be filled, with resultant increase in power gain, until the inter-element spacing become of the order of 2 m. Therefore an array whose aperture was 150 m could accommodate a maximum of about 64 elements and according to Figure 52 the maximum power gain that would be achieved is 17 dBi. Although not indicated in Figure 52 it is expected that the power gain of an array with an aperture of 150 m will level off at about 64-elements for a frequency of 10 MHz.

The directivity gain in Figure *52* increases montonically with the number of elements in the array until it contains 8-elements. At this point the array is filled with no further increase in directivity gain taking place as the number of elements is increased. Actually little increase in directivity gain is achieved at 10 MHz once there are 4-elements in the array. If the array were to be used solely as a receiving antenna there would be little advantage, except for increased efficiency, in adding more than 8-elements provided that the upper frequency was limited to 10 MHz. The number of elements, in actual fact, should be doubled to 16 in order that the array be free of grating lobes up to 20 MHz.

Initially the efficiency of the array in Figure 52 is about 1.0 per cent which is simply the efficiency of a single element. It increases slowly with the number of elements until the array is filled. Beyond this point there is a fairly rapid increase and it is expected that a maximum efficiency of approximately 32 per cent would occur when the array contained 64-elements. Although not shown in Figure 52, it is expected that this curve will also level off when the array contains 64-elements just as the directivity gain leveled off when the array contained 4-8 elements.

4.4.2 Beverage Array as a Point-to-Point Communications Antenna

Some initial measurements which are corroborated by more extensive measurements at Debert, N.S. have been conducted at Ottawa to evaluate the performance of a linear array as a point-to-point communications antenna. An 8-element array with an aperture of 149.3 m has been erected and pointed towards Alert. The performance of the array has been compared to that of a resonant $\lambda/4$-monopole antenna. A skywave signal emanating from a transmitter located at Alert was monitored simultaneously on both antennas. Each antenna was attached to a Hewlett Packard spectrum analyzer and the spectrum analyzers were set to perform repititious scans over a 50 kHz frequency band that was centred on the frequency being monitored. The video output of the spectrum analyzer was recorded on a chart recorder. Figure 53 gives an example of the records obtained using this technique. Two traces are shown, one is the video output of the spectrum analyzer attached to the Beverage antenna array and the other is the video output of the spectrum analyzer attached to the monopole antenna. The IF bandwidth of the spectrum analyzer was 100 Hz and the total scan time was 100 sec. In each case the predominant vertical traces as indicated in Figure 53 represent the Alert signal. Although the horizontal axis is calibrated in units of time it could also be calibrated in units of frequency.

It is to be noted in this example that the signal-to-interference ratio achieved with the monopole antenna is about 23 dB whereas that achieved with the Beverage array is about 11 dB greater or 34 dB. Similarly the signal-to-background noise level (SNR) of the monopole antenna is about 45 dB whereas

that of the Beverage array is about 60 dB. The distinction between inter-
ference and noise used here is the following; interference is coherent and
therefore emanates from other HF transmitters, whereas noise is broadband and
emanates from electrical power lines, electrical machines, atmospherics and
extra-stellar sources. Since the directivity gain of a monopole antenna is
about *4* dB and that of the Beverage array is 23 dB it is seen that the improve-
ment in *SNR* realized on the Beverage array over that of the monopole antenna
is roughly equal to the difference in the directivity gains.

Further results obtained from a comparison of the linear array and a
reference $\lambda/4$ monopole antenna are given for a 3-hour period on 7 October 1974
in Figure 54. This figure shows the difference in SNRs achieved on the *two*
antennas. The median difference value is 15 dB, which **is** somewhat short of
the expected value of 19 dB given by the difference in directivity gains of
these two antennas. It is to be expected that a longer sampling of data would
have resulted in a median value which would have been in closer agreement with
the expected value.

4.4.3   Efficiency of a Linear Beverage Array

In an attempt to verify the basic assumption of independent elements
used to derive Figure 52, records such as those shown in Figure 53, were
scaled to determine the gain of the Beverage array with respect to that of
a monopole antenna. Using the theoretical gain of a monopole antenna with
respect to an isotropic antenna for skywaves the gain of the Beverage array
with respect to an isotropic antenna is then readily determined. Results
showing the gain of the Beverage array with respect to that of a monopole are
given for a **3** hour interval in Figure 55. The median value of gain of the
Beverage array with respect to a monopole antenna was found to be 10 dB.
Since the gain of a monopole antenna at an elevation angle of 13°, which is
the predominant angle of arrival of the skywave signals from Alert, is −1.5
dBi and the total Beverage array losses due to attenuation in linking cables
and power dividers were about 2.0 dB it follows that the gain of the Beverage
array is 10.5 dBi.

The power gain G of an antenna (Kraus, 1950) is given by

$$G = \in D$$

where $\in$ = the efficiency of the antenna (fraction of the power fed into
the antenna that is actually transmitted)

D = directivity gain

The directivity gain of an antenna is determined primarily by the two dimen-
sional geometrical shape of the antenna's radiation pattern and is given to
good approximation for small beamwidths by

$$D = \frac{41,253}{BW_A \times BW_V}$$

where, the numerator is the number of square degrees in a sphere.

Since the directivity gain of the Beverage array is 23 dB at the frequency of the Alert signal and its power gain, as just determined, is 10.5 dBi it follows that its efficiency is −12.5 dB or 5.6 per cent. The efficiency on the other hand of a single Beverage element of the type used in the array is about 1 per cent. Therefore this array of 8−elements has an efficiency which is about *4.6* per cent greater than that of a single Beverage element. This finding is in close agreement with increase in efficiency predicted by Figure 52 with 3−elements in the array aperture rather than a single element.

An explanation for the increased efficiency that can be realized by the arraying of inefficient antennas is most easily arrived at by considering the antenna as a receiving antenna. If the power received by one antenna monitoring a signal is P, the power received by 2 antennas, provided there is sufficient separation between them so that they are independent, is 2 P. If these two antennas are phased together the gain of the resulting antenna is, as a receiving antenna, 3 dB greater than a single antenna. It follows from the reciprocity theorem for antennas that the gain of this antenna as a transmitting antenna has also increased by the same amount over that of a single antenna. For an array of n independent antennas the power received is n times as great as that received with a single antenna and therefore the power gain of the array of antennas is greater than that of a single antenna by the factor

$$AG = 10 \log n$$

where AG, is the increase in gain of an array over that of a single antenna.

When antennas with an efficiency of 1.0 are arrayed together the power gain realized with the array relative to a single element can only be due to the increased directivity gain of the array. On the other hand when inefficient antennas are arrayed together the resulting increase in the power gain can stem from an increase both in the directivity gain and efficiency of the array with respect to a single element. The increase in efficiency of an array over a single element arises from a reduction in ground losses brought about by the array's lower electrical energy density which is less, simply because the total electrical energy is spread over a larger area (De Santis, 1973).

As an example of highly inefficient antennas let us consider Beverage antennas, which are postulated (Travers et al, 1964) to maintain a fairly high degree of isolation until their spacing is less than their height above ground. *An* approximate relationship between the azimuthal beamwidth of an antenna, in particular, of an array of antennas, and its aperture is given by

$$BW_A = \frac{51.7}{N_\lambda}$$

where N_λ = the aperture of the antenna in wavelengths.

Since the azimuthal beamwidth of a Beverage antenna (f = 10 MHz, H = 2 m, L − 110 m, average soil − dry) is *40″* its effective aperture is 1.3λ. This suggests that at 10 MHz the directivity gain of an array of these Beverage antennas is essentially equal to the directivity gain of a single Beverage

antenna until the array aperture is greater than **39** m. From what has been said above, up to approximately 20 non–interacting Beverage elements could be phase together in an aperture of **39** m. At 10 MHz the increase in power gain that would be realized is 13.0 dB. The majority of this increase must be attributed to the increased efficiency of the array relative to a single element since the directivity gain of the array is essentially that of a single Beverage element or 18 dB. **It** follows that the gain of this array would be 12.0 dBi if the gain of a single element is assumed to be –1 dBi. The efficiency then of this array would be –6.0 dB or about 25 per cent whereas the efficiency of a single element is only about 1 per cent.

There is another point of view that can be brought to bear in explaining the increase in efficiency that is achieved with arrayed antennas. It can be also used to determine the maximum power gain that can be achieved with an array whose physical dimensions are fixed.

It is a relatively well known fact in antenna theory that the minimum effective proximity of the elements in an array is determined by the size of the elements' effective apertures. In other words, for a one or two dimensional array of fixed physical aperture the maximum gain that can be achieved is realized when a sufficient number of elements is placed in the aperture so that the perimeters of the effective apertures of adjacent antennas are essentially touching one another. A small degree of overlapping is possible since the region near the centre of the effective apertures of each element has greater weight than the region near the perimeters.

The gain of an array with N elements arrayed such that the effective apertures are not overlapping, is given by N x A where A is the effective aperture of one of the array elements. The gain of the array is then given by

$$g_N = \frac{4\pi NA}{\lambda^2}$$

where g_N = gain of the array

A = effective aperture of one element $(= g\lambda^2/4\pi)$

N = number of elements

If in a first approximation one approximates the effective aperture **A** of an element with a square the length of one side in wavelengths is given by

$$L_\lambda = \sqrt{\frac{g}{4\pi}}$$

where   g = gain of an element

L_λ = linear dimension of effective aperture of array element

Table IV gives the gain and efficiencies of a Beverage antenna array with a physical aperture of 150 m for 16, **22** and **32** Beverage elements. **It** is assumed that the array is on average soil (dry), element lengths are 150 m

and element heights are 2 m. The gain of a single element varies between −4.5 dBi and 2.3 dBi in the frequency range 5 MHz to 20 MHz. In the same frequency interval the effective aperture of a single Beverage antenna varies from 101.7 m² to 30.4 m² and correspondingly the width of its effective aperture varies between 10.1 m and 5.52 m. It follows that if there is to be no overlapping of effective apertures in this frequency range the minimum inter−element spacing must be 10.1 m. The remainder of the table gives the gains and efficiencies of the array antenna for 16, 22 and 32 elements when overlapping of effective apertures takes place the total effective aperture N x A is adjusted to ensure that the common areas are only counted once and the resultant is given as N x A'.

TABLE IV

Gain and Efficiency of a Beverage Antenna Array Determined From Effective Areas

Aperture = 150 m
Average Soil (Dry)

Frequency	5 MHz	10 MHz	15 MHz	20 MHz
N	1	1	1	1
G	−4.5 dB	−1.0 dBi	1.0 dBi	2.3 dBi
L_λ	.168	.251	.317	.368
L	10.1 m	7.53 m	6.34 m	5.52 m
A	101.7 m²	56.9 m²	40.11 m²	30.4 m²
	1.8 %	.0 %	2.2 %	2.3 %
N	16	6	16	16
S	10 m	0 m	10 m	10 m
N x A	1627.2 m²	710.4 m²	641.7 m²	486.4 m²
G_N	7.53 dBi	1.0 dBi	13.04 dBi	14.34 dBi
	5.66 %	31 %	6.82 %	6.82 %
N	22	2	22	22
S	7 m	7 m	7 m	7 m
N x A	2237.4 m²	1151.8 m²	882.2 m²	668.8 m²
N x A'	1565.8 m²	1164.2 m²	882.2 m²	668.2 m²
G_N	7.37 dBi	1.1 dBi	14.4 dBi	15.7 dBi
	5.45 %	8.12 %	9.33 %	9.33 %
N	32	32	32	32
S	4.84 m	4.84 m	4.84 m	4.84 m
N x A	3254.4 m	1320.8 m²	1283.4 m²	972.8 m²
N x A'	1529.6 m	1170.8 m²	979.2 m²	789.9 m²
G_N	7.3 dBi	12.1 dBi	14.9 dBi	16.4 dBi
	5.4 %	8.12 %	10 %	10.96 %

G = gain w.r.t. dBi
L_λ = width of effective area in wavelength
L = width of effective area in metres
A = effective area

A' = effective area adjusted to account for overlapping
S = separation of elements (metres]
N = number of elements

The results in Table IV for 16 elements are equivalent to those of Figure 52. The efficiency at 10 MHz, for example, has increased from **2** per cent for a single element to 6.31 per cent for the array of 16 elements. The results of Table IV and Figure *52* diverge for N equal to 22 and 32 because correction for overlapping of effective areas was not taken into account in the derivation of Figure 52.

5. CONCLUSIONS AND RECOMMENDATIONS

5.1 SITING OF HF ANTENNA

A. **An** effective means of measuring the homogeneity of a potential antenna site is to erect a monopole antenna and measure its radiated field with an airborne receiver and short dipole antenna (**RELEDOP**).

B. The electrical constants of the ground are probably most easily determined with a temporary Beverage antenna. The attenuation of the current-wave on the antenna is measured at a number of frequencies in the HF band and the soil constants (soil type) are determined by reference to Appendix I.

5.2 BEVERAGE ANTENNA PARAMETERS

A. Extensive measurements were made of Beverage antenna parameters and compared with theoretical results. The complement of measured parameters include the following;

- input impedance
- characteristic impedance
- current-wave attenuation
- current-wave phase velocity
- isolation between elements
- space-wave power gain
- surface-wave power gain
- azimuthal radiation patterns (space wave)
- elevation radiation patterns (space wave)

The agreement between the experimental and theoretical results was, except for a few instances, reasonably good. It follows that the theoretically derived parameters can be used with confidence in the design of communications circuits using Beverage antennas and in the design of Beverage antenna systems.

B. Theoretical design parameters are given in Appendices I, **II** and 111. Appendix I gives the current-wave attenuation and characteristic impedance of Beverage antennas. These can be used to determine the power rating require-ments and magnitudes of terminating resistors. The remaining design parameters are given in Appendix II. These consist of azimuthal beamwidth, vertical

beamwidth, take-off angle and power gain. Appendix III gives the power gain of Beverage antennas for surface waves.

C. It was shown that the Beverage antenna is a highly effective HF receiving antenna. This stems from its high directivity gain ($\sim$ 17 dB), broad band characteristics (3-30 MHz) and low take-off angle ($\sim$ 15.0"). Its other attributes consist of low real estate requirements and low procurement, installation and maintenance costs. As a receiving antenna it has been found to be more than, or at least as effective as, classical HF antennas in maximizing the SNR of received signals.

5.3   BEVERAGE ANTENNA SYSTEMS

A.   A rosette array of Beverage antennas was shown to be an effective HF receiving antenna with a mean directivity gain of about 17 dB and an effective azimuthal steer capability of 360". It was also shown to have potential as an HF direction finding antenna system.

B.   Linear phased arrays of Beverage antennas were shown to be effective OTH and HF point-to-point communications antennas. HF receiving arrays having mean directivity gains of *23* dB have been tested and found to be effective in achieving high SNRs on communications circuits. Maximum directivity gains achieved by classical HF antennas are usually about 16-18 dB.

C.   It was shown that an array of Beverage antennas can have greater efficiency than a single Beverage antenna. Efficiencies of up to 10 per cent can be achieved using Beverage elements whose efficiencies individually are about *2* per cent. It was shown that construction of antenna arrays with power gains which varied from 7 dBi to 16 dBi in the frequency interval 5 MHz to *20* MHz are possible using Beverage antennas as array elements. The real estate requirements are 150 m by 150 m. These gains compare very favorably with the larger classical HF antennas and the costs are about 1/8 - 1/10 those of classical antennas.

5.4   THEORY

A fairly complete description of the equations used in deriving the theoretical Beverage parameters used in the body of this report is given in Appendix IV. Equations are also given for calculation of the electrical parameters of arrays of Beverage antennas. A listing and discussion of the CRC Beverage antenna computer program is also given.

A.   A prototype transmitting Beverage antenna should be built, tested and demonstrated.

Purely economic considerations serve as the major justification for this recommenation. On the basis of the results given in this report, it appears highly probable that transmitting Beverage antennas can be designed, built and maintained at a fraction of the cost of classical antennas, such as rhombics and log periodics, with a performance which equals or exceeds that of these classical antennas. Detailed measurements need to be made to verify that the power gains which have been predicted in this report can be realized

in practice.   If one considers the savings in capital expenditures that could
be realized by agencies using Beverage antennas rather than classical antenna ,
in long range circuit applications, and the relatively modest resources
required to have these tests performed, one is forced to acknowledge with the
validity of this recommendation.

   B.   Extensive measurements should be made of a Beverage antenna's power
gain and radiation pattern using the RE'LEDOP techniques.

   Effort and resources dedicated to obtaining detailed radiation
pattern measurements are justified, even at this stage in the development of
the Beverage antenna, to determine the degree to which their measured patterns
depart from the theoretical model.   The description of the Beverage antenna
in terms of measurements is not yet as complete as is the theoretical model
of the antenna.   Future applications of this antenna as adaptive radar antennas
and direction finding antennas are likely to require detailed knowledge of
its radiation patterns.   It will be particularly important to discover to
what extent wide aperture linear arrays, for example, are degraded by in-
homogeneous ground and also to determine the limitation imposed by a Beverage
antenna's environment on the beam shaping of wide aperture arrays.

   C.   A prototype HF direction finding Beverage array system should be
built, tested and referred to industry for further development.

   Once again economic consideration come to the fore as justification
for further work in this area.   Existing high frequency direction finding
systems are extremely expensive due largely to their antennas and goniometers.
As a consequence they are used only where large expenditures can be justified.
An inexpensive HFDF system is likely to find fairly widespread application in
areas where large initial capital expenditures are not justified, such as;

   - tracking of radio buoys at sea to measure ocean currents,

   - radio tracking of oil spills at sea,

   - regulatory location of transmitters,

   - measurement of variations in angle of arrival of HF signals for
     scientific purposes,

   - portable HFDF system for gathering of intelligence,

   - systems requiring multiple, automated DF stations.

6.   ACKNOWLEDGEMENTS

7. REFERENCES

1. Beverage, H.H., C.W. Rice and E.W. Rellogg, *The Wave Antenna, a New Type of Highly Directive Antenna,* Trans. A.I.E.E., Vol. 42, February 1923.

2. Travers, D.N, P.E. Martin and W.M. Sherrill, *Use of the Beverage Antenna in Wide Aperture High Frequency Direction Finding (Part IV: Theory),* Interim Report for Contract NObsr-89345, Southwest Research Institute, 23 March 1964.

3. Martin, P.E., D.N. Travers and R. Lorenz, *Circular Arrays* of *Beverage Antennas* for *High Frequency Radio Direction Finding,* Paper submitted for Technical Program Southwestern IEEE, April 1965.

4. Terman, F.E., Electronic and Radio Engineering, McGraw-Hill Book Company, Inc., New York, 1955.

5. Ramo, S., J.R. Whinnery and T. Van Duzer, *Fields and Waves in Communication Electronics,* John Wiley & Sons, Inc., New York, 1967.

6. Litva, J. and E.E. Stevens, *Performance and Evaluation of the Cambridge Bay Beverage Array,* Proceedings of the OHD Technical Review Meeting, May 2-3, 1975, Colorado Springs, Colorado, 1973.

7. Jenkins, R.W. and E.L. Hagg, *Final Report on the Canadian Polar Cap 3 Experiment at Cambridge Bay, N.W.T.,* CRC Report No. 1975.

8. Litva, J. and E.E. Stevens, *Rapid Azimuthal Determination* of *Radio Signals,* CRC 1340-144, Patent Pending, 30 January 1975.

9. DeSantis, C.M., D.V. Campbell and F. Schwering, *An Array Technique for Reducing Ground Losses in thi HF Range,* IEEE Trans. on Ants. and Prop., Vol. AP-21, No. 6, November 1973.

10. Herlitz, Ivan, *Appendix B, Analysis* of *Action* of *Wave Antennas,* An Appendix to the paper by Beverage, Rice, and Kellog, *The Wave Antenna, a New Type of Highly Directive Antenna),* Transactions of the American Institute of Electrical Engineers, Volume 42, 1923, pp. 260-266.

11. Skilling, H.H., *Electric Transmission Lines,* McGraw-Hill Book Company, Inc., 1951.

12. The Royal Signals Handbook of Line Communication, Vol. 1, 1947, Seventh Impression 1964, p. 747.

13. Ramo Winnery Van Duzer, op. cit., **p.** 17.

14. Kraus, J.D., *Antennas,* McGraw-Hill Book Company, Inc., 1950, p. 53.

15. Stratton, J.A., *Electromagnetic Theory,* McGraw-Hill, New York, 1941, Secs. 9.4 and 9.9.

16. Feldman, C.B., *The Optical Behaviour of the Ground for Short Radio Waves,* Proceedings of the I.R.E., Vol. 21, No. 6, June 1933, pp. 764-801.

46

17. Carson, .R., *Wave Propagation in Overhead Wire with Ground Return,* Bell, Systems Technical Journal, Vol. 5, 1926, pp. 539–554.

18. Wise, W.H., *Propagation of High Frequency Currents in Ground Return Circuits,* Proceedings of the Institute of Radio Engineers, Vol. 22, April 1934, pp. 5221527.

19. Kraus, op. cit., pp. 76–77.

20. Kraus, ibid, p. 66.

21. Orr, William, Herbert G. Johnson VHF Handbook 1956 pp. 90–97.

22. Gold, Bernard and Charles M. Rader, *Digital Processing of Signals,* McGraw Hill Book Company, 1969, pp. 162–164.

23. Gilchrist, A.W.R., *The Use and Properties of Window Functions in Spectrum Analysis,* CRC Report No. 1221, November 1971, Ottawa.

24. Taylor, T.T., *Design of Line-Source Antennas for Narrow Beamwidth and Low Sidelobes,* IRE Transactions on Antenna Propagation, Volume AP-3, Number 1, January 1955, pp. 16–28.

25. Ross, W., E.N. Bramley, and G.E. Ashwell, *A Phase-Comparison Method of Measuring the Direction of Arrival of Ionospheric Radio Waves,* Proc. I.E.E., 1951, 98, Pt. 111, p. 294.
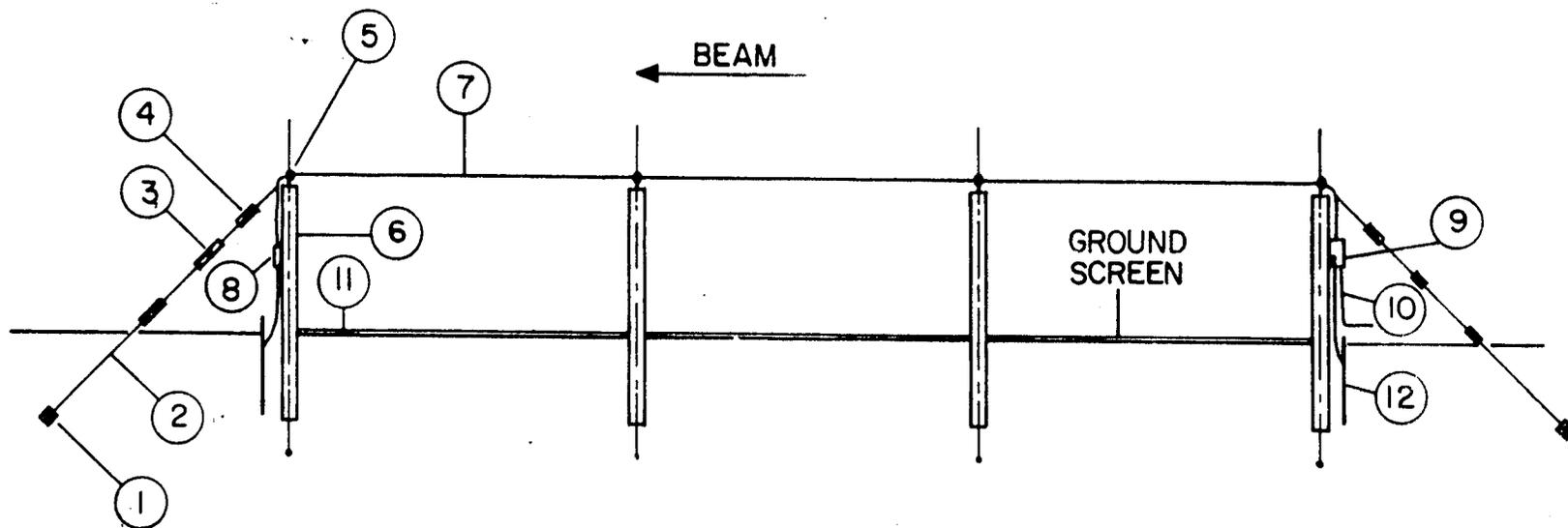
① ANCHOR	⑤ INSULATOR WET TYPE	⑨ TRANSFORMER, MATCHING 400/50
② ROD ANCHOR	⑥ POST CEDAR	⑩ CABLE RF
③ TURN BUCKLE	⑦ ANTENNA WIRE, STRANDED AWG 14	⑪ GROUND SCREENS
④ INSULATOR STRAIN	⑧ RESISTOR	⑫ GROUND ROD

Figure 1. .Components of an H F Beverage antenna. Typically the height above ground is 1 to 2 metres and the length is 100 to 150 metres.

47

Figure 2. Cambridge Bay antenna site showing the location of three antennas, linear phased array, rosette array and monopole antenna. Field intensity measurements were made on the dashed circle, whose radius is 610 m, at increments of $15°$ of azimuth.
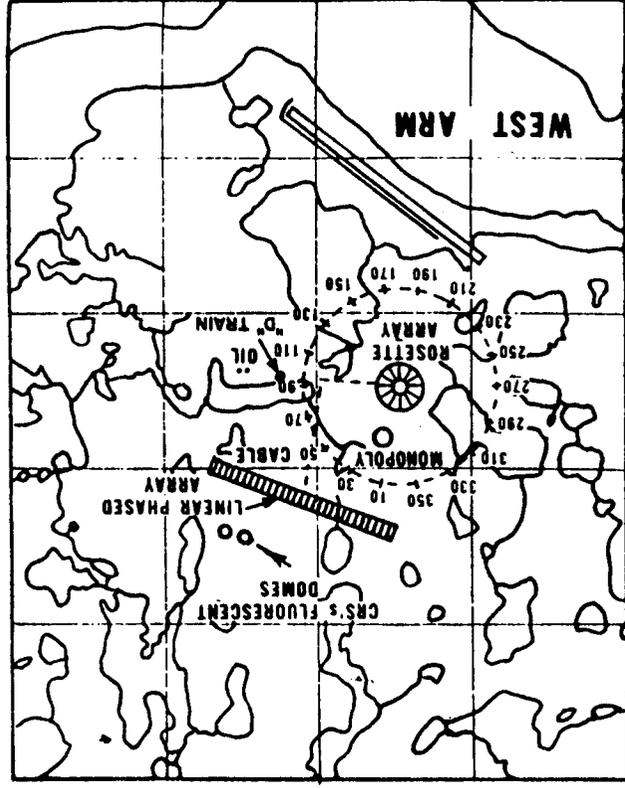
Figure 3. Same as Figure 2, except that the location of the test monopole is displaced by 300 m to the northeast. The dashed circle now defines the outer extent of the first Fresnel region for radio waves radiated by the monopole with an elevation of angle of $12°$.
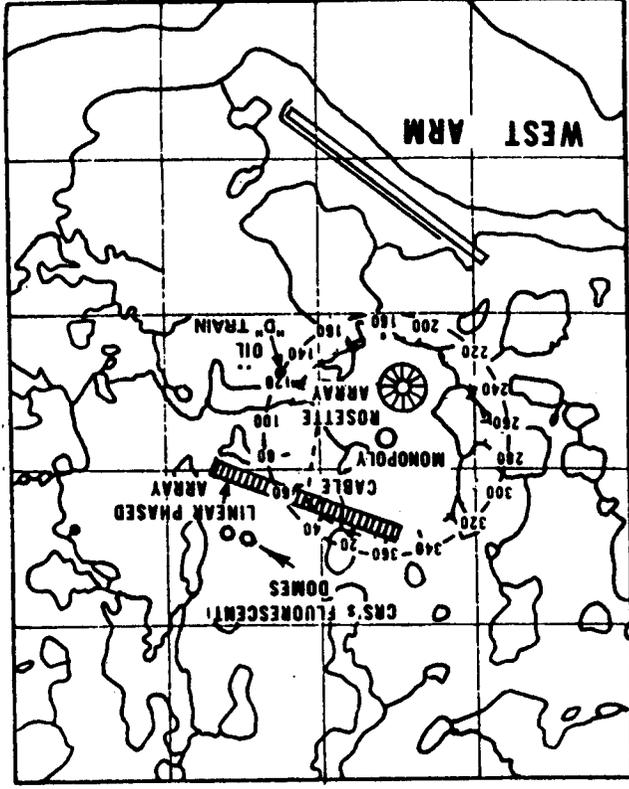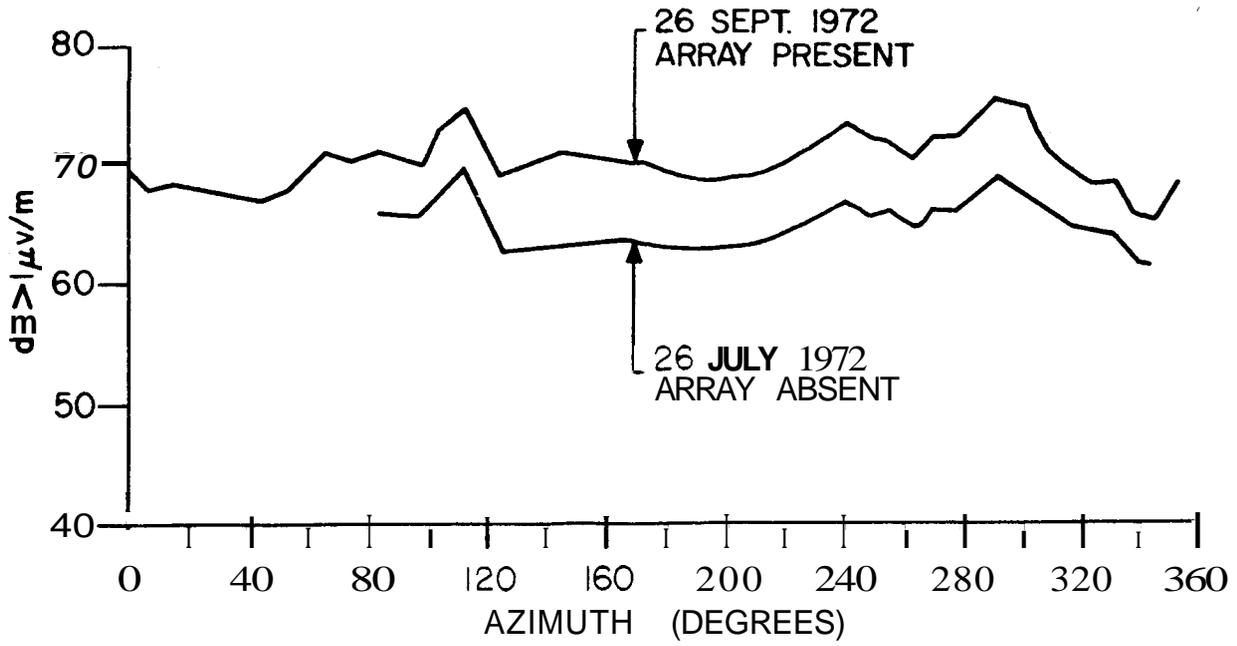
Figure 4. Field Intensity at a Distance **of** 610m vs. Azimuth from a Quarterwave Monopole at the Centre of the Array (U).
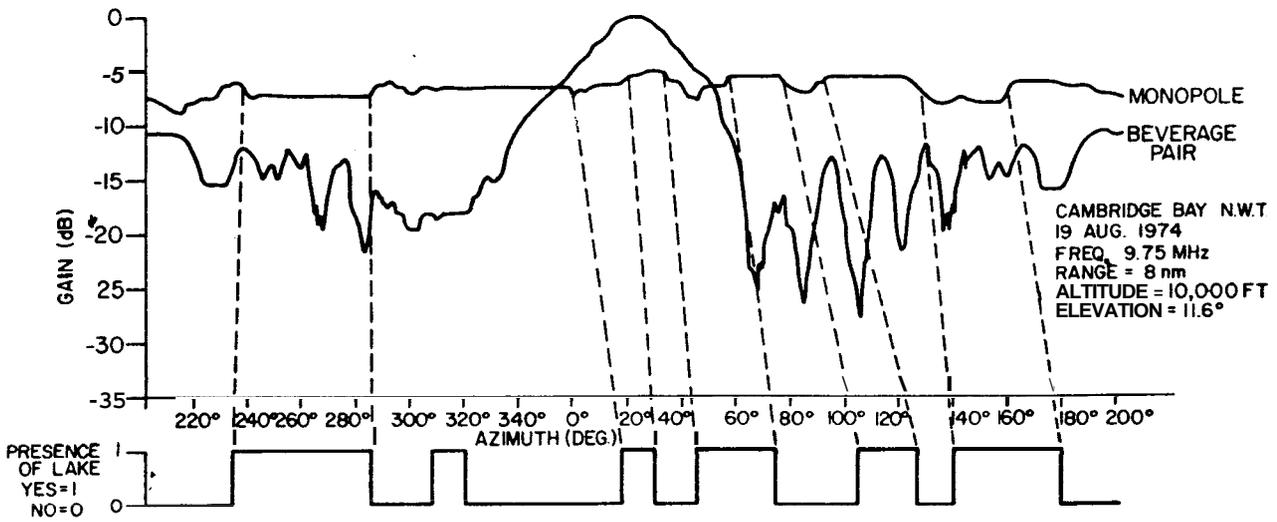
Figure 5. Relative Field Intensity Measured at a Range of 14.8km **from** a Monopole Antenna and Beverage Pair Antenna both Excited by a 9.75 MHz Transmitter.
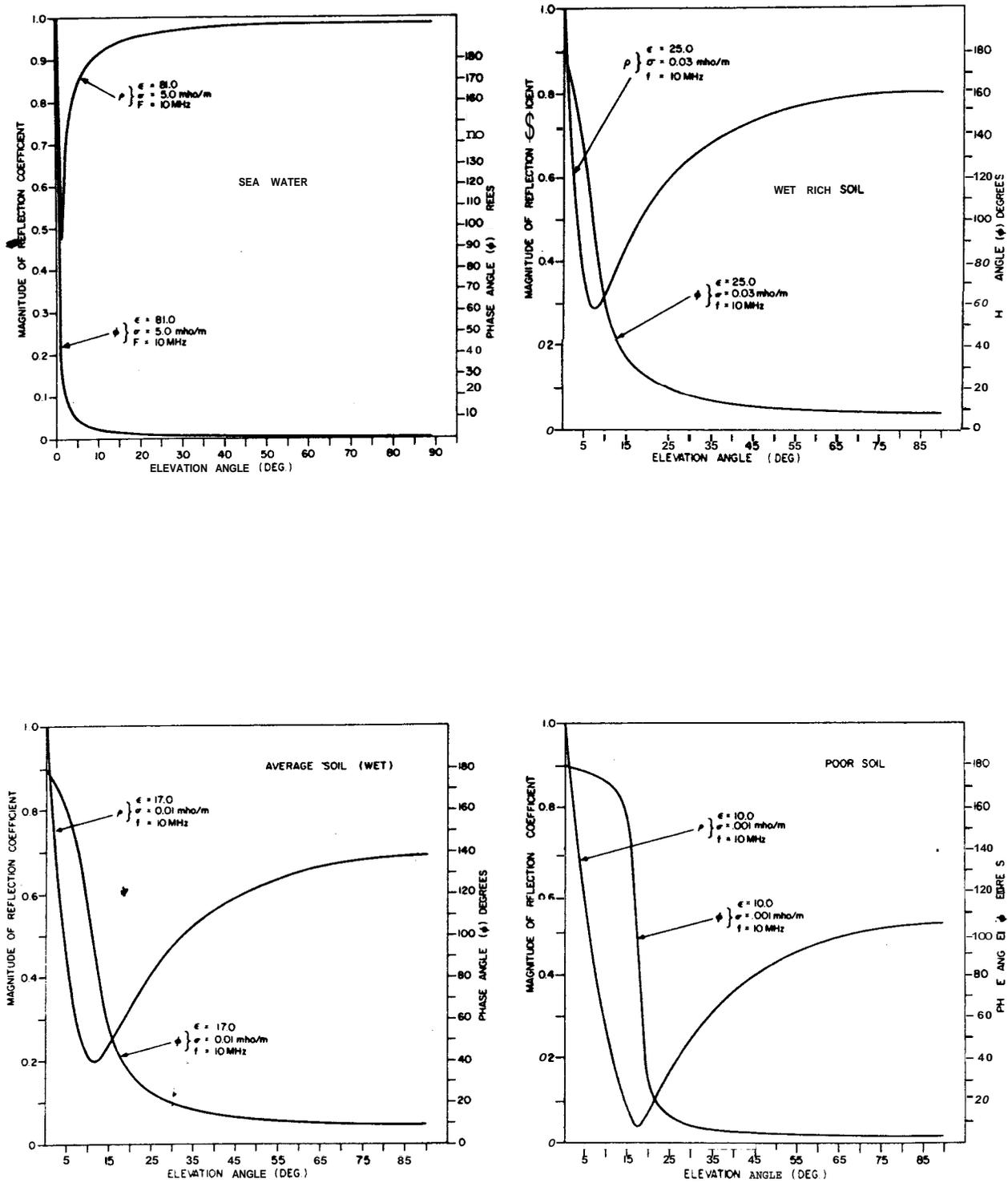
Figure 6. Reflection Coefficients at 10MHz for Sea Water, Wet Rich Soil, Average Soil (Wet) and Poor Soil.
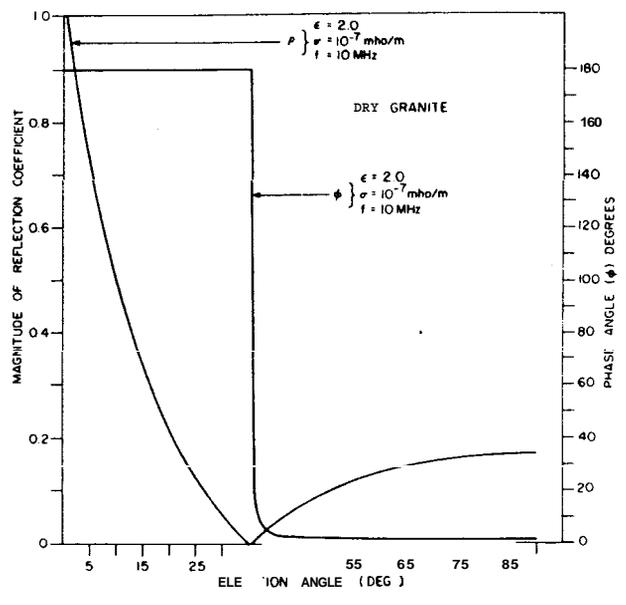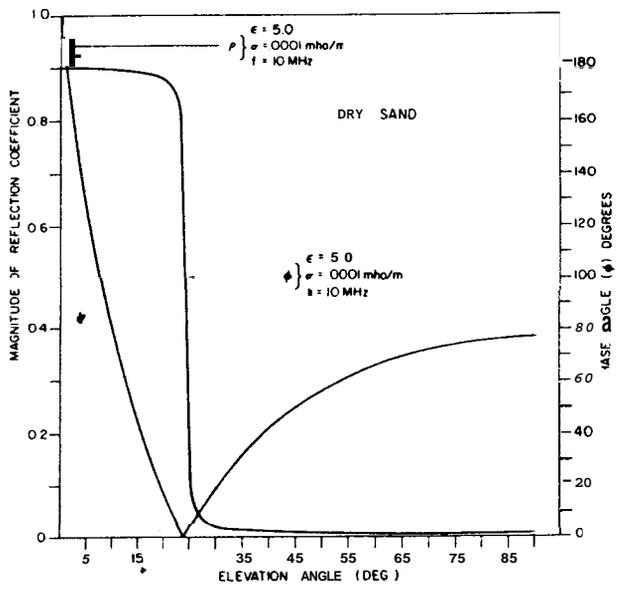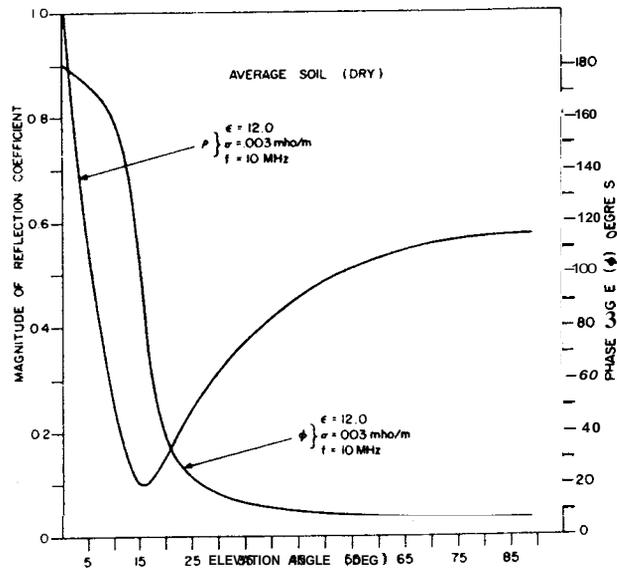
Figure 7. *Reflection Coefficients at 10 MHz for Average Soil (Dry), Dry Sand and Dry Granite.*
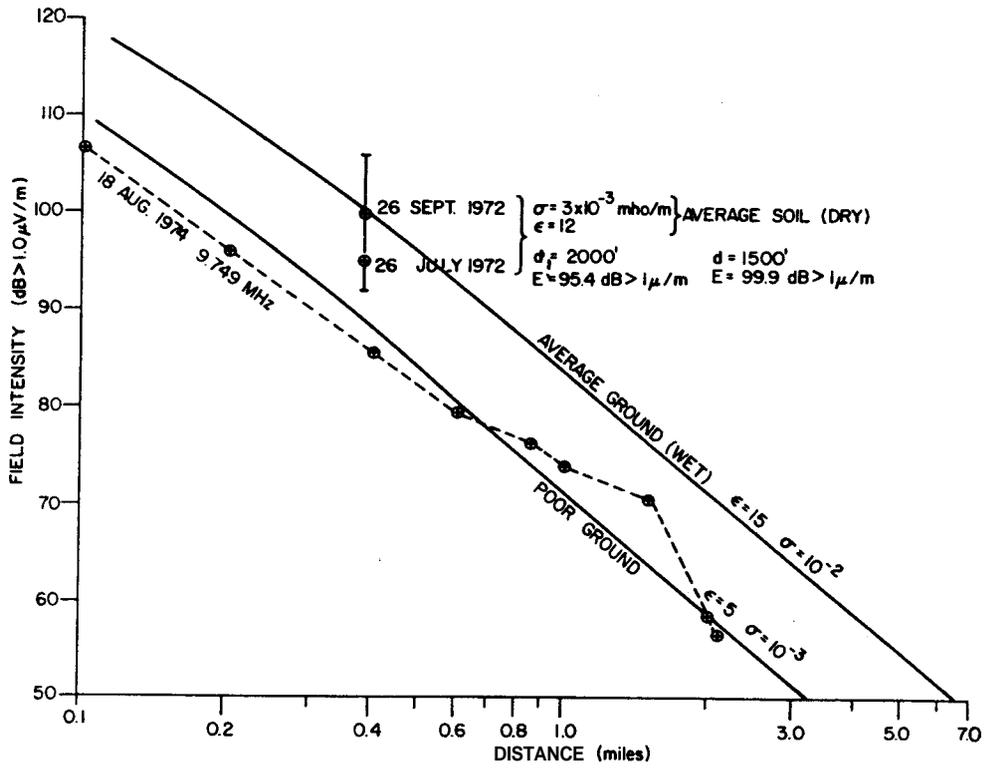
Figure 8. Measured field intensity from a λ/4 monopole antenna excited with a 9.75 MHz transmitter. Transmitter power has been normalized to 1 kw. Theoretical results are included and show fall off of field intensity with distance for average ground (wet) and poor ground.
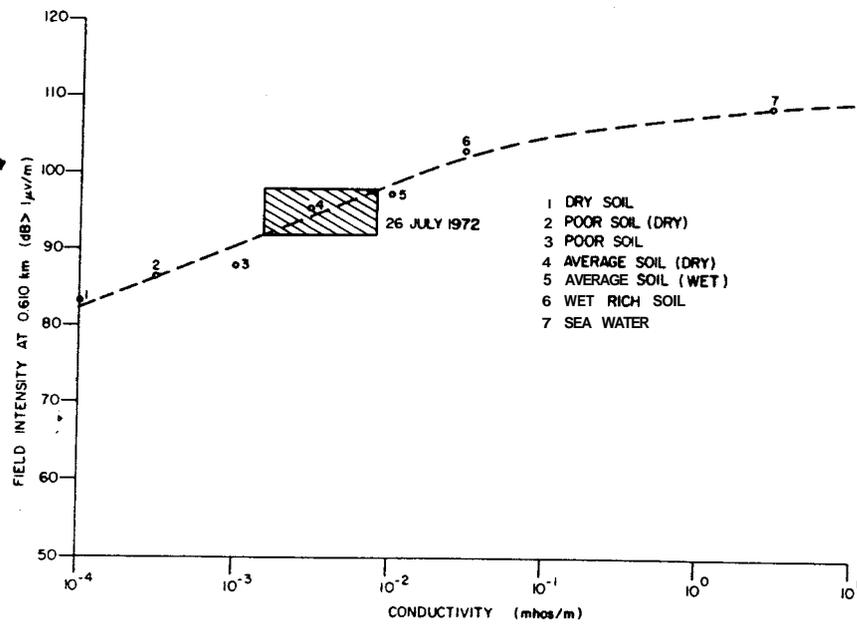
Figure 9. Comparison of field intensity measured at a distance of 0.610 km from position of the center of the rosette array with theoretical values for earth types varying from dry sand to sea water.
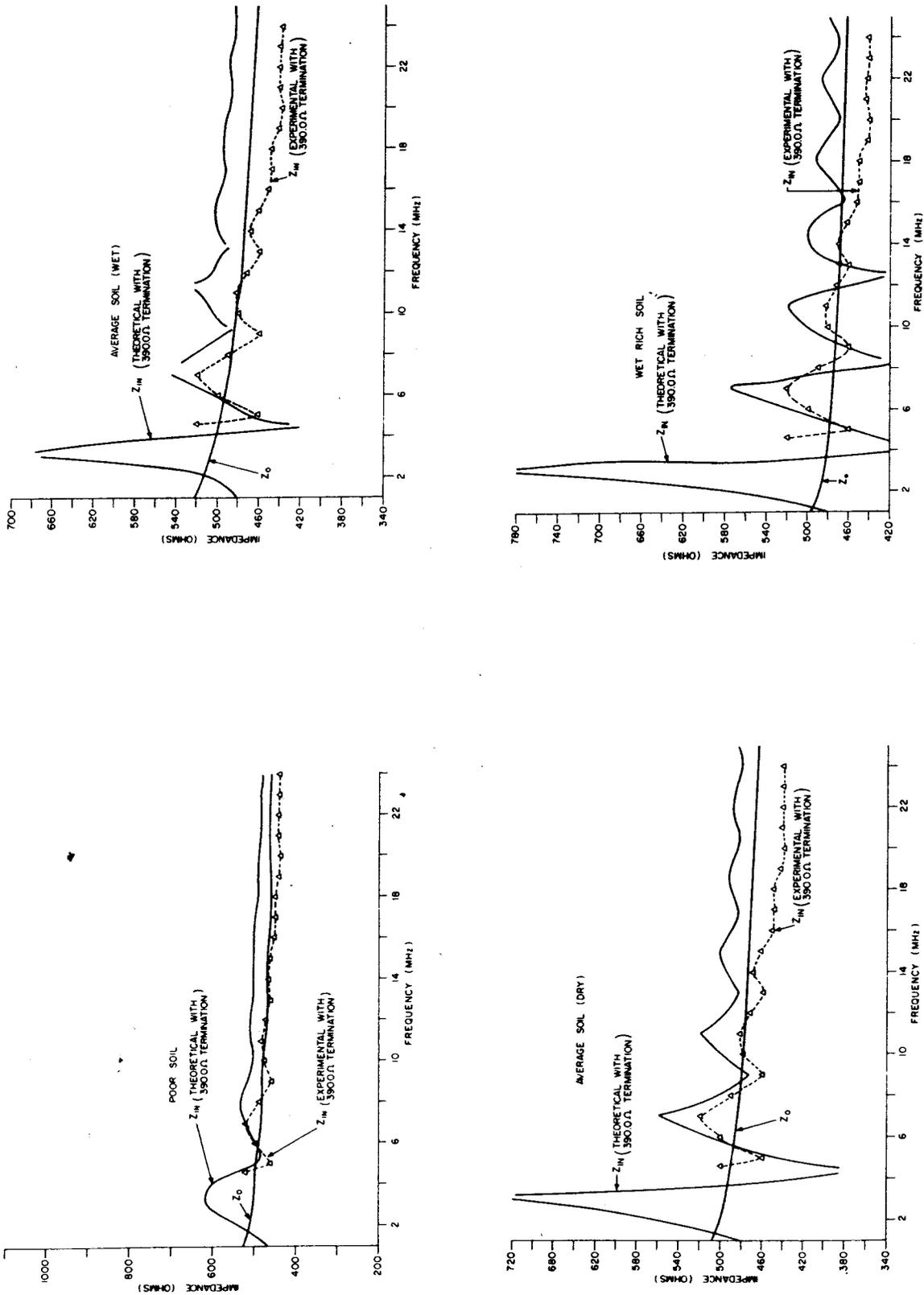
Figure 10. *Measured input impedance for a Beverage antenna with a height above ground of 1 meter terminated in 390 ohms. Theoretical curves are included for antennas terminated in 390 ohms and Z_0 over poor soil, average soil (dry), average soil (wet) and wet rich soil.*
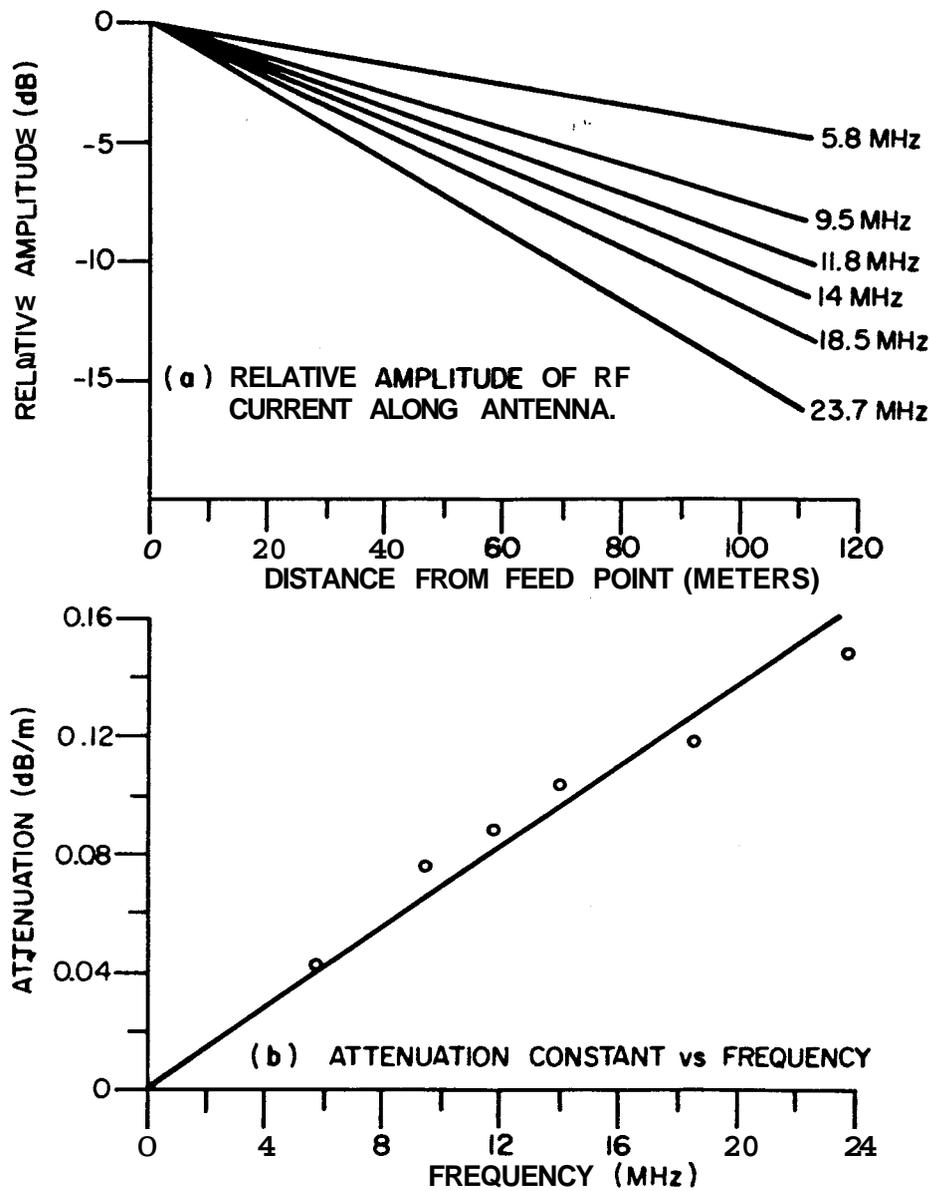
Figure 11. *Relative Amplitude and Attenuation Constant* vs. *Frequency for a Beverage Antenna.*
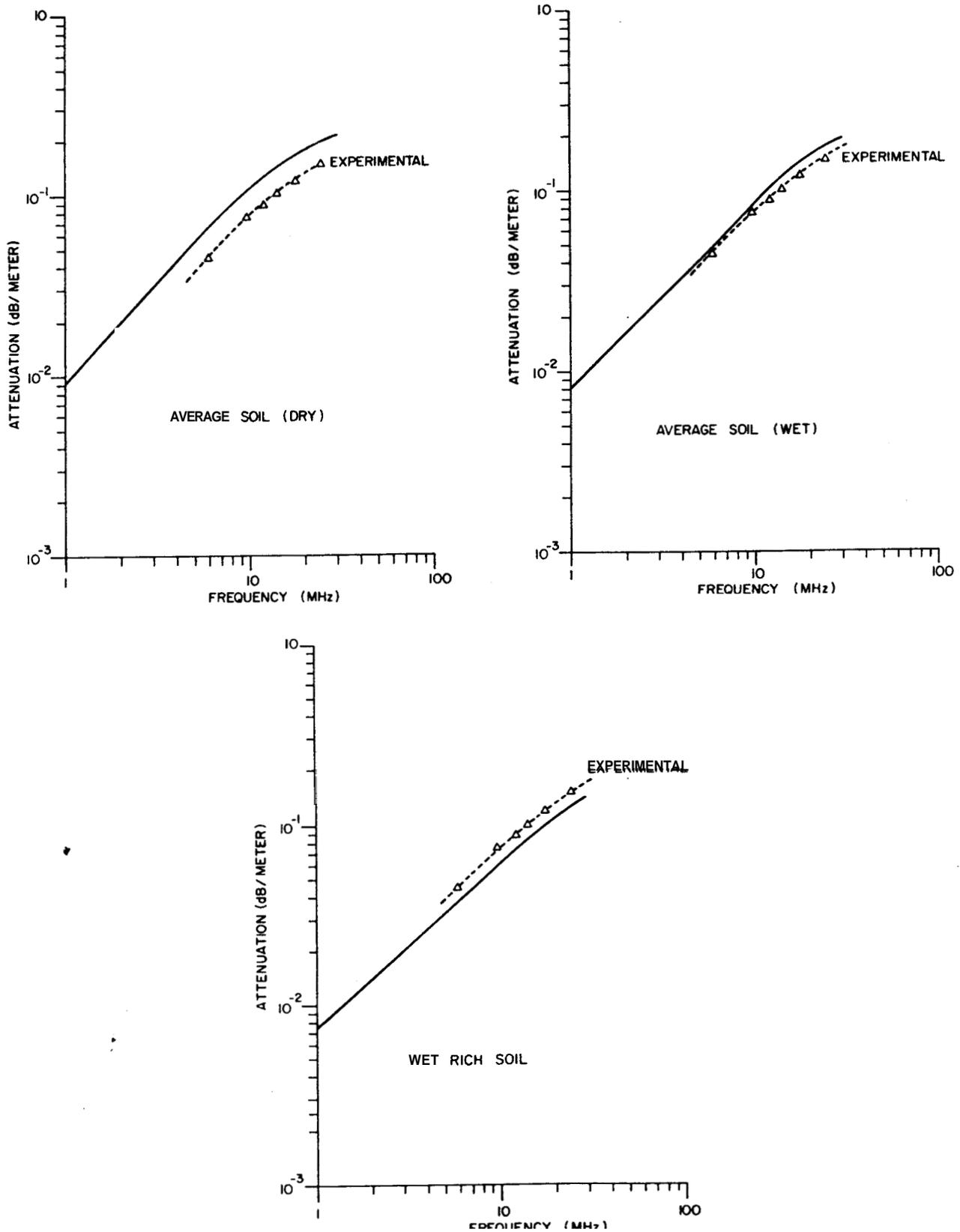
Figure 12. *Comparison* of experimental current-wove ottenuotion ot *Cambridge Boy and theoreticol current-wove ottenuotions for overoge soil (dry), average soil (wet) and wet rich soil.*

56

Figure 13. Displacement of Current-wave Null from Terminated End Versus Null Number for 5, 10, 15 and 20 MHz.
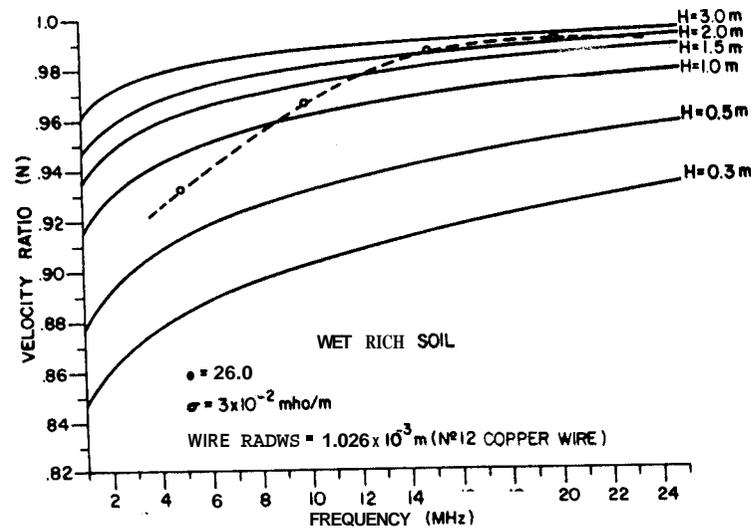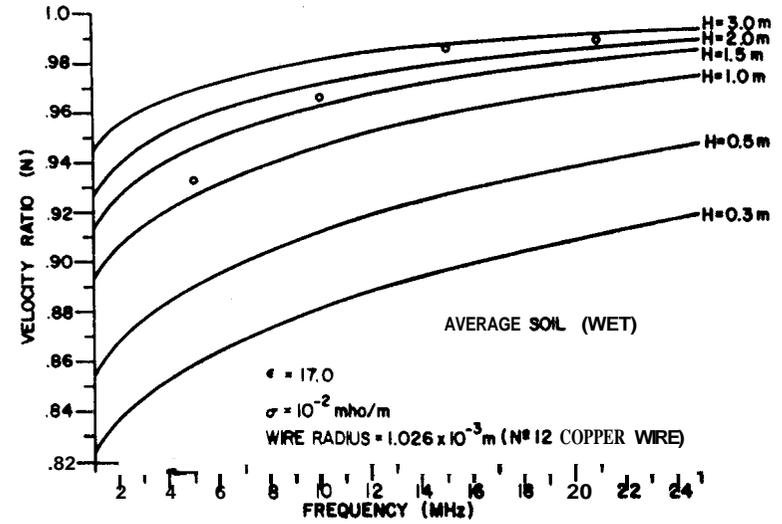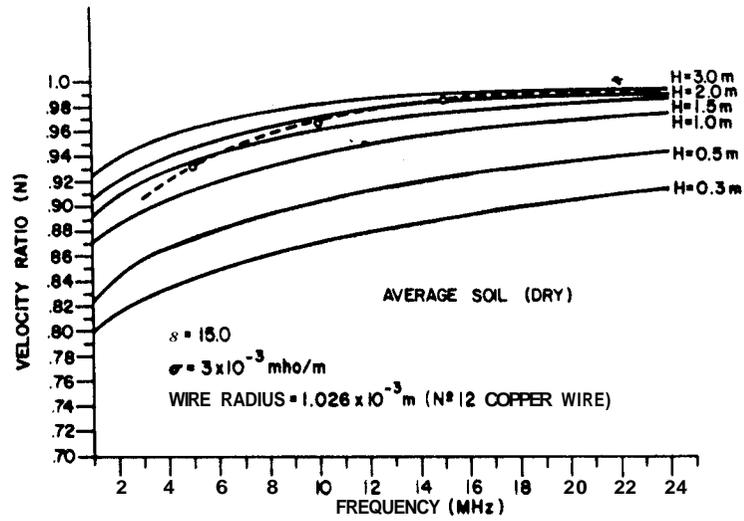
Figure 14. Comparison of theoretical and experimental values of the current-wave velocity factor as a function of frequency for average soil (dry), average soil (wet) and wet rich soil.
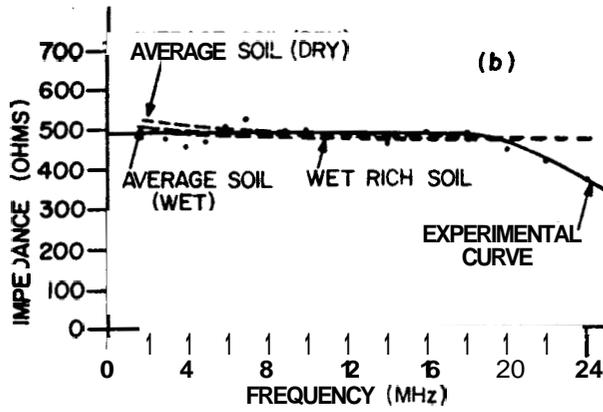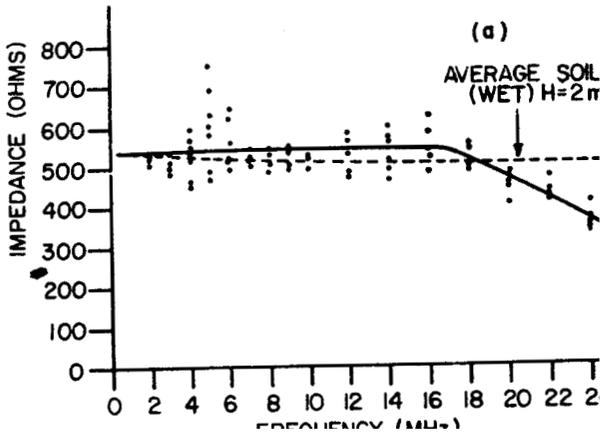
(a) Composite input impedance of 8-elements.

(b) Comparison of experimental and theoretical input impedance for element #1.
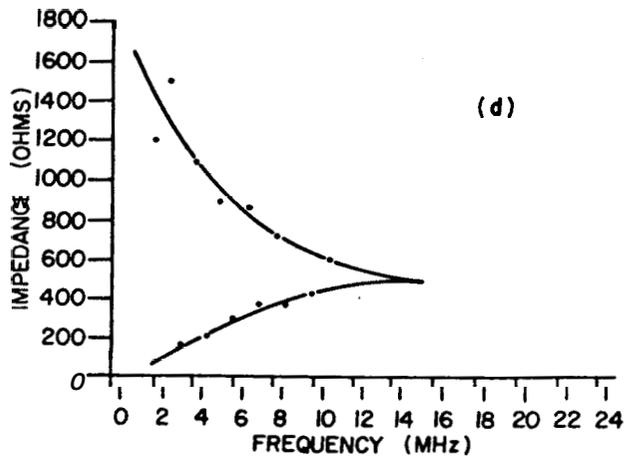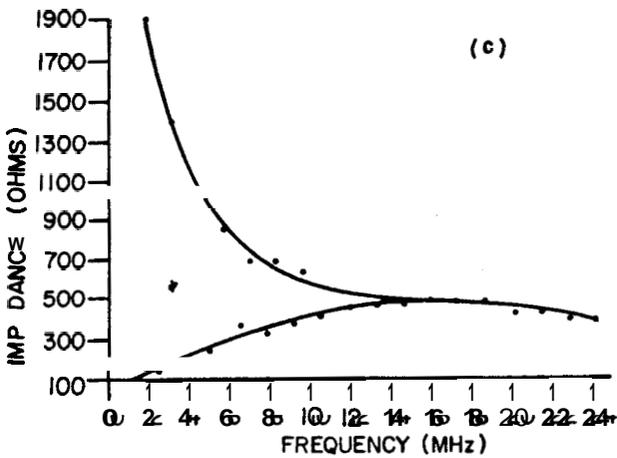
(c) Input impedance of element #1 terminated in a short circuit.

(d) Input impedance of element #1 terminated in an open circuit.

Figure 1: Debert Input Impedance Measurements on Beverage Antennas Terminated in an Open Circuit, a Short Circuit and the Antenna's Characteristic Impedance.
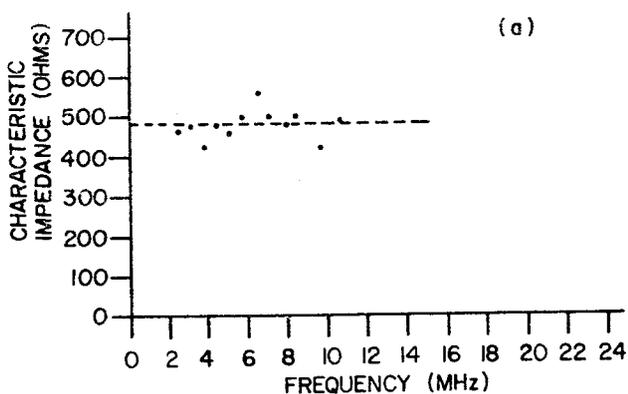
(a) Characteristic input impedance of element #1 derived from open and short circuit input impedance measurements.
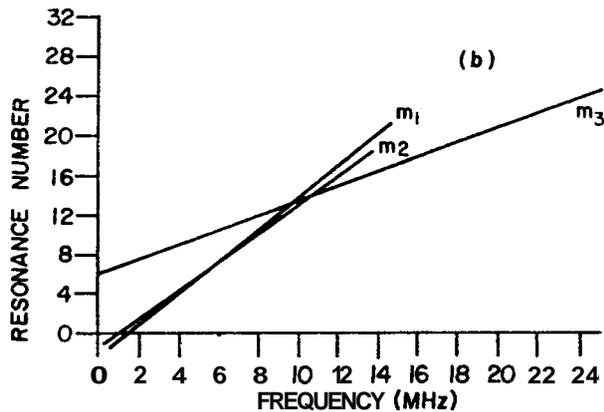
(b) Open and short circuit resonance number versus frequency.
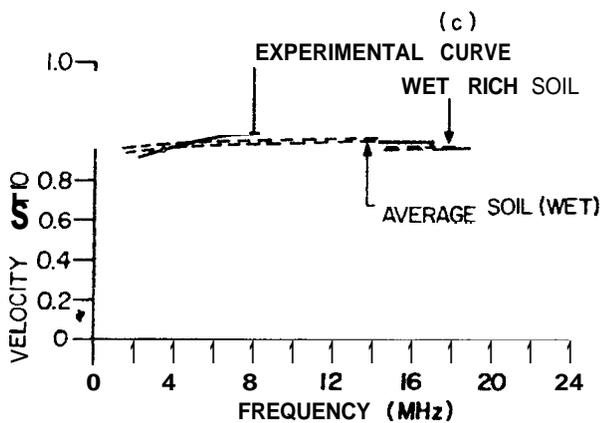
(c) Comparison of experimental and theoretical current-wave phase velocity for element #1.
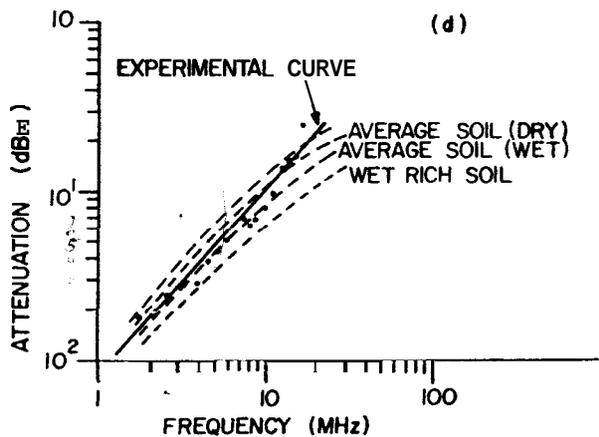
(d) Comparison of experimental and theoretical attenuation for element #I.

Figure 76. Debert Element #1 Measured Chorocteristic Impedance, Current-wove Phase Velocity and Comparison of Meosured Current-Wove Attenuation with Some Theoretical Curves
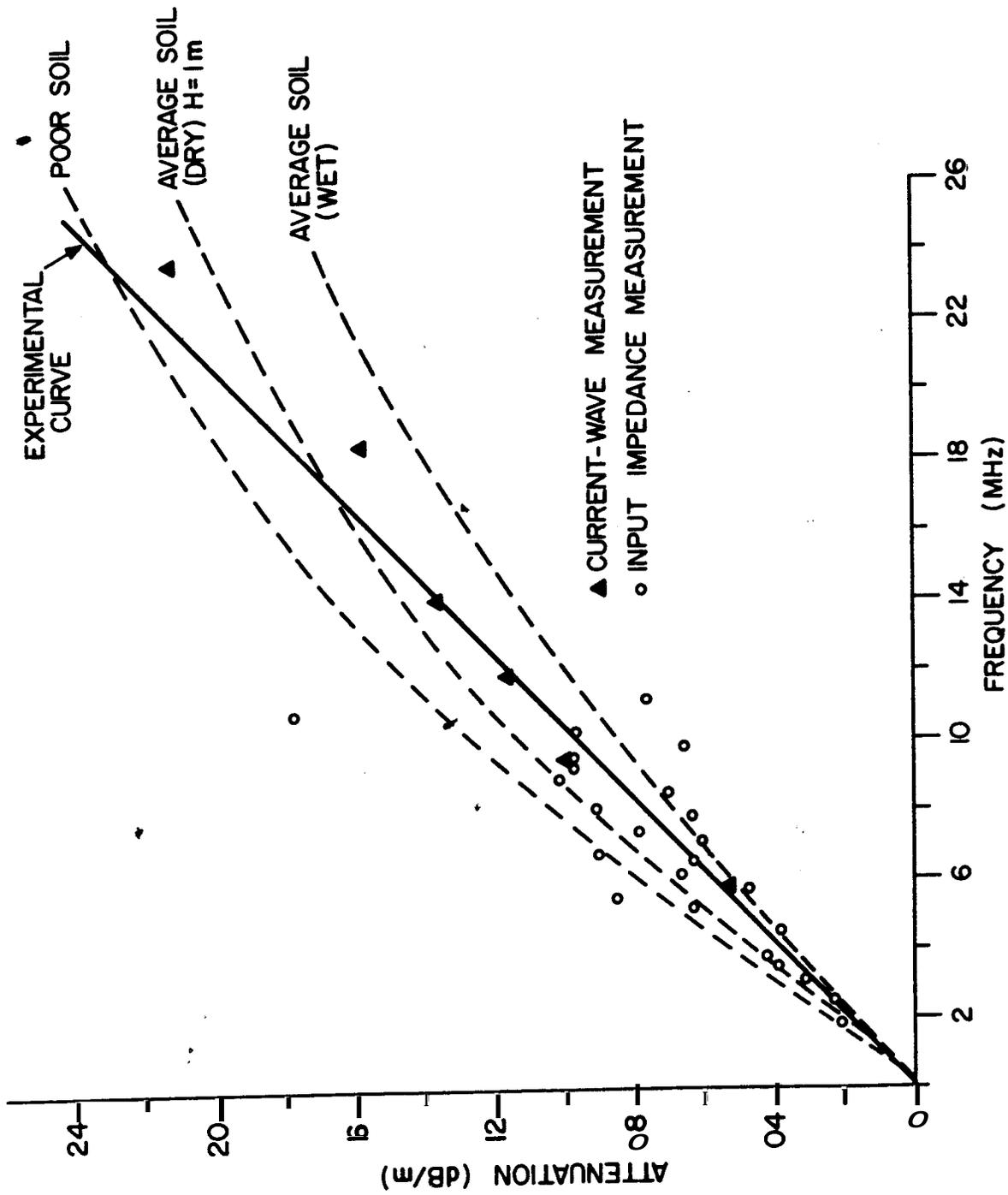
Figure 17. *Comparison of Theoretical and Measured Current-wave Attenuation on a Beverage Element at Shirley Bay, 110 m long and 1 m high.*
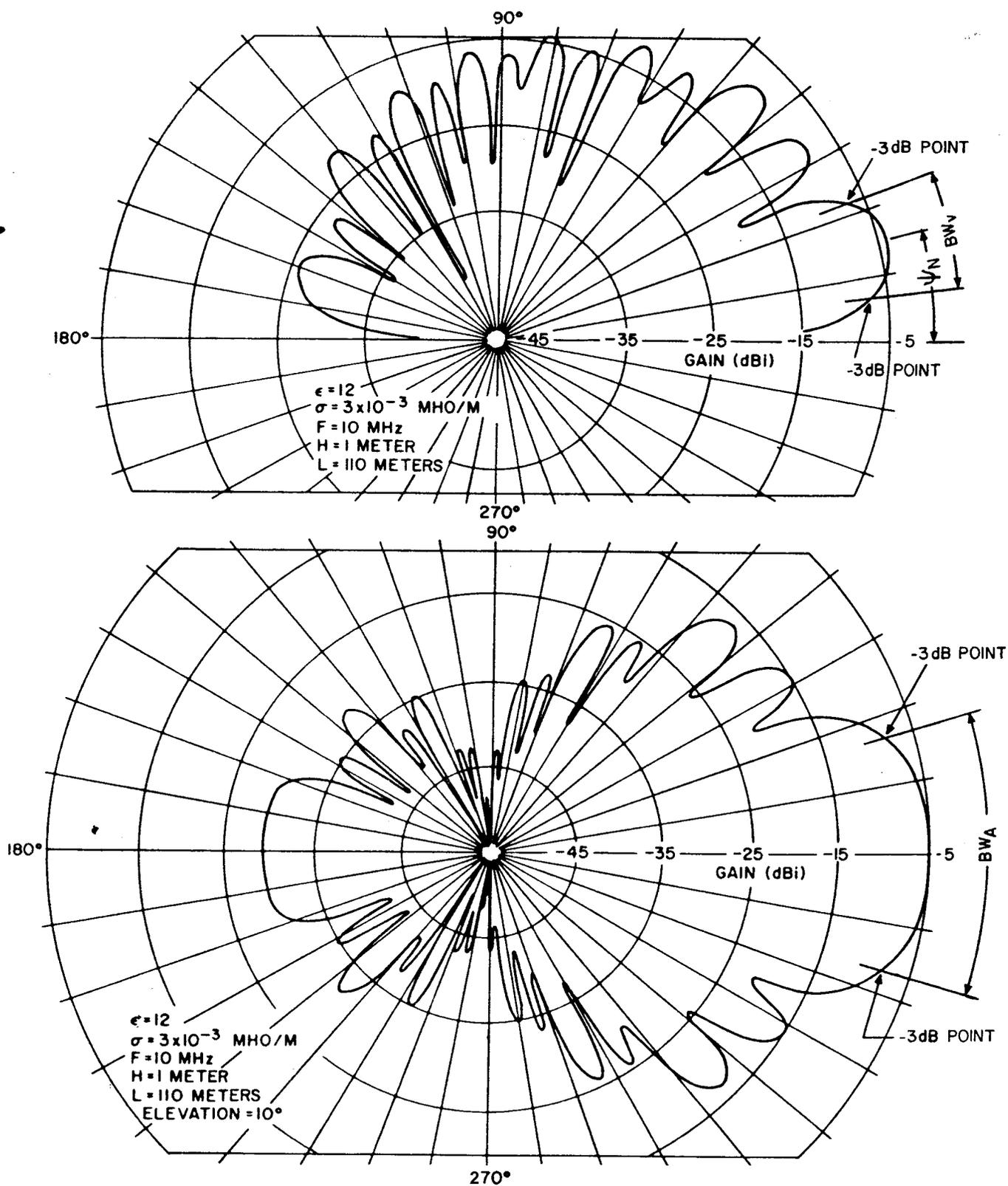
Figure 18. Typical theoretical elevation and azimuthal radiation patterns for a Beverage element situated over average soil (dry) and whose length and height are 110 m and 1 m, respectively. The 3-dB vertical beamwidth BW_V, take-off angle ψ_N, gain G_N and 3-dB azimuthal beamwidth BW_A as defined in Section 3.1 are illustrated.

62
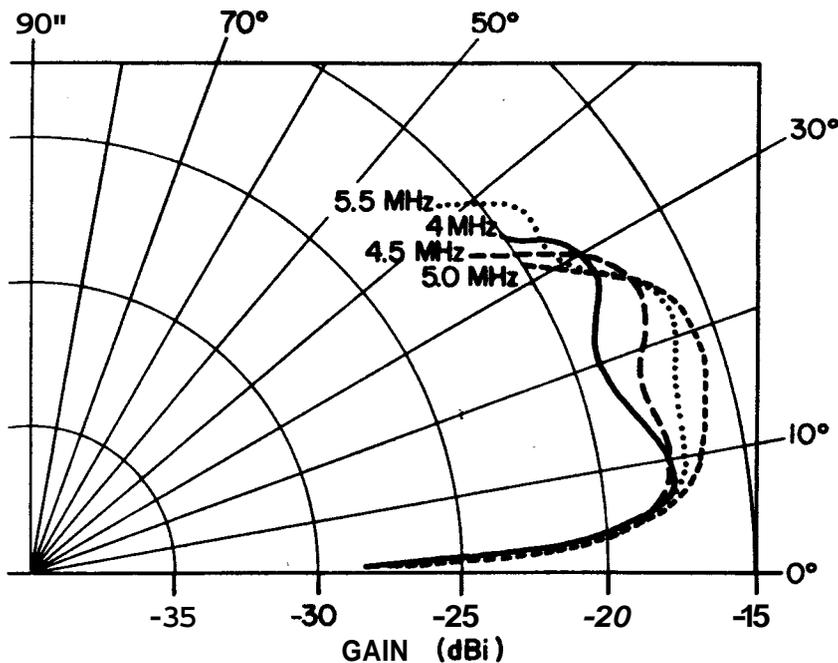
Figure 19. This diagram demonstrates the source of the discontinuities in Figs. 11-1 to 11-48. In particular, it shows that the discontinuities in Fig. 11-36 are caused by a secondary lobe growing in magnitude with increasing frequency and surpassing the main lobe.
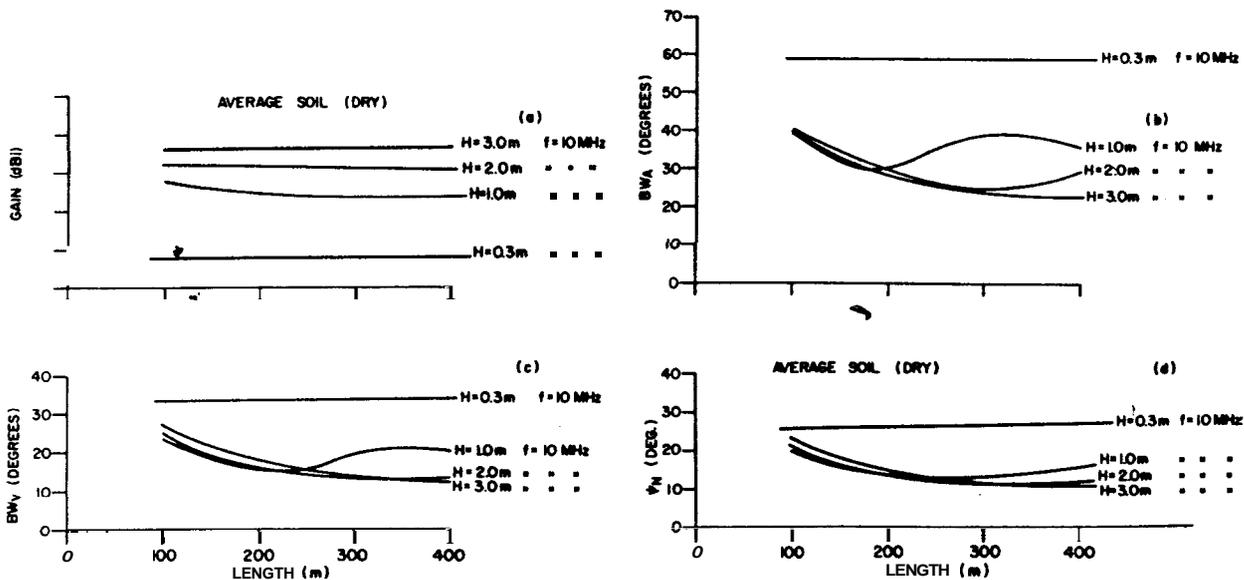
Figure 20. Gain, azimuthal beamwidth, vertical beamwidth and take-off angle of a Beverage antenna on average soil (dry) at 10MHz for lengths between 100 and 400 m and heights between 0.3 and 3.0 m.
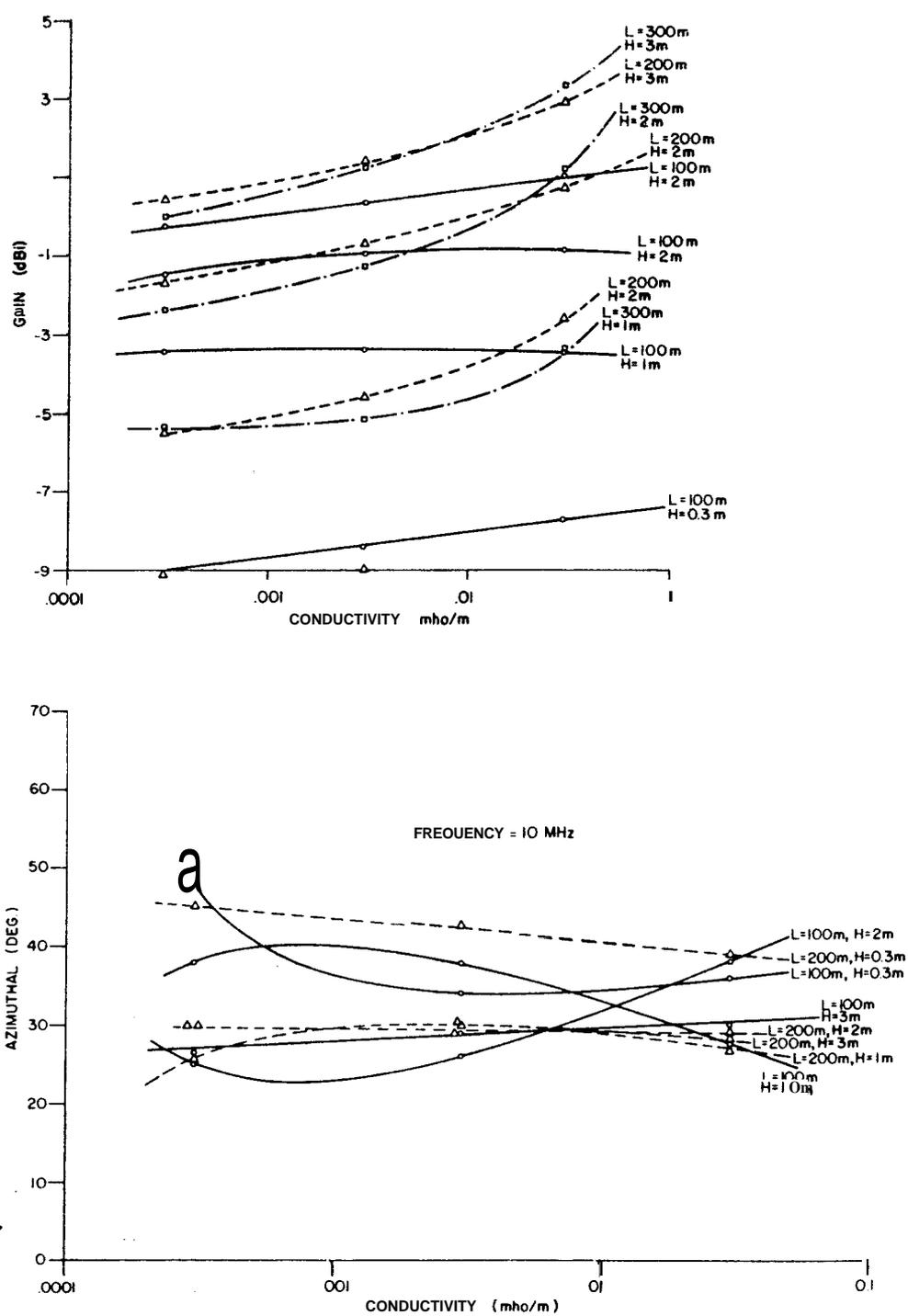
Figure 21. Gain, and azimuthal beamwidth of a Beverage antenna at 10 MHz as a function of soil conductivity, length and height.
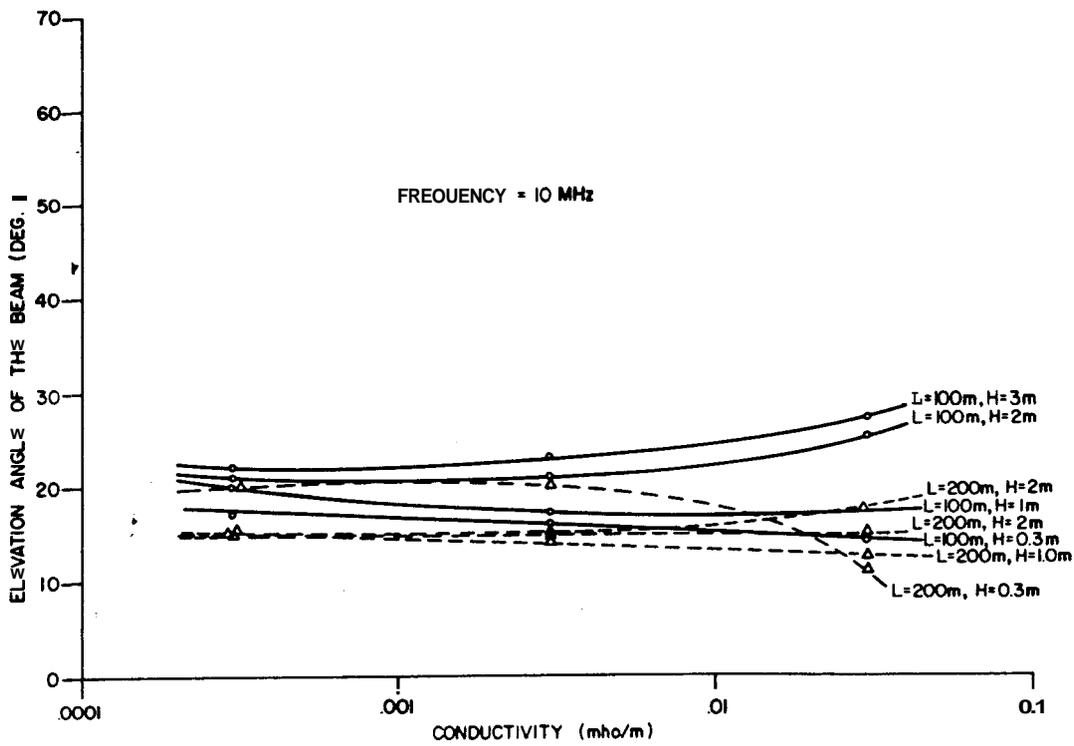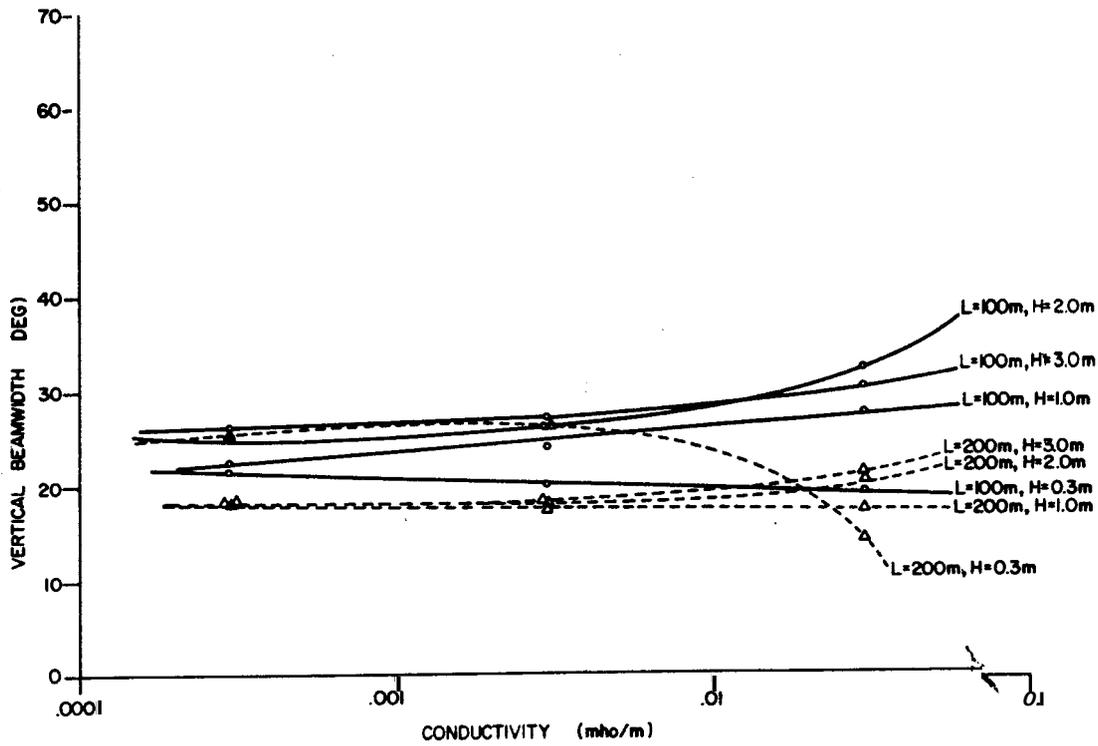
Figure 22. *Vertical Beamwidth and Take-off Angle of a Beverage Antenna at 10 MHz as a Function of Soil Conductivity, Length and Height.*
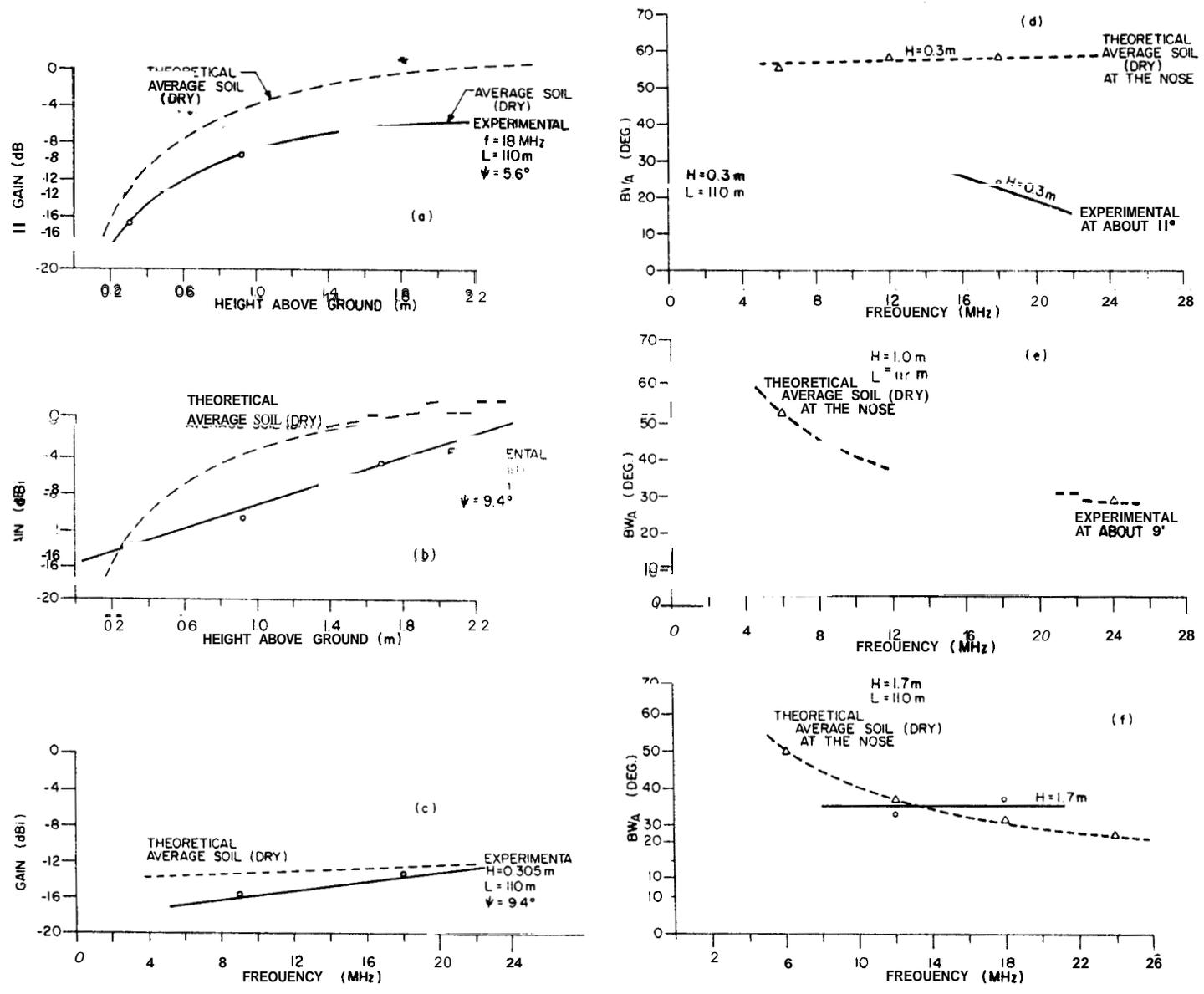
Figure 23. Comparison of Theoretical and Measured Values of Gain G_N and Azimuthal Beamwidth BW_A of a Beverage Antenna. The Measurements were made at Shirley Bay with the Antenna on Average Soil (Dry).
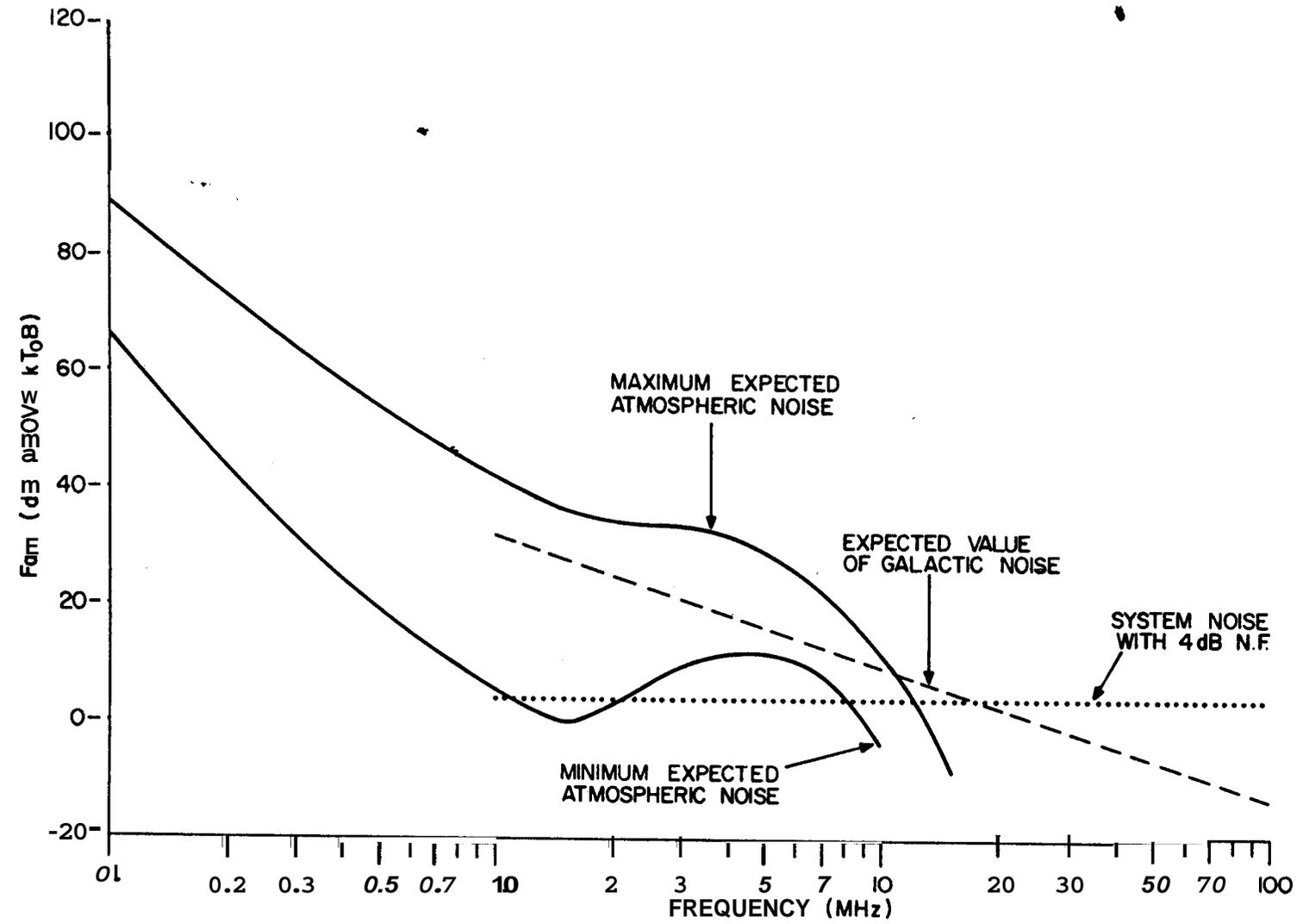
Fam = Median of the hourly values of Fa within a time block.

Fa = Effective antenna noise factor which results from the external noise power available from a loss-free antenna.

Figure 24. Variation of Radio Noise with Frequency for a Receiving Beverage Antenna. Noise Data was Obtained from CCIR Report 322.
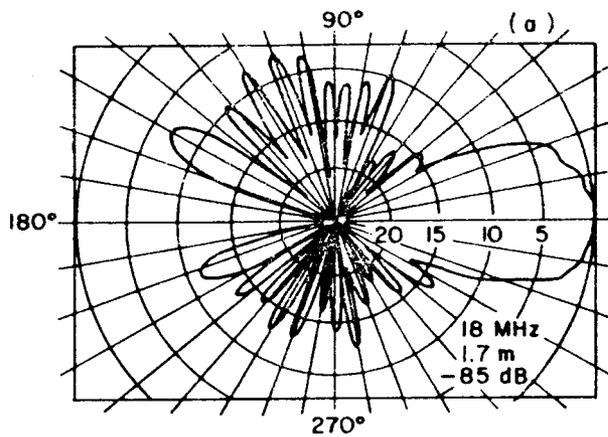
(a) Azimuthal pattern for Beverage antenna, L=110m, H=1.7m and f=18MHz.
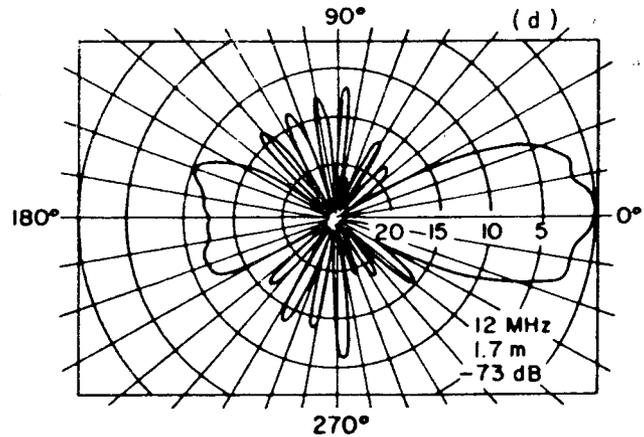
(d) Azimuthal pattern for Beverage antenna, L=110m, H=1.7m and f=12MHz.
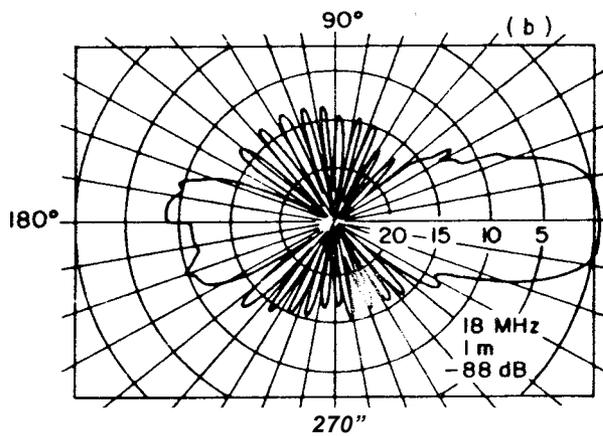
(b) Azimuthal pattern for Beverage antenna L=110m, H=0.9 and f=18MHz.
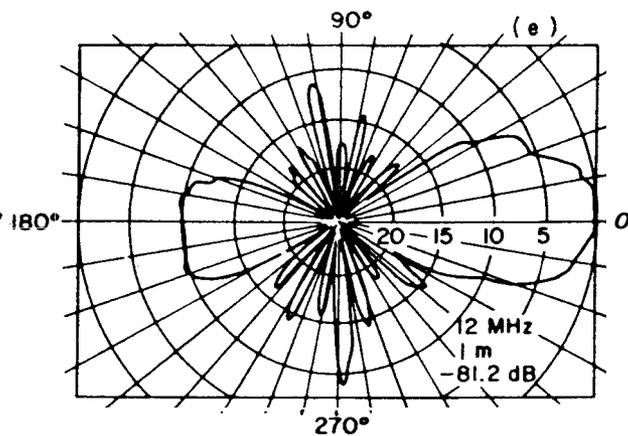
(e) Azimuthal pattern for Beverage antenna, L=110m, H=9.9m and f=12MHz.
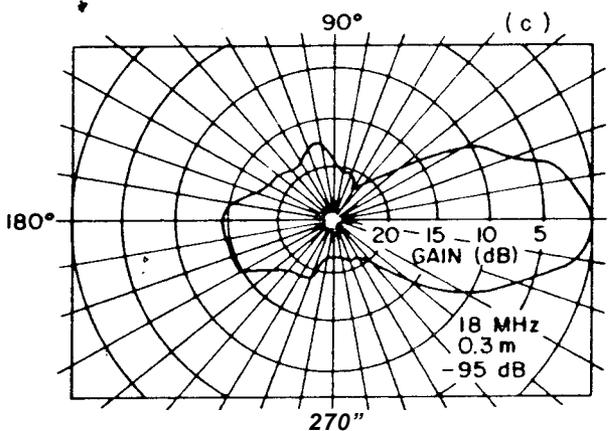
(c) Azimuthal pattern for Beverage antenna, L=110m, H=0.3m and f=18MHz.
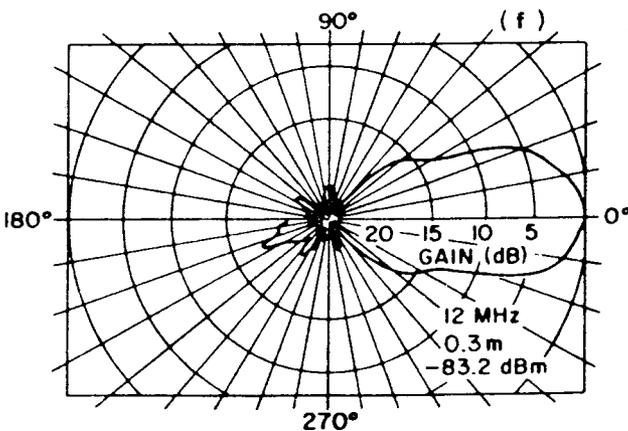
(f) Azimuthal pattern for Beverage antenna, L=110m, H=0.3m and f=12MHz.

Figure 25. Measured azimuthal radiation patterns of Beverage antennas for 12 and 18 MHz. The length of the antenna was 110 m and height was varied between 0.3 and 1.7 m.
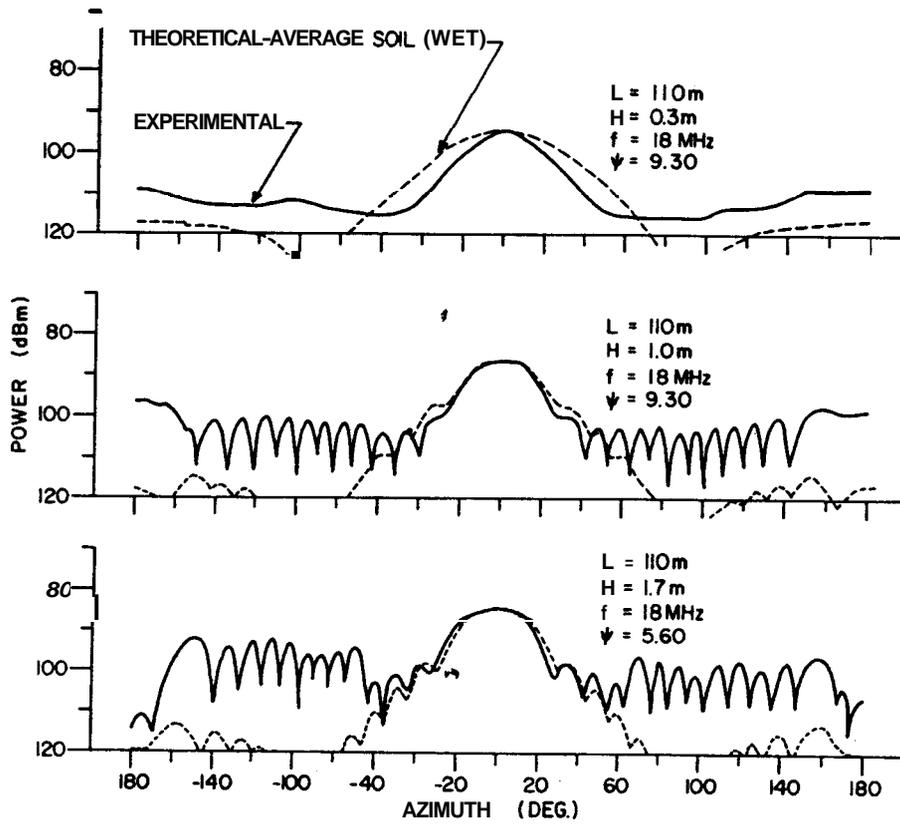
Figure 26. Comparison of theoretical and experimental patterns at 18 MHz for a Beverage antenna. The experimental patterns are those shown in polar form in Fig. 25 (a, b, c).
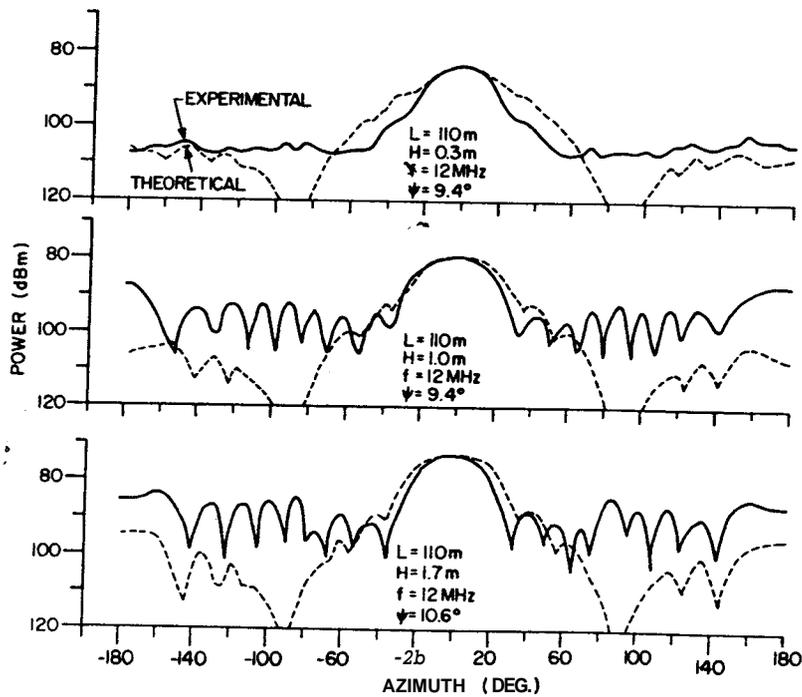
Figure 27. Comparison of theoretical and experimental patterns at 12 MHz for a Beverage antenna. The experimental patterns are those shown in polar form in Fig. 25 (d, e, f).
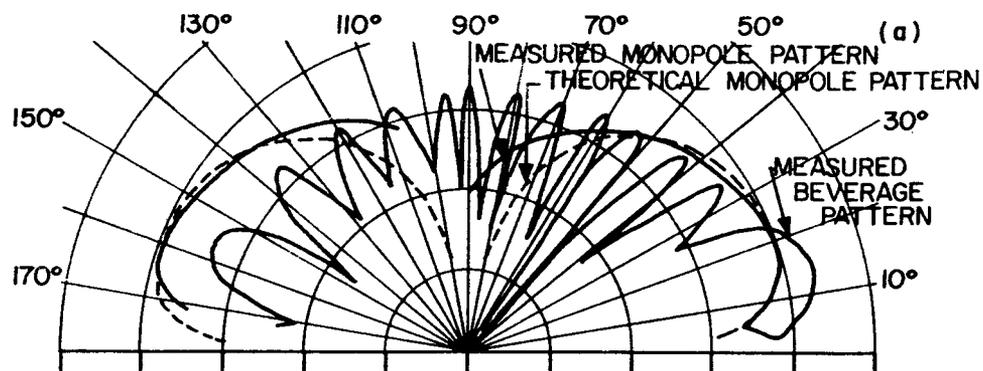
(a) The solid curves give the measured vertical radiation patterns for Beverage and $\lambda/4$ monopole antennas obtained with a horizontally polarized XELEDOP. The dashed curve gives the theoretical pattern for a $\lambda/4$ monopole antenna.
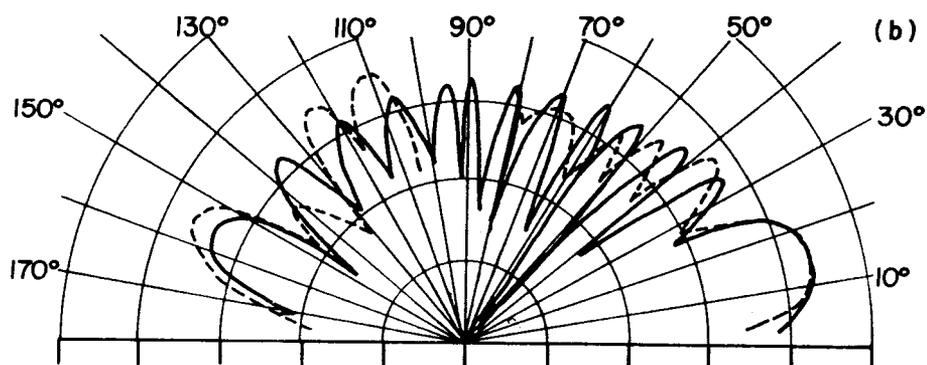
(b) Comparison of measured vertical radiation patterns for a Beverage antenna obtained with horizontally and vertically polarized XELEDOPs.
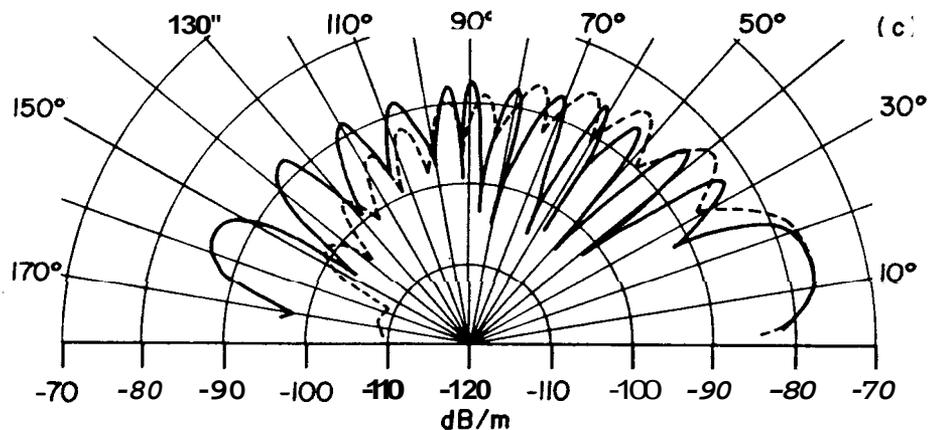
(c) Comparison of measured and theoretical vertical radiation patterns for a Beverage antenna.

figure 28. Comparison of theoretical and measured vertical radiation for a Beverage antenna at 78 MHz. The measurements were made at Shirley Bay on a Beverage antenna whose length was 110 m and height was 1.7 m.
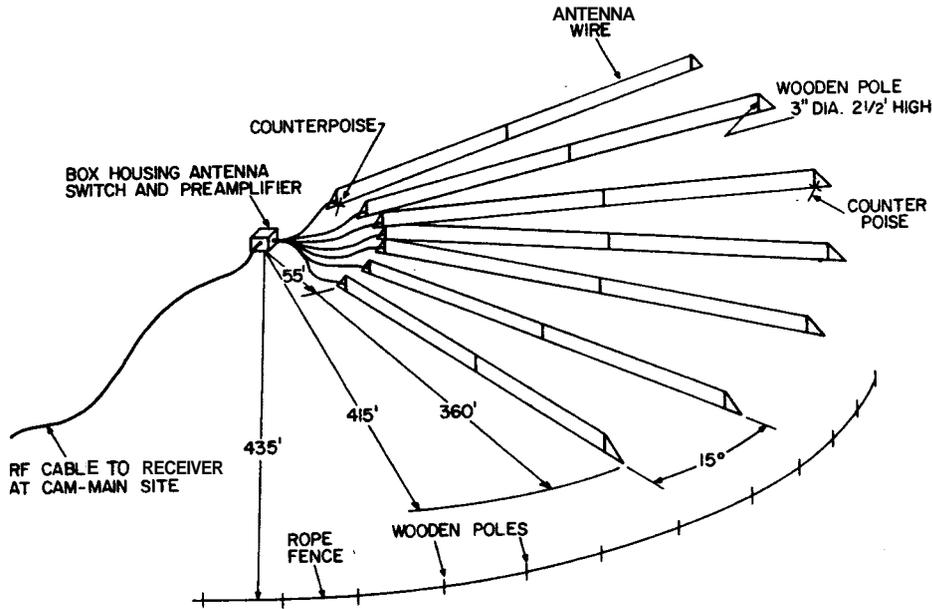
Figure 29. A Portion of the Beverage Rosette Array.
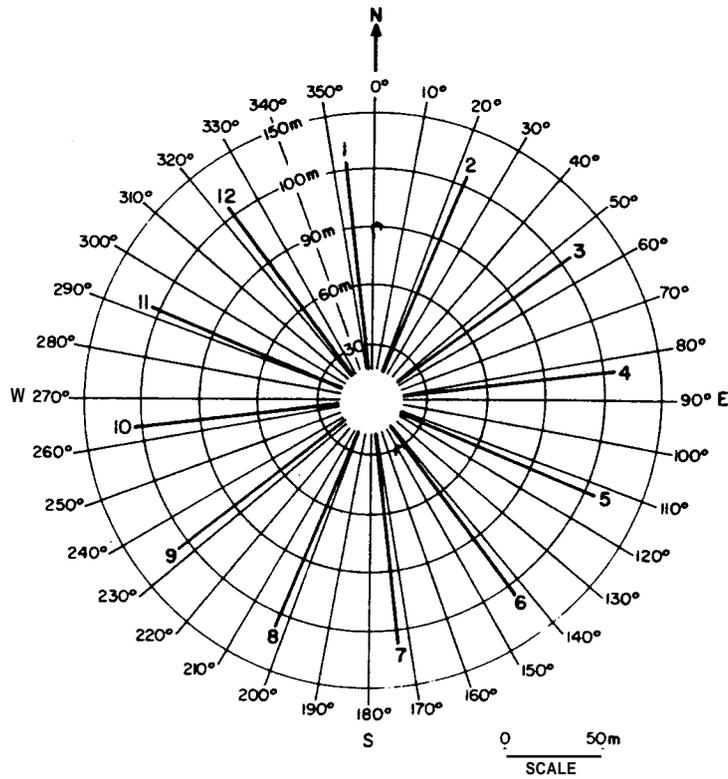
Figure 30. Modified Plan View of the Beverage Antenna Array Showing the Azimuths of the 72 Fixed Beams.
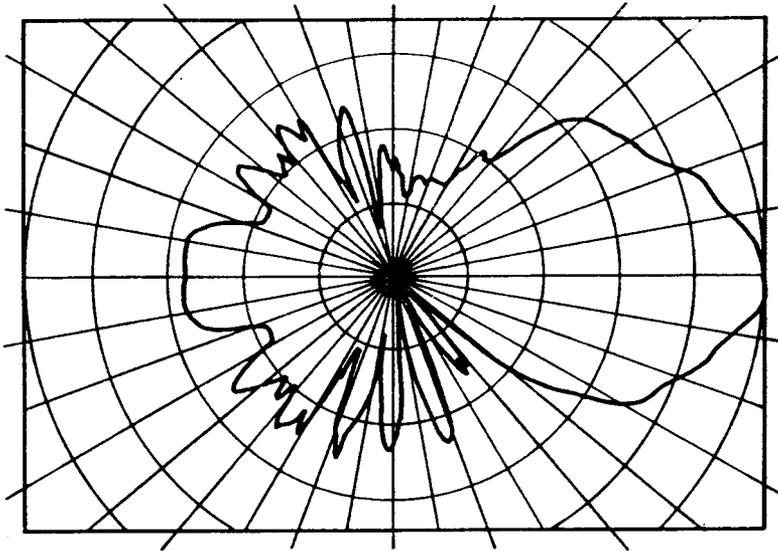
(a) Azimuthal pattern of Beverage pair
    antenna. Measurement was made
    with a vertically polarized **XELEDOP**
    antenna. This pattern was shown
    in rectilinear form in Fig. 5.
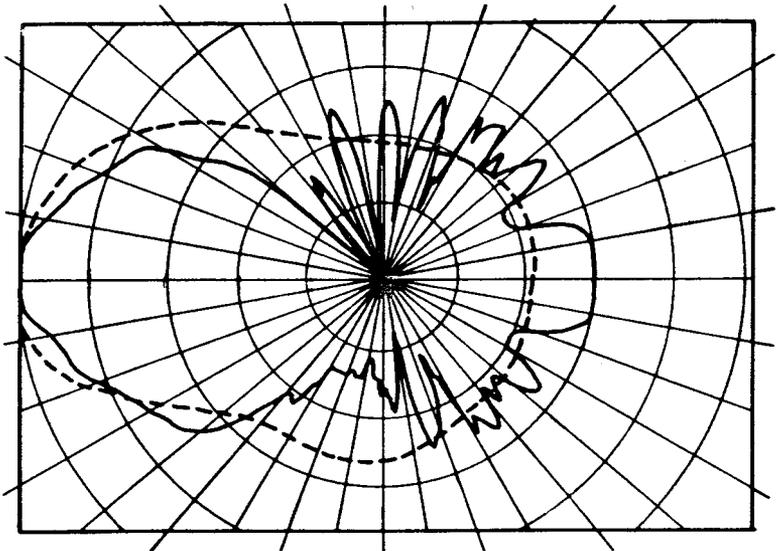
(b) Comparison of azimuthal pattern
    obtained with the vertically
    polarized **XELEDOP** and skywave
    of opportunity.
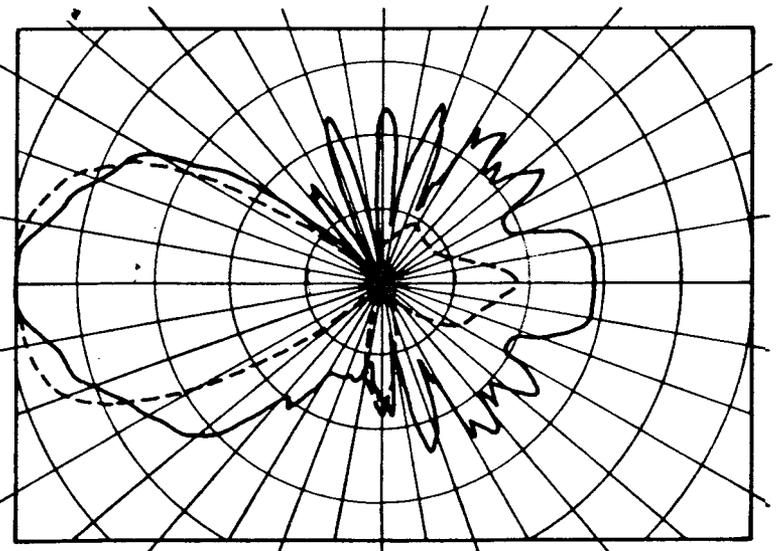
(c Comparison of azimuthal patterns
    obtained with the vertically
    polarized **XELEDOP** and a
    vertical dipole and transmitter
    suspended from a Balloon.

*Figure 31. Comparisons of measured azimuthal radiation patterns at 9.75 MHz for a Beverage pair antenna
at Cambridge Bay.*
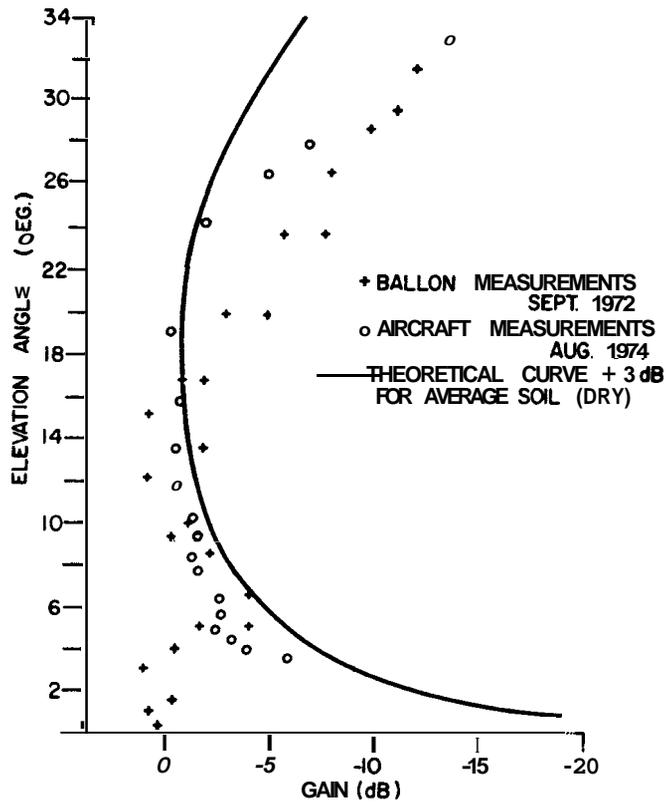
Figure 32. Vertical Radiation Pattern for the Beverage Pair Antenna Pointed Towards Alert at a Frequency of about 9.5 MHz.
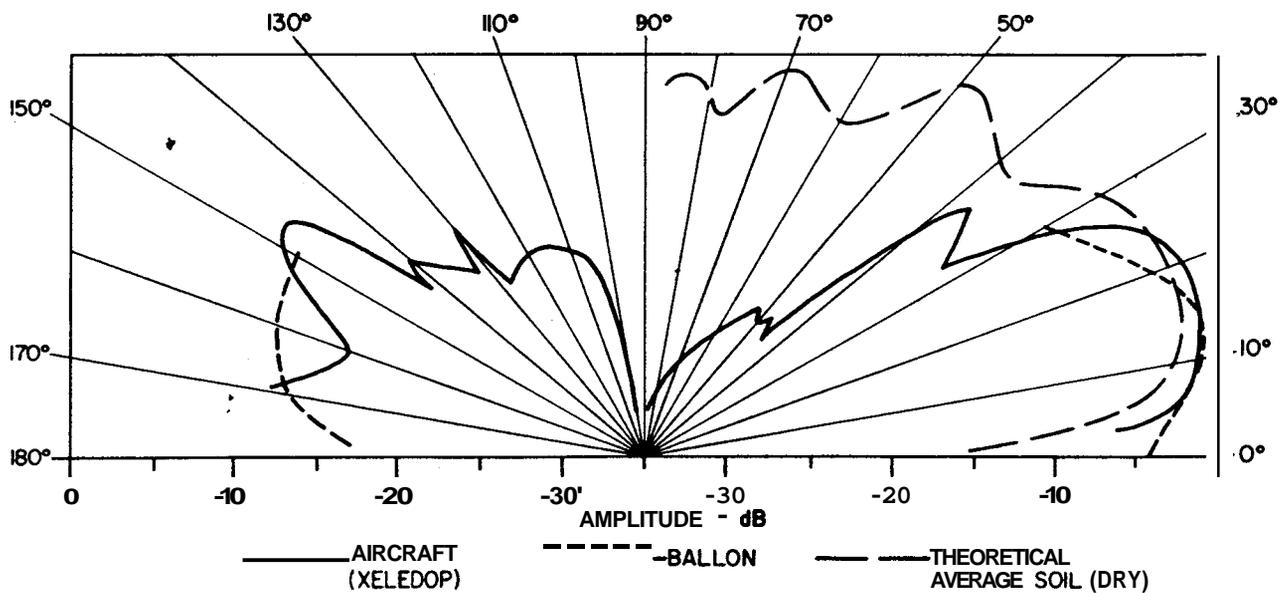
Figure 33. Comparison of theoretical and measured radiation patterns for a Cambridge Bay Beverage pair antenna. The balloon measurements were made at 9.0 MHz and the XELEDOP measurements were made at 9.75 MHz. The theoretical curve was derived for a frequency of 9.5 MHz and average soil (dry).
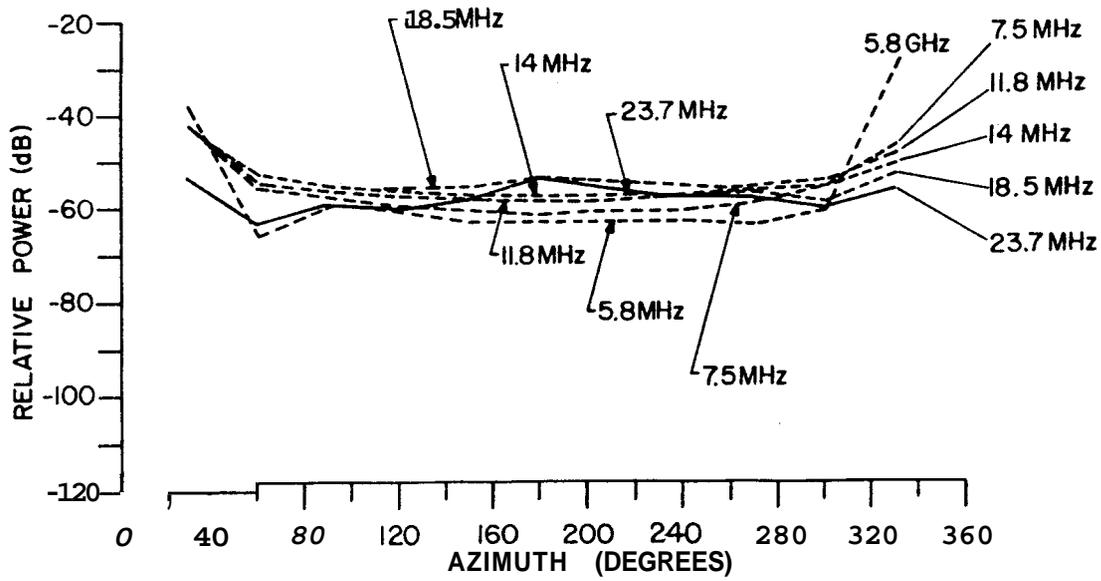
Figure 34.   Mutual Coupling Between Antenna Elements of the Rosette Array.
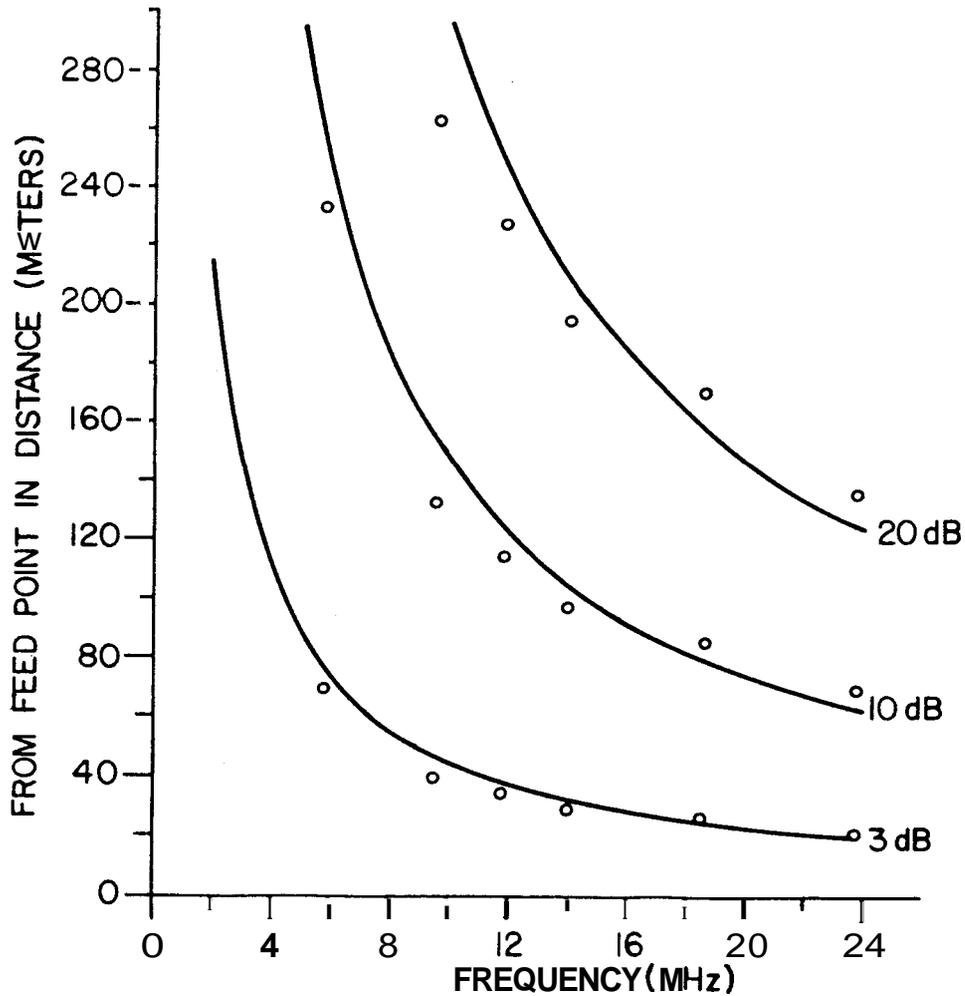
Figure 35.   Attenuation Contours for RF Currents on a Beverage Antenna.

74
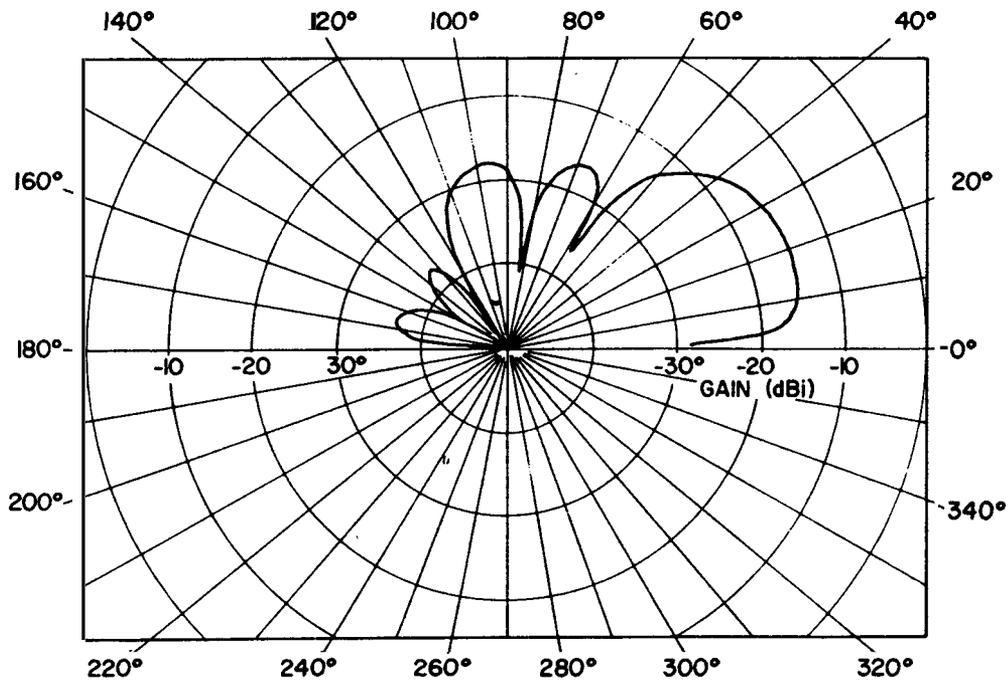
(a) Theoretical vertical radiation pattern for a Beverage antenna at 125 kHz over poor soil (dry).
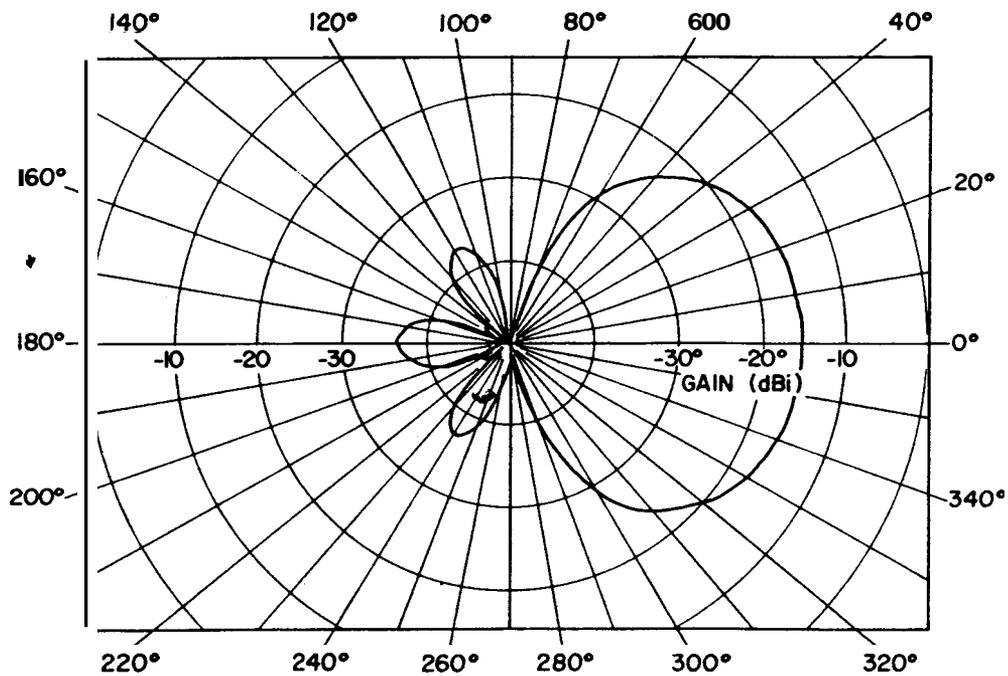
(b) Theoretical azimuthal radiation pattern for a Beverage antenna at 125 kHz over poor soil (dry).

Figure 36. Theoretical radiation patterns for Beverage antennas situated on poor soil.
The length of the antenna is 2.4 km and its height is 7.62 m.
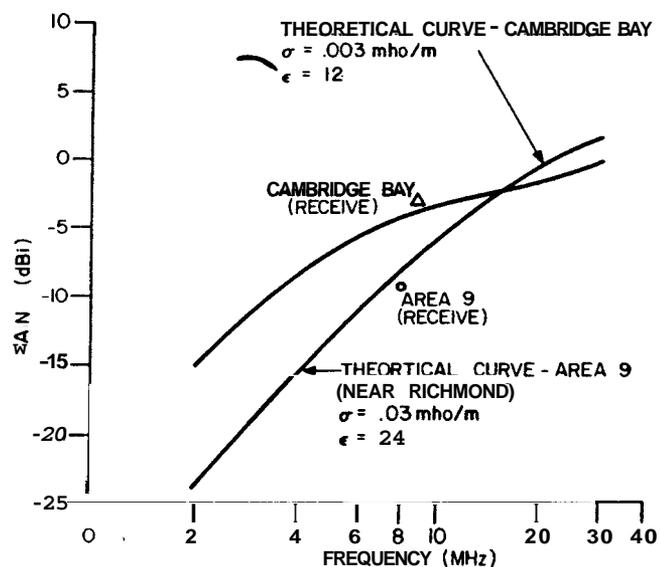
Figure 37. Comparison of Experimental and Theoretical Surface Wave Gains of Beverage Pair and Single Beverage Antennas for Average Soil (dry) and Wet Rich Soil, Height = I m and Length = 110 m.
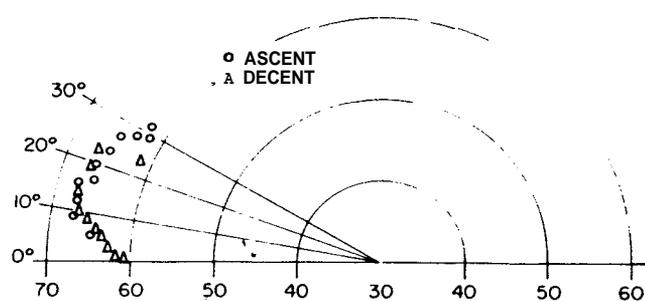
Figure 38. Field Intensity at the Center of the Array From a Balloon-Suspended Transmitter.
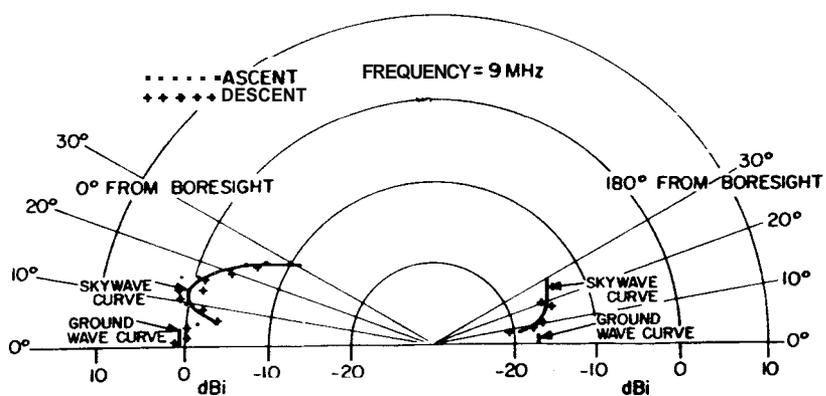
Figure 39. Gain of Beverage Element vs. Elevation Angle.

BEVERAGE
PAIR
ANTENNA
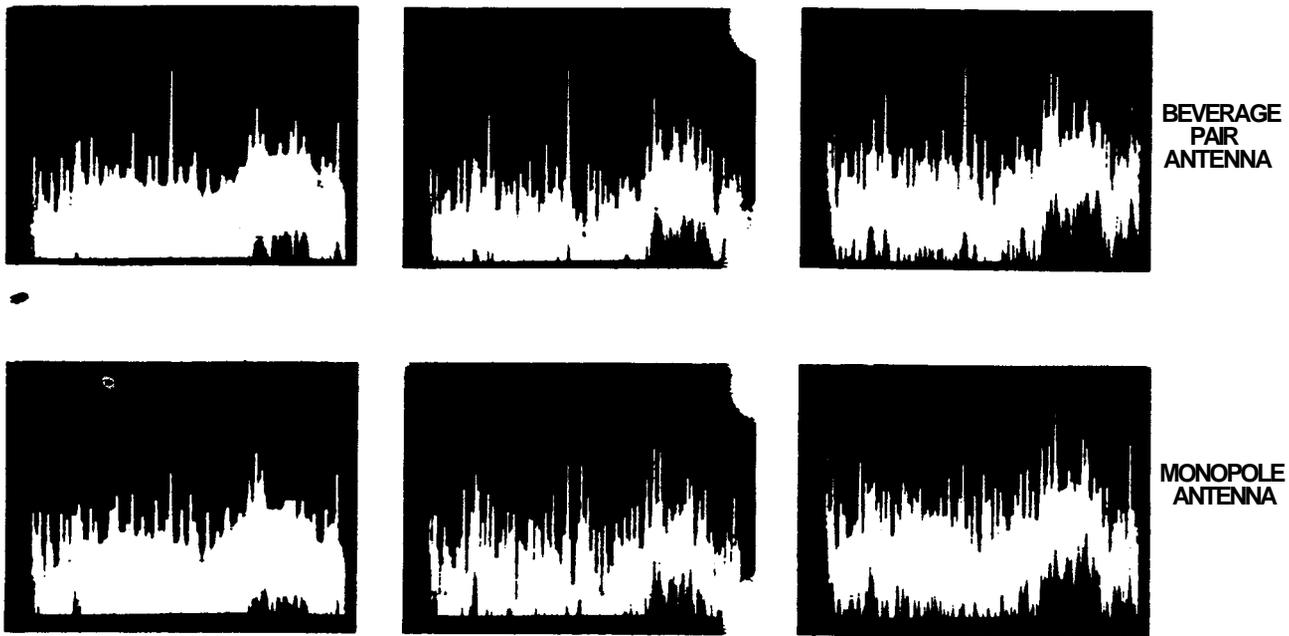
MONOPOLE
ANTENNA

Signal-to-interference taken almost simultaneously on a Beverage pair antenna and a quarter wave monopole antenna for 12 consecutive time intervals.

	Signal-To-Interference Ratio (dB)	
Interval	Beverage Pair	Monopole
1	+5	− 13
2	+14	− 3
3	+30	+12
4	+19	+8
5	+21	+10
6	+15	−2
7*	+34	+4
8*	+23	0
9*	+26	−16
10	+37	+6
11	+14	+16
12	+5	+16

*   Spectrum analyzer outputs shown above.

Figure 40. CRT displays of a spectrum analyzer connected alternately to a monopole antenna and a Beverage pair antenna. In each instance the Alert signal appears at the center of the display and the other signals are interferring signals. The IF bandwidth of the spectrum analyzer was 3 kHz; the width of the spectrum window scanned was 2 MHz and the scan time was 0.1 sec/div. Table show some measured signal-to-interference ratios on the two antennas.
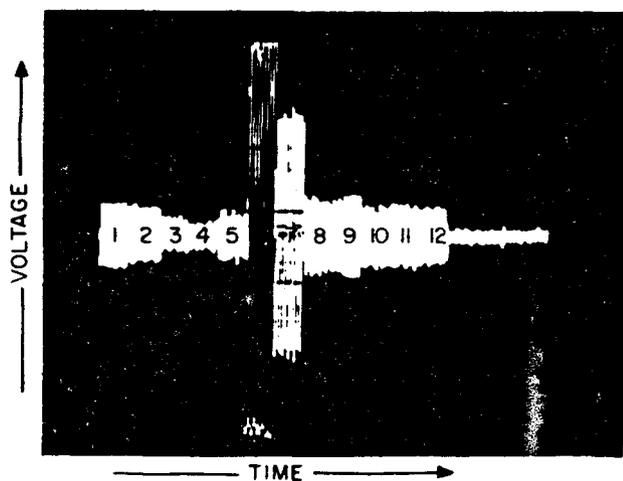
(a) Sequential sampling of the terminal voltages of the 12 Beverage pair antennas at Cambridge Bay, monitoring wwv on 10 MHz. The sampling time for each antenna was 1.2 μsec and the IF bandwidth of the receiver was 10 kHz.
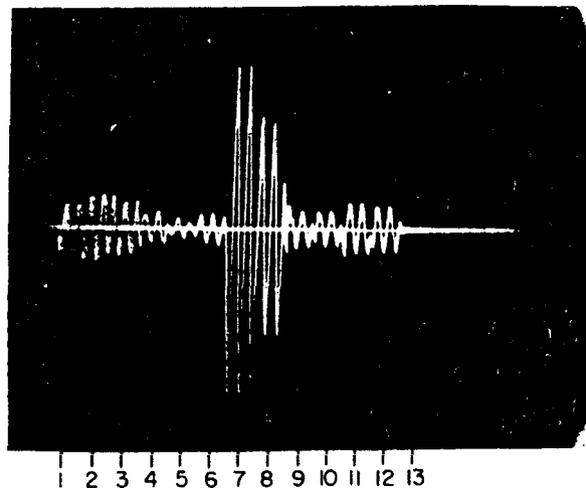
(c) Sequential sampling of the terminal voltages of the 12 Beverage pair antennas at Cambridge Bay monitoring wwv on 15 MHz somewhat latter in time *than* (b).
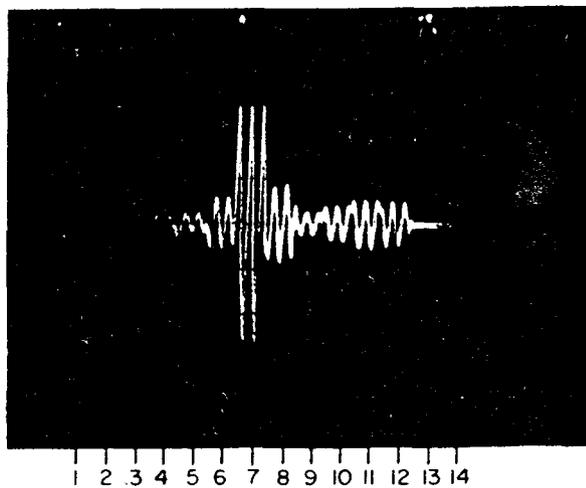
(b) Sequential sampling of the terminal voltages of the 12 Beverage pair antennas at Cambridge Bay, monitoring wwv on 15 MHz.
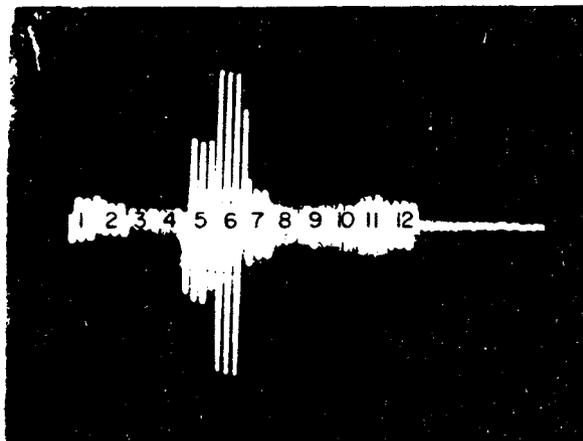
(d) Sequential sampling of the terminal voltages of the 12 Beverage pair antennas at Cambridge Bay, monitoring wwv on 15 MHz, somewhat latter in time than (c).

Figure 41. Photographs of the CRT display of an oscilloscope monitoring the video output of a receiver whose input is connected in rapid succession by a diode switch to the 12 Beverage pair antennas at Cambridge Bay monitoring **wwv.**
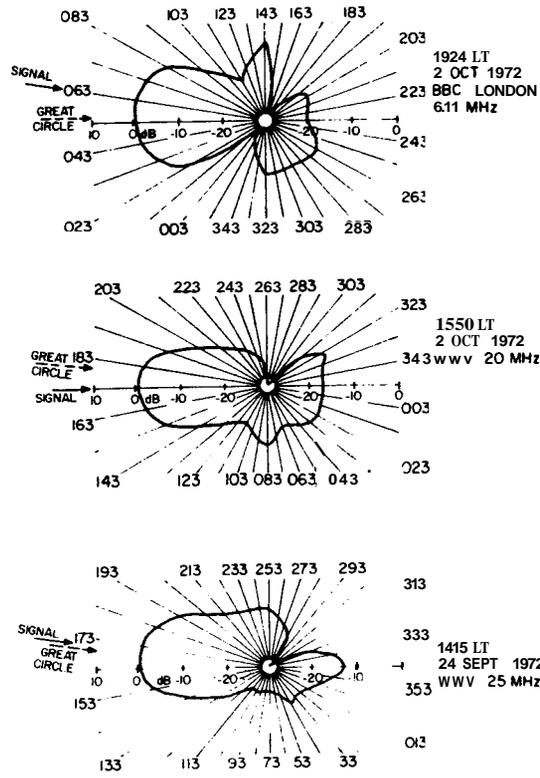
Figure 42. Direction Finding Patterns Obtained With the Beverage Array from Known Transmitters.
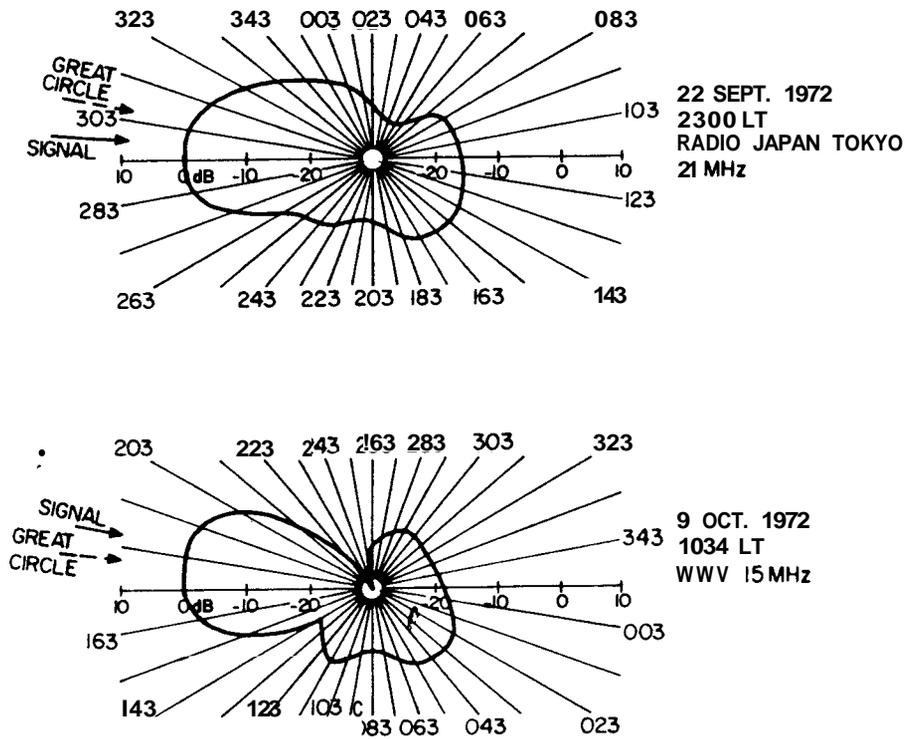
Figure 43. Further Examples of Direction-Finding Patterns on Signals from Known Transmitters.

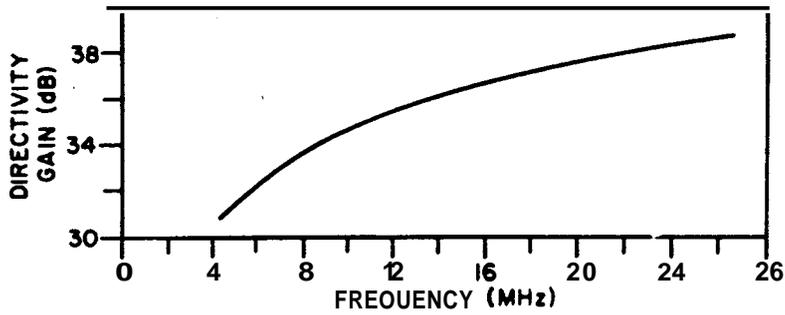BEVERAGE ANTENNA

TO OPERATIONS BUILDING

4134.55'

TO ALERT

o   4:1 POWER COMBINER
□   SWITCH BOX WITH PHASING CABLES
⌐   2:1 POWER COMBINER
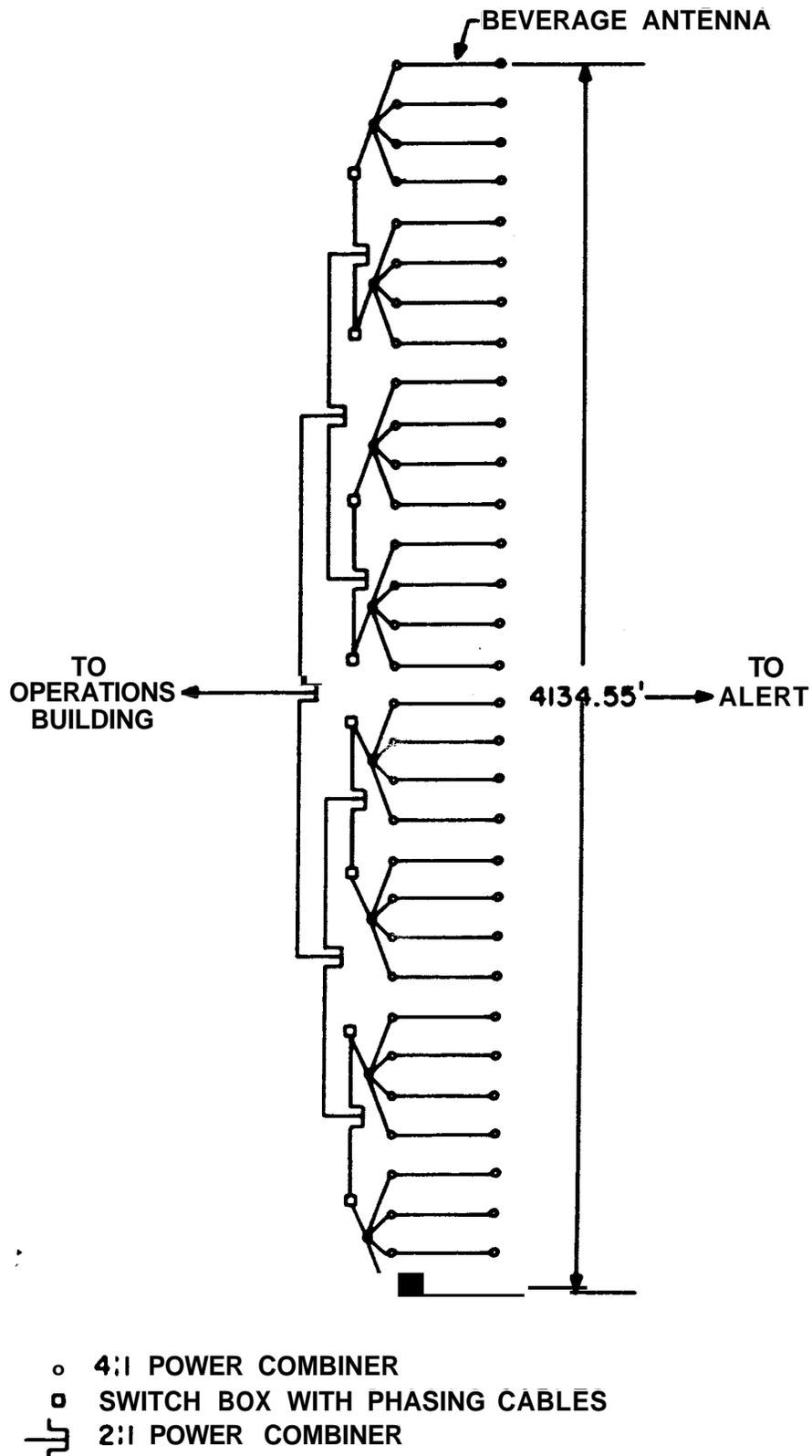
Figure 44. Schematic of the 32-Element Linear Phased Beverage Array Installed at Cambridge Bay, N.W.T.

80
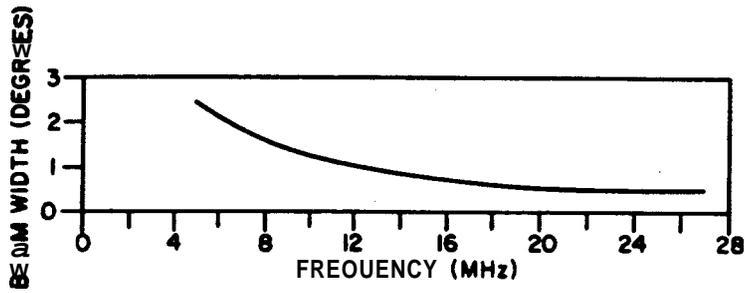
(a) Azimuthal beamwidth of the Cambridge Bay linear array.

(b) Directivity gain of the Cambridge Bay linear array.

PRIMARY GRATING LOBE
SECONDARY GRATING LOBE

B— PRIMARY LOBES DOWN AT LEAST 13 dB
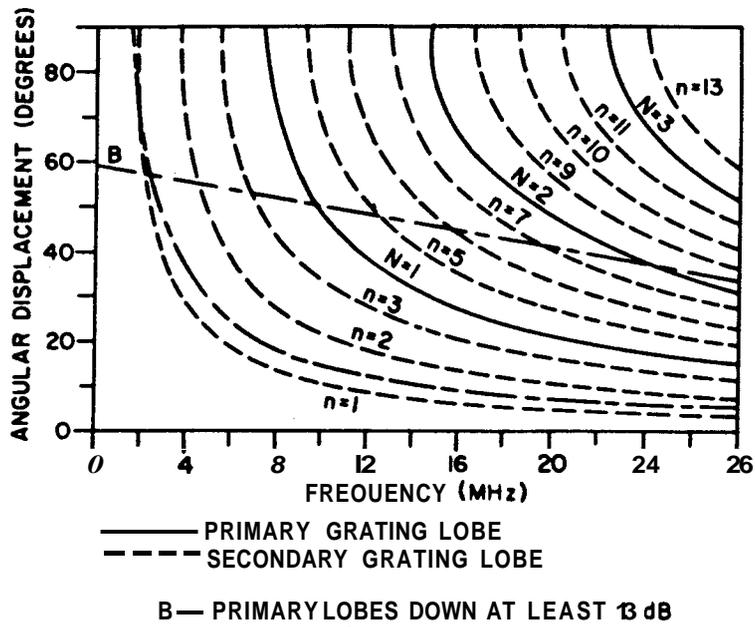
(c) Azimuths of the primary and secondary grating lobes of the Cambridge Bay linear array.

Figure 45. Azimuthal Beamwidth, Directivity Gain and Location of Grating Lobes for the Cambridge Bay Array.
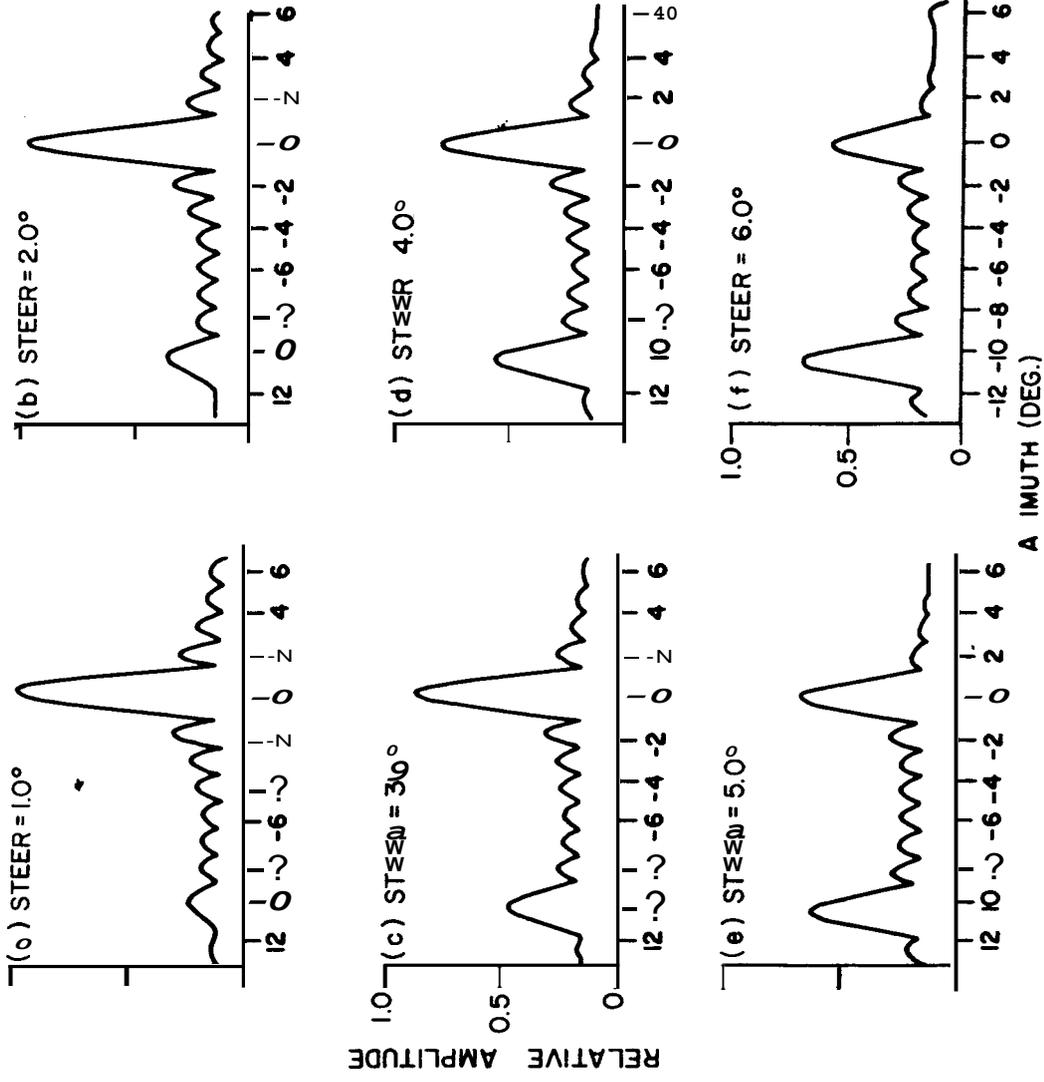
Figure 46. Theoretical azimuthal radiation patterns of the Cambridge Bay linear array at 10 MHz for azimuths adjacent to the main beam as the array is slewed through angles varying from 1 to 6 degrees.

FREQUENCY 9.75 MHz
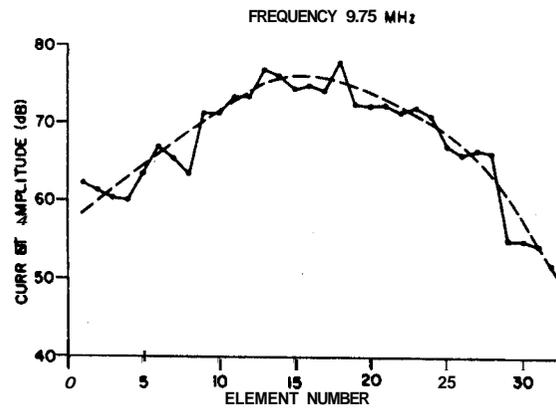
(a) Current amplitude measured across the aperture of the Cambridge Bay linear phased array at the terminated ends of the Beverage elements.
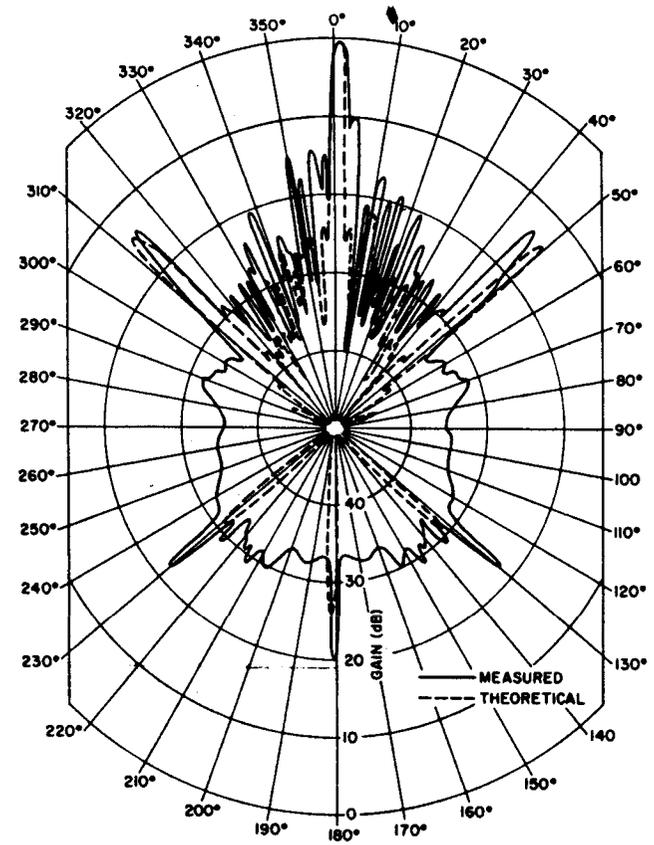
(b) Comparison of the theoretical and measured radiation patterns o for the Cambridge Bay linear array at 9.75 MHz.

Figure 47. Sampling of the Current Amplitude Across the Aperture of the Cambridge Bay Linear Phased Array and a Comparison of Theoretical and Experimental Radiation Patterns.

(b) Theoretical azimuthal pattern at **10 MHz** *of* a   weighted 8-element linear phased Beverage array with an aperture of **149m.** Cos^2 weighting was applied to the antenna aperture.
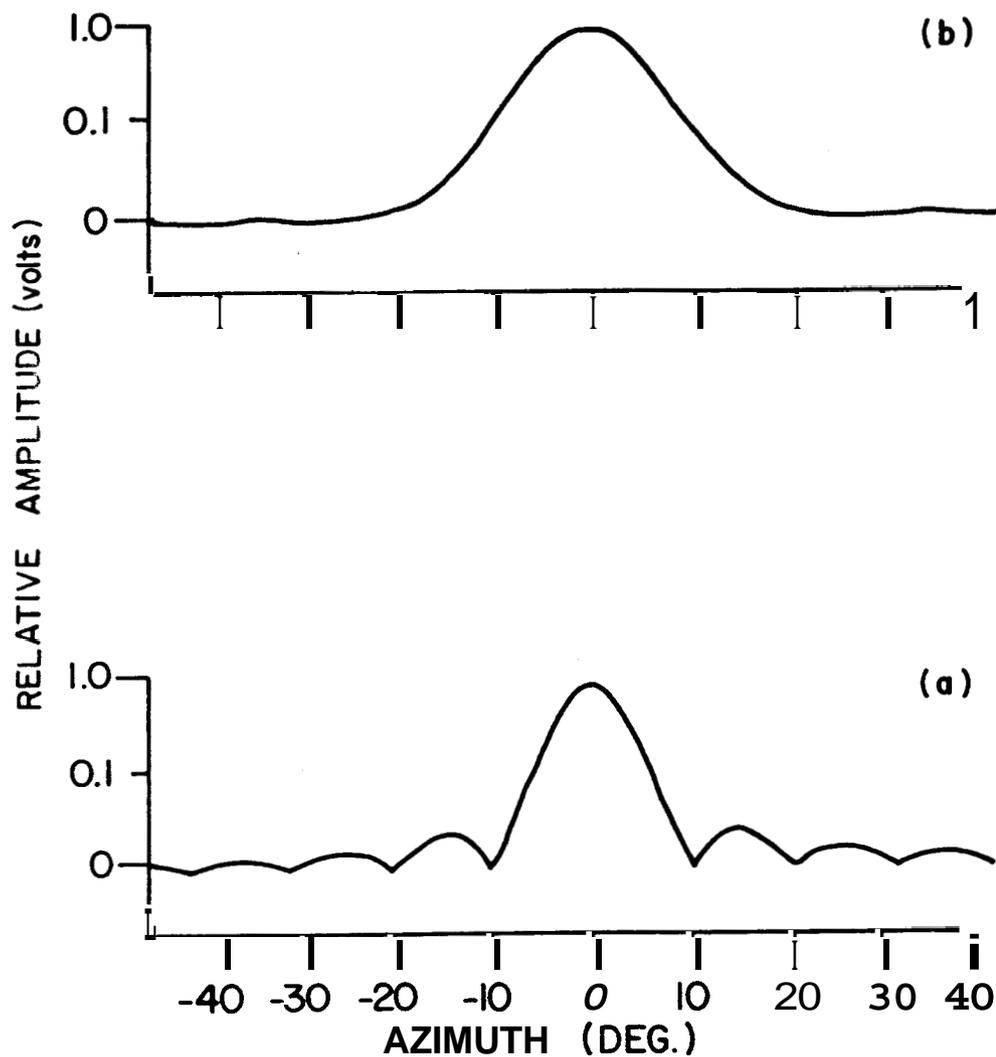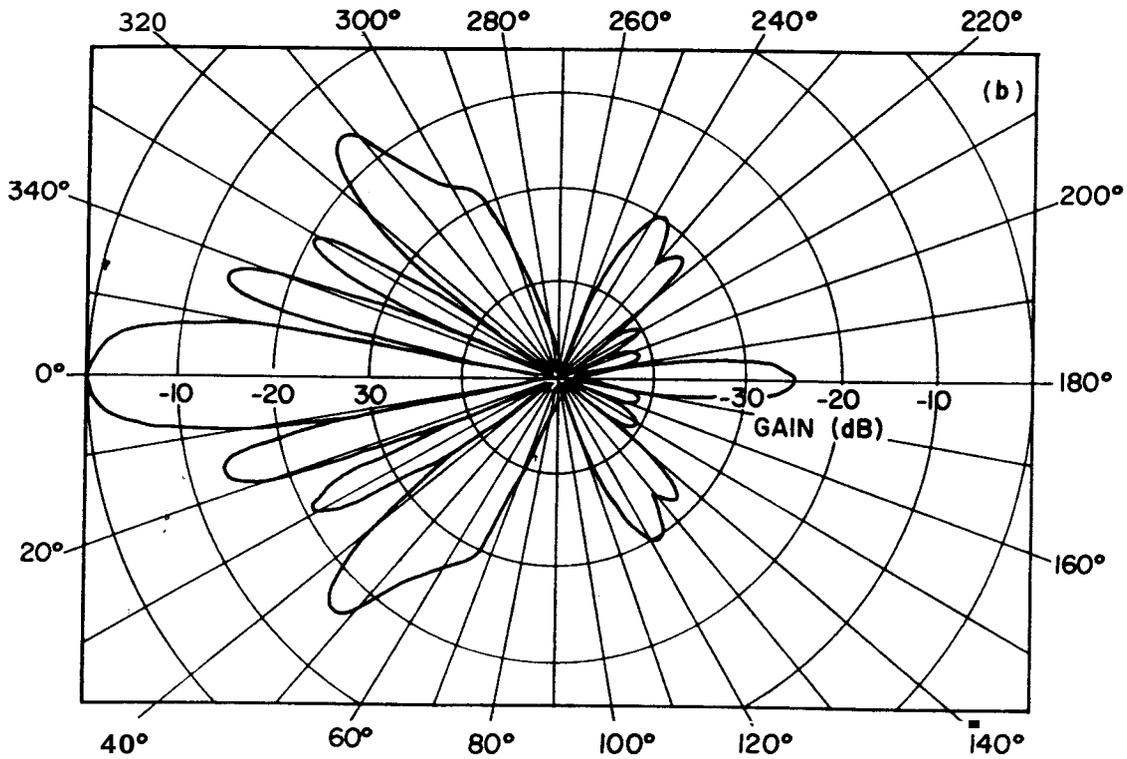

(a) Theoretical azimuthal pattern at **10 MHz** of an unweighted 8-element linear phased Beverage array with an aperture of **149m.**

Figure 48.   Theoretical Patterns at 10MHz of an Unweighted and Weighted Linear Beverage Array With an Aperture of 150m.
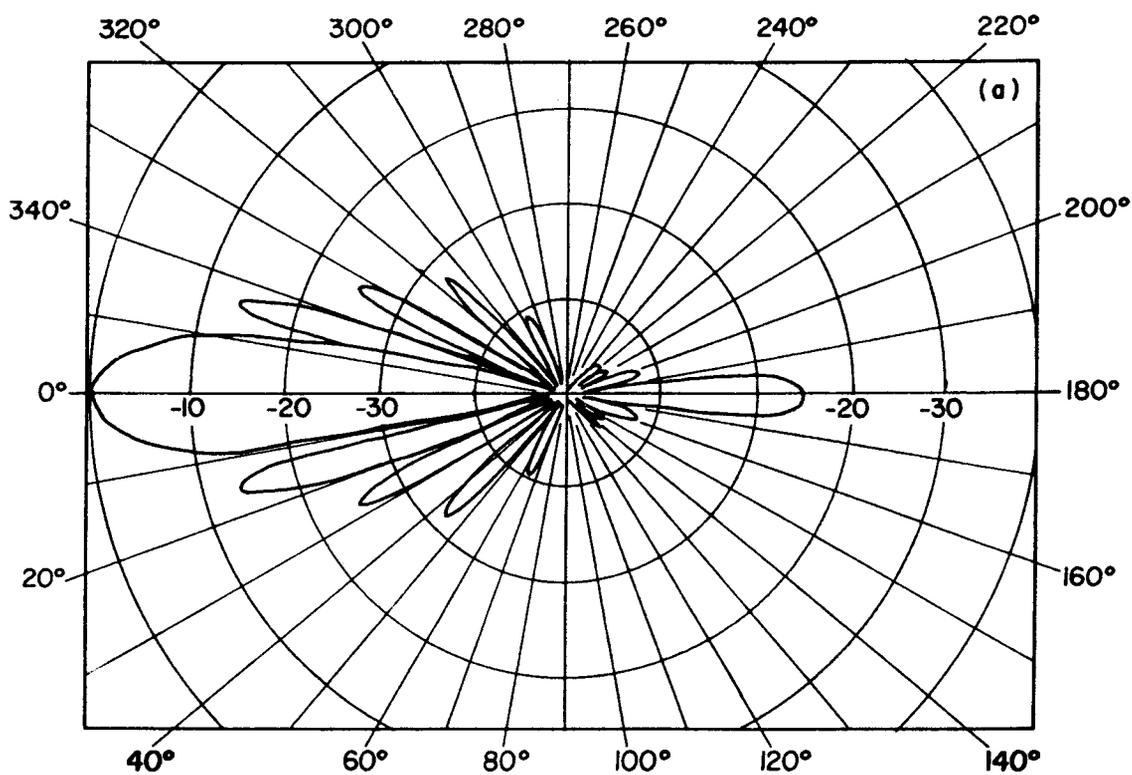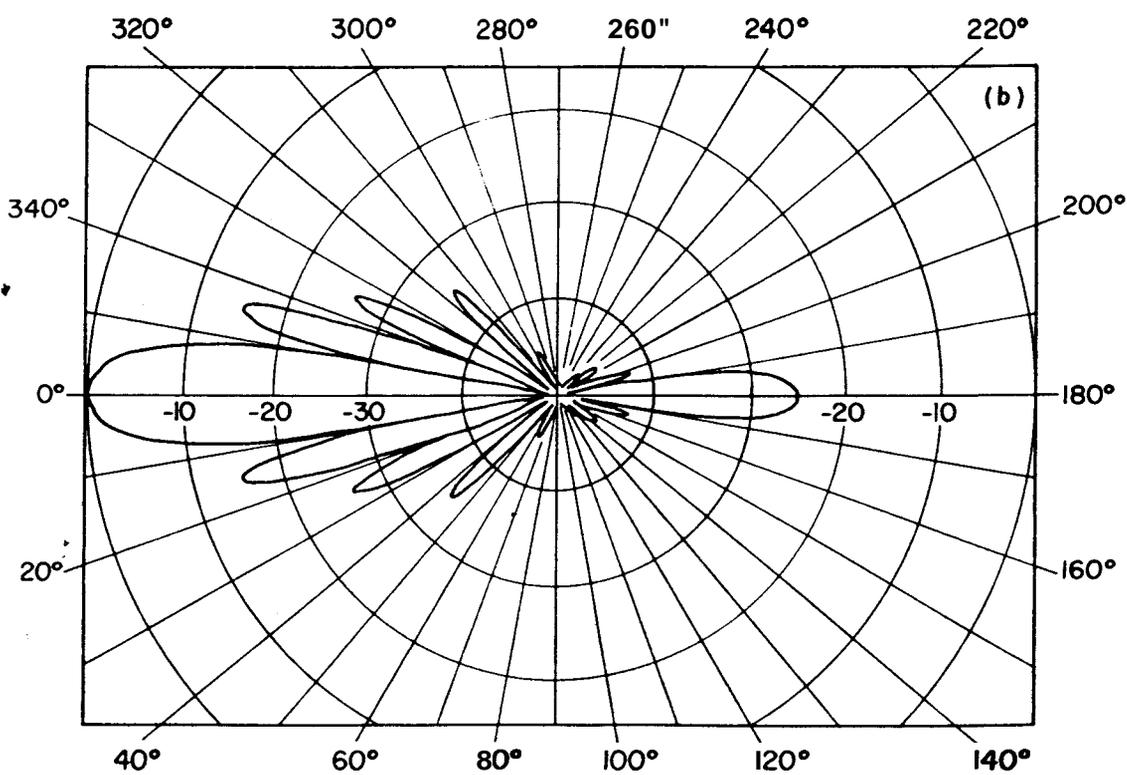
84
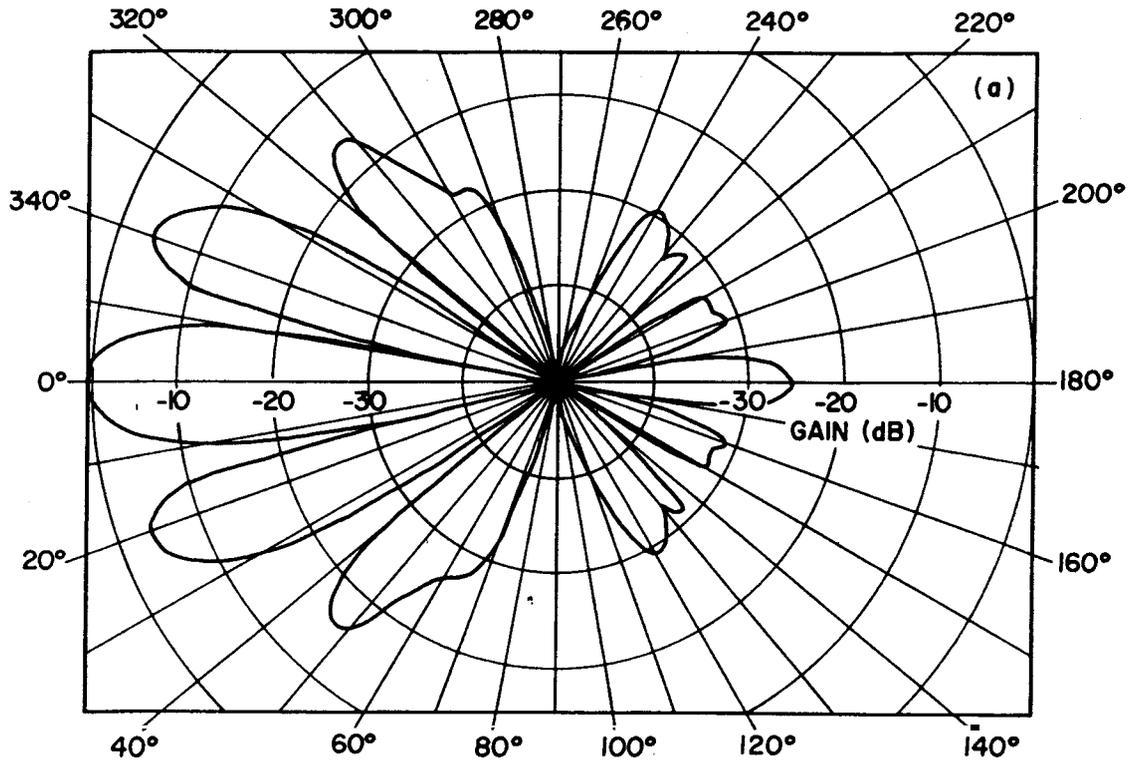
(a) Two-elements

(b) Four-elements

Figure 49. Theoretical 1 0 MHz azimuthal pattern for a Beverage antenna array with a 150m aperture. The elements are 110m long and their height above ground is 2m.
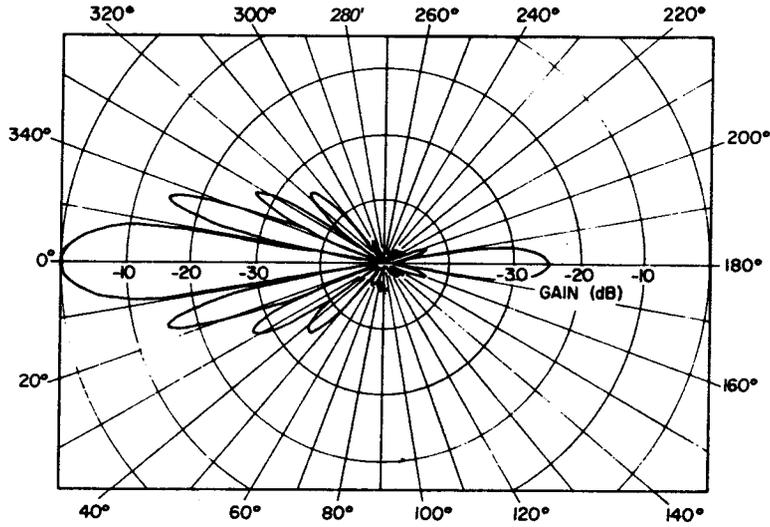
(a) Eight-elements

(b) Sixteen-elements

Figure 50. Theoretical 10 MHz azimuthal pattern for a Beverage antenna array with a 150m aperture. The elements are 110m long and their height above ground is 2m.

(a) **Thirty-two** elements

Figure 51. Theoretical 10MHz azimuthal pattern for a Beverage antenna array with a 150m aperture. The elements are 110m long and their height above ground is 2m.
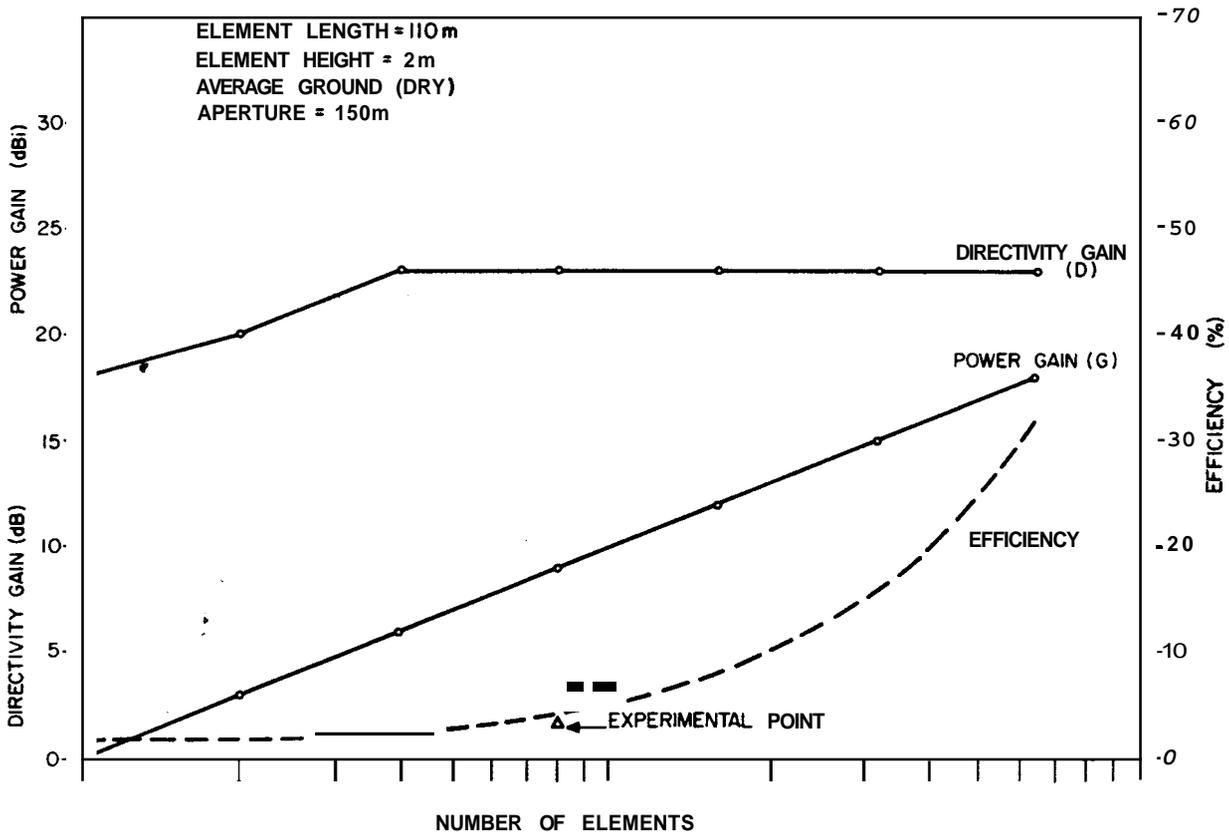

Figure 52. Directivity gain, power gain and efficiency at 10MHz of a Beverage array with an aperture of 150m as the number of elements in the array is increased from 1 to 64. The length of each element is 110m, its height above ground is 2m and the elements are sited on average ground (dry).
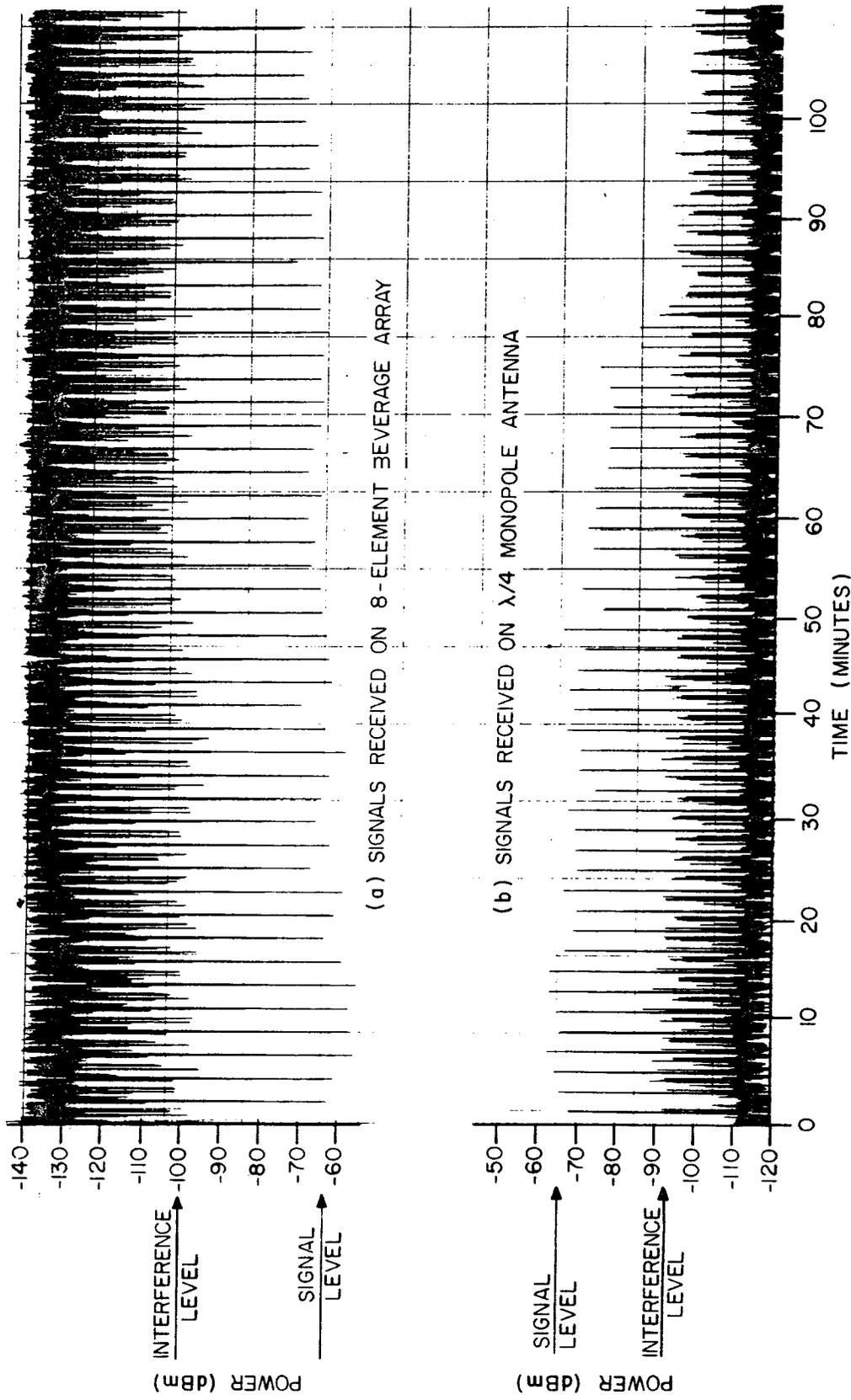
Figure 53. Comparison of signal received by 8-element Beverage array and λ/4 monopole antenna the larger amplitude vertical lines separated by 100 sec intervals in both (a) and (b) represent the amplitude of the wanted Alert signal. The other vertical lines represent amplitudes of interfering signals located in the frequency window ± 25 KHz centered on the frequency of the Alert signal which remained constant throughout.
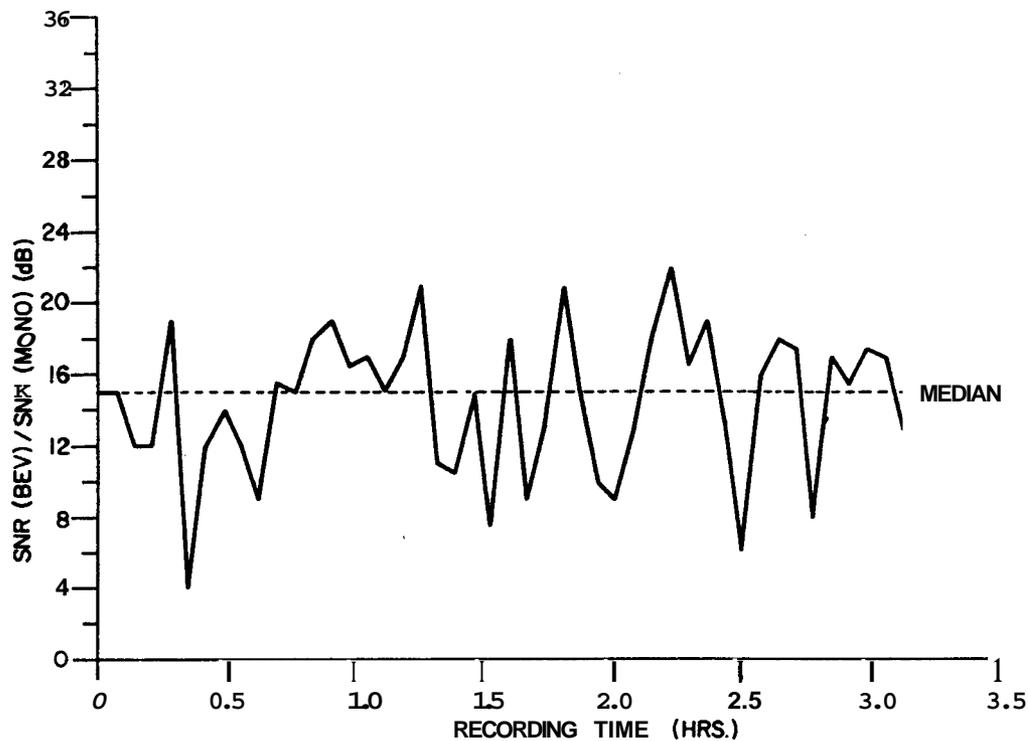
Figure 54. Difference in the SNR of the 10.6 MHz Alert signal received on the 8-element Beverage array with that received simultaneously on a Xλ/4 monopole antenna. This data was taken on 7 October 1974 between 1210 and 1530 LT.

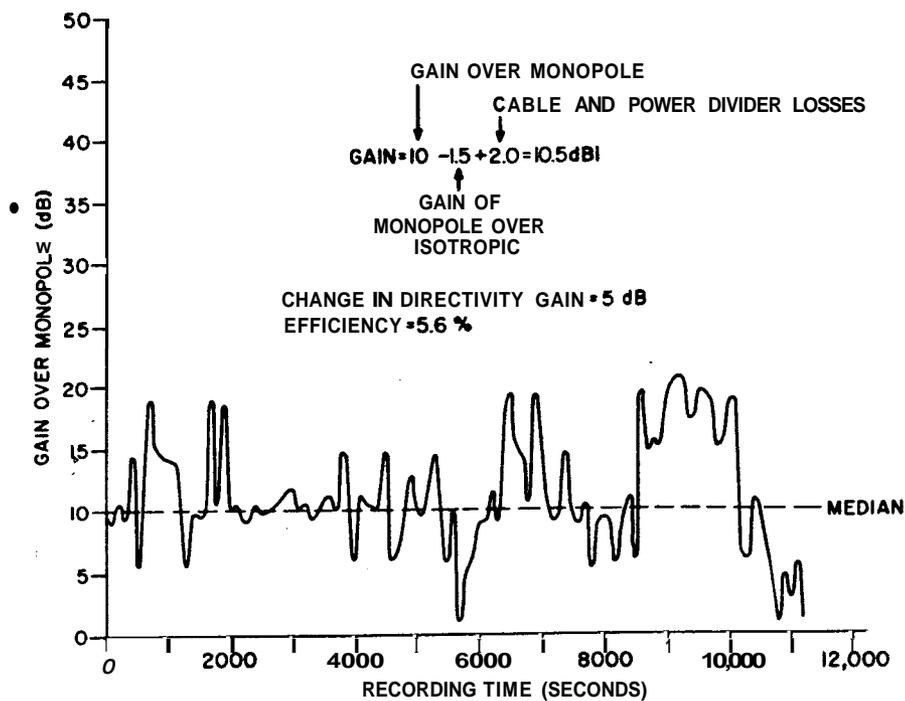figure 55. Gain of an 8-element Beverage array with respect to o λ/4 monopole. Both antennas were located ot Ottawa and were simultaneously monitoring o sky wave signal emanating from a transmitter ot Alert.

APPENDIX   I

Theoretical Curves for Attenuation, Characteristic Impedance

and Velocity Ratio

Figure I-1. Theoretical Values for Attenuation, Impedance and Wave Velocity for a Beverage Antenna on Dry Granite.

Figure 2. *Theoretical Values for Attenuation, Impedance and Wave Velocity for a Beverage Antenna on Dry Sand.*
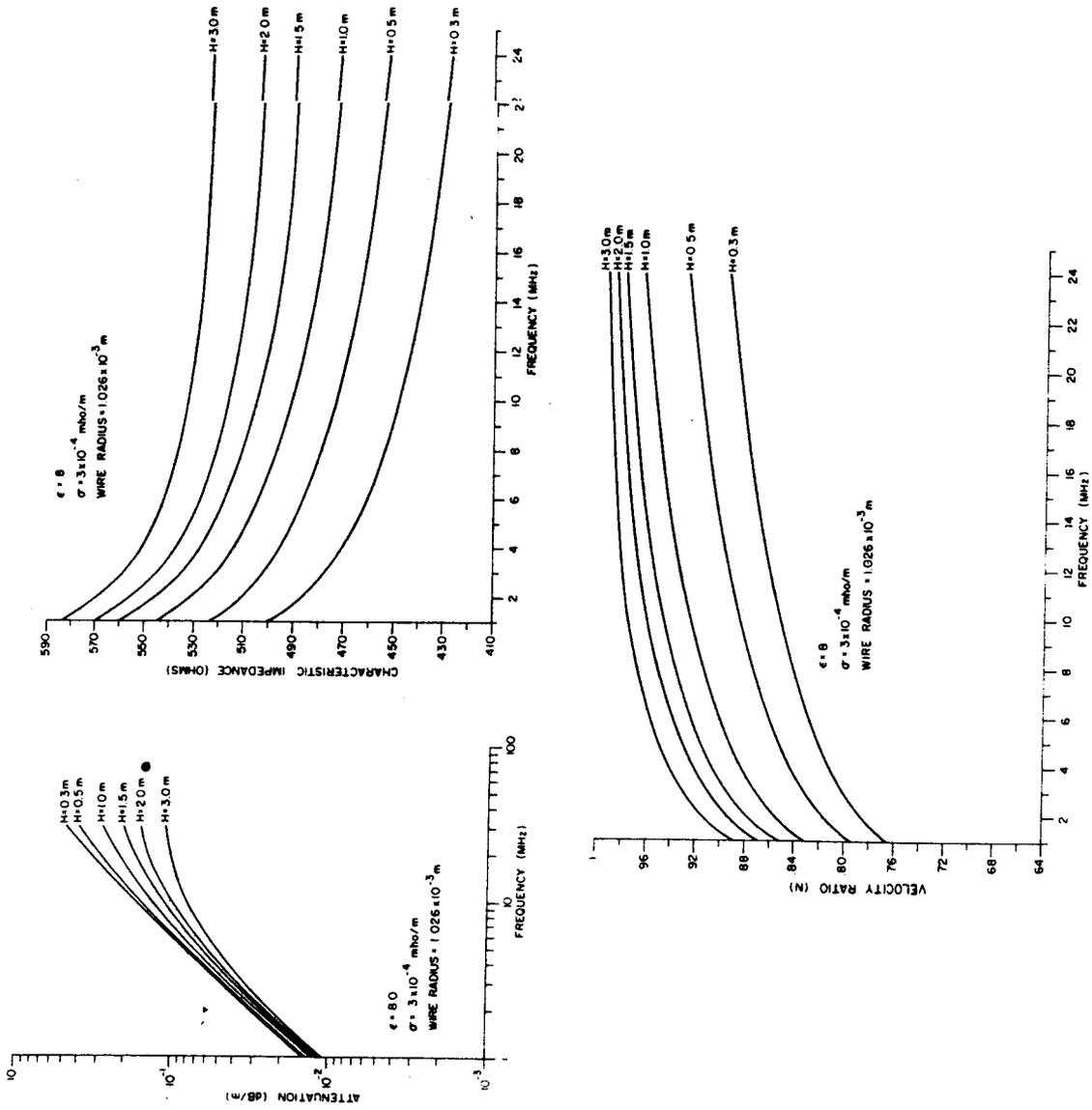
Figure I-3. Theoretical Values for Attenuation, Impedance and Wave Velocity for a Beverage Antenna on Poor $\angle q_{\parallel}$ (Dry).
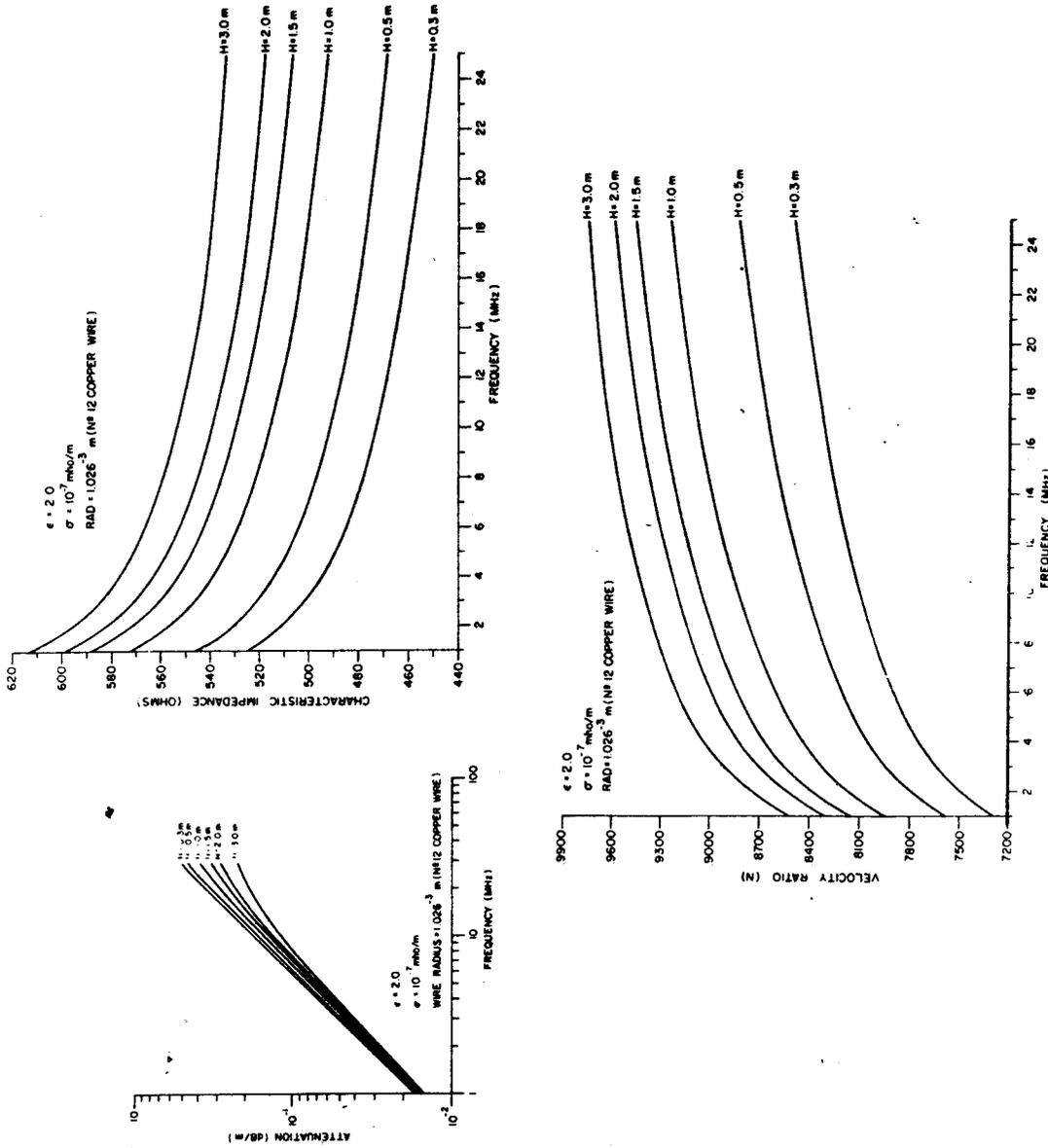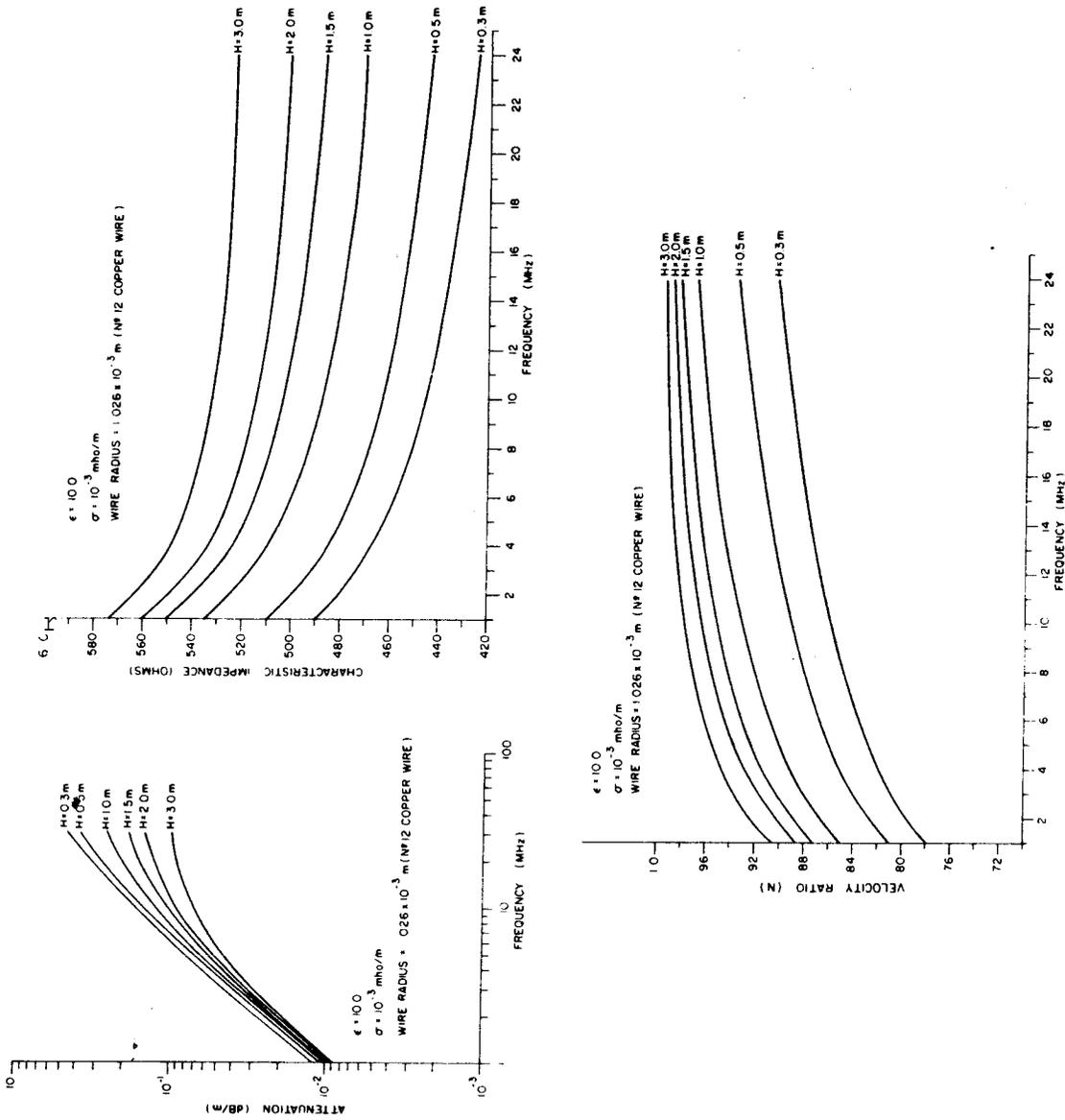
Figure I-4. Theoretical Values for Attenuation, Impedance and Wave Velocity Ratio for a Beverage Antenna on Poor Soil.
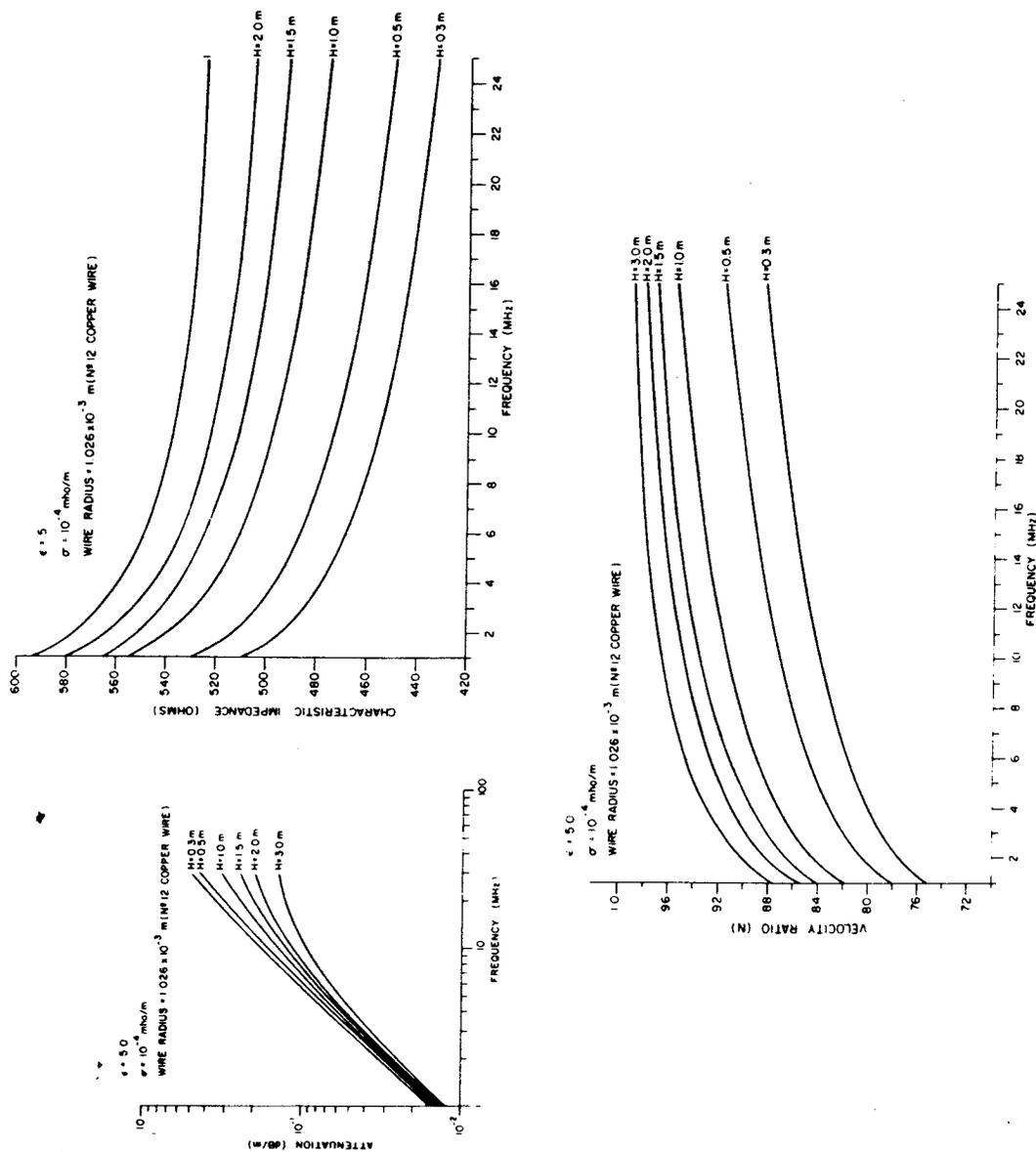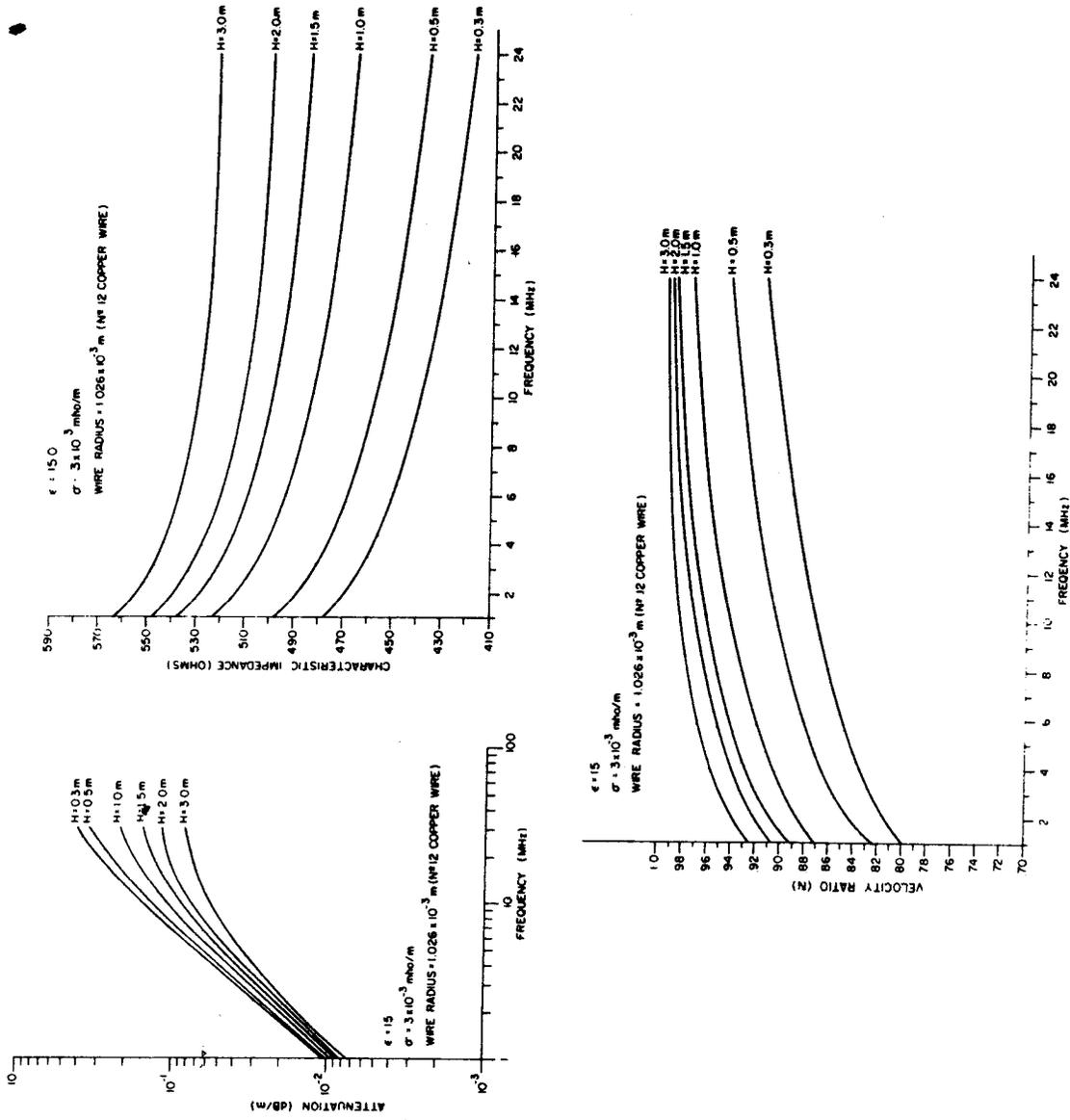
Figure I-5. Theoretical Values of Attenuation, Impedance and Velocity Rato for a Beverage Antenna on Dry Average Soil.
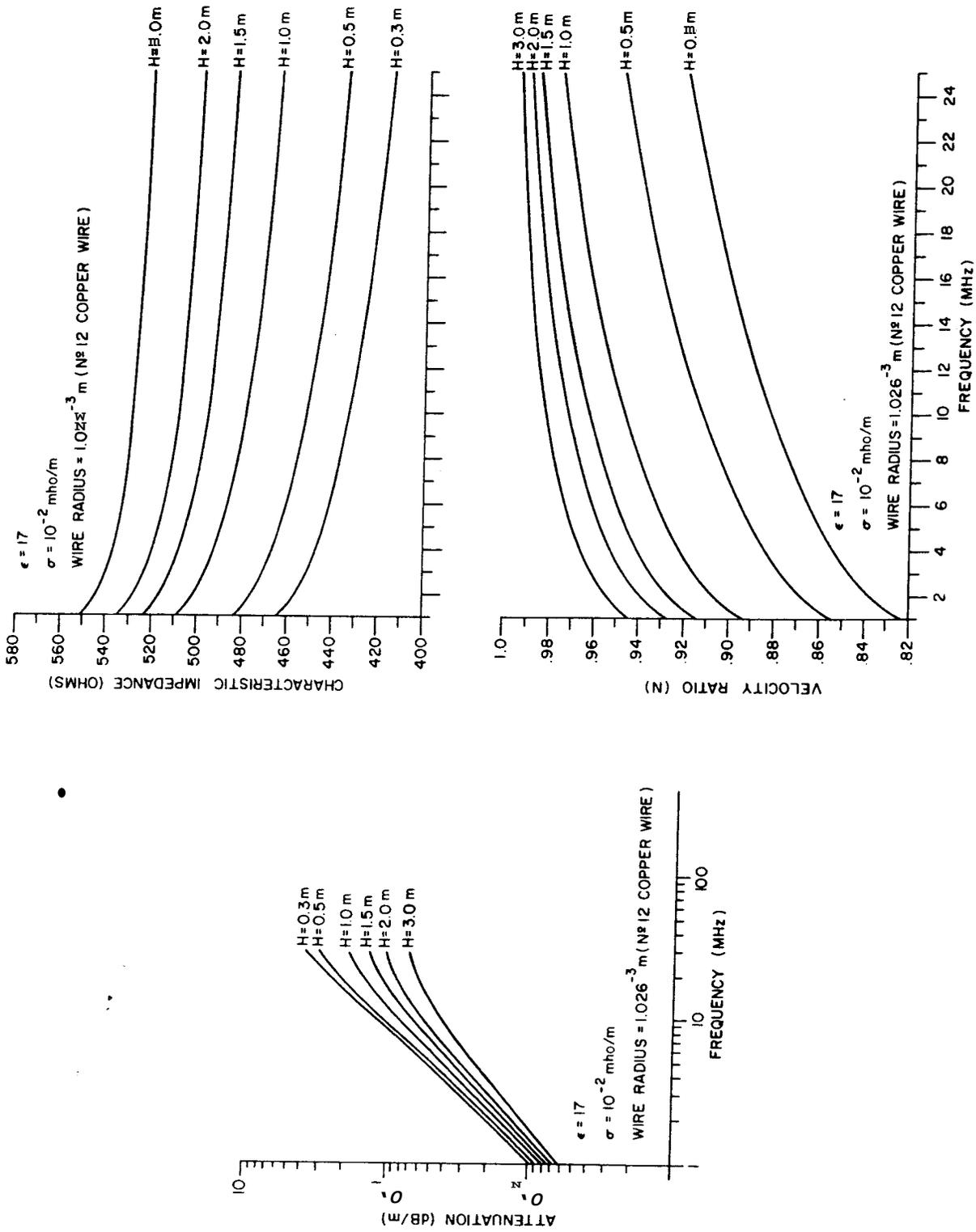
Figure I-6. Theoretical Values of Attenuation, Impedance and Velocity Ratio for a Beverage on Average Soil (Wet).
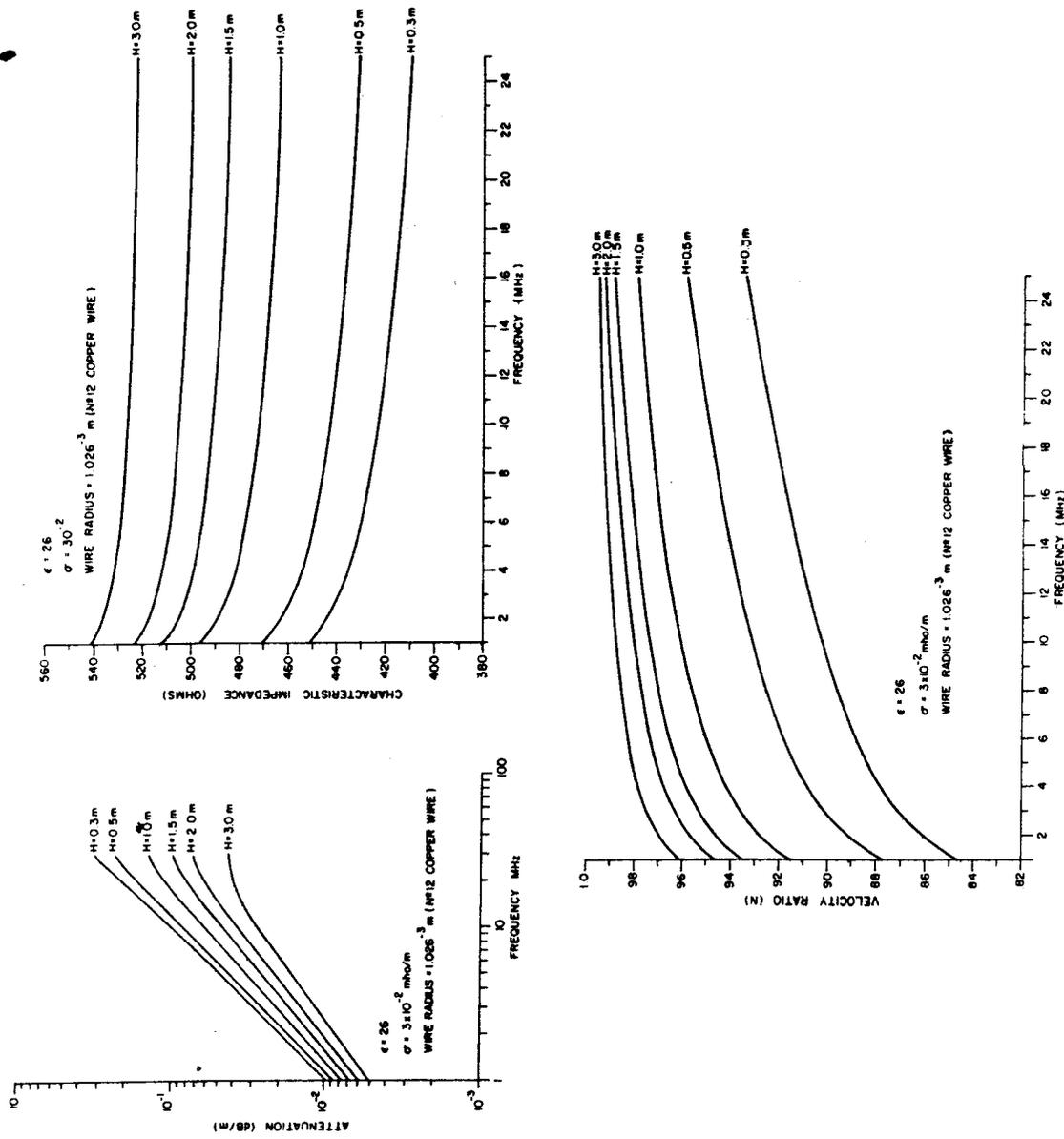
Figure I-7. Theoretical Values of Attenuation, Impedance and Velocity Ratio for a Beverage Antenna on Wet Rich Soil.

A P P E N D I X   I I

Theoretical Curves for Azimuthal Beamwidth, Vertical Beamwidth,

Gain, and Take-Off Angle

Figure II-1. *Design Parameters for Poor Soil (Dry), H = 0.3m, L = 100m.*

Figure 11-2. *Design Parameters for Poor Soil (Dry), H= 0.3m, L = 200m.*
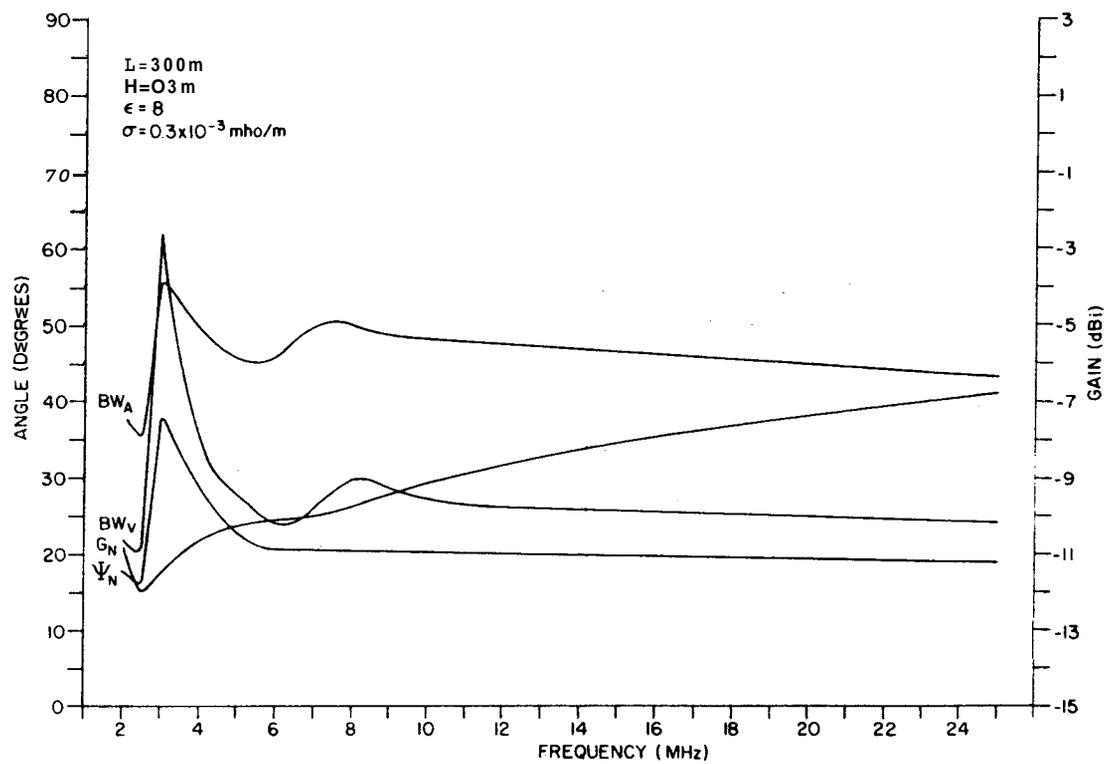
Figure II-3.   Design Parameters for Poor Soil (Dry), H = 0.3m, L = 300m.
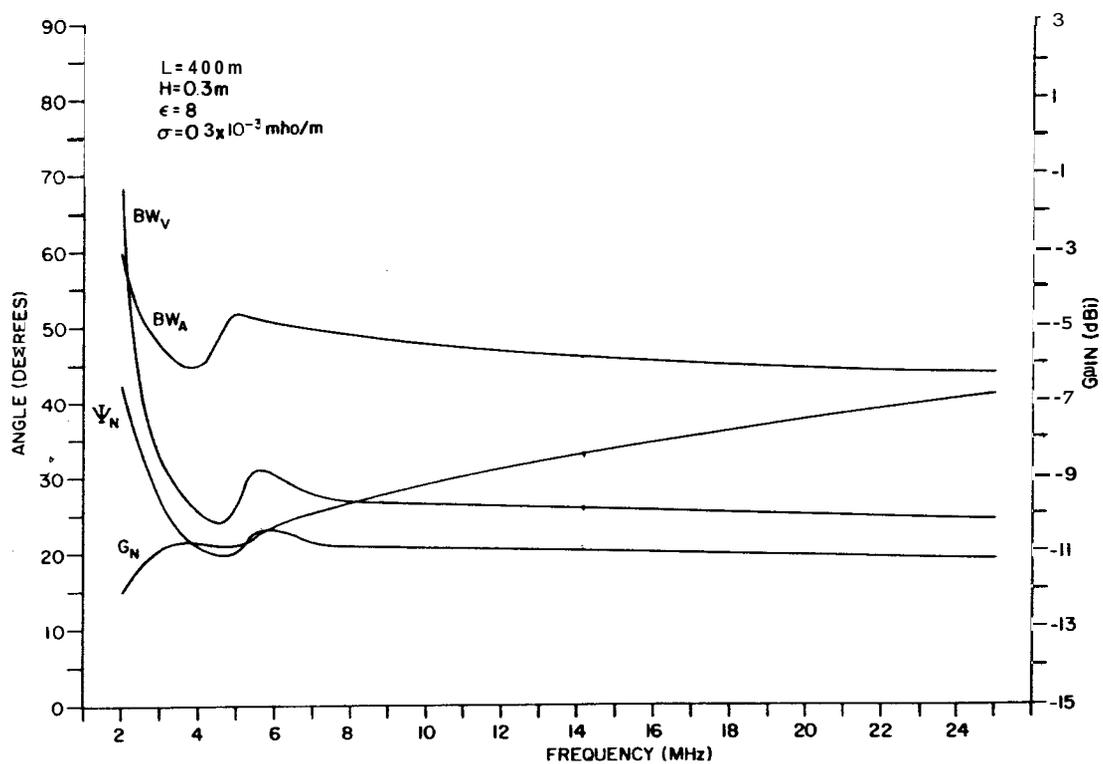
figure II-4.   Design Parameters for Poor Soil (Dry), H = 0.3m, L = 400m.
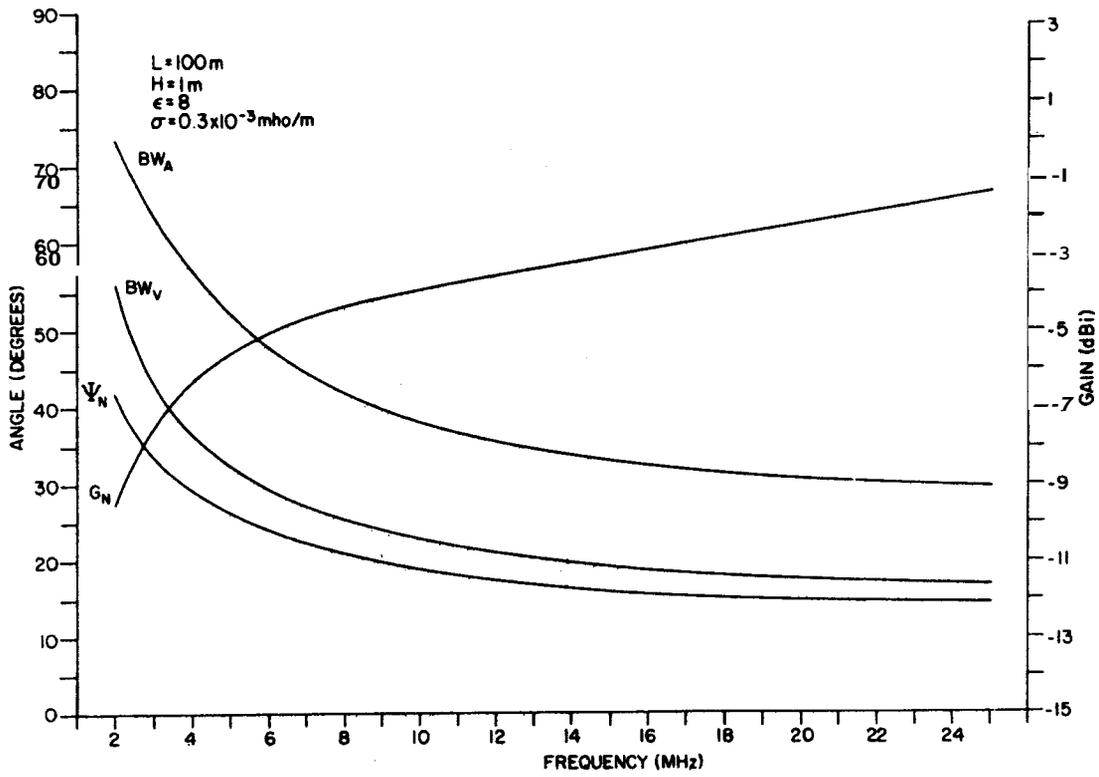
Figure II-5.   Design Parameters for Poor Soil (Dry), H = 1m, L = 100m.
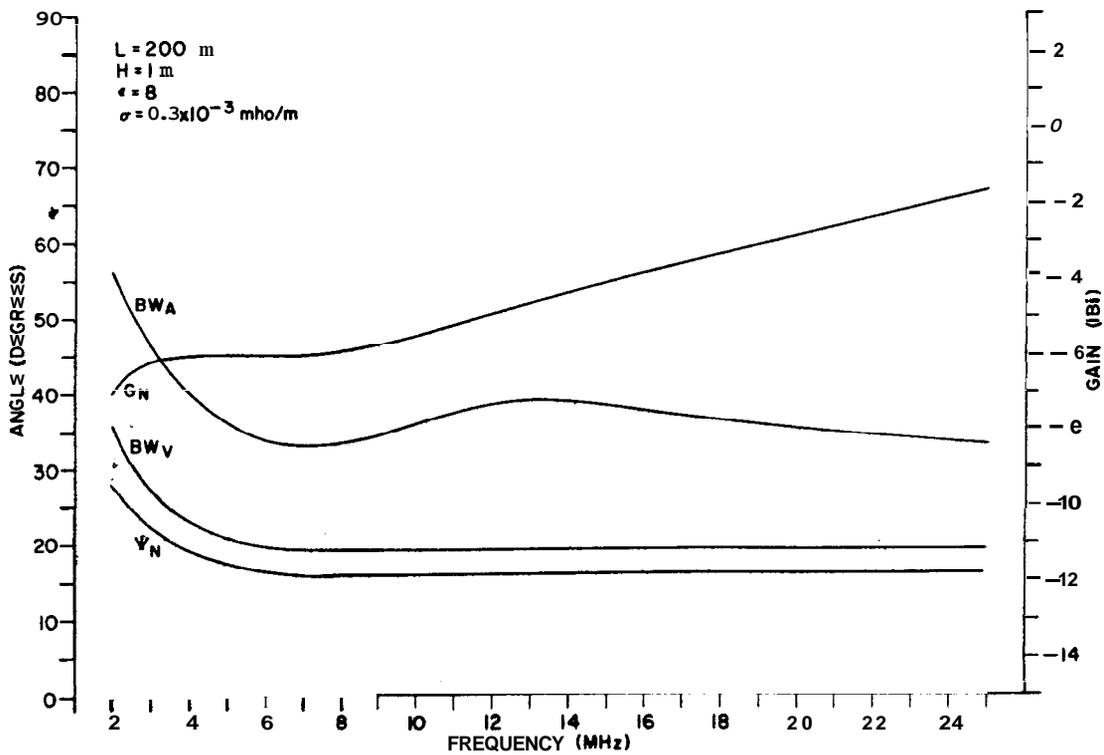
Figure II-6.   Design Parameters for Poor Soil (Dry), H = 1m, L = 200m.
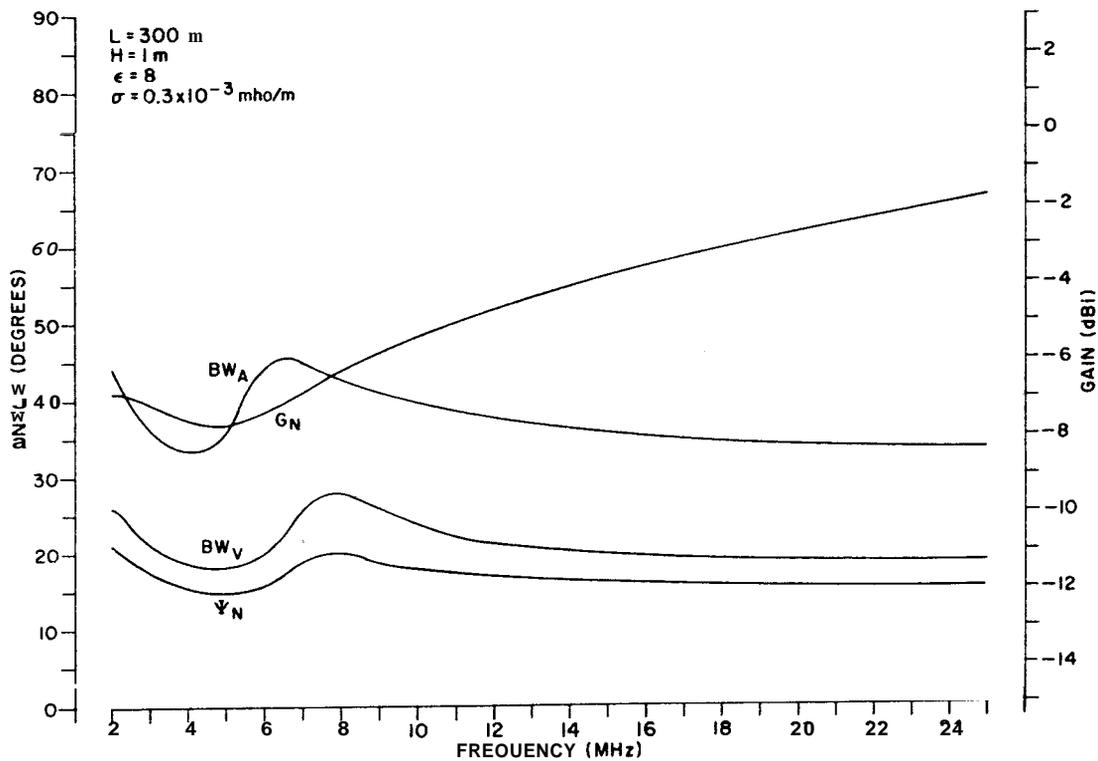
Figure II-7. Design Parameters for Poor Soil (Dry), H = 1m, L = 300m.
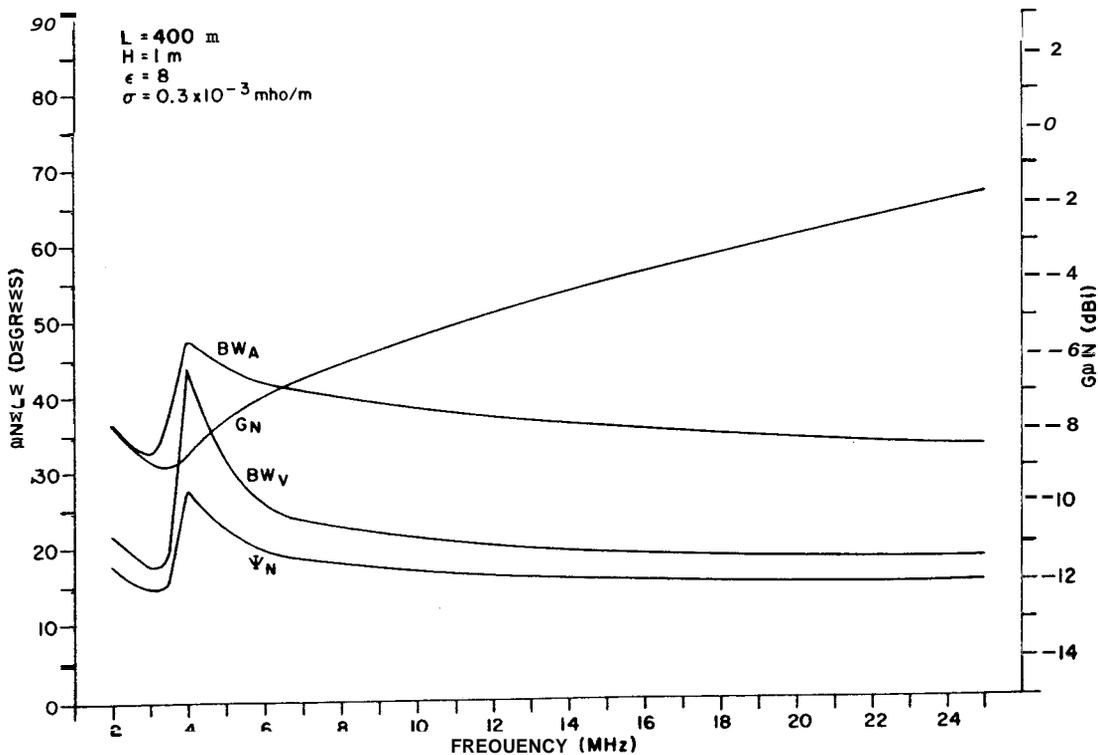
Figure 11-8. Design Parameters for Poor Soil (Dry), H = 1m, L = 400m.
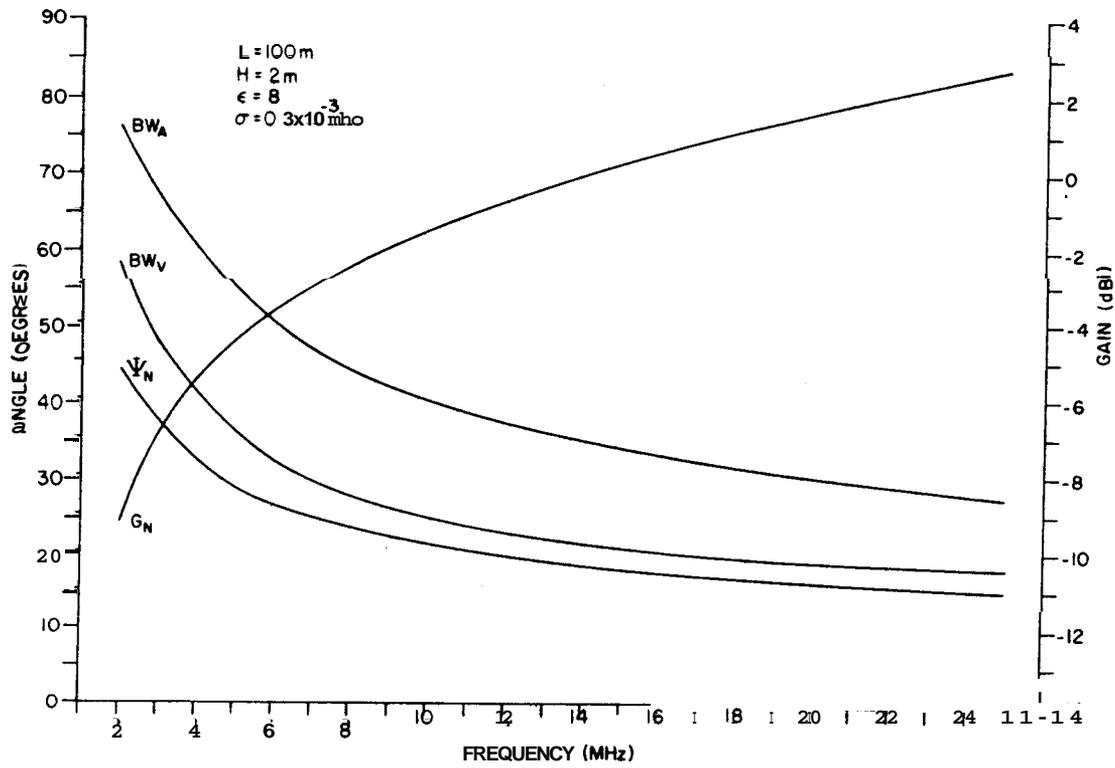
Figure 11-9. Design Parameters for Poor Soil (Dry), H = 2m, L = 100m.
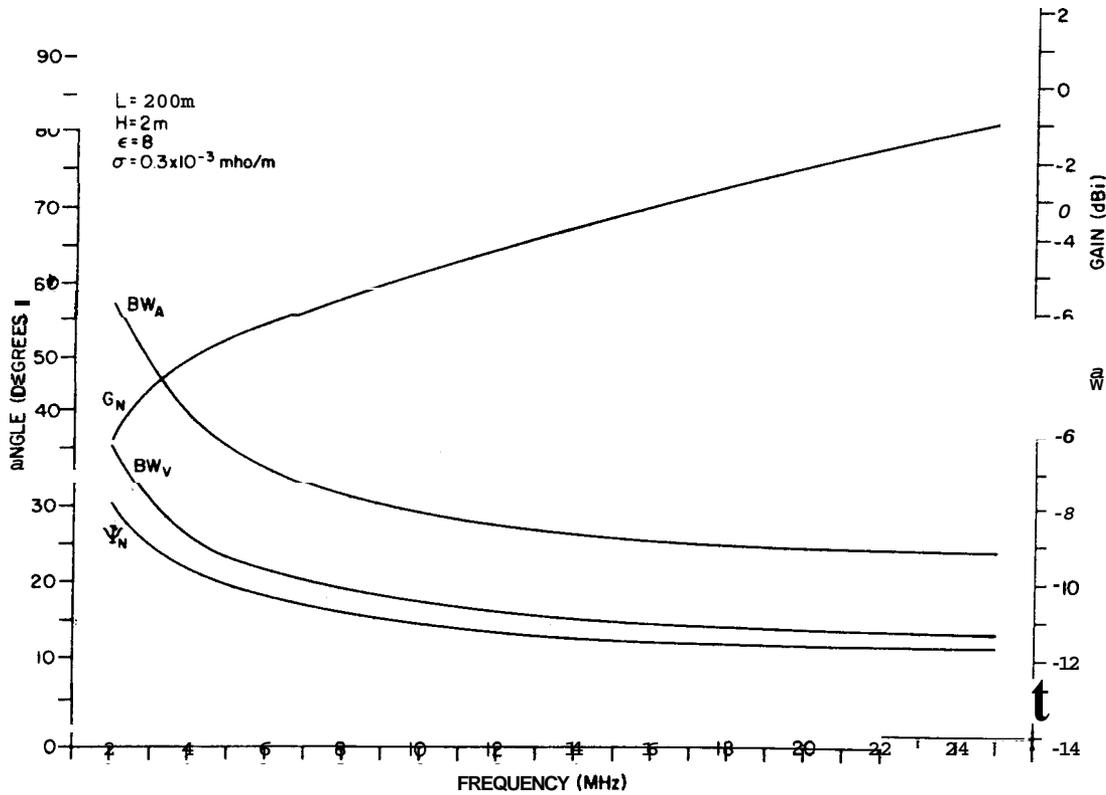
Figure II-10. Design Parameters for Poor Soil (Dry), H = 2m, L = 200m.
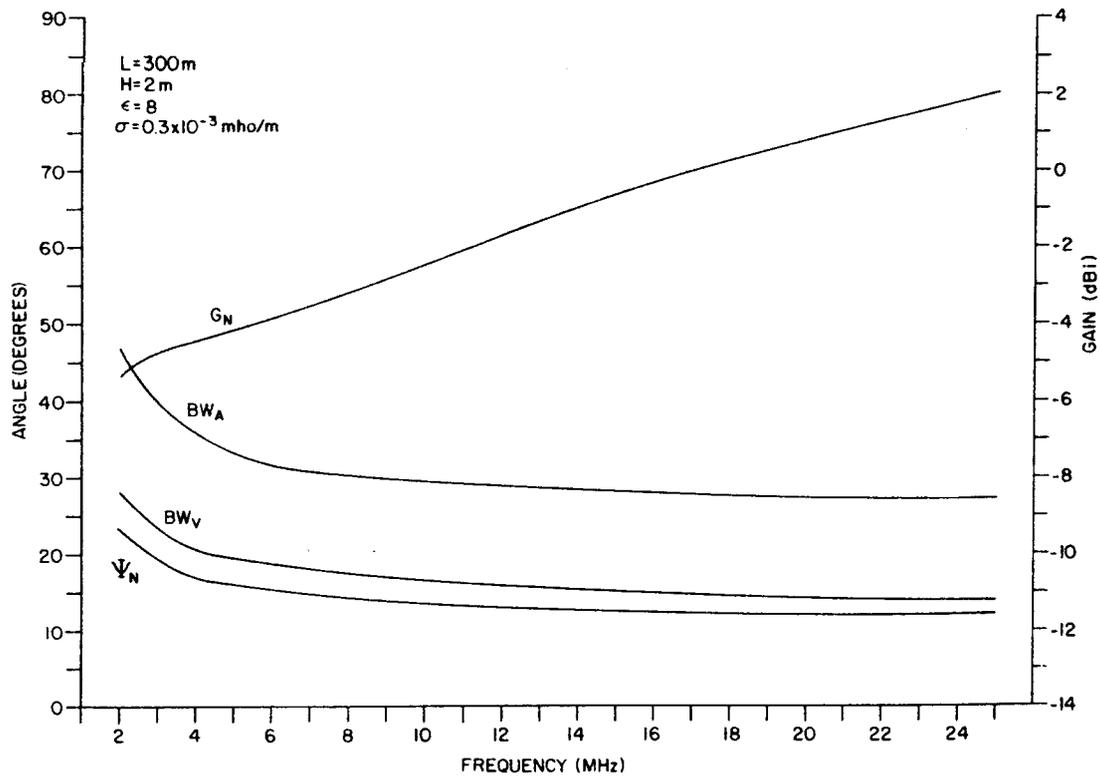
Figure II-11. Design Parameters for Poor Soil (Dry), H = 2m, L = 300m.
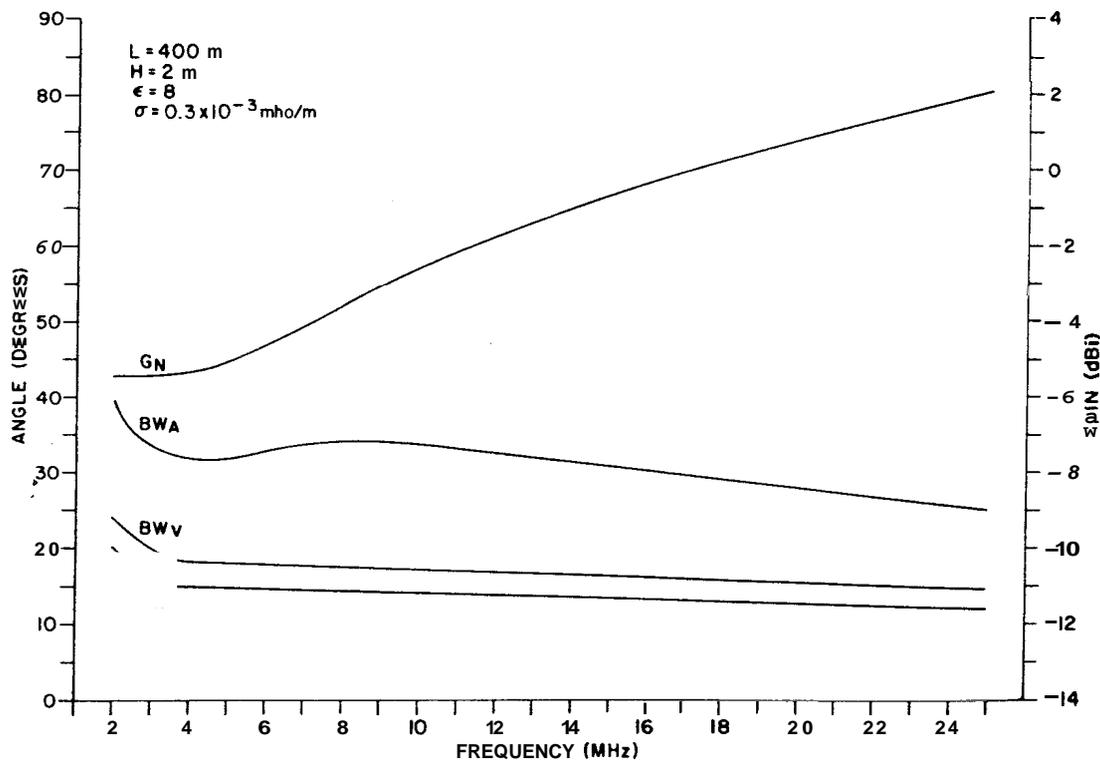
Figure II-12. Design Parameters for Poor Soil (Dry), H = 2m, L = 400m.
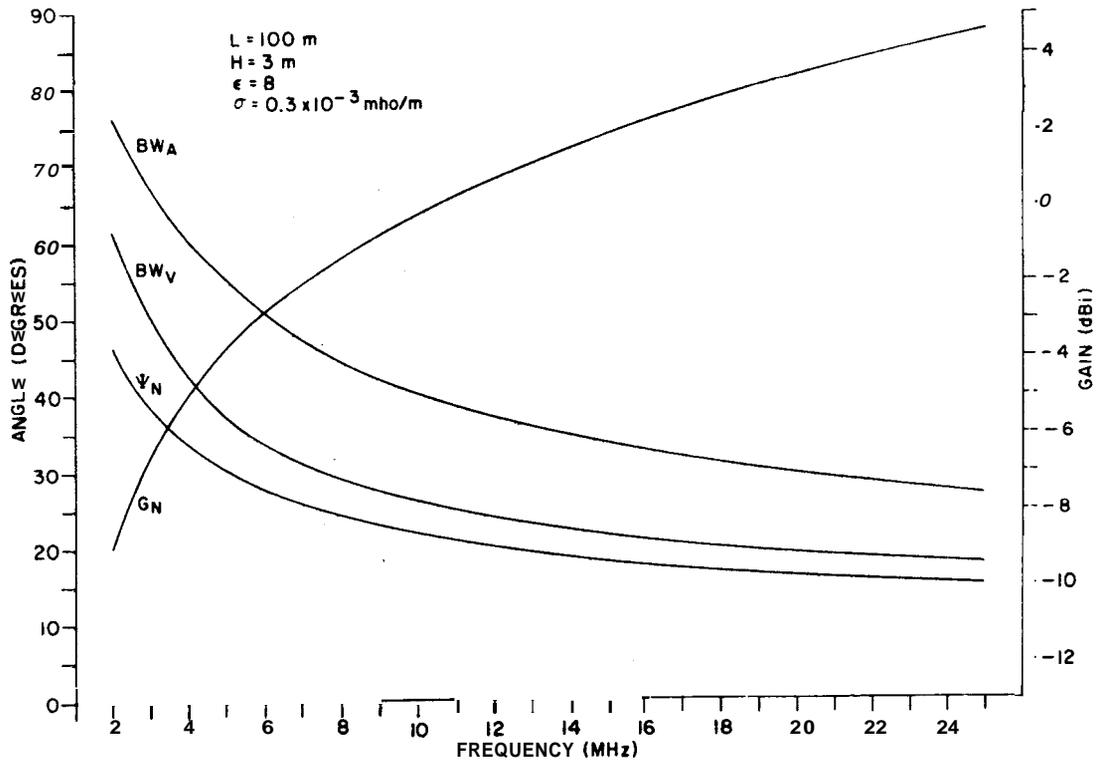
Figure II- 13. Design Parameters for Poor Soil (Dry), H = 3m, L = 100m.
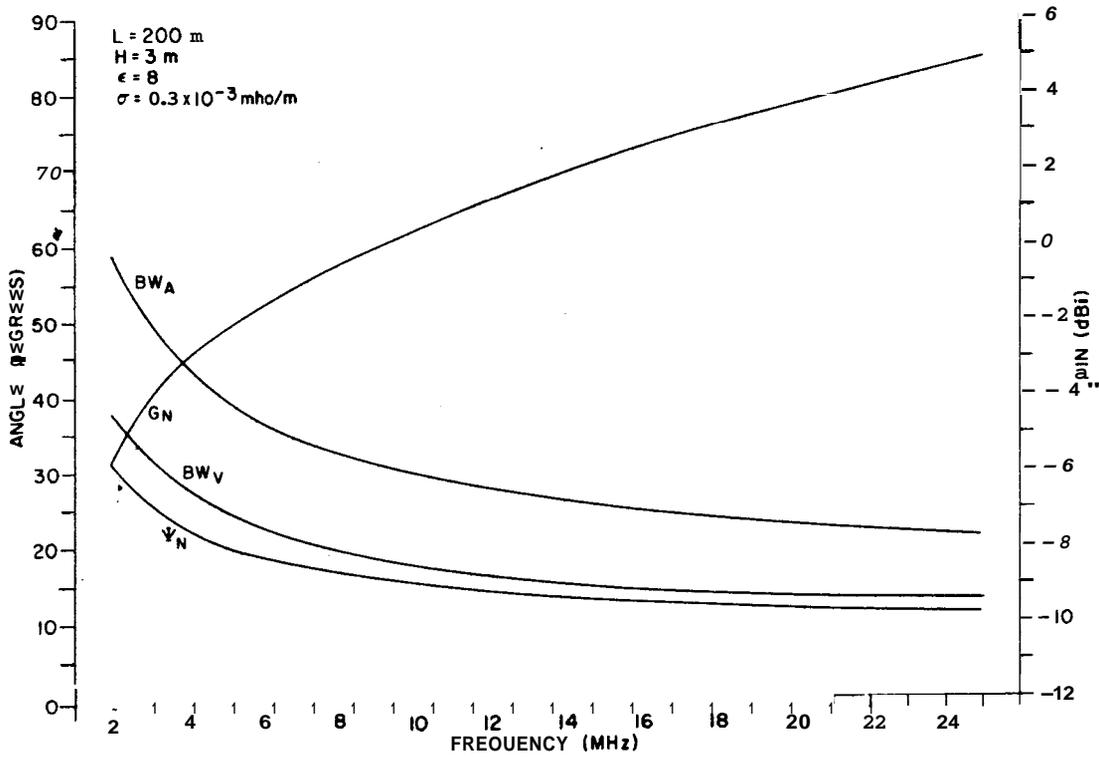
Figure II- 14. Design Parameters for Poor Soil (Dry), H = 3m, L = 200m.
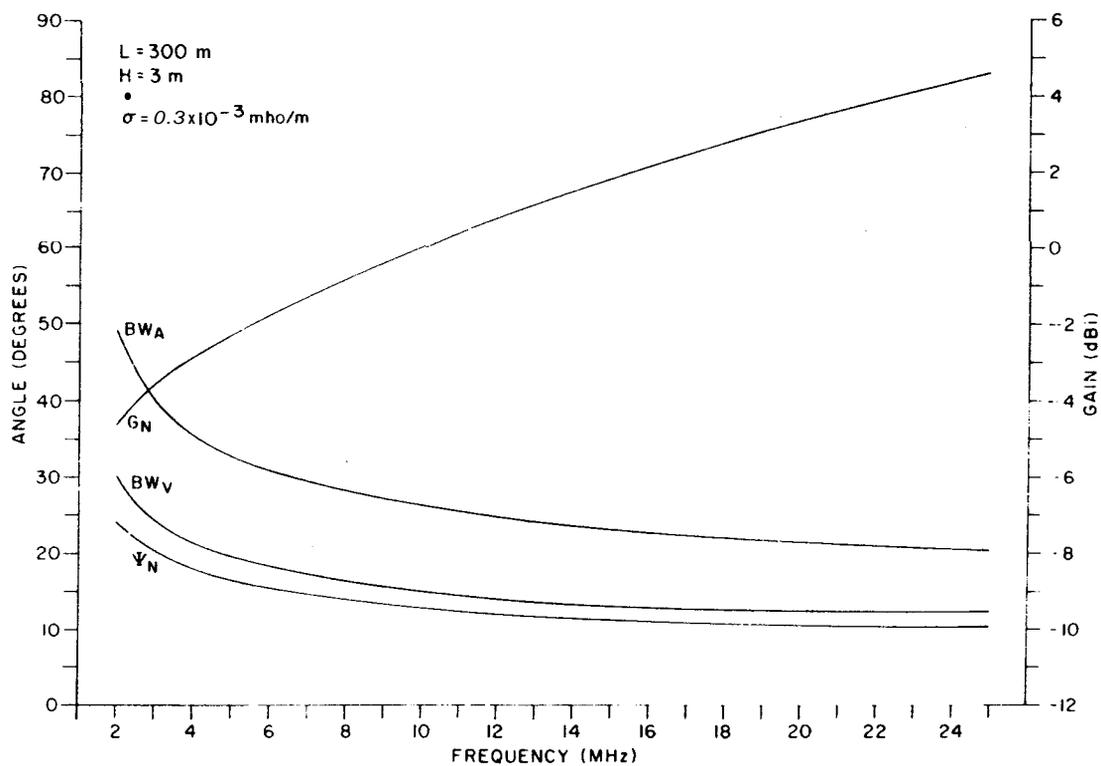
Figure II-15. Design Parameters for Poor Soil (Dry), H = 3m, L = 300m.
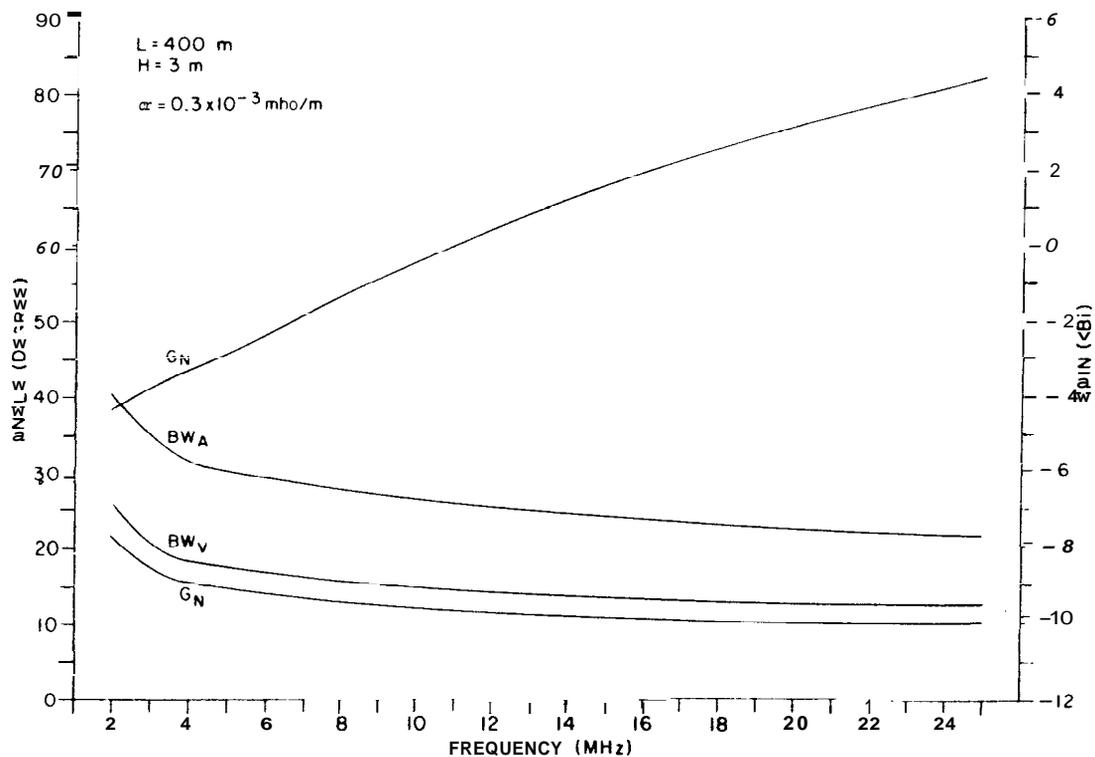
Figure II- 16. Design Parameters for Poor Soil (Dry), H = 3m, L = 400m.
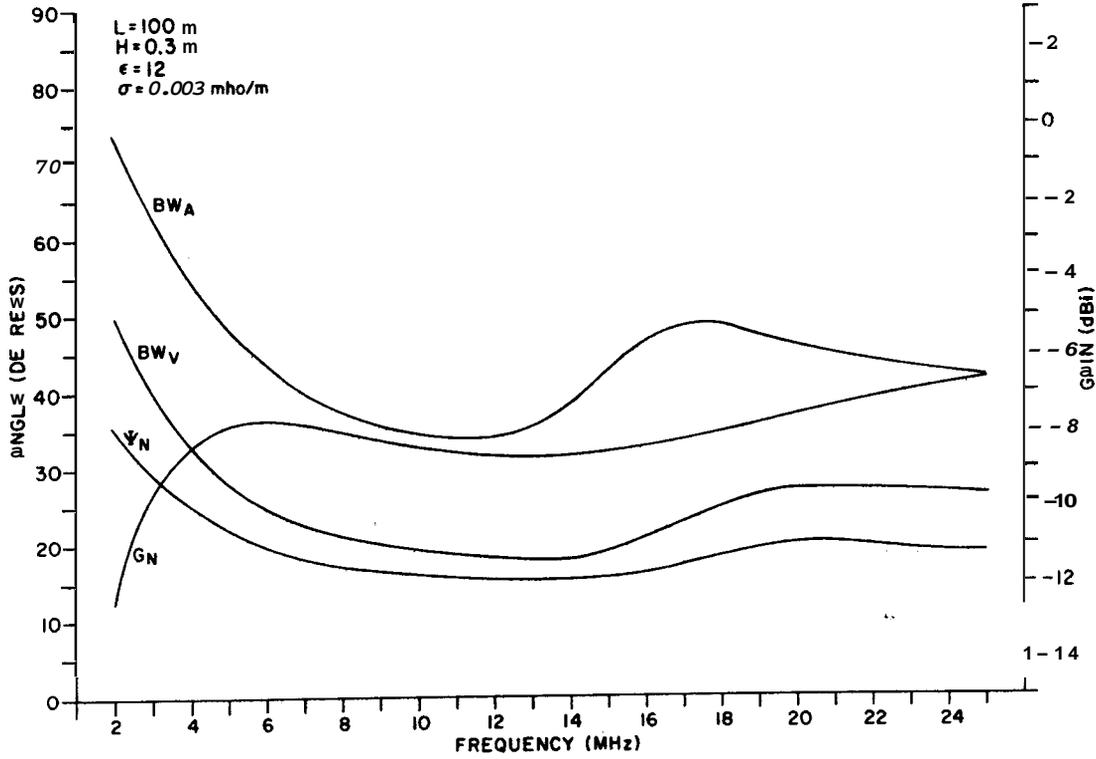
Figure *II-17.* Design Parameters *for Average Soil (Dry),* $H = 0.3m$, $L = 100m$.
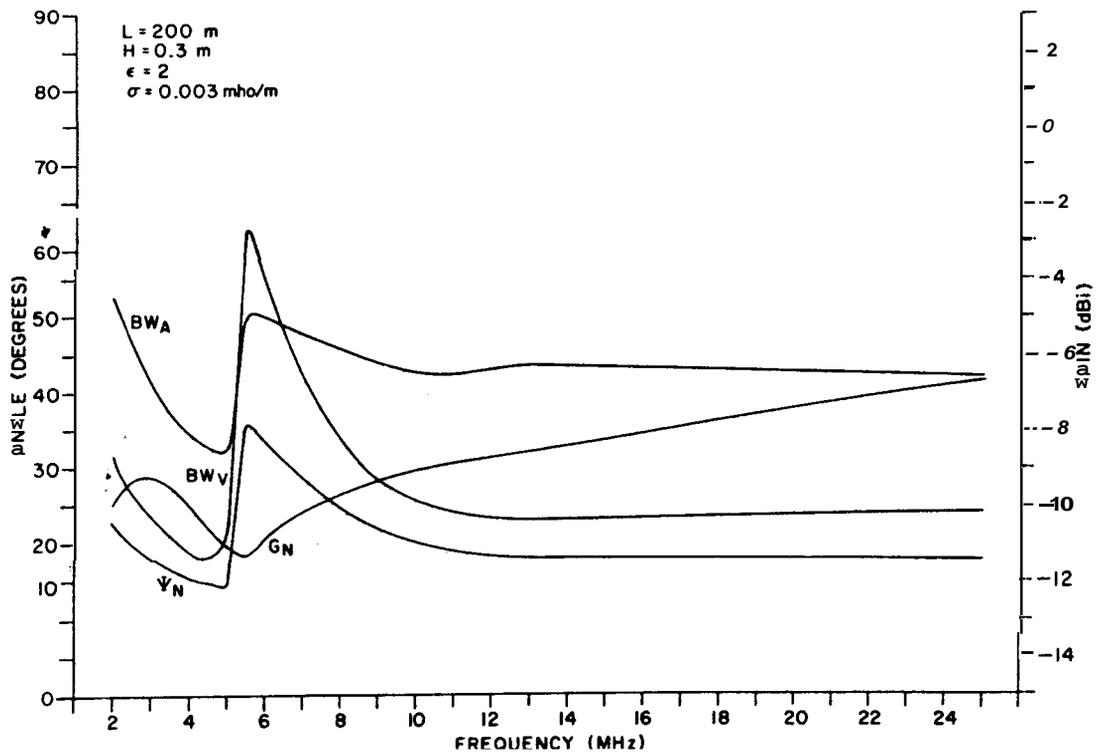
Figure *II- 18.* Design Parameters *for Average Soil (Dry),* $H = 0.3m$, $L = 200m$.
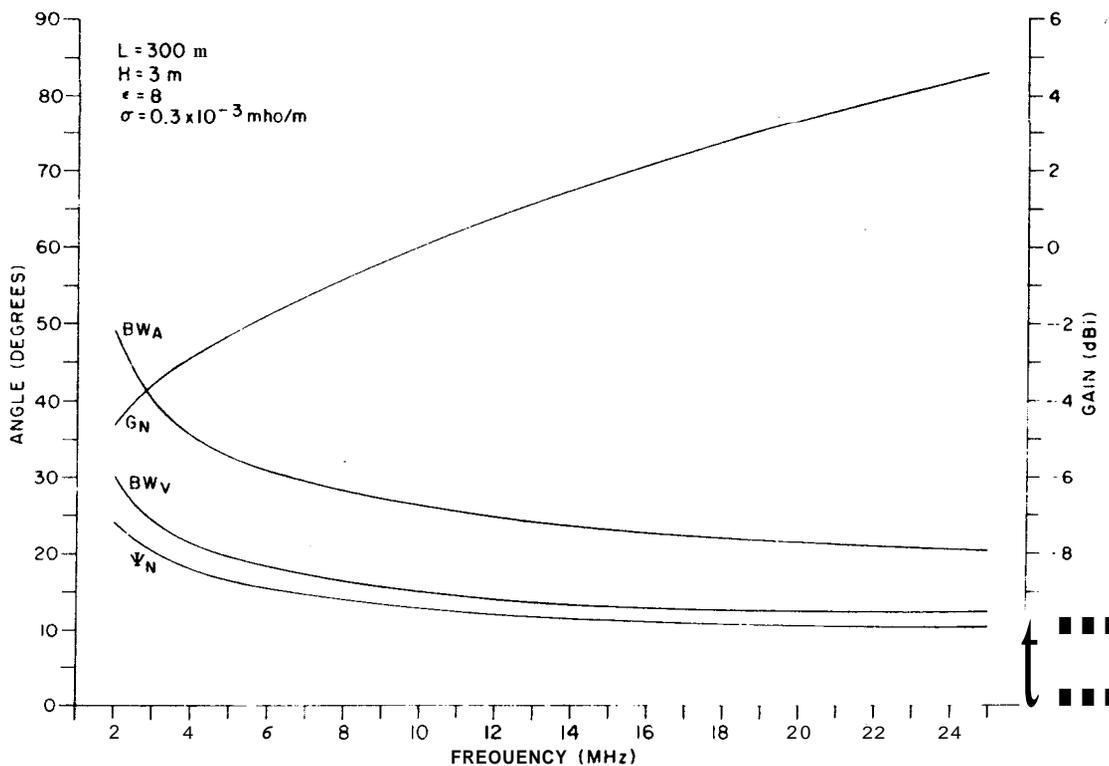
Figure II-15. **Design Parameters** for **Poor** Soil *(Dry)*, H = 3m, L = 300m.
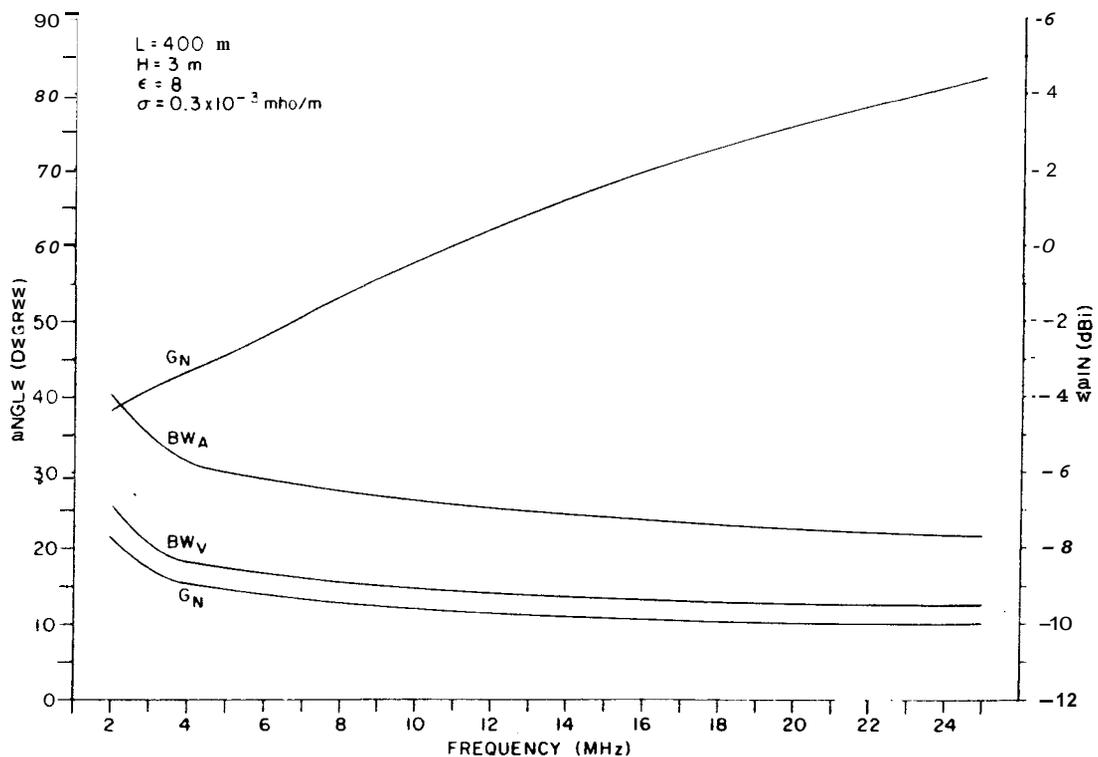
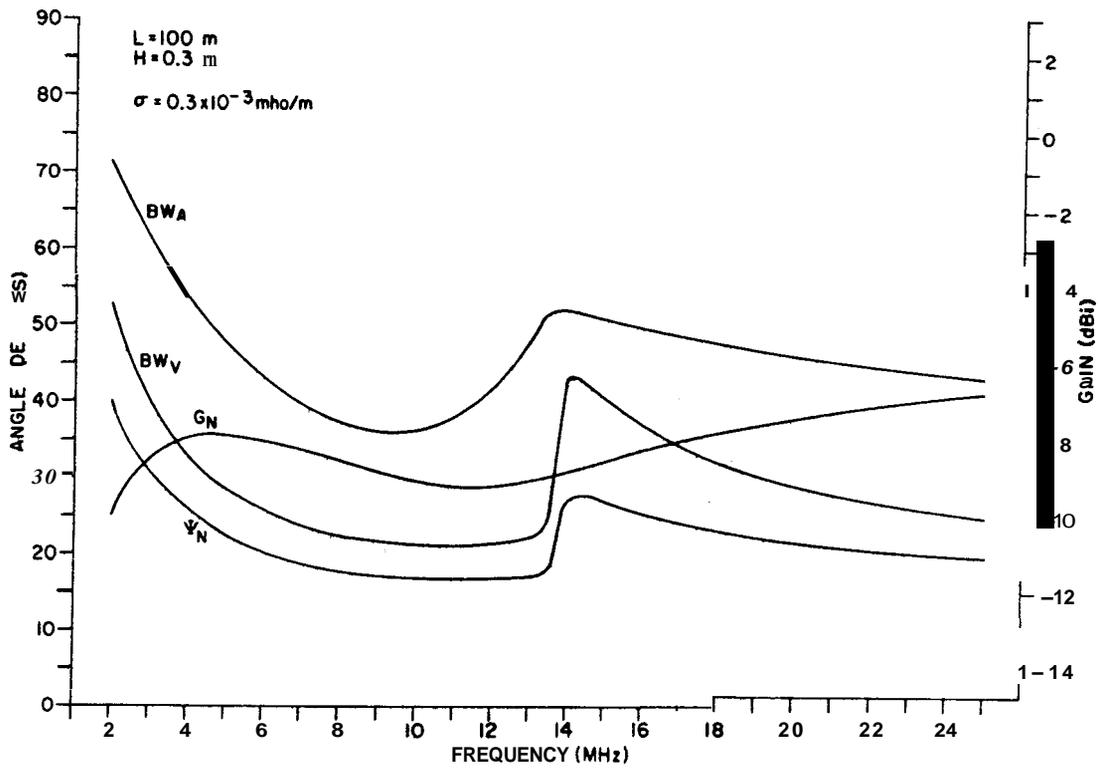**Figure II-16. Design Parameters for Poor Soil (Dry),** H = 3m, L = 400m.
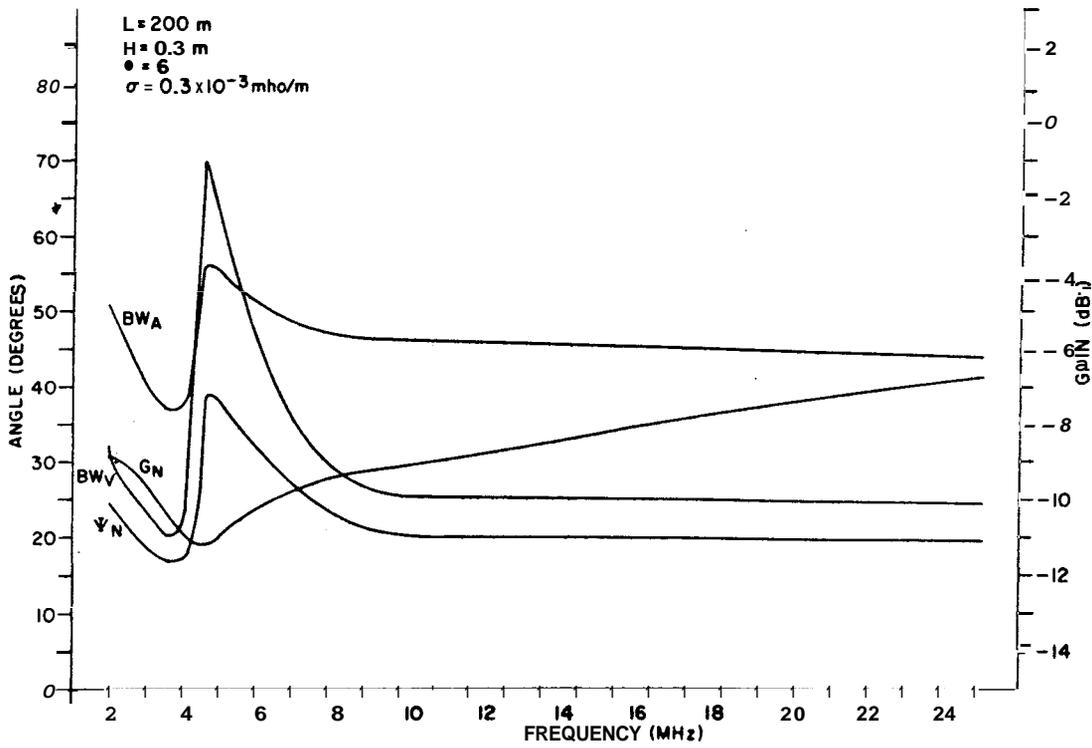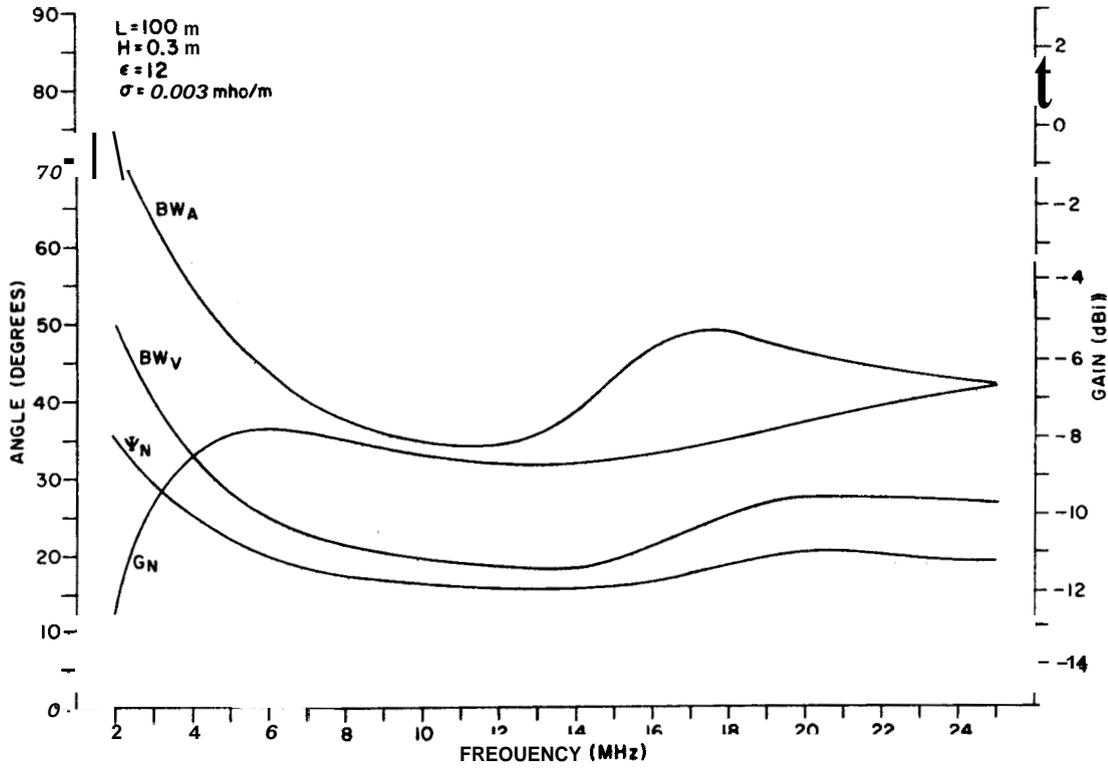
Figure 11-17. Design Parameters for Average Soil (Dry), $H = 0.3m$, $L = 100m$.
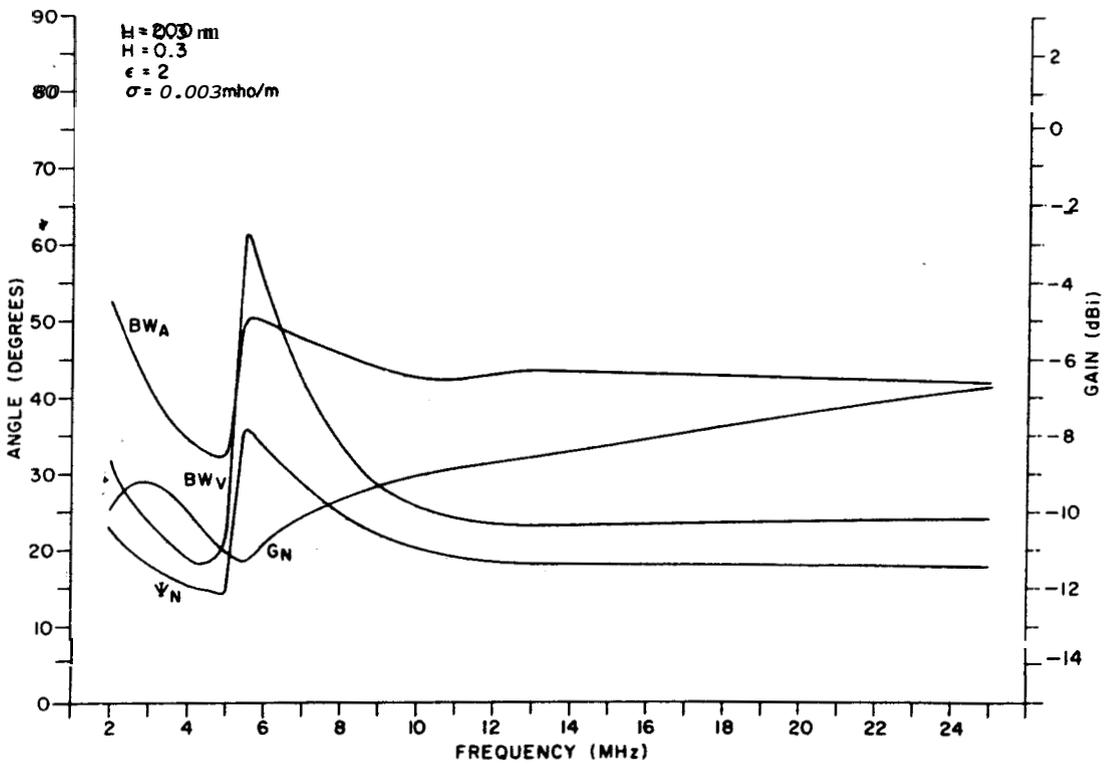
Figure II-18. Design Parameters for Average Soil (Dry), H = 0.3m, L = 200m.
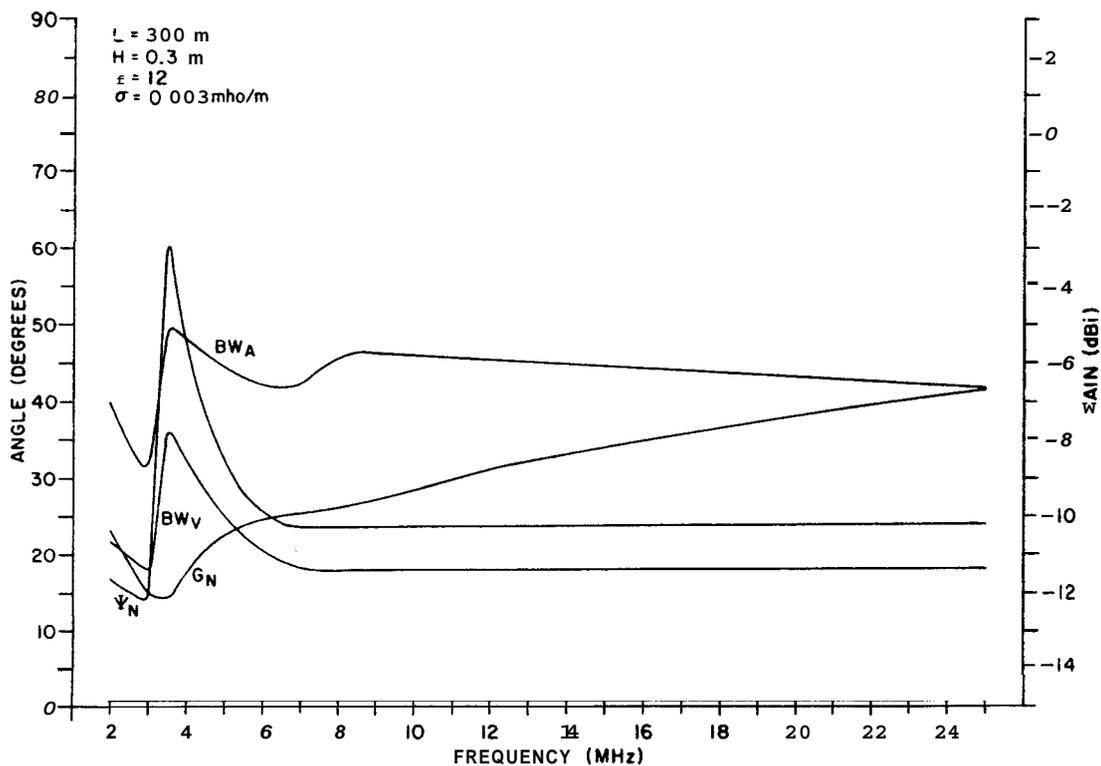
Figure 11-19. *Design Parameters for Average Soil (Dry), H = 0.3m, L = 300m.*
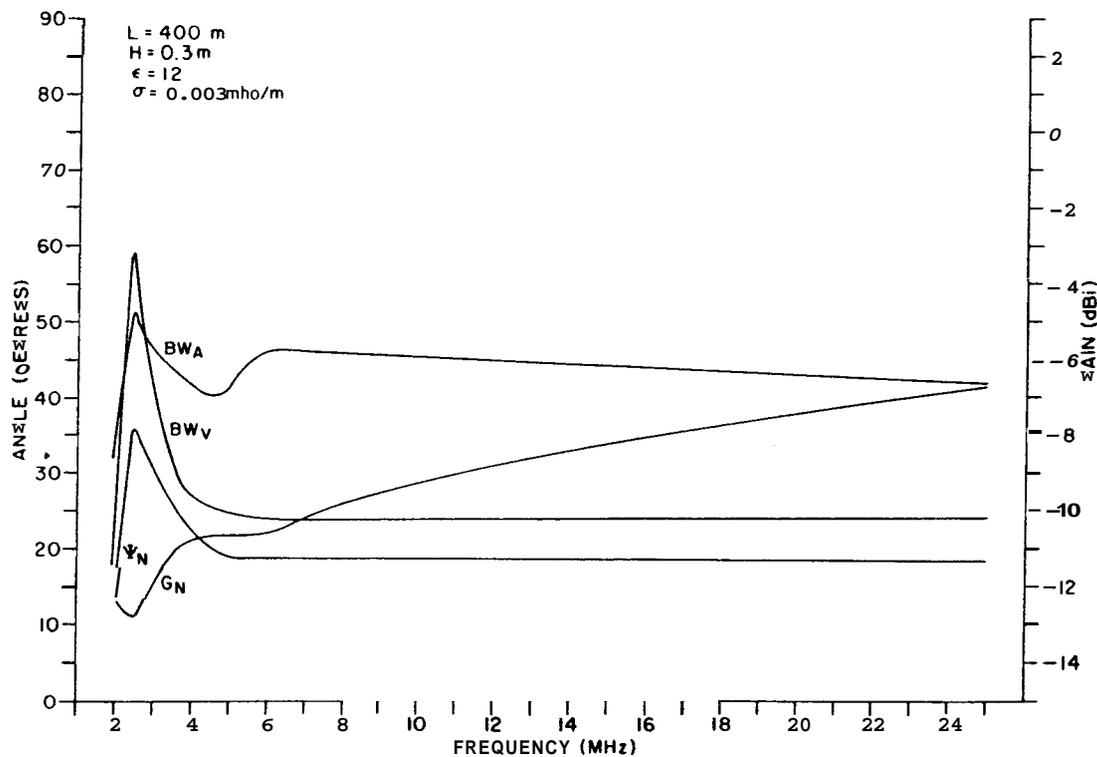
Figure 11-20. *Design Parameters for Average Soil (Dry), H = 0.3m, L = 400m.*
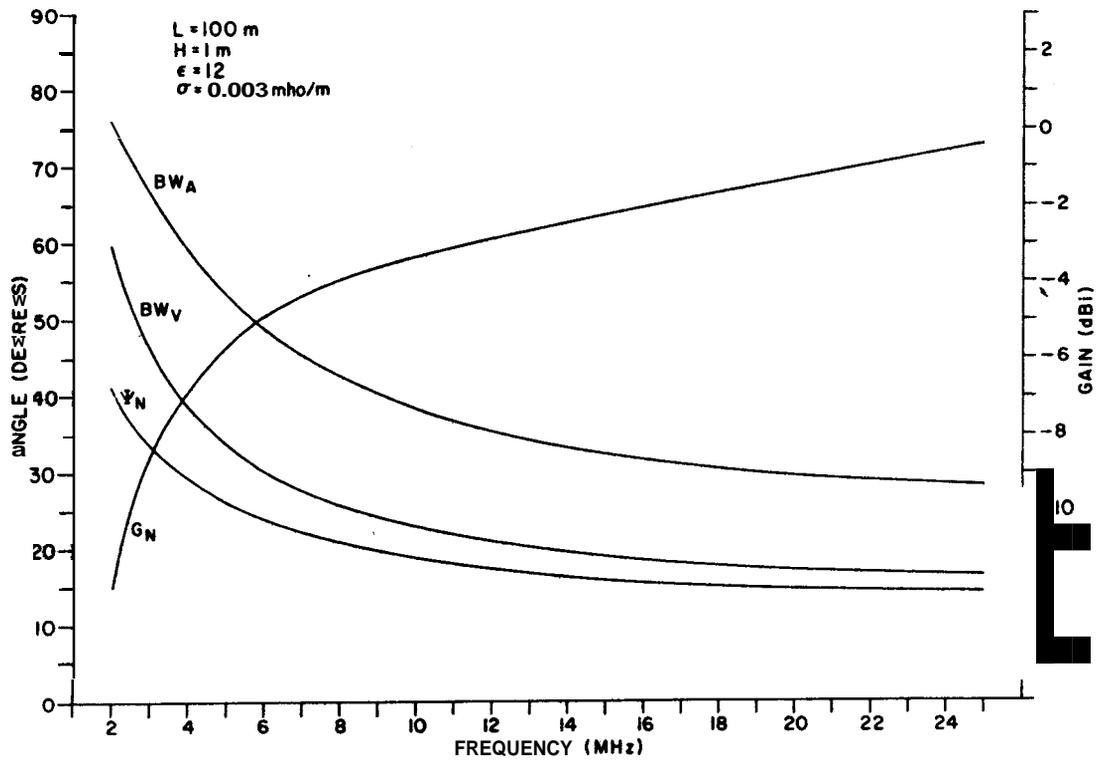
Figure 11-21. Design Parameters for Average Soil (Dry), H = 1m, L = 100m.
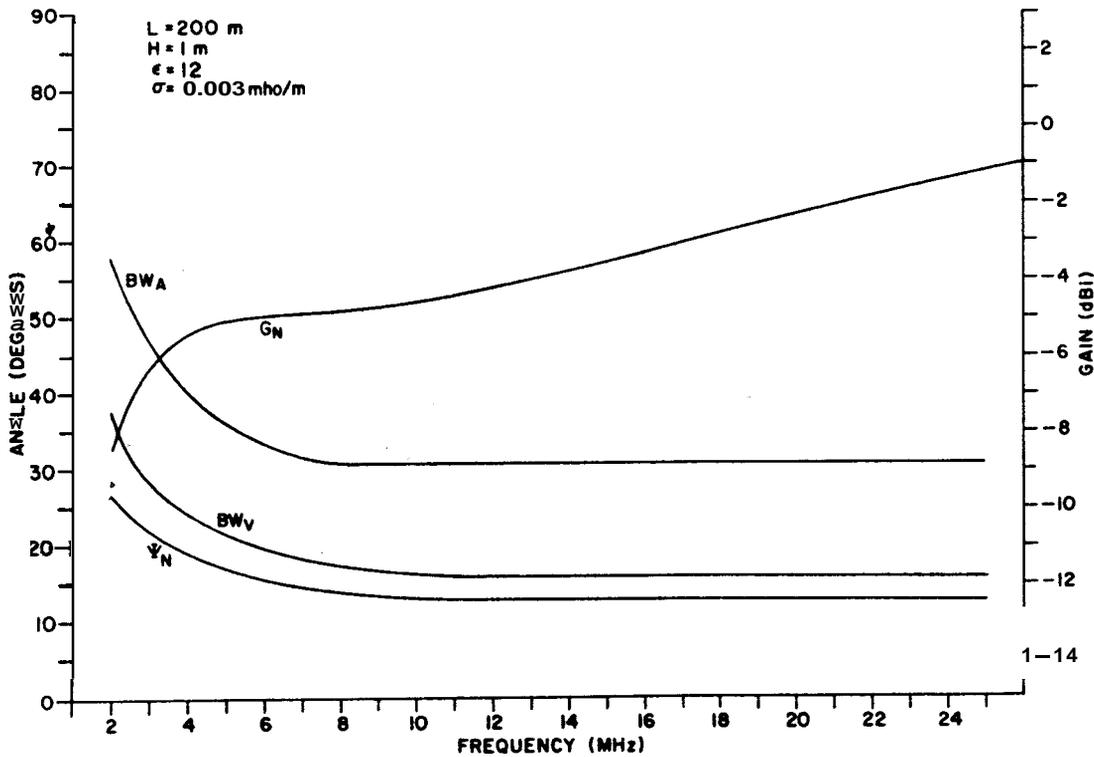
Figure 11-22. Design Parameters for Average Soil (Dry), H = 1m, L = 200m.
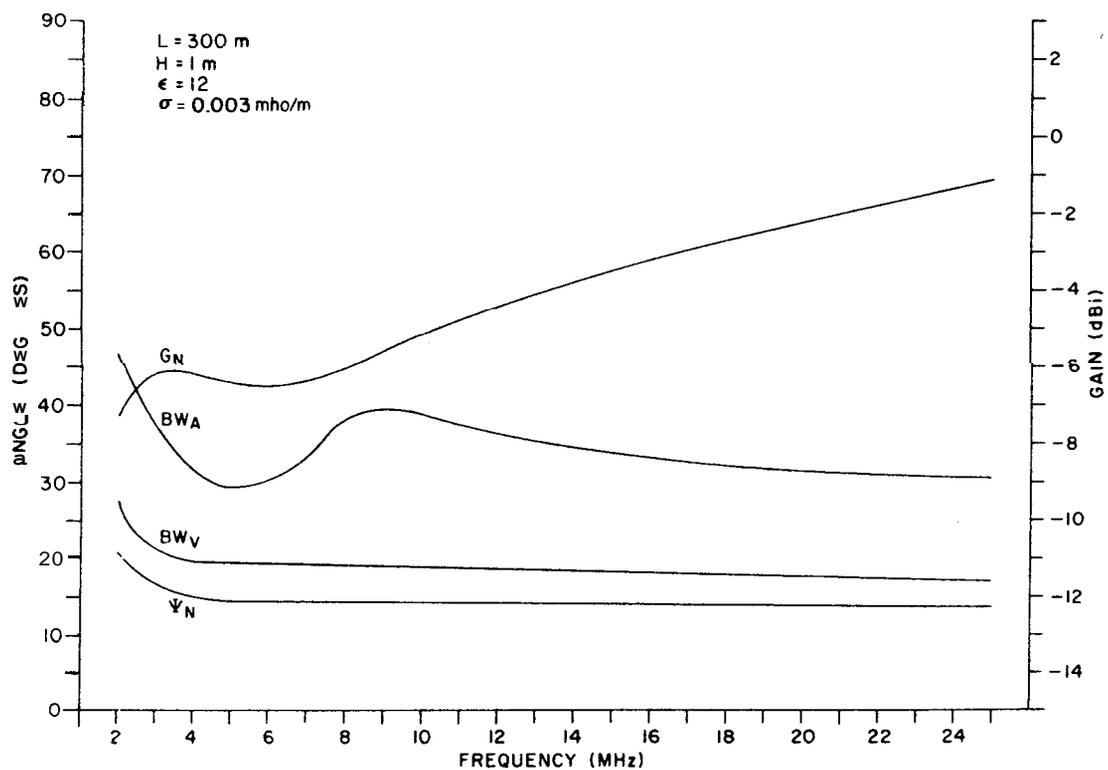
Figure 11-23. *Design Parameters for Average Soil (Dry), H = 1m, L = 300m.*
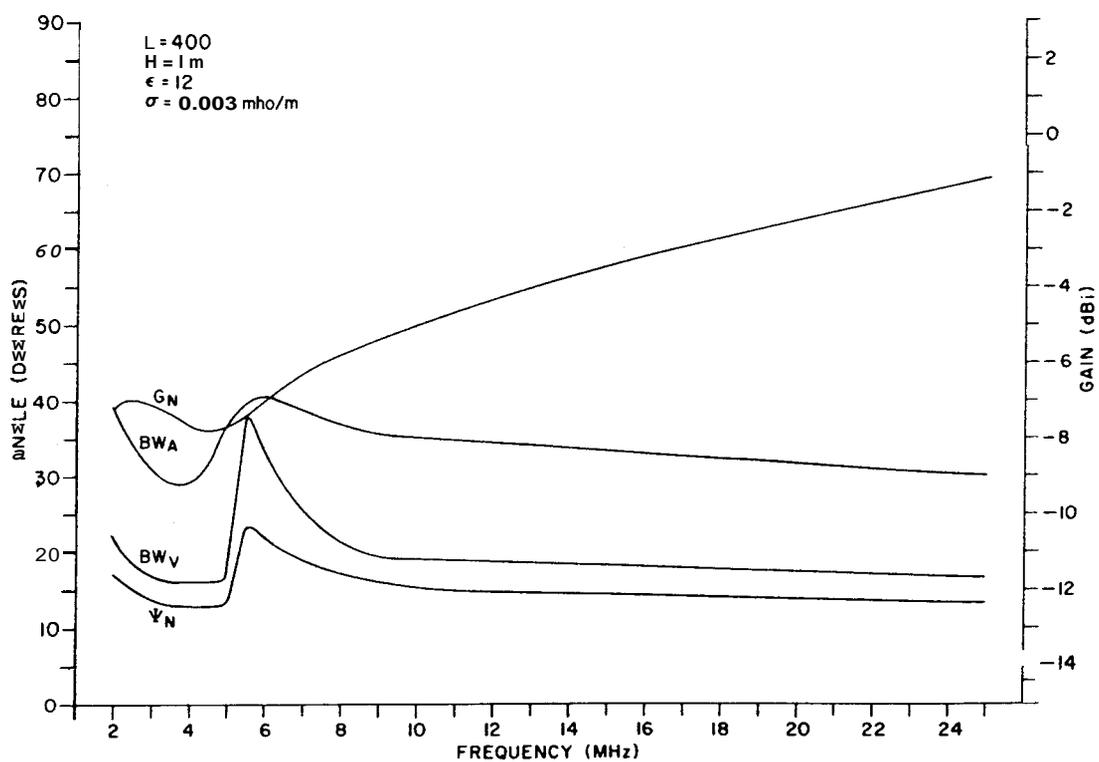
Figure 11-24. *Design Parameters for Average Soil (Dry), H = 1m, L = 400m.*
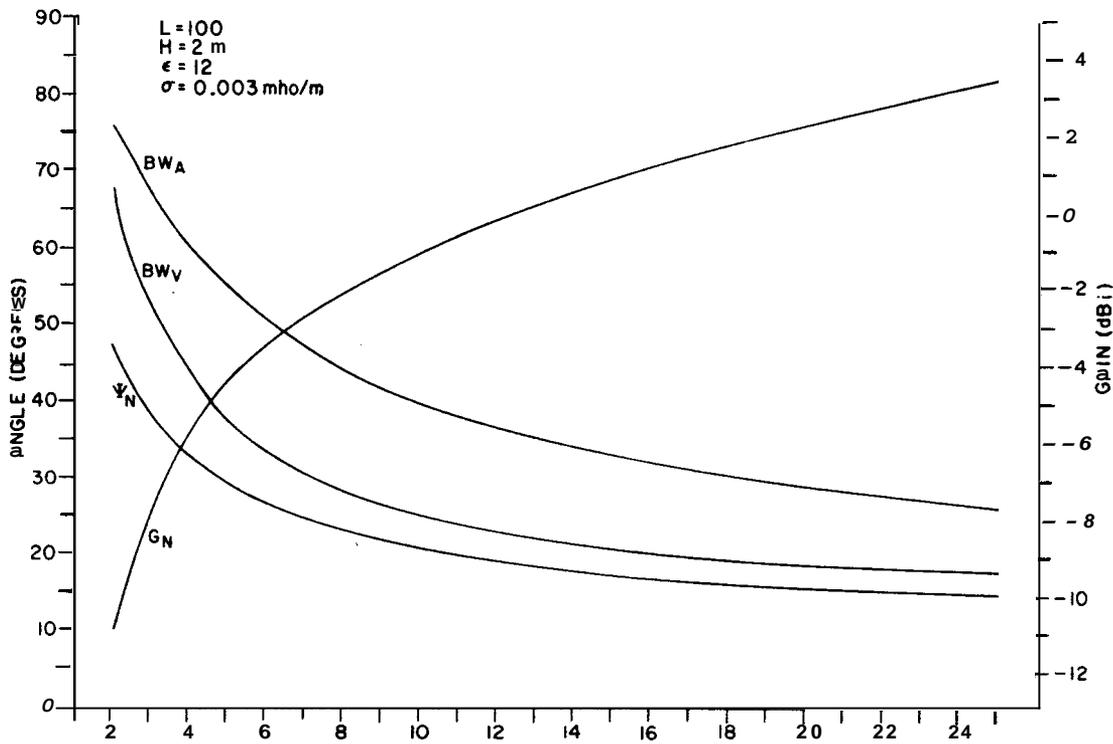
Figure II-25. *Design Parameters for Average Soil (Dry), H = 2m, L = 100m.*
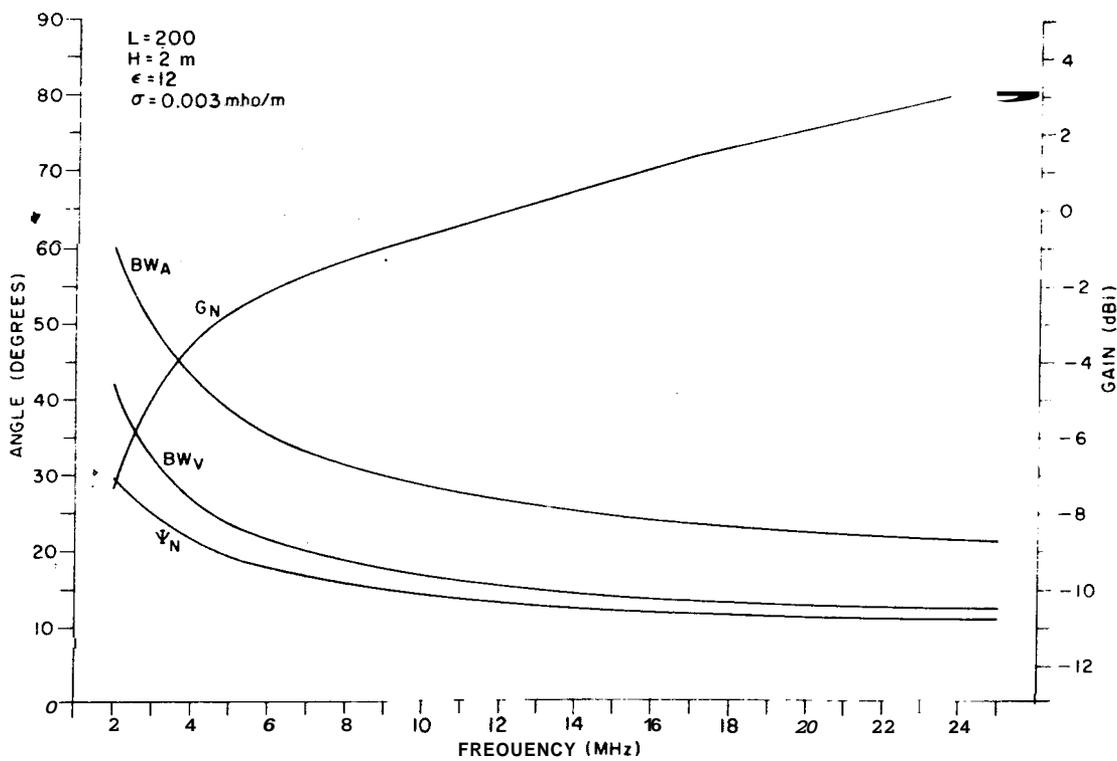
Figure 11-26. **Design Parameters for Average Soil (Dry), H = 2m, L = 200m.**
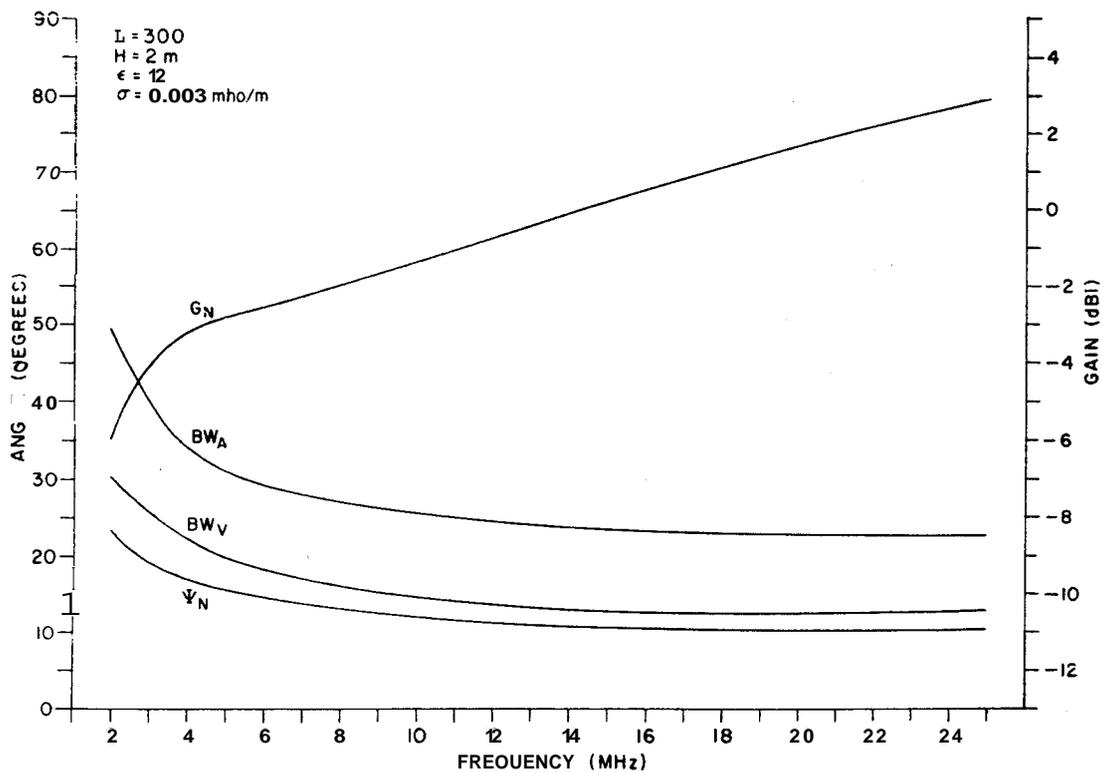
Figure 11-27. Design Parameters for Average Soil (Dry), H = 2m, L = 300m.
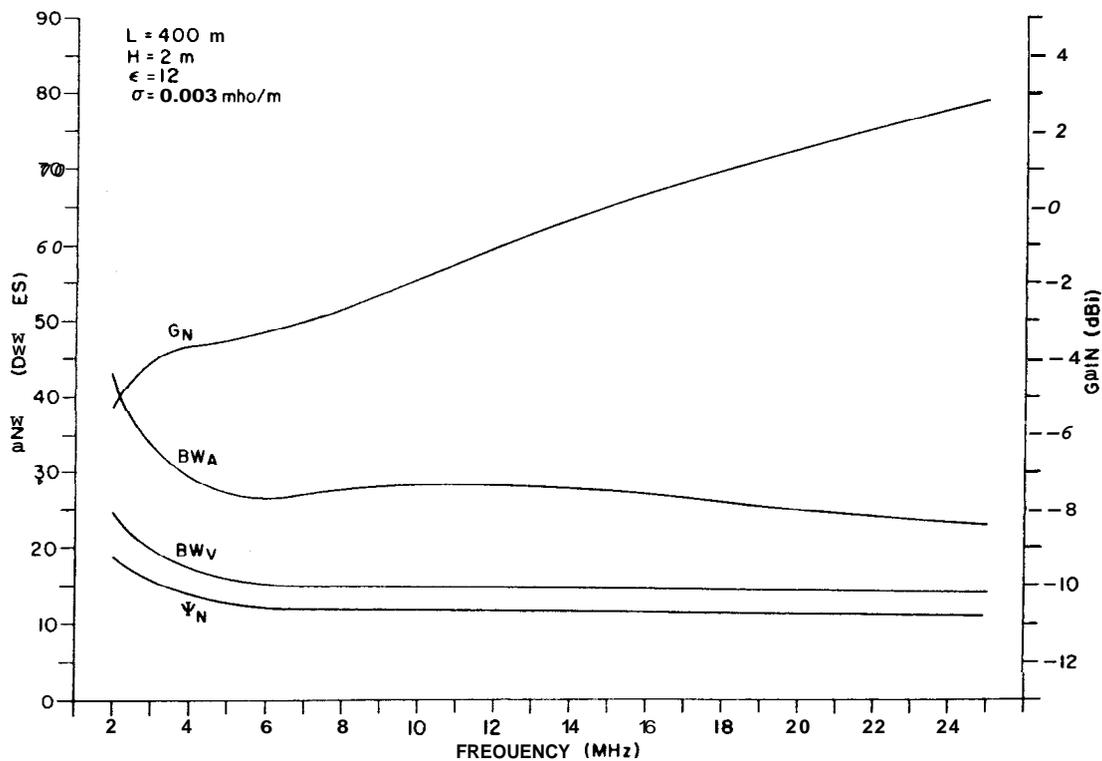
Figure 11-28. Design Parameters for Average Soil (Dry), H = 2m, L = 400m.
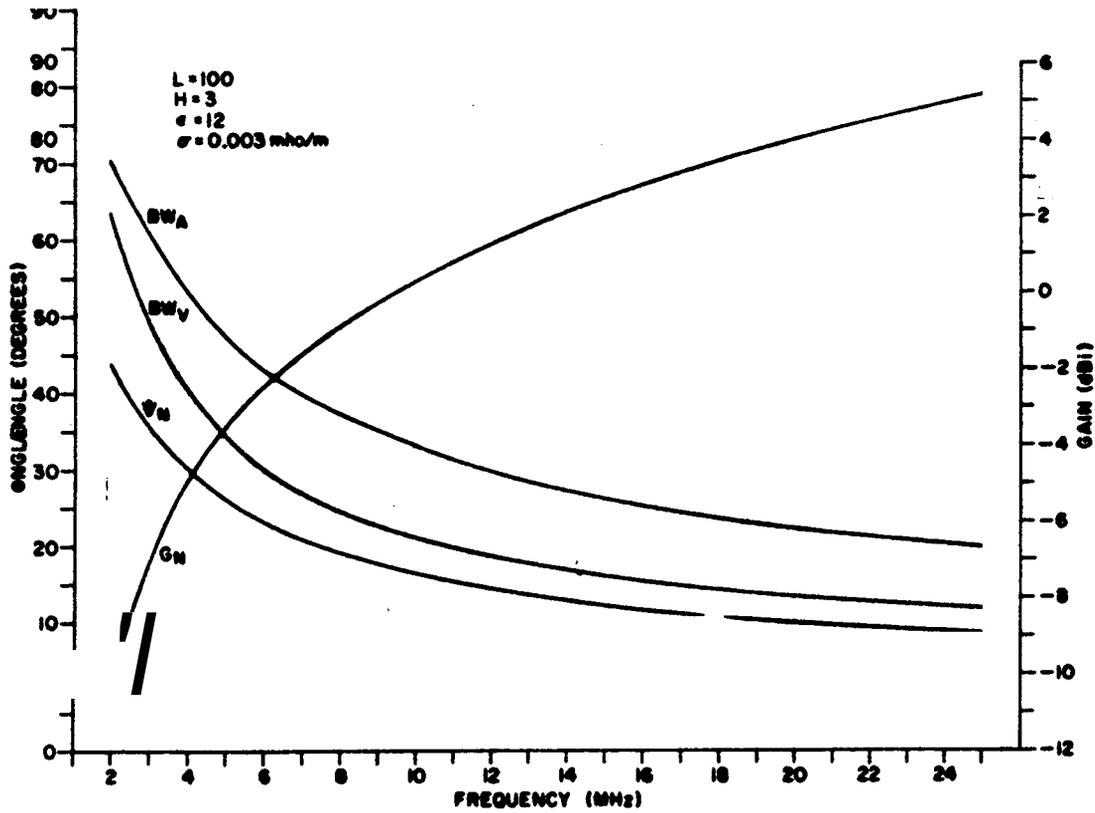
Figure II-29. Design Parameters for Average Soil (Dry), H = 3m, L = 100m.
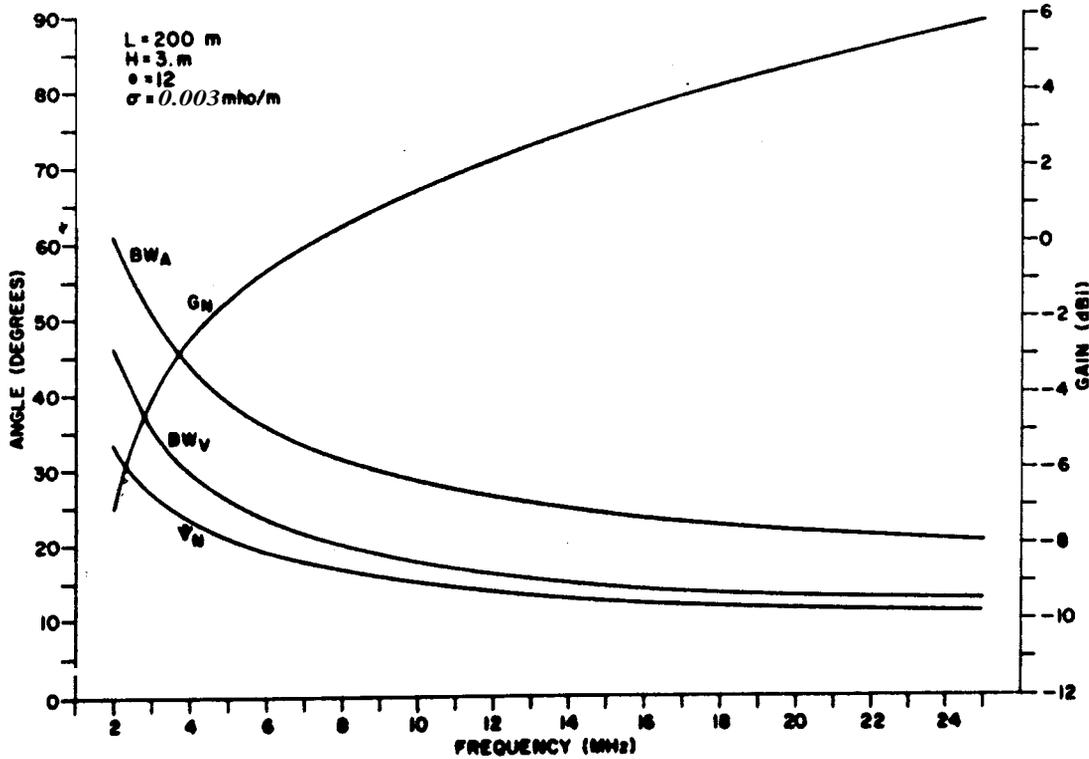
Figure II-30. Design Parameters for Average Soil (Dry), H = 3m, L = 200m.
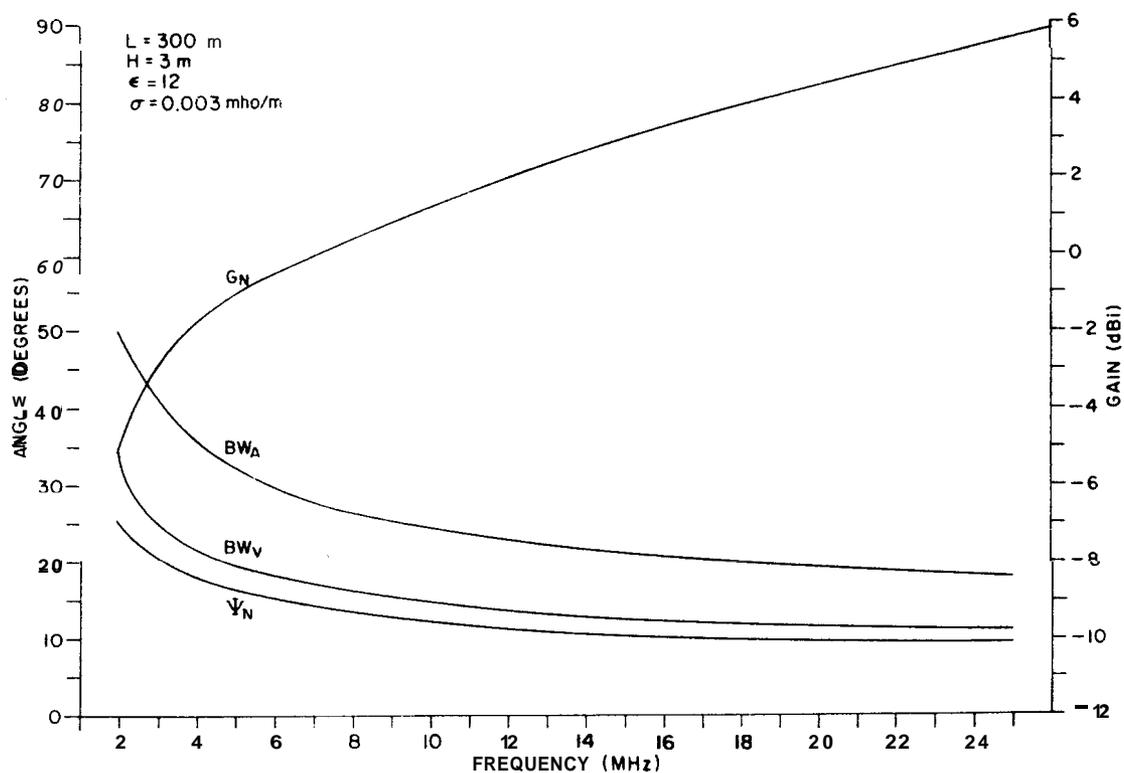
Figure 11-31. *Design Parameters for Average Soil (Dry), H = 3m, L = 300m.*
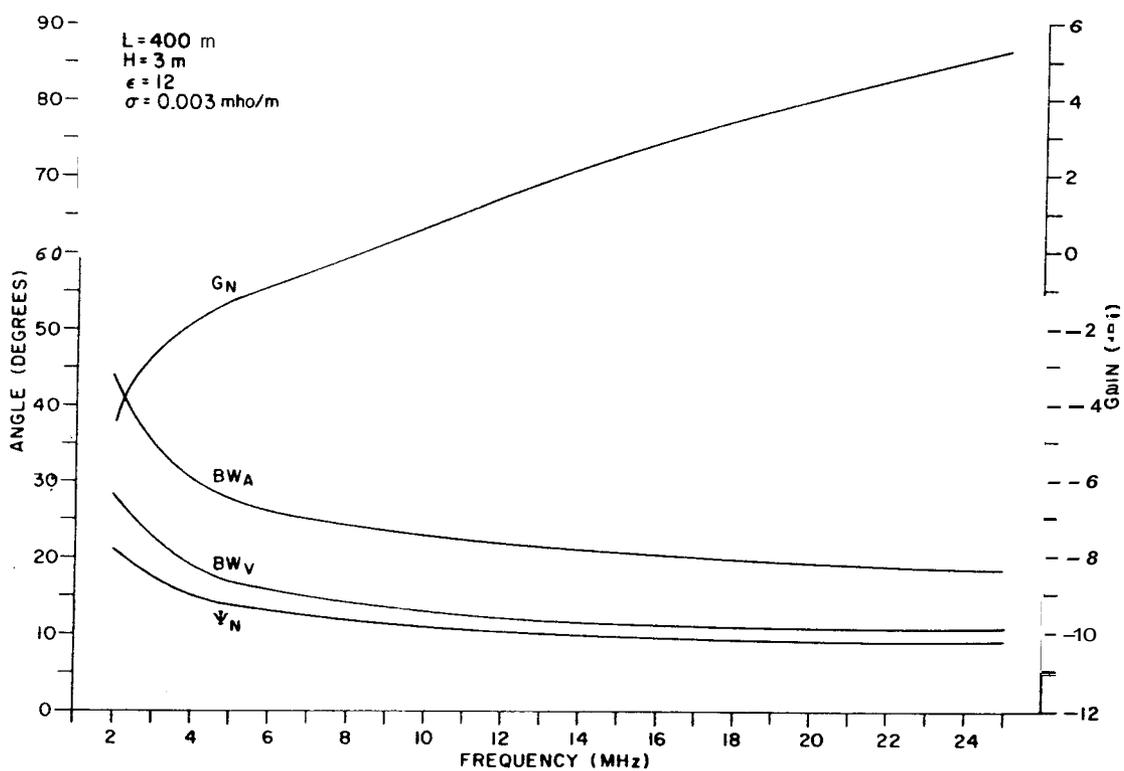
Figure 11-32. *Design Parameters for Average Soil (Dry), H = 3m, L = 400m.*
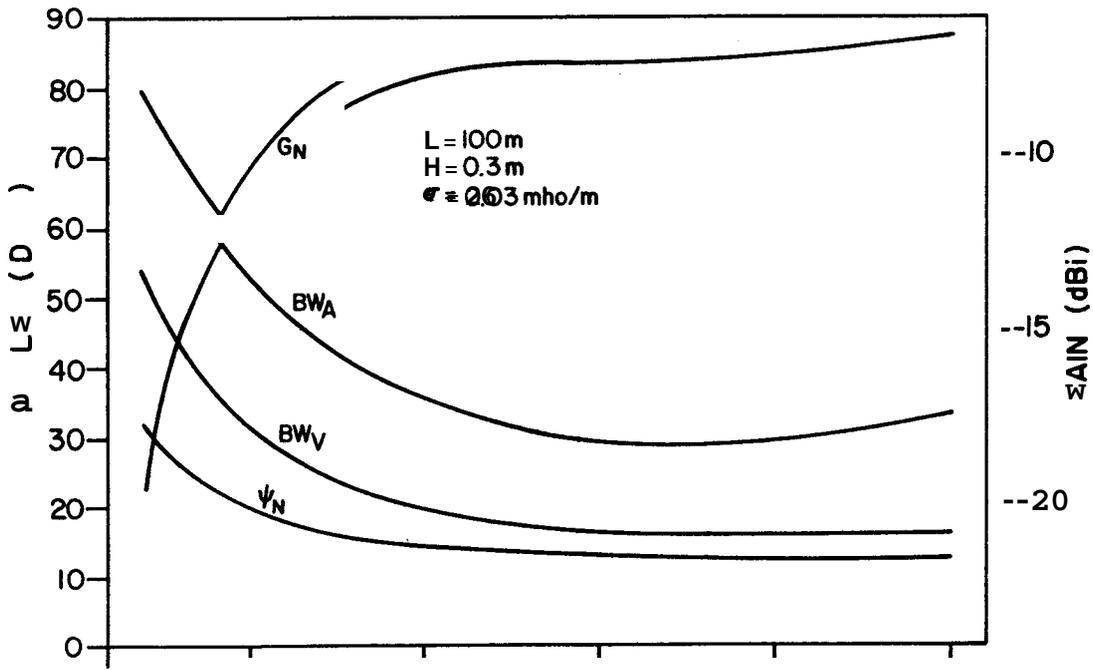
Figure 11-33. Design Parameters for Wet Rich Soil, H = 0.3m, L = 100m.
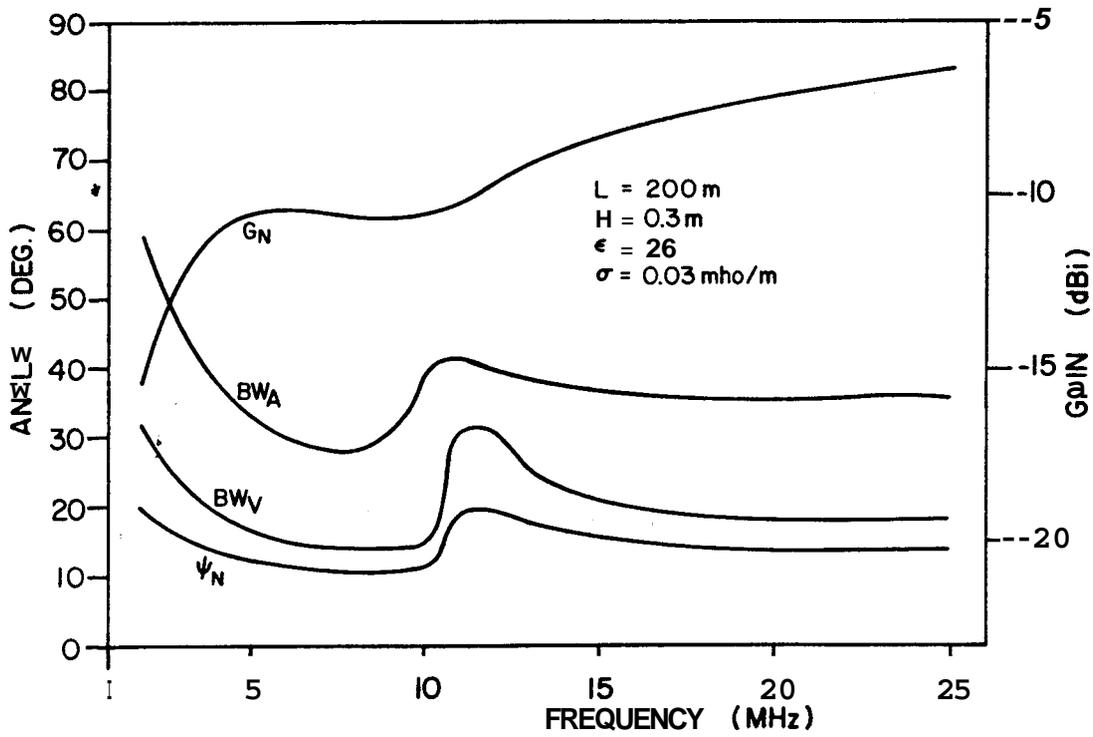
Figure 11-34. Design Parameters for Wet Rich Soil, H = 0.3m, L = 200m.
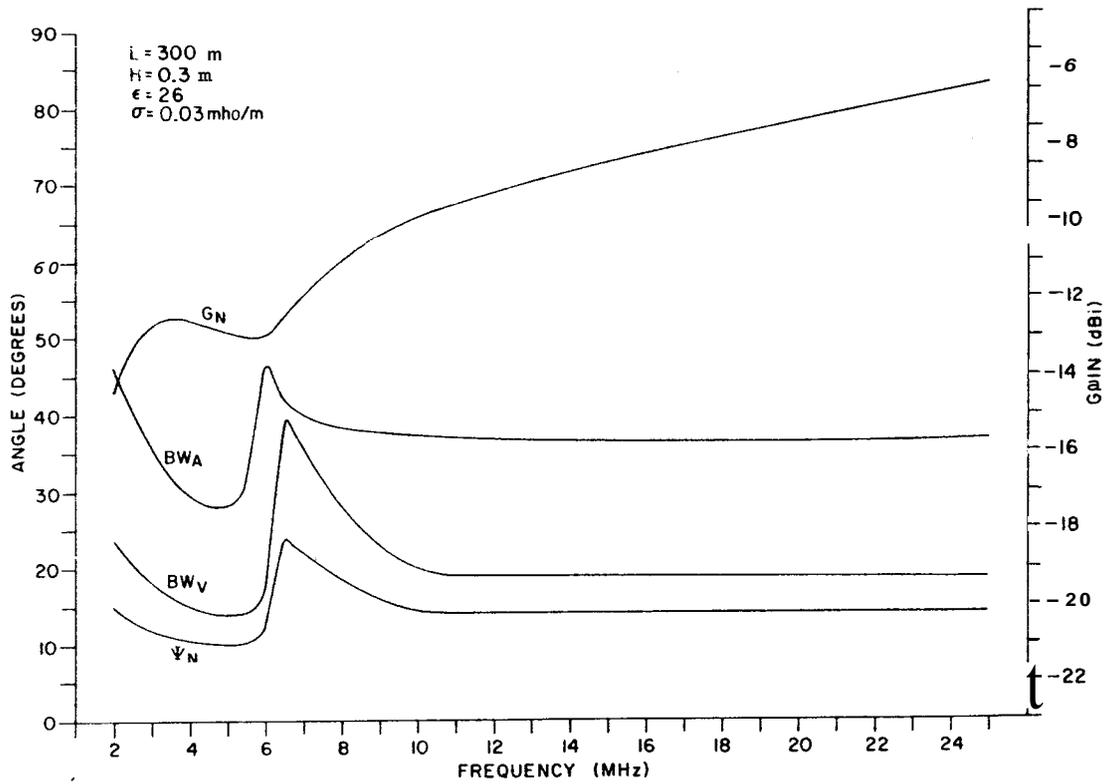
Figure II-35.   Design Parameters for Wet Rich Soil, H= 0.3m, L = 300m.
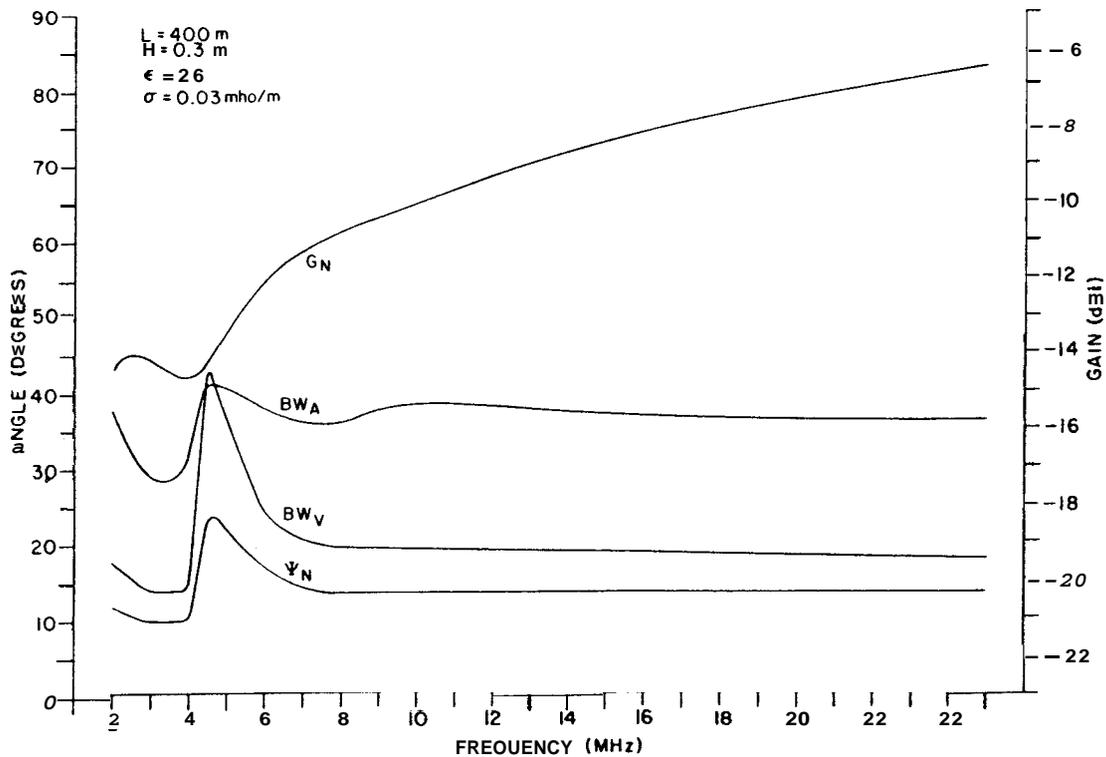
Figure 11-36.   Design Parameters for Wet Rich Soil, H= 0.3m, L = 400m.
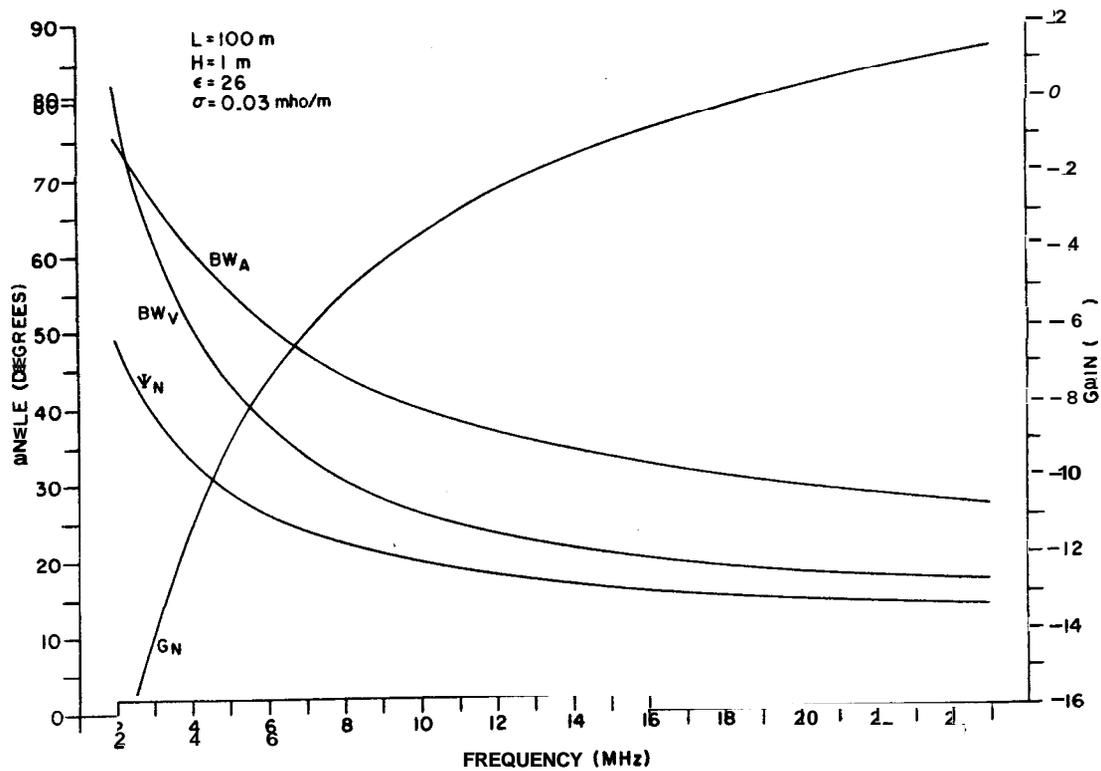
Figure 11-37. Design Parameters for Wet Rich Soil, H= 1m, L = 100m.
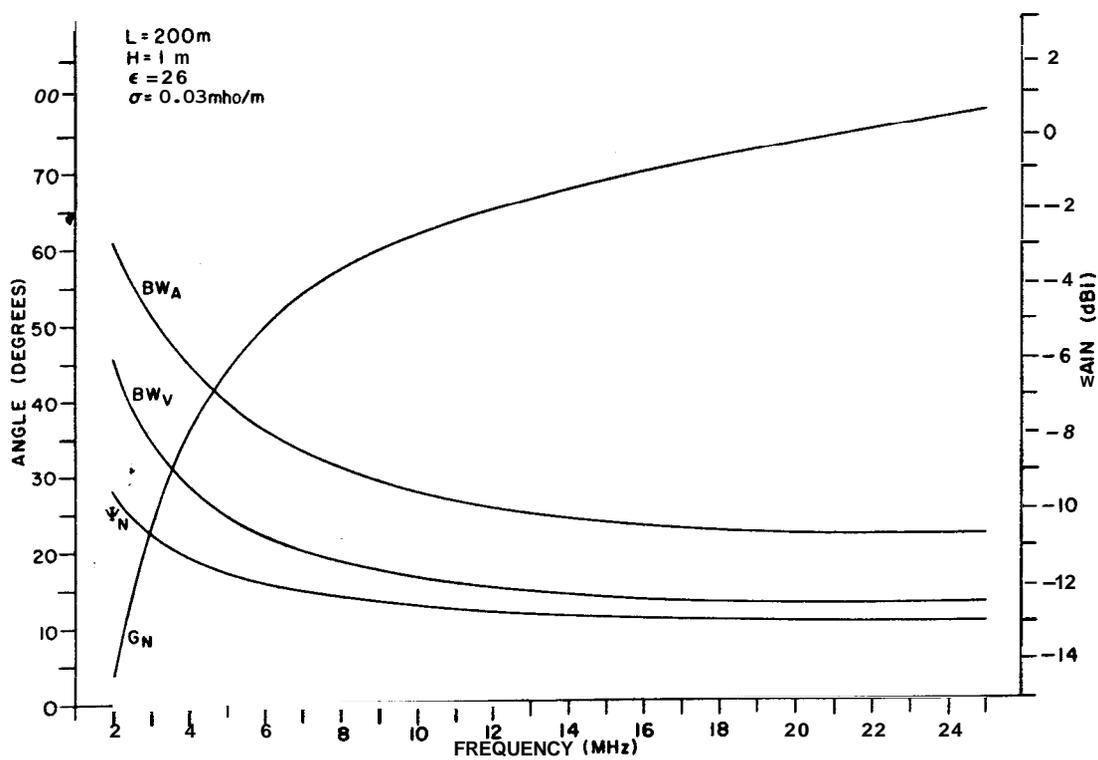
Figure 11-38. Design Parameters for Wet Rich Soil, H= 1m, L = 200m.
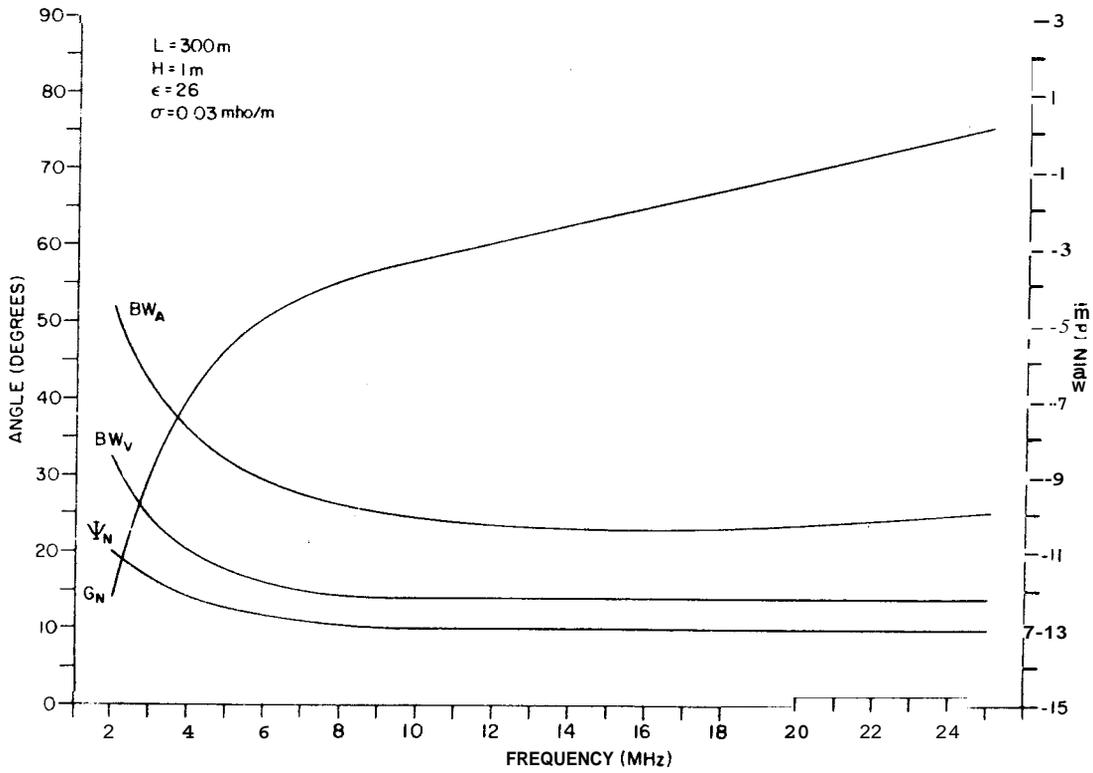
Figure 11-39. Design Parameters for Wet Rich Soil, $H = 1m$, $L = 300m$.
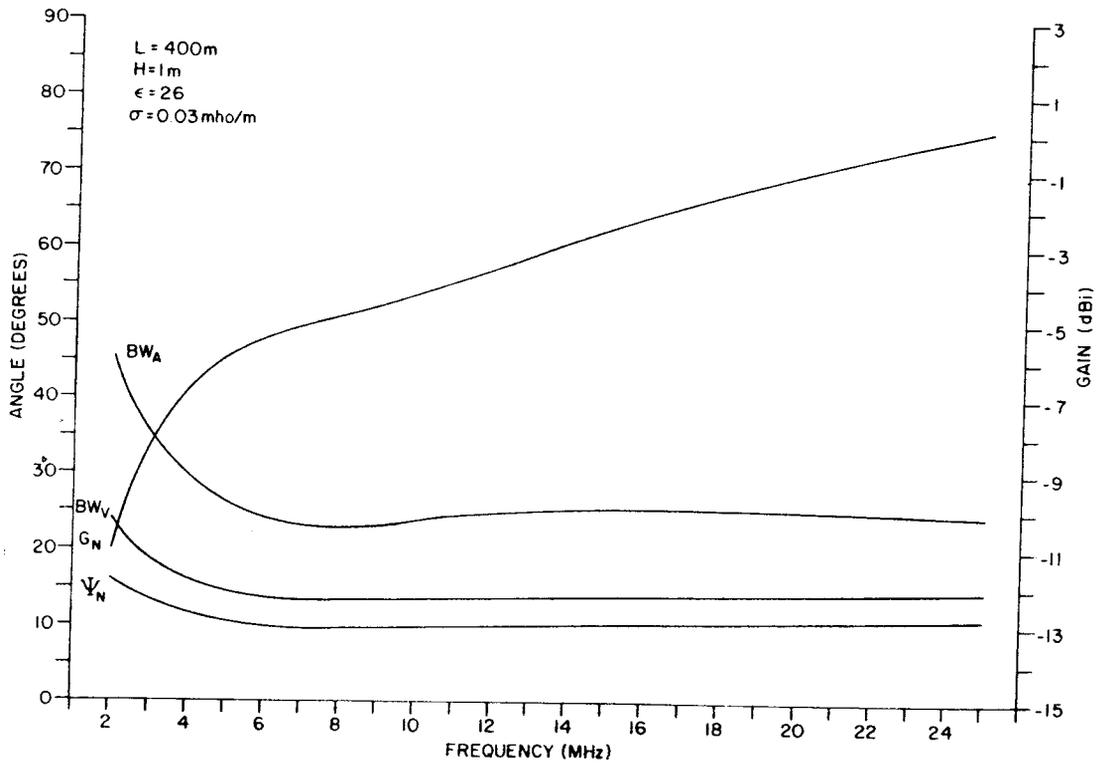
Figure 11-40. Design Parameters for Wet Rich Soil, $H = 1m$, $L = 400m$.
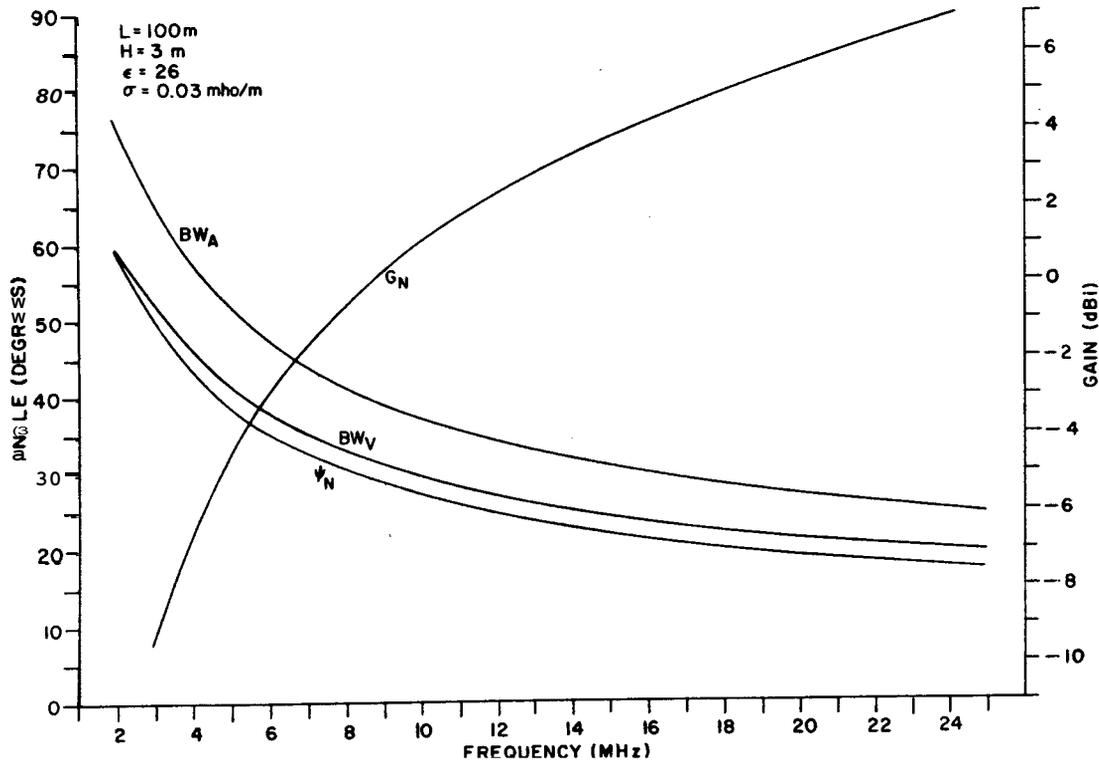
Figure 11-41. Design Parameters for Wet Rich Soil, H = 2m, L = 100m.
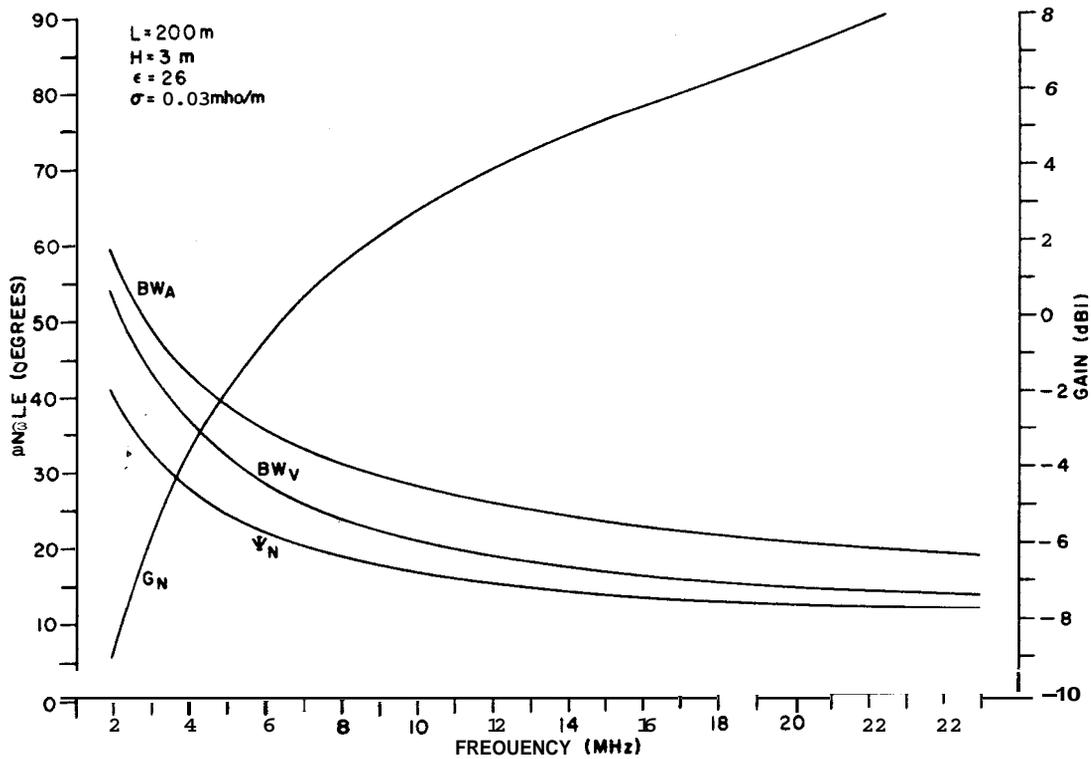
Figure 11-42. Design Parameters for Wet Rich Soil, H = 2m, L = 200m.
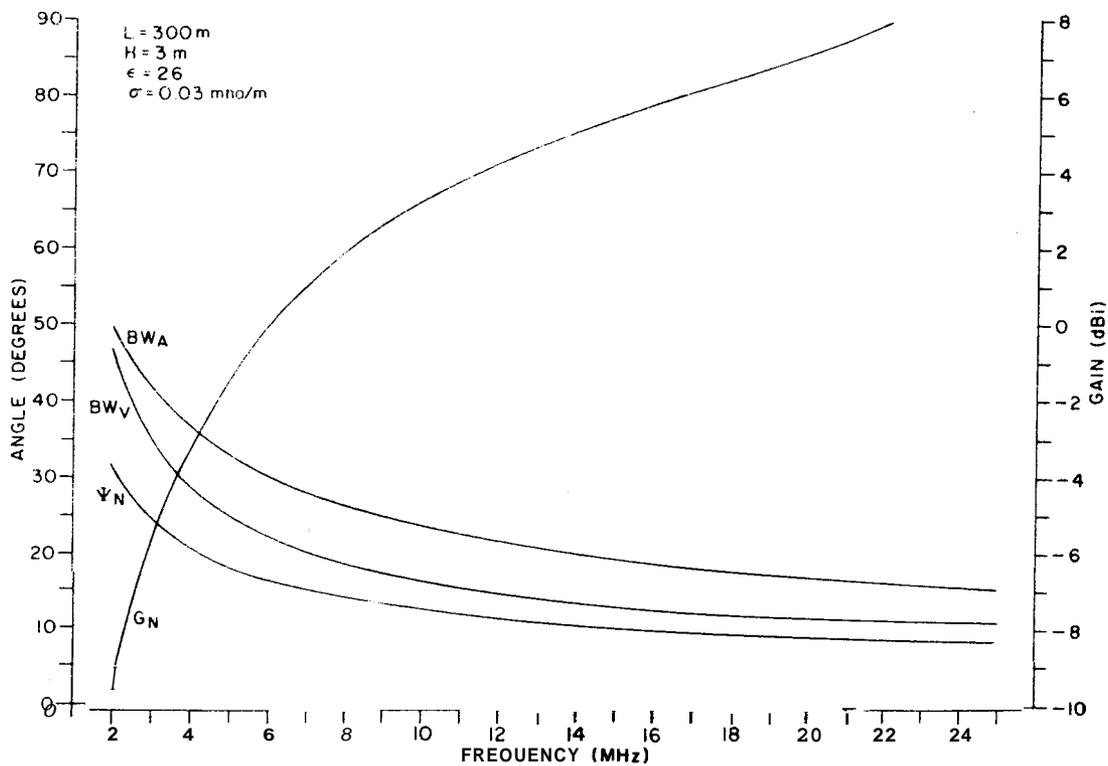
Figure 11-43. Design Parameters for Wet Rich Soil, H = 2m, **L** = 300m.
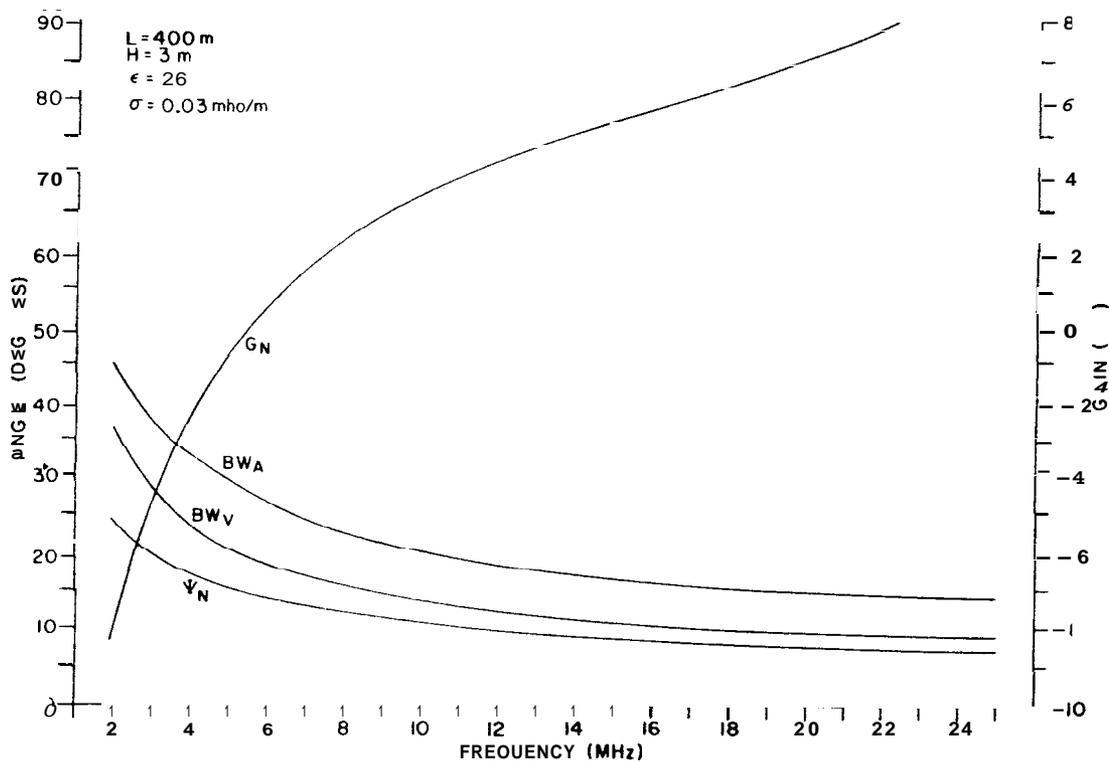
Figure 11-44. Design Parameters for Wet Rich Soil, H = 2m, L = 400m.
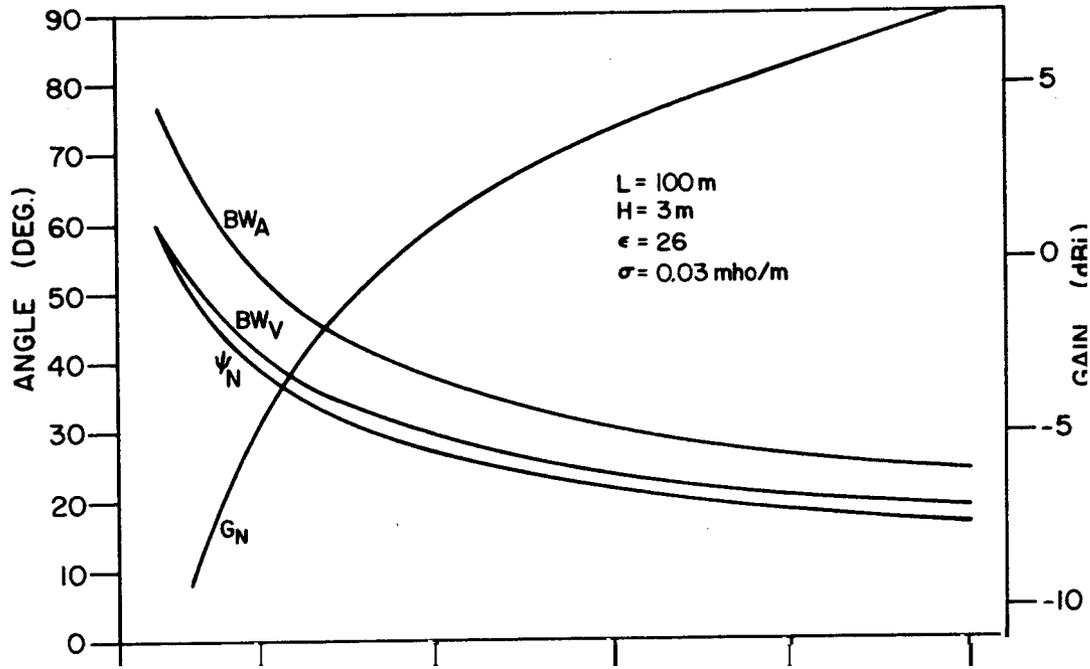
Figure 11-45. Design Parameter for Wet Rich Soil, H = 3m, L = 100m.
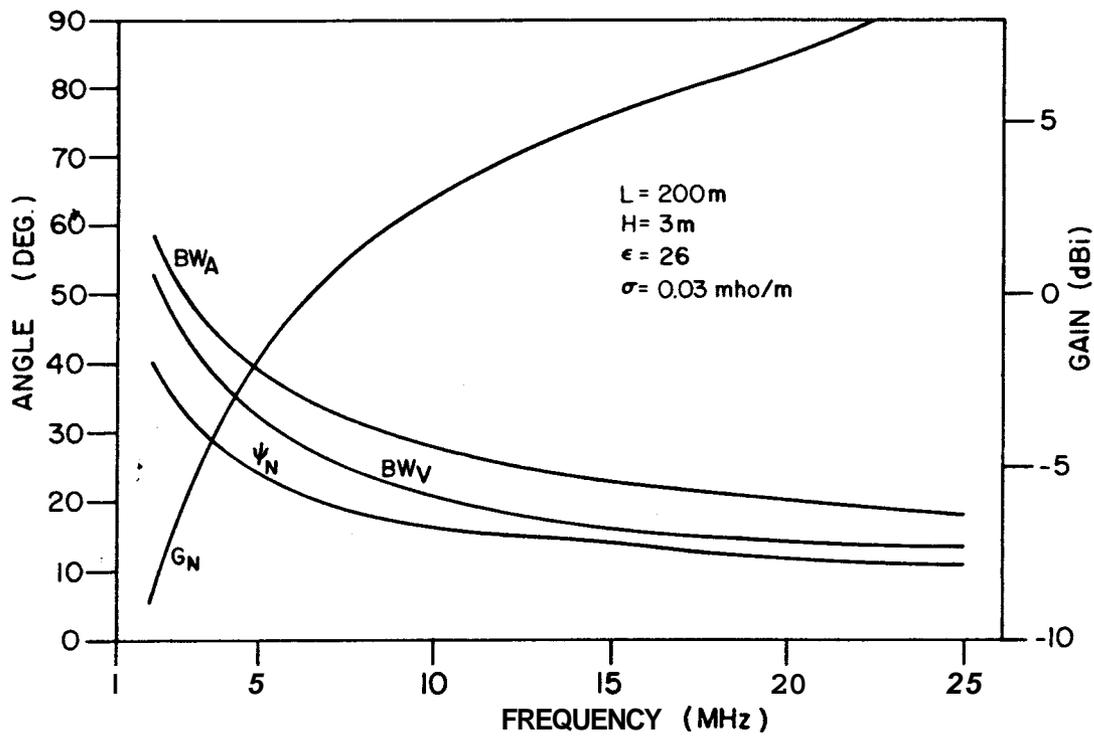
Figure 11-46. Design Parameters for Wet Soil, H = 3m, L = 200m.
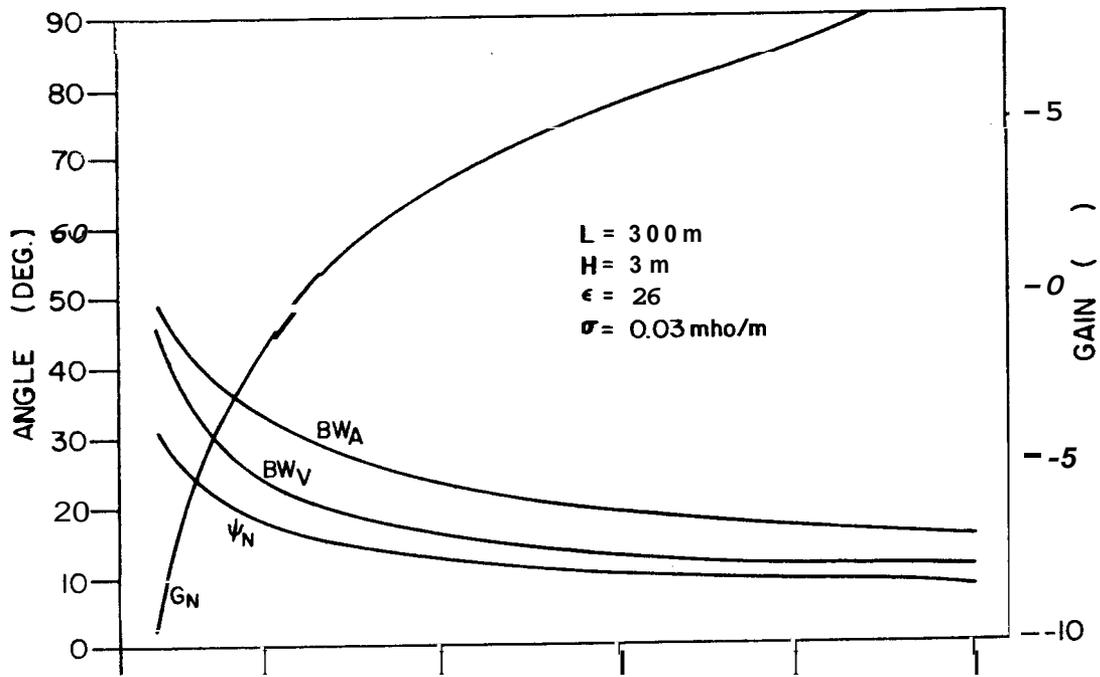
Figure 11-47. Design Parameters for Wet Rich Soil, H = 3m, L = 300m.
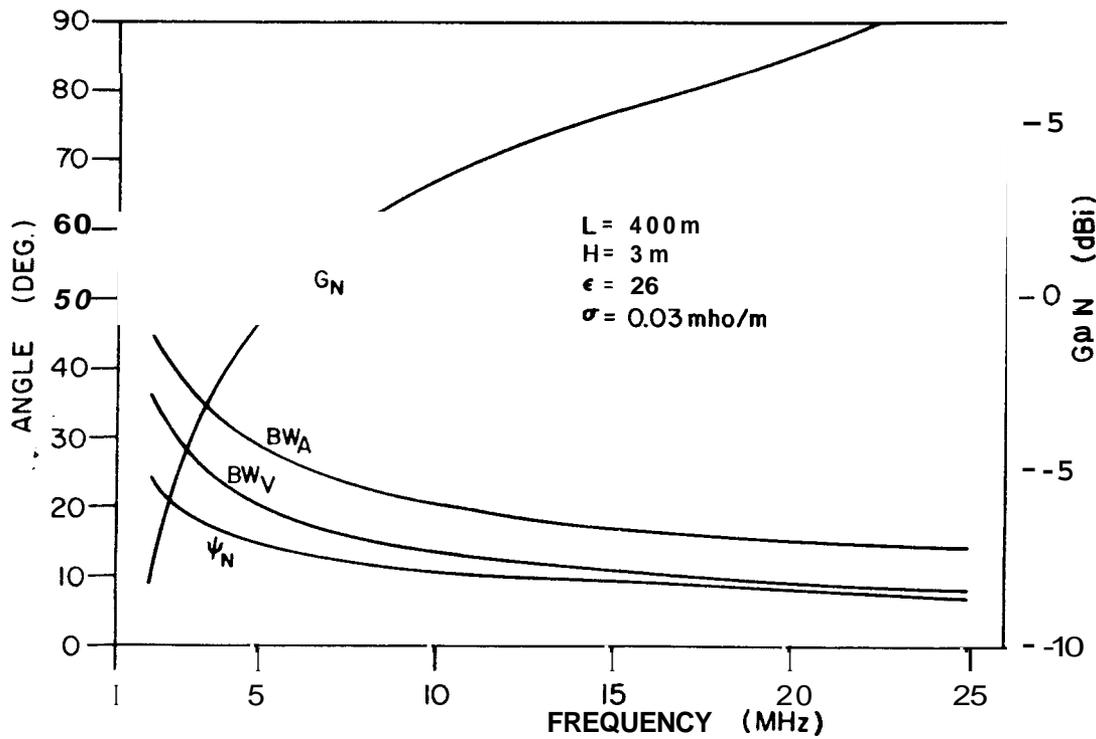
Figure 11-48. Design Parameters for Wet Rich Soil, H = 3m, L = 400m.

A P P E N D I X   I I I

Theoretical Curves for Surface Wave Gain
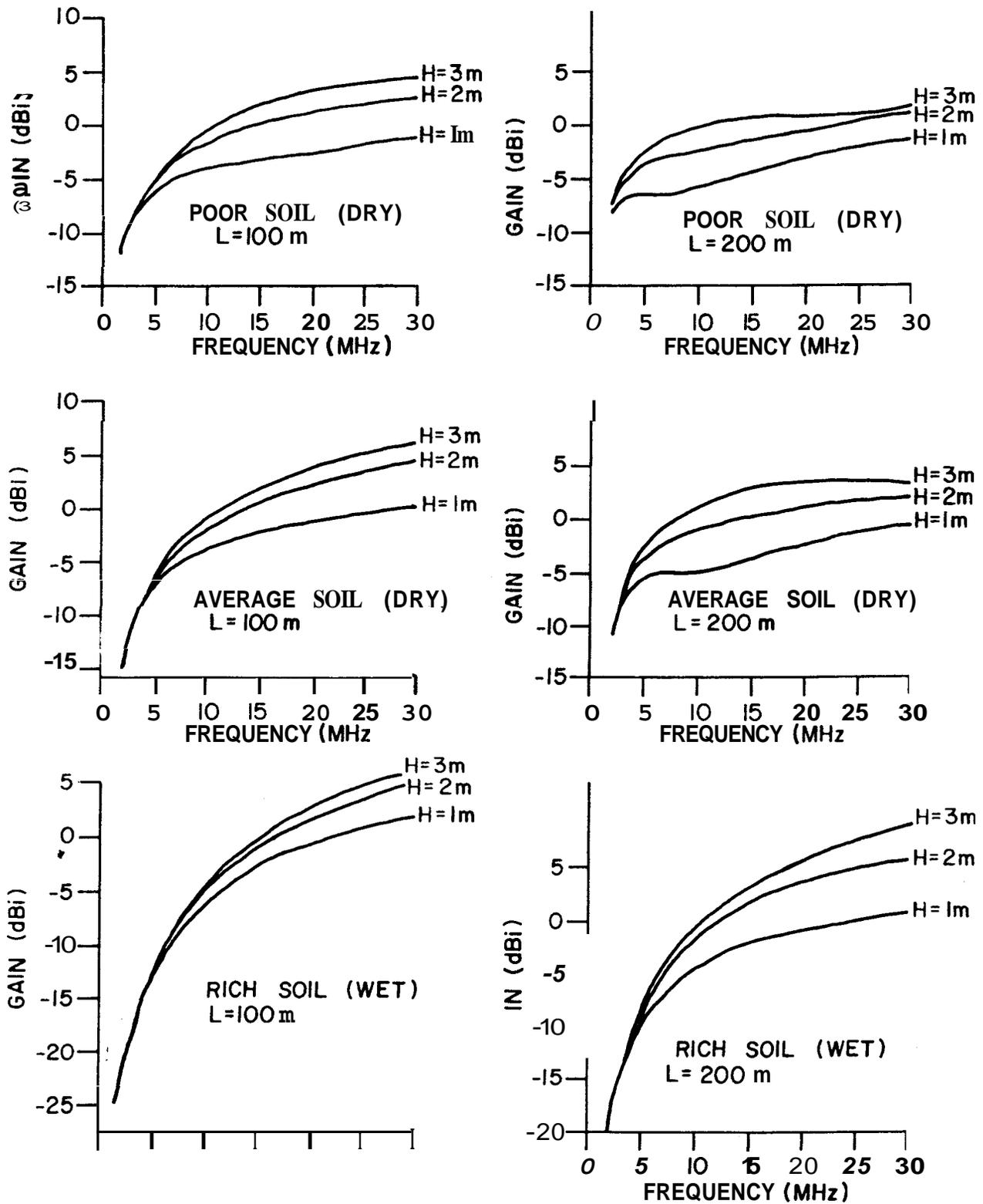
Figure III-1. Theoretical Surface Wave Gain of Beverage Antennas with Lengths of 100 and 200m, Heights of 1, 2, and 3m Over Poor Soil (Dry), Average Soil (Dry), and Rich Soil (Wet).
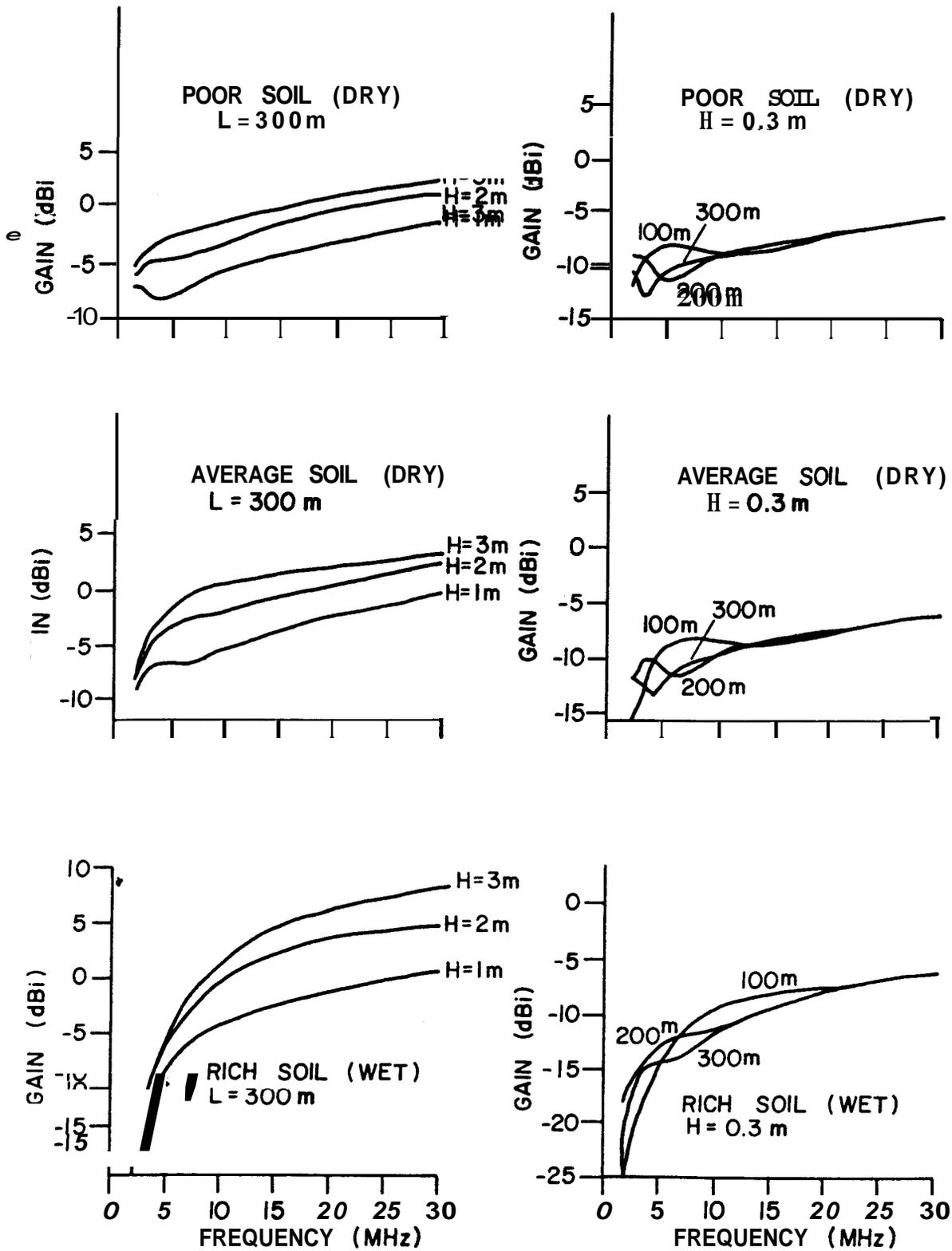
Figure III-2. Theoretical Surface Wove Gain of Beveroge Antennas with o Length of 300m, Heights of 1, 2, ond 3m over Poor Soil (Dry), Averoge Soil (Dry) ond Rich Soil (Wet). Curves ore also Given for o Height of 0.3m, Lengths of 100, 200 ond 300m and Poor Soil (Dry), Averoge Soil (Dry) ond Rich Soil (Wet).

A P P E N D I X   I V

An Analysis of the Beverage Antenna and Its Applications to Linear

Phased Arrays

In the analysis which follows consideration is given to the formulation of the elevation radiation pattern for the Beverage antenna. The work follows the notation of Beverage and Herlitz[1,10] and is extended in order to consider the effects of mismatching at the terminating end. Since the response of this antenna is greatly affected by the ground constants over which the antenna may be installed, an in-depth analysis is included in order to determine the antenna response for varying ground parameters that are likely to be encountered. The work also includes the application of the Beverage antenna to linear phased array systems.

)

SECTION 1

Analysis of the Beverage Antenna

*

Consider a plane wave incident on the Beverage antenna at some elevation angle ψ and propagating in the direction as shown in Figure IV-1. For an elemental length dx from point P, where P is midway between A and B, a voltage $V_g dx$ will be induced on the line. The magnitude of this voltage will be dependent on the parallel component $\overline{E_P}$ of the vertically polarized electric field $\overline{E_v}$ such that

$$\overline{E_P} = \overline{E_v} \sin I\!) \cos 8 \qquad (1:1)$$

where 8 is the azimuthal angle of the plane wave with respect to the antenna. However, if we assume for the moment that θ is zero then

$$\overline{E_P} = \overline{E_v} \sin I\!) \qquad (1:2)$$

Since $\overline{E_P}$ lies parallel to the line a potential gradient results giving

$$\frac{dv}{dx} = \overline{E_P} \qquad (1:3)$$

Therefore the voltage induced in the line is

$$V_g dx = \frac{dv}{dx} dx \qquad (1:4)$$

Equation (1:4) may be thought of as a voltage generator on the line in series with two impedances $Z_{IN}(A)$ and $Z_{IN}(B)$, where $Z_{IN}(A)$ is the impedance looking in at P towards A and $Z_{IN}(B)$ is the impedance looking in at P towards B, giving rise to an elemental current i_s where

$$i_s = \frac{V_g dx}{Z_{IN}(A) + Z_{IN}(B)}$$
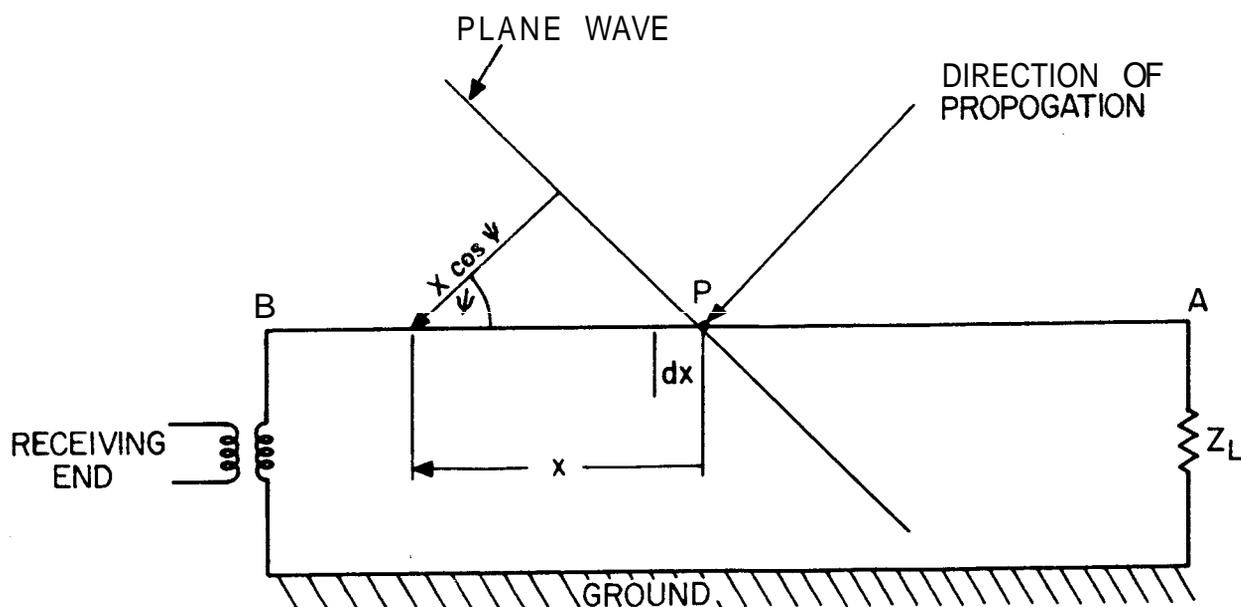
Figure IV-I.   Model of the Beverage Antenna

$Z_{IN}(A)$ and $Z_{IN}(B)$ may be expressed through the usual transmission line equations (See for example skilling[11]) as

$$Z_{IN}(A) = Z_0 \left[\frac{Z_L - jZ_0 \tanh \gamma \left(\frac{\ell}{2} - x \right)}{Z_0 + jZ_L \tanh \gamma \left(\frac{\ell}{2} - x \right)} \right] \qquad (1:5)$$

and

$$Z_{IN}(B) = Z_0 \left[\frac{Z_B + jZ_0 \tanh \gamma \left(\frac{\ell}{2} - x \right)}{Z_0 + jZ_B \tanh \gamma \left(\frac{\ell}{2} - x \right)} \right] \qquad (1:6)$$

γ in equations (1:5) and (1:6) is the complex line constant defined as

$$\gamma = \alpha + j\beta \qquad (1:7)$$

where α is the attenuation constant in nepers per unit length

β is the phase constant in radians per unit length

Z_B in equation (1:6) represents the terminating impedance at B.   However, **if** we assume a perfectly matched system, then

$$Z_{IN}(A) = Z_{IN}(B) = Z_0 \qquad (1:8)$$

128

then,

$$i_s = \frac{V_g \, dx}{2Z_0} \tag{1:9}$$

At point x the phase angle of the current i_s with respect to P will be determined through the propagation length $x \cos \psi$ to be

$$i_s = \frac{V_g \, dx}{2Z_0} \, e^{-j\frac{\omega x \cos \psi}{c}} \tag{1:10}$$

where   c is the velocity of light

           ω is the radian frequency

The induced current i_s will cause a current wave to traverse the wire in the direction of propagation, that is, towards B. This current wave may be expressed as[12]

$$i_b = i_s \, e^{-\gamma \left(\frac{\ell}{2} - x\right)} \tag{1:11}$$

and therefore

$$i_b = \frac{V_g \, dx}{2Z_0} \, e^{-j\frac{\omega x \cos \psi}{c}} \, e^{-\gamma \left(\frac{\ell}{2} - x\right)} \tag{1:12}$$

Combining the exponents in x and factoring out the constant term results in

$$i_b = \frac{V_g \, dx}{2Z_0} \, e^{-\frac{\gamma \ell}{2}} e^{\left(\gamma - j\frac{\omega \cos \psi}{c}\right)x} \tag{1:13}$$

Since $\gamma = \alpha + j\beta$ then,

$$i_b = \frac{V_g}{2Z_0} \, dx \, e^{-(\alpha + j\beta)\frac{\ell}{2}} e^{\left(\alpha + j\beta - j\frac{\omega \cos \psi}{c}\right)x} \tag{1:14}$$

The phase constant of the line β, may be expressed as

$$\beta = \frac{\omega}{\mu} \tag{1:15}$$

where μ is the velocity of propagation of the wire, therefore

$$i_b = \frac{V_g}{2Z_0} \, dx \, e^{-(\alpha + j\beta)\frac{\ell}{2}} e^{[\alpha + j\beta(1 - N \cos\psi)]x} \tag{1:16}$$

where $N = \dfrac{\mu}{c}$

The total current at B as a function of the elevation angle ψ will be the sum of the elemental currents over the total length of the line, or in other words, the integral of equation (1:16). Since P has been chosen as the reference point, we may integrate them $-\dfrac{\ell}{2}$ to $\dfrac{\ell}{2}$ thus,

$$I_B(\psi) = \frac{V_g}{2Z_0} e^{-\frac{\gamma \ell}{2}} \int_{-\frac{R}{2}}^{\frac{\ell}{2}} e^{[\alpha + j\beta(1 - N\cos\psi)]x} dx \qquad (1:17)$$

which results in

$$I_B(\psi) = \frac{V_g}{2Z_0} e^{-(\alpha + j\beta)\frac{\ell}{2}} \left\{ R \sinh \frac{\left[\frac{\gamma_1 \ell}{2}\right]}{\frac{\gamma_1 \ell}{2}} \right\} \qquad (1:18)$$

where $\gamma_1 = \alpha + j\beta(1 - N\cos\psi)$ \qquad (1:19)

Thus equation (1:18) may be used to calculate the elevation radiation pattern of a perfectly matched Beverage antenna that is, when $Z_L = Z_0$. However, achieving a perfectly matched system is extremely difficult, especially when operating over a wide frequency range, and therefore one must consider the effects of a mismatched system.

In order to understand the effects of mismatching, consider a signal impinging on the antenna wire from the reverse direction (i.e. $\psi > 90°$). A current wave i_a will result and will propagate towards A where

$$i_a = \frac{V_g}{2Z_0} dx\, e^{j\frac{\omega x \cos\psi}{c}} e^{-\gamma\left(\frac{\ell}{2} - x\right)} \qquad (1:20)$$

Combining the exponents in x and factoring out the constant term in the same manner as for i_b (equation(1:16)) results in

$$i_a = \frac{V_g dx}{2Z_0} e^{-\frac{\gamma \ell}{2}} e^{[\alpha + j\beta(1 + N\cos\psi)]x} \qquad (1:21)$$

The total current I at A as a function of ψ the elevation angle is simply the integral of equation (1:21) thus,

$$I_A(\psi) = \frac{V_g}{2Z_0} e^{-\frac{\gamma \ell}{2}} \left\{ \int_{-\frac{\ell}{2}}^{\frac{\ell}{2}} e^{[\alpha + j\beta(1 + N\cos\psi)]x} dx \right\} \qquad (1:22)$$

which results in

$$I_A(\psi) = \frac{V_g}{2Z_0} e^{-\frac{\gamma \ell}{2}} \frac{\ell \sinh\left[\frac{\gamma_2 \ell}{2}\right]}{\frac{\gamma_2 \ell}{2}} \tag{1:23}$$

where $\gamma_2 = \alpha + j\beta (1 + N \cos \psi)$ $\tag{1:24}$

At point **A**, the termination end, a reflecting current i_{b_2} will result if $Z_L \neq Z_0$ and will proceed to propagate towards the receiving end B. Thus

$$i_{b_2} = \frac{V_g}{2Z_0} e^{-\frac{\gamma \ell}{2}} \frac{\ell \sinh\left[\frac{\gamma_2 \ell}{2}\right]}{\frac{\gamma_2 \ell}{2}} P_L \tag{1:25}$$

Where P_L is the reflection coefficient given by [11]

$$P_L = \frac{Z_L - Z_0}{Z_L + Z_0} \tag{1:26}$$

Thus the reflected current i_{b_2} at B will be

$$i_B = \frac{V_g}{2Z_0} e^{-\frac{\gamma \ell}{2}} \frac{\ell \sinh\left[\frac{\gamma_2 \ell}{2}\right]}{\frac{\gamma_2 \ell}{2}} P_L e^{-\gamma \ell} \tag{1:27}$$

The total current at B, the receiving end, will then be

$$L_T(\psi) = I_R(\psi) + i_R \tag{1:28}$$

or

$$L_T(\psi) = \frac{V_g}{2Z_0} e^{-\frac{\gamma \ell}{2}} \ell \left[\frac{\sinh\left[\frac{\gamma_1 \ell}{2}\right]}{\frac{\gamma_1 \ell}{2}} + P_L e^{-\gamma \ell} \frac{\sinh\left[\frac{\gamma_2 \ell}{2}\right]}{\frac{\gamma_2 \ell}{2}} \right] \tag{1:29}$$

The above analysis assumes that no reflecting currents occur at B (i.e. the line is correctly terminated at the receiving end).

In order to complete the full two dimensional radiation pattern, the term $\cos \psi$ must be multiplied by $\cos \theta$ in γ_1 and γ_2 (equations (1:19) and (1:24)) thus

$$\gamma_1 = \alpha + j\beta (1 - N \cos \psi \cos \theta) \tag{1:30}$$

$$\gamma_2 = = + \beta (1 + N \cos \psi \cos \theta) \tag{1:31}$$

The resultant equation for the two dimensional radiation pattern then becomes,

$$I_T(\psi,\theta) = \frac{V_g}{2Z_0} e^{-\frac{\gamma \ell}{2}\ell\cos \theta} \left[\frac{\sinh\left[\frac{\gamma_1\ell}{2}\right]}{\frac{\gamma_1\ell}{2}} + P_L e^{-\gamma \ell} \frac{\sinh\left[\frac{\gamma_2\ell}{2}\right]}{\frac{\gamma_2\ell}{2}} \right] \quad (1:32)$$

Power Developed in the Load Impedance at the Receiving End: Although it was assumed that the line was correctly terminated at the receiving end, this assumption is not strictly correct because the impedance Z_i as seen looking into the line at B (Figure IV-1) towards A will vary according to the degree of mismatch at the terminating end B and with frequency. The impedance Z_i nay be derived from either Equation (1:5) or Equation (1:6) to be

$$Z_i = Z_0 \left[\frac{Z_L + jZ_0 \tanh \, y \, \ell}{Z_0 + jZ_L \tanh \, \gamma \, \ell} \right] \quad (1:33)$$

However, if the terminating impedance Z_L is chosen such that the degree of mismatch is minimal, then for a reasonable line length and attenuation, Z_i will tend towards Z_0. Thus if we choose a terminating impedance at B to be the characteristic impedance Z_0 of the line, then to a reasonable degree of accuracy the line may be said to be correctly terminated at the receiving end.

The power developed in the load impedance at the receiving end may be given as [1]

$$P = Re\{VI^*\} \text{ watts} \quad (1:34)$$

where V and I are the r.m.s. values of the complex voltage and the complex current respectively. However, since we are dealing with complex currents and complex impedances then

$$V = I_T(\psi,\theta)Z_0 \quad (1:35)$$

where $I_T(\psi,\theta)$ is the total current at the receiving end (Equation (1:32)). Thus the power developed in the load at the receiving end may be given as

$$P_T = Re(Z_0) \left| I_T(\theta,\psi) \right|^2 \text{ watts} \quad (1:36)$$

Power Gain Referred to an Isotropic Radiator: In order to compare the gain of a Beverage antenna to that of other more widely used antenna systems, one would have to take simultaneous field intensity measurements of both the unknown and a known chosen standard antenna. The standard antenna selected for this purpose would be chosen on the basis that its characteristics are well known. The field intensity measurements obtained from the Beverage antenna may then be referred to the field intensity measurements obtained from the standard antenna in order to make gain comparisons. From a computer—

study standpoint, the isotropic radiator may be used as the standard because its characteristics are precisely known.

The isotropic radiator may be considered to be a point source suspended in free space and radiating equally in all directions. At some radial distance R from the point source the power passing through the sphere is $(\overline{S})$ $(4\pi R^2)$ where $\overline{S}$ is the average value of the Poynting vector at the surface of the sphere. This must equal P where

$$P = \overline{S}4\pi R^2 \qquad (1:37)$$

Thus the power density P_d is simply the average value of the Poynting Vector S. S may be defined as

$$\overline{S} = \frac{1}{\mu_0} \widetilde{E} \; \overline{B} \qquad (1:38)$$

where $\overline{E}$ and $\overline{B}$ are the electric and magnetic vectors respectively, and μ_0 is the permeability of free space $(4\pi \times 10^{-7})$. Using the relationship that

$$\overline{E} = c \; \overline{B} \qquad (1:39)$$

then

$$\overline{S} = \frac{\overline{E}^2}{\mu_0 c} \qquad (1:40)$$

The average value of $\overline{E}$ over one cycle is $\frac{1}{2}E_{vmax}^2$ and this leads to

$$P_d = \frac{E^2}{P_{0} \sim} \qquad (1:41)$$

where E is the rms value of the electric vector. The effective aperture of an isotropic radiator at a unit distance may be given in terms of the wave-length squared (λ^2) to be [14]

$$A = \frac{\lambda^2}{\cdot} \qquad (1:42)$$

Thus the power P passing through the sphere at a unit distance is

$$P = \frac{E^2 \lambda^2}{\mu_0 c 4\pi} \quad \text{watts} \qquad (1:43)$$

Thus the power gain of the Beverage antenna referred to that of an isotropic radiator is

$$P_G = \frac{4\pi\mu_0 c \left| I_T(\psi,\theta) \right|^2 \text{Re}(Z_0)}{\lambda^2} \qquad (1:44)$$

(assuming E to be unity)

Thus the gain in decibels referred to an isotropic radiator is

$$P_i = 10 \log (P_G) \text{ dBi} \qquad (1:45)$$

SECTION 2

The Effects of Ground on the Beverage Antenna Radiation Pattern

So far the preceding analysis has considered only the direct wave. However, the resultant induced voltage $V_g dx$ from point P (Figure (IV-1)) comprises three waves namely the direct, ground reflected and surface waves (excluding sky wave propagation). If the source of these waves is at a sufficiently large distance from the point of detection such that the magnitude of the surface wave is negligably small, then we may consider only the direct and ground-reflected waves. Consider the diagram in Figure (IV-2); at point P the resultant E vector $\bar{E}_r$ is the vector addition of the horizontal components of the E vectors for the direct and ground-reflected waves. The path length r, which is a function of the antenna height h above the ground plane and the elevation angle $, constitutes a phase shift ϕ_r with respect to the direct wave, where

$$\phi_r = \frac{2\pi}{A} (2h) \sin \psi \tag{2:1}$$

In addition, the reflecting properties of the ground will introduce a further phase shift nd lso a reduction in the magnitude of the E vector. This change in magnitude and phase is revealed through the reflection coefficient (ρ_v) of the ground for vertically polarized waves and is given by[15]

$$\rho_v = \rho e^{j\phi} = \frac{\sqrt{\epsilon_C} \sin \psi - \sqrt{\epsilon_c^2 - \cos^2 \psi}}{\sqrt{\epsilon_C} \sin \psi + \sqrt{\epsilon_c^2 - \cos^2 \psi}} \tag{2:2}$$

where E_C is complex and is given by:-

$$\epsilon_c = \epsilon_r - j \frac{\sigma g}{\omega \epsilon_0} \tag{2:3}$$

where ϵ_r is the ratio of the permativity of the ground to that of free space

σ_g is the ground conductivity in mho/meter

ϵ_0 is the permativity of free space (8.85×10^{-12} Farads/meter)

At point P on the wire, the resultant horizontal component of the E vector may then be determined thus

$$\overline{E}_r = \overline{E}_v \, \sin \psi \, (1 - \rho_v e^{-j\frac{2\pi}{\lambda}2h \, \sin \psi}) \qquad\qquad (2:4)$$

The negative sign in equation (2:4) indicates that the horizontal components of the direct and ground-reflected waves are oppositely directed in space. This condition is illustrated in Figure IV-2.
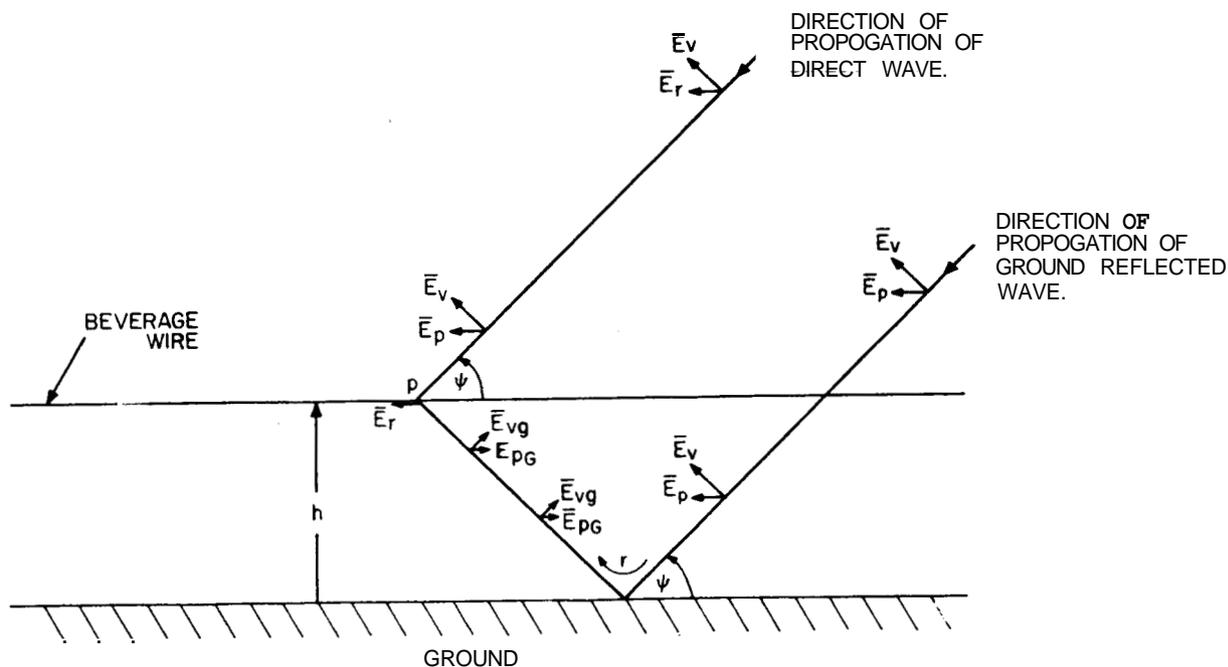
Figure IV-2. Illustration of the Resultant Parallel Component of the E Vector $(\overline{E}_r)$ from the Direct and Ground Reflected Waves

Beverage Antenna Response to Vertically Polarized Ground Waves: As the vertically polarized ground waves traverse the imperfectly conducting ground, they tilt forward in the direction of propagation by an angle δ with respect to the vertical. The magnitude of this tilt angle, which is a function of the ground constants and frequency, may be given as[16]

$$\delta = \tan^{-1} \left[\frac{(\epsilon_r - 1)^2 + \left(\dfrac{\sigma_g}{\epsilon_0 \omega}\right)^2}{\left[\epsilon_r^2 + \left(\dfrac{\sigma_g}{\epsilon_0 \omega}\right)^2\right]^2} \right]^{\frac{1}{4}} \qquad (2:5)$$

Thus the parallel component $\overline{E}_p$ of the vertically polarized ground wave may be determined as a function of δ to be

$$\overline{E}_{gp} = \overline{E}_v \sin \delta$$

Therefore the Beverage antenna response for a vertically polarized ground wave may be determined by using equation (1:32) giving

$$I(\delta,\theta) = \frac{\overline{E}_{gp}}{2Z_0} \; e^{-\frac{\gamma \ell}{2}} \; \ell \; \cos \theta \left\{ \sinh \frac{\dfrac{\gamma_1 \ell}{2}}{\dfrac{\gamma_1 \ell}{2}} + P_L e^{-\gamma \ell} \sinh \frac{\dfrac{\gamma_2 \ell}{2}}{\dfrac{\gamma_2 \ell}{2}} \right\} \qquad (2:6)$$

where $\quad \gamma_1 = \alpha + j\beta \;\; (1 - N \cos \delta \cos \theta) \qquad\qquad (2:7)$

and $\quad \gamma_2 = \alpha + j\beta \;\; (1 + N \cos \delta \cos \theta) \qquad\qquad (2:8)$

S E C T I O N   3

Determination of the Characteristic Impedance (Z_0)

and the Complex Propagation Constant (y)

For a uniform transmission line, the characteristic impedance Z_0, and the complex propagation constant γ may be expressed through the usual transmission line equations as[11]

$$Z_0 = \sqrt{\frac{Z}{Y}} \text{ ohms} \qquad (3:1)$$

and

$$\gamma = \sqrt{Z.Y} \qquad (3:2)$$

where   Z is the series impedance and Y the shunt admittance per unit length
of the line expressed as

$$Z = R + j\omega L \qquad (3:3)$$

where R and L is the resistance and inductance per unit length of the line respectively, and

$$Y = G + j\omega C \qquad (3:4)$$

where G and C is the conductance and capacitance per unit length of the line respectiyely.

The Beverage antenna is essentially a transmission line with the[17] ground providing the current return path. For such a circuit,   Carson provides the following formula for the series impedance

$$Z = R + j2w \ln \left(\frac{2h}{b}\right) + 4\omega \int_o^\infty (\sqrt{-\mu^2 + j} - \mu)e{-2h'\mu d\mu} \qquad (3:5)$$

The first two terms in equation (3:5) formulates the series impedance of the transmission line if the ground is a perfect conductor and the last term takes into account the ground's finite conductivity. The infinite integral in equation (3:5) may be evaluated to give

$$Z = R + j2w \ln\left(\frac{2h}{b}\right) + 4 \ (P + jQ) \quad \text{e.m.u.} \tag{3:6}$$

where P and Q are functions derived by Carson and are given below:

subscript "2" added per program listi g

$$P = \frac{\pi}{8} \ (1 - S_4) + \frac{S_2}{2} \ln\left(\frac{2}{\gamma r}\right) - \frac{\sigma_1}{\sqrt{2}} + \frac{\sigma_2}{2} + \frac{\sigma_3}{\sqrt{2}} \tag{3:7}$$

$$Q = \tfrac{1}{4} + \tfrac{1}{2}\ln\left(\frac{2}{\gamma r}\right) \ (1 - S_4) + \frac{\sigma_1}{\sqrt{2}} - \frac{\pi\sigma_2}{8} + \frac{\sigma_3}{\sqrt{2}} - \sigma_4 \tag{3:8}$$

In equations (3:7) and (3:8), $\gamma = 1.7811$ and σ_1, σ_2, σ_3, σ_4, S_2 and S_4 are infinite series defined as follows:

$$S_2 = \sum_{n=0}^{\infty} (-1)^n \frac{(r/2)^{(4n+2)}}{(2n+1)!(2n+2)!} \tag{3:9}$$

$$S_4 = \sum_{n=0}^{\infty} (-1)^n \frac{(r/2)^{4n+4}}{(2n+2)!(2n+3)!} \tag{3:10}$$

$$\sigma_1 = \sum_{n=0}^{\infty} (-1)^l \frac{r^{4n+1}}{[(3)(5)(7)\ldots(4n+1)]^2(3+4n)} \tag{3:11}$$

$$\sigma_2 = \sum_{n=0}^{\infty} (-1)^n [1 + \tfrac{1}{2} + \tfrac{1}{3}\ldots + \frac{1}{2(n+1)} - \frac{1}{4(n+1)}][\frac{(r/2)^{4n+2}}{(2n+1)!(2n+2)!}] \tag{3:12}$$

$$0_3 = \sum_{n=0}^{\infty} (-1)^n \frac{r^{(4n+3)}}{[(3)(5)(7)\ldots(3+4n)]^2(4n+5)} \tag{3:13}$$

$$\sigma_4 = \sum_{n=0}^{\infty} (-1)^n [1 + \tfrac{1}{2} + \tfrac{1}{3} + \cdots \frac{1}{2(n+1)} - \frac{1}{4(n+1)}][\frac{\left(\frac{r}{2}\right)^{4n+}}{(2n+2)!(2n+3)!}]$$

$$\tag{3:14}$$

where $\qquad r = 2h\sqrt{4\pi\sigma_g\omega}$ e.m.u. $\hfill$ (:15)

If the ground conductivity σ_g, and the height h, of the antenna above the ground plane are in **M.K.S.** units, then to comply with the results obtained for P and Q in Carson's paper,

$$r = 2h\sqrt{4\pi\sigma_g\omega} \quad (\sqrt{10} \times 10^{-4}) \text{ e.m.u.} \qquad (3:16)$$

Thus the series impedance Z (equation (3:6)) may **be** rewritten in the **M.K.S.** units as

$$Z = R + j2\omega.10^{-7}\ln\left(\frac{2h}{b}\right) + 4\omega(P + jQ).10^{-7} \text{ ohms/meter} \qquad (3:17)$$

Carson has set limits for the range of r (i.e., $0.25 < r \leq 5.0$), in determining the value of P and Q. For values of $r > 5.0$, he (Carson), has derived an assymptotic expansion in order to compute P and Q. However, P and Q may be determined for $r > 5.0$ by computing S_2, S_4, σ_1, σ_2, σ_3, and σ_4 in logarithmic form as follows:

$$S_2 = \sum_{n=0}^{\infty} (-1)^n \exp\{(4n+2)\ln\left(\frac{r}{2}\right) - \sum_{P=1}^{2n+1}\ln P - \sum_{q=1}^{2n+2}\ln q\} \qquad (3:18)$$

$$S_4 = \sum_{n=0}^{w} (-1)^n \exp\{(4n+4)\ln\left(\frac{r}{2}\right) - \sum_{P=1}^{2n+2}\ln P - \sum_{q=1}^{2n+3}\ln q\} \qquad (3:19)$$

$$\sigma_1 = \sum_{n=0}^{m} (-1)^n \exp\{(4n+1)\ln\left(\frac{r}{2}\right) - \sum_{P=1}^{1+2n}[2\ln(1+4n)] - \ln(3+4n)\} \qquad (3:20)$$

$$\sigma_2 = \sum_{n=0}^{\infty} (-1)^n [1 + \tfrac{1}{2} + \dots + \frac{1}{2(n+1)} - \frac{1}{4(n+1)}]$$

$$[\exp\{(4n+2)\ln\left(\frac{r}{2}\right) - \sum_{P=1}^{2n+1}\ln P - \sum_{q=1}^{2n+2}\ln q\}] \qquad (3:21)$$

$$\sigma_3 = \sum_{n=0}^{n=\infty} (-1)^n \exp\{(4n+3)\ln r - \sum_{P=1}^{1+2n} [2\ln(3+4n)] - \ln(4n+5)\} \qquad (3:22)$$

$$\sigma_4 = \sum_{n=0}^{w} (-1)^n [1 + \tfrac{1}{2} + \tfrac{1}{3} \cdots \left(\frac{1}{2(n+1)} - \frac{1}{4(n+1)}\right)$$

$$[\exp\{(4n+4)\ln \left(\frac{r}{2}\right) - \sum_{P=1}^{2n+2} \ln P - \sum_{q=1}^{2n+3} \ln q\} \qquad (3:23)$$

This method of computing the infinite series' prevents computer overflow and allows the range of r to be extended to the value of 10. For r > 10.0 Carson provides a much simpler expression to computer P + jQ and this is given by

$$P + jQ = \frac{1+j}{\sqrt{2}\,r} - \frac{1}{r^2} \qquad (3:24)$$

The value of r as deduced by Carson assumes that ε_r the relative dia- [18] lectric constant has little effect on the series impedance Z. However, Wise states that above 60 KHz this assumption no longer holds and therefore he (Wise) has derived a correction factor for r giving a new parameter

$$r_W = r\xi e^{jN} = r \sqrt{1 + j\frac{(\varepsilon_r - 1)}{2(\lambda\sigma_g \cdot 10^{-7})}} \quad \text{e.m.u.} \qquad (3:25)$$

x IMAG

where σ_g is in MKS units.   RCW, RRCW

An examination of equation (3:25) reveals that Wise's correction factor is also applicable for lower conductivities. Thus r may be replaced by r_W in the infinite series' and in the simpler expression (equation (3:24)), in order to compute the'values of P and Q. For r < .25 Wise's series for the computation of P and Q are employed thus:—

$$P = \frac{\pi}{8} - \frac{r\xi}{3\sqrt{2}} (\cos N - \sin N) + \frac{\pi r^2 \xi^2}{64} \sin 2N + \frac{r^2 \xi^2}{16}$$

$$[\cos 2N(0.6728 + \ln \left(\frac{2}{r\xi}\right)] \quad + N \sin 2N + \frac{71}{2} + \cdots \qquad (3:26)$$

$$Q = -0.03861 + \tfrac{1}{2}\ln\left(\frac{2}{r\xi}\right) + \frac{r\xi}{3\sqrt{2}}(\cos N - \sin N) + \frac{r^2\xi^2}{16}$$

$$\{\sin 2N[0.6728 + \ln\left(\frac{2}{r\xi}\right)] - N\cos 2N\} - \frac{\pi r^2\xi^2}{64}\cos 2N + \ldots \quad (3:27)$$

Up to this point we have been evaluating the series impedance Z and now, the shunt admittance Y must be considered. Generally, the conductance G, the real part of the admittance, is quite small and for all practical purposes may be ignored. **Thus** the shunt admittance Y may be given as

$$Y = j\omega C = j\frac{\omega 2\pi\epsilon_0}{\ln\left(\frac{2h}{b}\right)} \quad (3:28)$$

Thus the characteristic impedance Z_0 and the complex propagation constant γ may now be determined as a function of w, h and the ground parameters to be

$$Z_0 = \sqrt{\frac{R + j2\omega.10^{-7}\ln\left(\frac{2h}{b}\right) + 4\omega(P + jQ).10^{-7}}{j\dfrac{\omega 2\pi\xi_0}{\ln\left(\frac{2h}{b}\right)}}} \quad \text{ohms} \quad (3:29)$$

and

$$\gamma = \left[(R + j2\omega.10^{-7}\ln\left(\frac{2h}{b}\right) + 4\omega(P + jQ).10^{-7}) \Big/ \left(j\dfrac{\omega 2\pi\xi_0}{\ln\left(\frac{2h}{b}\right)}\right)\right]^{\frac{1}{2}} \quad (3:30)$$

where b is the radius of the wire in meters.

$_{by}(11)$ The value of the series resistance per unit length R, may be determined by

$$R = \frac{2K\sqrt{f}}{b} \quad \text{ohms/unit length} \quad (3:31)$$

Where $K = 41.6 \times 10^{-9}$ for copper wire, and f is the frequency in Hz.

Equation (3:29) shows that the characteristic impedance Z_0 is complex and probably accounts for the difficulty in selecting a terminating impedance to optimize the design of a Beverage antenna system particularly when operating over a wide frequency range.

SECTION 4

Radiation Pattern of a Linear Array

Consider an array of **N** isotropic elements with equal amplitudes of unity and spaced evenly by a distance D as shown in Figure **IV-3.** Following Kraus[19] the radiation pattern E for such an array system may be expressed in the following way:-

$$E' = \sum_{n=0}^{N-1} e^{nj\phi} \tag{4:1}$$

where ϕ is the phase difference between any two adjacent sources. Equation (4:1) is a geometric series and may be expressed as,

$$E = 1 + e^{j\phi} + e^{2j\phi} + \text{------} + e^{(N-1)j\phi} \tag{4:2}$$

Equation (4:2) may be manipulated into the following form,

$$E = \frac{\sin (N\phi/2)}{\sin (\phi/2)} \, e^{j\xi} \tag{4:3}$$

where ξ is the phase referred to source one of the linear array. However, if the phase is referred to the centre of the array then,

$$E = \frac{\sin (N\phi/2)}{\sin (\phi/2)} \tag{4:4}$$

The phase angle ϕ, the phase difference between any two adjacent sources, may be given as

$$\phi = \frac{2\pi}{\lambda} \, D \sin \theta \tag{4:5}$$

Thus, the radiation pattern E as a function of θ is
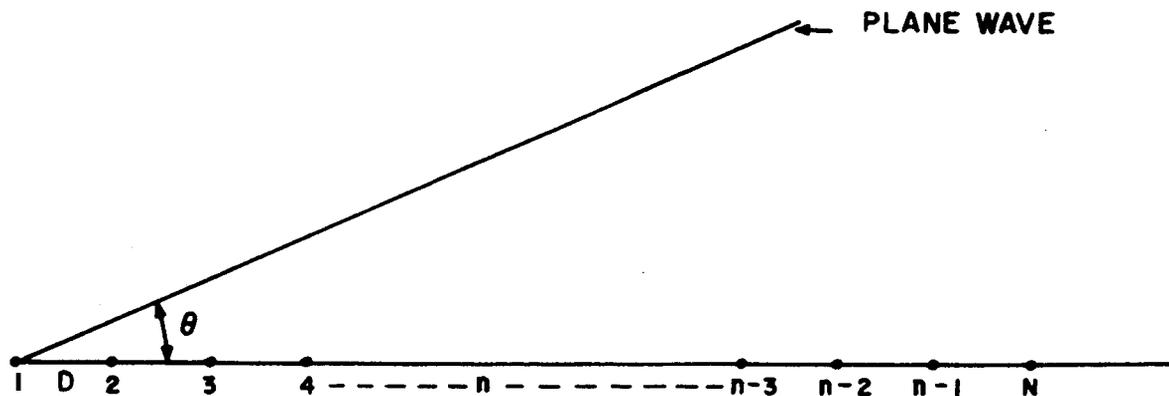
$$E(\theta) = \frac{\sin (\pi ND \sin \theta)}{\sin \left(\frac{\pi D}{\lambda} \sin \theta\right)} \tag{4:6}$$

Figure IV-3. *Illustration of a Plane Wave at the Angle θ with Respect to Linear Antenna Array of Spacing D.*

In the central region of the radiation pattern (I.E. where θ is small), then

$$\sin\left(\frac{\pi D}{\lambda} \sin \theta\right) \simeq \frac{\pi D}{\lambda} \sin \theta \qquad (4{:}7)$$

Therefore,

$$E = \frac{N \sin\left(\frac{\pi ND}{\lambda} \sin \theta\right)}{\frac{\pi ND}{\lambda} \sin \theta} \qquad (4{:}8)$$

Thus in the central region, the radiation pattern E (Equation **(4:8))**, approximates very closely to a sin(x)/x function where

$$x = \frac{\pi ND}{\lambda} \sin \theta \qquad (4{:}9)$$

The maximum value of E occurs when sin(x)/x is unity, that is when **x** = 0.0. Thus,

$$E_{max} = N \qquad (4{:}10)$$

Beamwidth and Aperture Length: The **3** dB beamwidth may be determined from equation **(4:9).** Let E = **0.707N,** then x **= 1.39** radians. Then from equation *(4:9),*

$$\sin \theta = \frac{0.442\lambda}{ND} \qquad (4{:}11)$$

If the angle θ, is radians, is approximately equal to its sine value, then the beamwidth, which is equal to 2θ may be given as

$$\text{Beamwidth} = \frac{50.65\lambda}{\text{ND}} \quad \text{degrees} \tag{4:12}$$

where ND is the aperture length in meters. Usually, in the design of a linear array system, the beamwidth will be specified for a given wavelength λ, therefore **two** choices remain in the design of a system in order to meet the beamwidth requirements, namely:-

    (1)   the number of elements;

    (2)   the inter-element spacing.

As an example, given a specified beamwidth of $1.2°$ at $\lambda = 30.0$ meters, the aperture length may be determined using equation (4:12). Thus,

$$N D = \frac{50.65 \times 30.0}{1.2} = 1266.25 \text{ meters}$$

The aperture length is ND rather than $(N - 1)D$ because the aperture distribution is dependent upon the total number of elements used. However, the physical length of the array system is $(N - 1)D$.

    Radiation Pattern of an Array of Non-Isotropic Elements: The foregoing analysis has considered *a* linear array of N isotropic elements with an inter-element spacing of D. To determine the radiation pattern for **a** similar array using non-isotropic elements, the method of beam pattern **multiplication**[20] may be used provided that all the non-isotropic elements are oriented in the same direction. The general expression for this method is given by,

$$E_r(\theta,\psi) = E(\theta) \cdot E_1(\theta,\psi) \tag{4:13}$$

where $E(\theta)$ is the radiation pattern for a linear array of isotropic elements as a function of θ.

    $E_1(\theta,\psi)$ is the radiation pattern for a non-isotropic element as a function of the same θ for a given elevation angle ψ.

    $E_r(\theta,\psi)$ is the resultant beam pattern for a linear array of non-isotropic elements.

    This method may be employed provided the equation for the radiation pattern of the non-isotropic element, as a function of θ and ψ, is known.

Power Gain of Linear Array: As the number of elements in a linear array system are increased the contributions of current from each element are added. Thus as the number of elements are doubled, the power gain will increase by 3 dB. Thus the power gain may be simply stated as

$$\text{power gain (dB)} = \frac{3 \log_{10}(N)}{\log_{10}(2)} \qquad (4:14)$$

where N is the number of elements used such that

$$N = 2^M \qquad (4:15)$$

and M an integer number.

Thus the power gain in decibels referred to that of an isotropic radiator is given by

$$P = P_i + \frac{3 \log_{10}(N)}{\log_{10}(2)} + W \text{ dBi} \qquad (4:16)$$

where W in equation (4:16) takes into account the effects of weighting to be discussed later.

Determination of the Minimum Spacing: A limiting point is reached, however, when the power gain no longer increases in proportion to a further increase in the number of elements for a given aperture. This limitation in the power gain occurs when the elements are so closely spaced that they interact with one another. This interaction may be thought of as an effect caused by the overlapping of the effective areas of the individual elements thereby reducing the power gain of the individual elements[21]. However, if the spacing is chosen such that the edges of the effective areas just touch one another then we may say that the spacing so chosen will be the minimum that may be used without violating the concept of overlapping effective areas. In order to calculate the minimum spacing, one would have to determine the horizontal length of the effective area, for it is this length that would give the minimum spacing. The effective area A_{em} of a Beverage antenna may be derived from Equation (1:42) giving

$$A_{em} = \frac{G\lambda^2}{4\pi} \quad \text{square meters} \qquad (4:17)$$

where G is the maximum power gain of the Beverage antenna referred to an isotropic radiator. The −3 dB beamwidth may be defined as θ_e and θ_h where the subscripts e and h represent the electric and magnetic vectors, therefore, θ_e and θ_h are in the planes of the electric and magnetic vectors. Since the Beverage antenna responds to vertically polarized waves then θ_e and θ_h are the half power beamwidths in elevation and azimuth respectively. Usually $\theta_h > \theta_e$ for the Beverage antenna and this suggests that the effective area will be

elliptical in nature with the major axis in the horizontal plane. Since we are interested in the minimum distance at which antennas may be sp ced then we need only to calculate the length of the major axis. The minimum spacing, which may be denoted by D_{min}, may then be given in terms of θ_e, θ_h and the effective area. Thus

$$D_{min} = 2\sqrt{\frac{A_{em}\,\theta_h}{\pi\,\theta_e}} \qquad (4:18)$$

where D_{min} in Equation (4:18) is expressed in wavelengths. θ_e and θ_h may be expressed either in radians or degrees.

Numerical **Procedures**

Sampled Aperture: Since the linear array system is a series of elements separated by a finite distance D, it can be regarded as a sampled aperture where sampling takes place at the element positions. If the wave field at the sampled positions is given by

$$E(nD) = e^{j\frac{2\pi}{\lambda}\,nD\,\sin\theta} \qquad (4:19)$$

then the far field angular distributi n is the Discr te Fourier Transform (DFT) [22] of the equation (4:17). **Thus,**

$$F(k) = \sum_{n=-\frac{N}{2}+1}^{\frac{N}{2}} E(nD)e^{-j\frac{2\pi}{ND}\,(nD)k} \qquad (4:20)$$

where $\frac{2n}{ND}$ is the chosen sampling frequency as a function of the aperture length ND. There are N distinct values computable by equation **(4:20)** namely, those for k in the range

$$-\frac{N}{2} + 1 \le k \le \frac{N}{2} \qquad (4:21)$$

If we now substitute for **E(nD)** in equation **(4:20)** the result becomes,

$$F(k) = \sum_{n=\frac{N}{2}+1}^{\frac{N}{2}} e^{j\frac{2\pi(nD)}{\lambda}\left\{\sin\theta - \frac{k}{ND}\right\}} \qquad (4:22)$$

where $\frac{A}{ND}$ may be defined as the sine of the angular estimates between the discrete points of **k.** Let α be defined as those angular estimates then,

$$\alpha = \text{arc sin } \frac{kh}{ND} \tag{4:23)'}$$

for k defined as above.

The limits of sin a are therefore

$$\sin \alpha_{max} = \frac{-N}{2} \cdot \frac{\lambda}{N \; D} \qquad \qquad \text{to} \qquad \sin a_{max} = \frac{N}{2} \cdot \frac{h}{ND} \tag{4:24}$$

$$\text{or} \qquad \sin a_{max} = \frac{\pm\lambda}{2D} \tag{4:25}$$

For a given wavelength λ in equation (4:25) three cases arise if the inter-element spacing D is varied.

Case (1) $D < \frac{A}{2}$

If the inter-element spacing D is less than half a wavelength then $|\sin \alpha_{max}| > 1$, and therefore only those angular estimates of a sector of the angular distribution out to some $K < \frac{N}{2}$ such that $\frac{K}{ND} \leq 1$ are valid.

Case (2) $D = \frac{A}{2}$

If the inter-element spacing D is half a wavelength, then $|\sin \alpha_{max}| = 1$, or $a = \frac{\pm\pi}{2}$, and therefore angular estimates are obtained over a sector of the angular distribution $\pm\frac{\pi}{2}$ from boresight.

Case (3) $D > \frac{A}{2}$

If the inter-element spacing D is greater than half a wavelength then $|\sin \alpha_{max}| < 1$, and the angular distribution will repeat beyond $|\alpha_{max}|$. From a sampled data theory point of view, sampling takes place at less than the Nyquist rate and therefore alliasing occurs.

Based upon the above procedure, a program was written in the Fortran IV language for use on the Sigma 9 computer at C.R.C. in order to determine the performance of linear array systems.

The program essentially computes the radiation pattern for an array of isotropic sources, utilizing the Discrete Fourier Transform (DFT), and then by the method of beam pattern multiplication with non-isotropic element, namely the Beverage antenna, calculates the resultant beam pattern for an array of non-isotropic elements or Beverage antennas. The beam pattern results are in the form of a linear plot of azimuth angle against gain in decibels normalised to the maximum value. A typical output result appears in Figure IV-4).

DISPLAY IN LINEAR FORM OF THE RADIATION PATTERN FOR A LINEAR ARRAY OF BEVERAGE ANTENNAS   B. ... -

THE NUMBER Of ELEMENTS USED = 16

INTER-ELEMENT SPACIYG (METERS) =   7.00

FREQUENCY IN MHZ = 5.00

BEVERAGE ANTENNA WIRE LENGTH (METERS) = 100.00

VELOCITY OF PROPOGATION RATIO = .911

ATTENUATION CONSTANT (DB/METER) = .054022

PHASE CONSTANT (RADIANS/METER) = .114989

HEIGHT OF ANTENNA ABOVE OROUND (METERS) = 1.00

RELATIVE CIALECTRIC CONSTANT OF GROUND = 12.0

GROUND CONDUCTIVITY (MHO/METER) = .003000

WIRE RADIUS IN METERS (COPPER WIRE) = .0010260

COMPLEX CHARACT. IMPED. ZO = (498.63, -26.97) OHMS

TERMINATING IMPEDANCE = 499.36 OHMS

ELEVATION ANGLE OF SIGNAL (DEGREES) = 22.00

POWER GAIN OF ANT. ARRAY REL. TO ISOTROPIC RADIATOR =   6.185DB
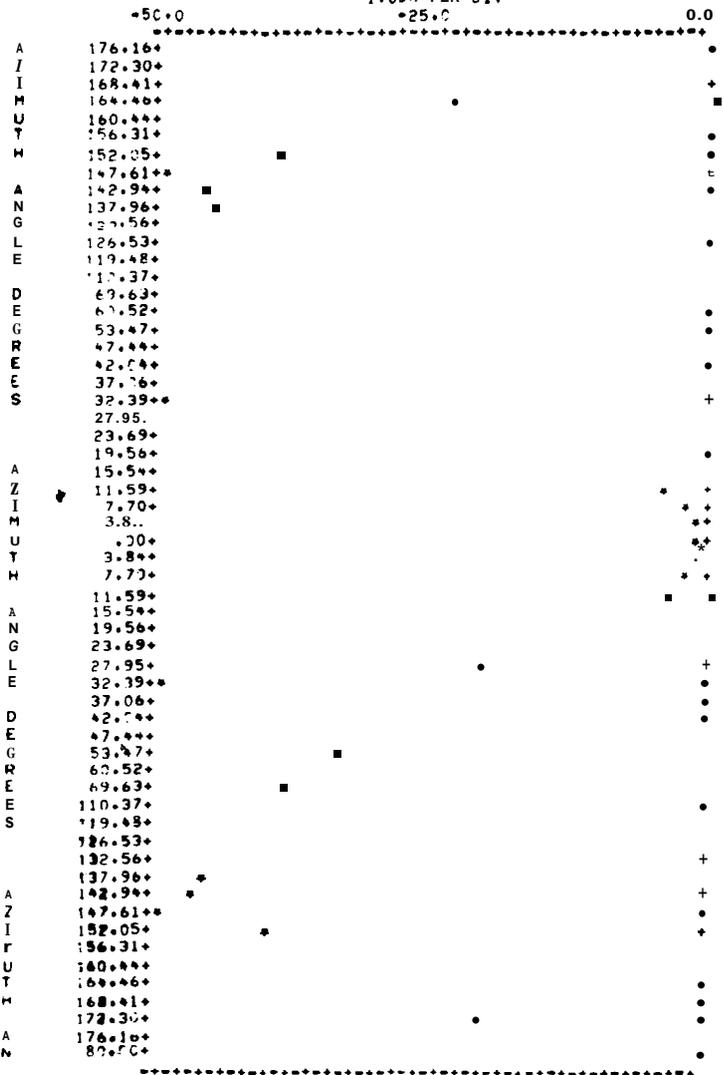
Figure IV-4.   Typical Computer Output Result

S E C T I O N   5

'Primary' Grating **Lobes**

Beyond the central regions the radiation pattern function reverts to,

$$E \; = \; \frac{\sin\left(\dfrac{\pi ND}{\lambda}\; \sin\,\theta\right)}{\sin\left(\dfrac{\pi D}{\lambda}\; \sin\,\theta\right)} \tag{5:1}$$

Note that at some value of θ such that $\frac{D}{\lambda}\sin\theta = 1$, $r\sin\theta = \frac{\lambda}{D}$, then for any value of $N \geq 1$, equation (5:1) is indeterminate. Equation (5:1) may be evaluated, however, by the use of L'Hospital's rule to give,

$$\left| \; E_{max} \; \right| \; = \; N \tag{5:2}$$

Thus a secondary lobe of amplitude N, which may be defined as the 'primary' grating lobe, will appear at some azimuthal angle θ given by

$$\theta \; = \; \text{arc}\,\sin\left(\pm\,\frac{\lambda}{D}\right) \tag{5:3}$$

The word, 'primary', is used here to distinguish this type of grating lobe from 'that of another type to be discussed in a later section.   The $\pm$ sign in equation (5:3) indicates that two grating lobes exist and are positioned symetrically at $\pm\theta$ from boresight.   For example, if the inter-element spacing D is equal to one wavelength $(D = \lambda)$, then two primary grating lobes will appear at $\pm\frac{\pi}{2}$ from boresight.   If, however, the inter-element spacing D is much greater than one wavelength $(D \gg \lambda)$, then for every wavelength λ contained in the inter-element spacing D such that

$$\frac{n\lambda}{D} \; \leq \; 1 \qquad\qquad n = 1, 2, 3, \text{---} \tag{5:4}$$

multiple grating lobes will exist.   Their positions in azimuth will then be given as

$$\theta_n \; = \; \text{arc}\,\sin\left(\pm\,\frac{n\lambda}{D}\right) \tag{5:5}$$

Since the value of $\sin \theta$ for any given value of n, takes on four possible values in complete azimuth, it can be concluded that the positions of the grating lobes in the second half of the radiation pattern is the mirror image of the first half. As an example, let λ = 30 meters and D = 40.65 meters, then for n = 1, the first grating lobes will appear at,

$$\theta = \text{arc} \sin \left(\pm \frac{30.0}{40.65} \right) = \pm 47.55° \qquad (5:6)$$

For the mirror image,

$$\theta = 180.0° \pm 47.55° \qquad (5:7)$$

$$= 132.45° \text{ and } 227.55' \qquad (5:8)$$

for n = 2, then $\frac{nh}{D} > 1$ and the second grating lobe extends beyond the 'visible' region (using antenna theory parlance), and therefore, is not valid.

The position of the primary grating lobes, which have been determined in the foregoing example, are exemplified in the polar plot of Figure IV–5.
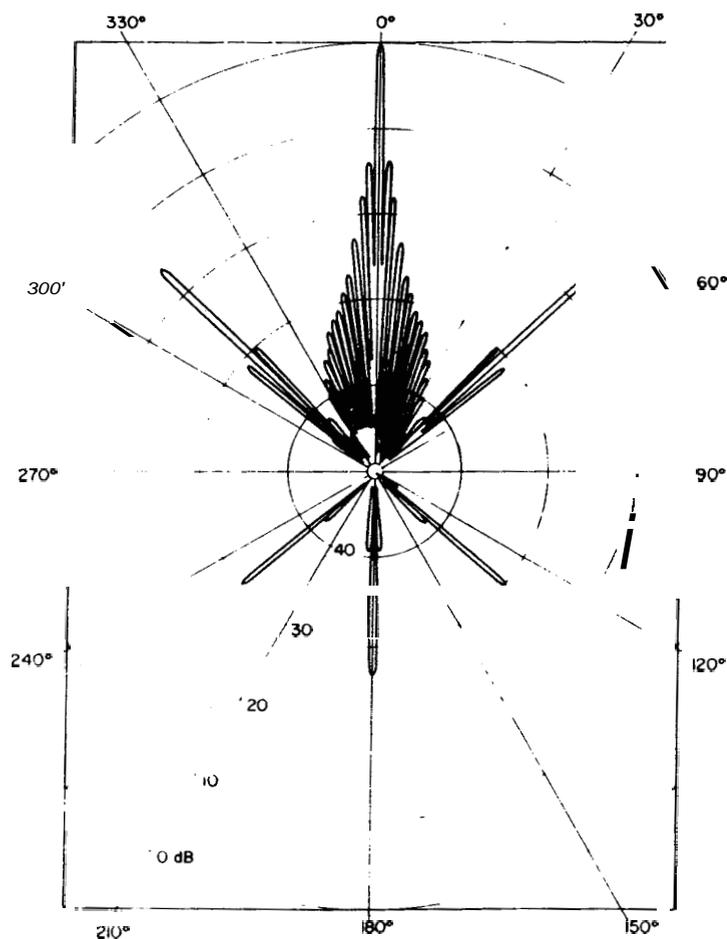
Figure IV-5. Polar Plot Illustrating the Position of the Grating Lobes for the Example Given on Page 150.

S E C T I O N   6

Beam Steering

For special requirements it may be necessary to steer the beam from boresight into the direction of the signal source. To meet this requirement, delay lines may be inserted into the array system in order to steer the beam. For example, if there are 32 elements in a given array system, 31 delay lines would be required (excluding the reference element), in order to steer the beam to a given angular position. Furthermore, if the beam were to be steered 210.0 degrees at intervals of 1.0 degree, it would require the use of 620 varying lengths of delay line in order to achieve this.   However, the maximum amount of beam−steering that may be achieved will be dependent on the beamwidth of any one element.

The 'Segmented' Array: In order to reduce the number of delay lines used for beam steering, the array may be arranged in groups or segments, with M segments of n elements per segment.   This method results in a secondary array system where each segment may be referred to as one element for M elements.   The spacing between the segments, or elements of the secondary array, will be n times the original inter−element spacing D of the primary array.

For the calculation of the delay lines refer to Figure IV−6.   The first segment (segment 1) is considered to be the reference segment.   The length L is calculated for the first element (element 5) in segment 2 for a given azimuthal steer angle.   The method as described is then repeated for the remaining segments in order to calculate the remaining delay lines.   Using the previous example, the number of delay lines required to steer the beam ±10.0 degrees from boresight will not be 140.   The method results in a con− siderable reduction in the number of delay lines required and in addition reduces the complexity of the associated switching system.   However, the method requires the payment of a penalty; as previously mentioned, the amount of beam−steering available is determined by the beamwidth of any one element and similarly, for this method, the amount of beam−steering available will be determined by the beamwidth of any one segment.
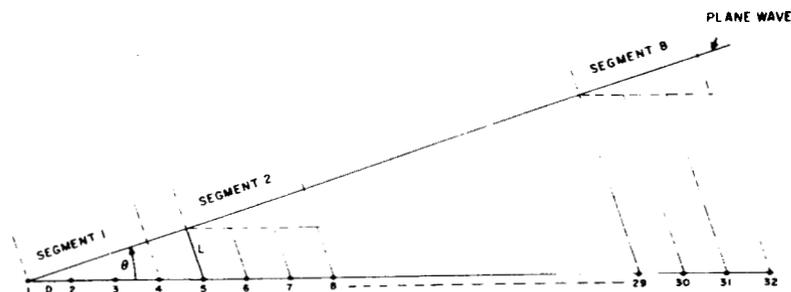
Figure IV-6.   Illustration of the Segmentation of the Linear Array.

Consider one segment of *4* elements.   The summation of the arbitrary phase ϕ is depicted in Figure **IV-7.**   Let A(x) be the x co-ordinate of A, and let A(y) be the y co-ordinate of **A** then,

$$A^2 = a^2(4 + 6\cos\phi + 4\cos 2\phi + 2\cos 3\phi) \tag{6:1}$$

The maximum value of A^2 occurs when $\phi = 0$.   Thus,

$$A^2_{max} = 16a^2 \tag{6:2}$$

For the half power points,

$$\frac{A^2_{max}}{2} = 8a^2 \tag{6:3}$$

and therefore,

$$2 = 3\cos 4 + 2\cos 2\phi + \cos 3\phi \tag{6:4}$$

Equation (6:4) is satisfied when $\phi = 41.0$ degrees, and therefore θ the azimuthal angle at which the half power points occur may be determined from equation (5:3) to give

$$\theta = \pm\text{arc}\ \sin\left(\frac{41}{360\ D}\right) \quad \textbf{degrees} \tag{6:5}$$

For an example let $\lambda = 30.0$ meters and $D = 40.65$ meters then,

$$\theta = \pm\text{arc}\ \sin\ (0.084)$$

$$= \pm 4.82\ \text{degrees}$$

Thus, the beam-steering limits are $\pm 4.82°$ from boresight for a wavelength $\lambda = 30.0$ meters.

Figure IV-8 shows plots of the radiation pattern in the central region for steer angles from boresight to *5.0* degrees in increments of 1.0 degree. The linear array was in the 'segmented' configuration, with 4 elements per segment, with an inter-element spacing **D** and wavelength λ of *40.65* meters and 30.0 meters respectively.
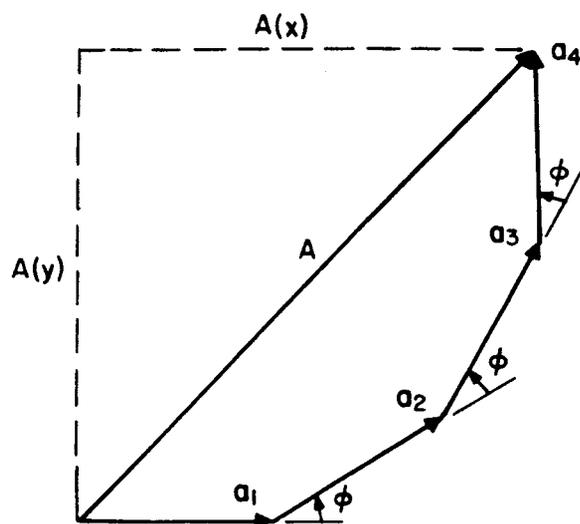
Figure I V-7. Phasor Diagram of One Segment of 4 Elements.
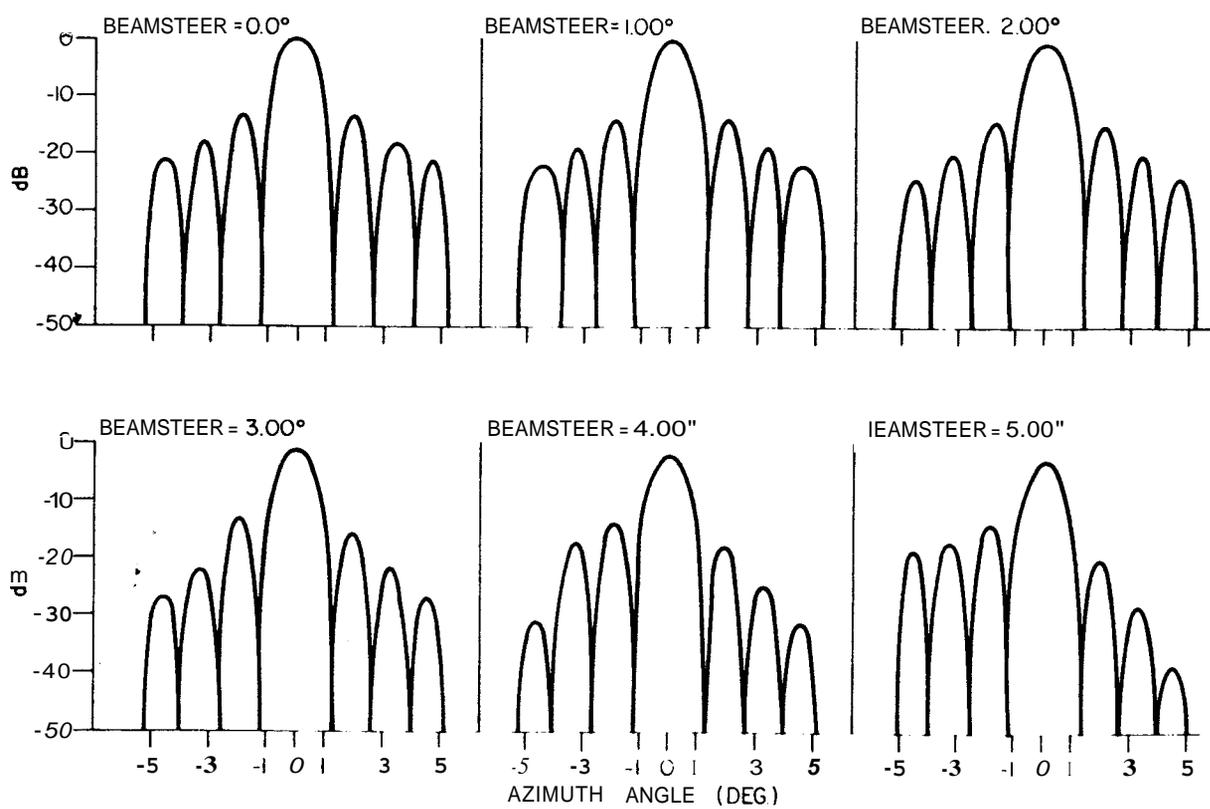
Figure IV-8. Radiation Patterns in the Central Region For the Beamsteers as Shown.

'Secondary' Grating Lobes: If the linear array system is in the segmented configuration, the system may be thought of as a secondary array system, where each segment represents one element in the array. The inter-segment spacing, denoted by D_s, is then given by

$$D_s = ND, \qquad\qquad (6:6)$$

where   N is the number of elements used in the segment.

         D is the original inter-element spacing.

If the inter-segment spacing D_s is much greater than a wavelength ($D_s \gg \lambda$), 'secondary' grating lobes will result. The word, 'secondary', distinguishes the type of grating lobes which is now under consideration from the type previously mentioned. To determine the position in azimuth of the secondary grating lobes equation (5:5), previously used for determining the positions in azimuth of the primary grating lobes, may **be** used, except that D must be replaced by D_s thus,

$$\theta_n = \text{arc sin} \left(\pm \frac{n\lambda}{D_s} \right) \quad , \qquad\qquad (6:7)$$

for n = 1,2,3,--- , such that $\frac{n\lambda}{D_s} \leq 1$.

Figures IV-9 to IV-13 illustrate the presence of the secondary grating lobes resulting from the array system being in the segmented configuration. Four elements were used per segment with an inter-element spacing of **40.65** meters. The total number of elements used in the array was **32.** These results were obtained at a frequency of 10 MHz (λ = 30.0 meters) and may be compared to the result obtained in Figure IV-5 where the array was not in the segmented configuratidn.
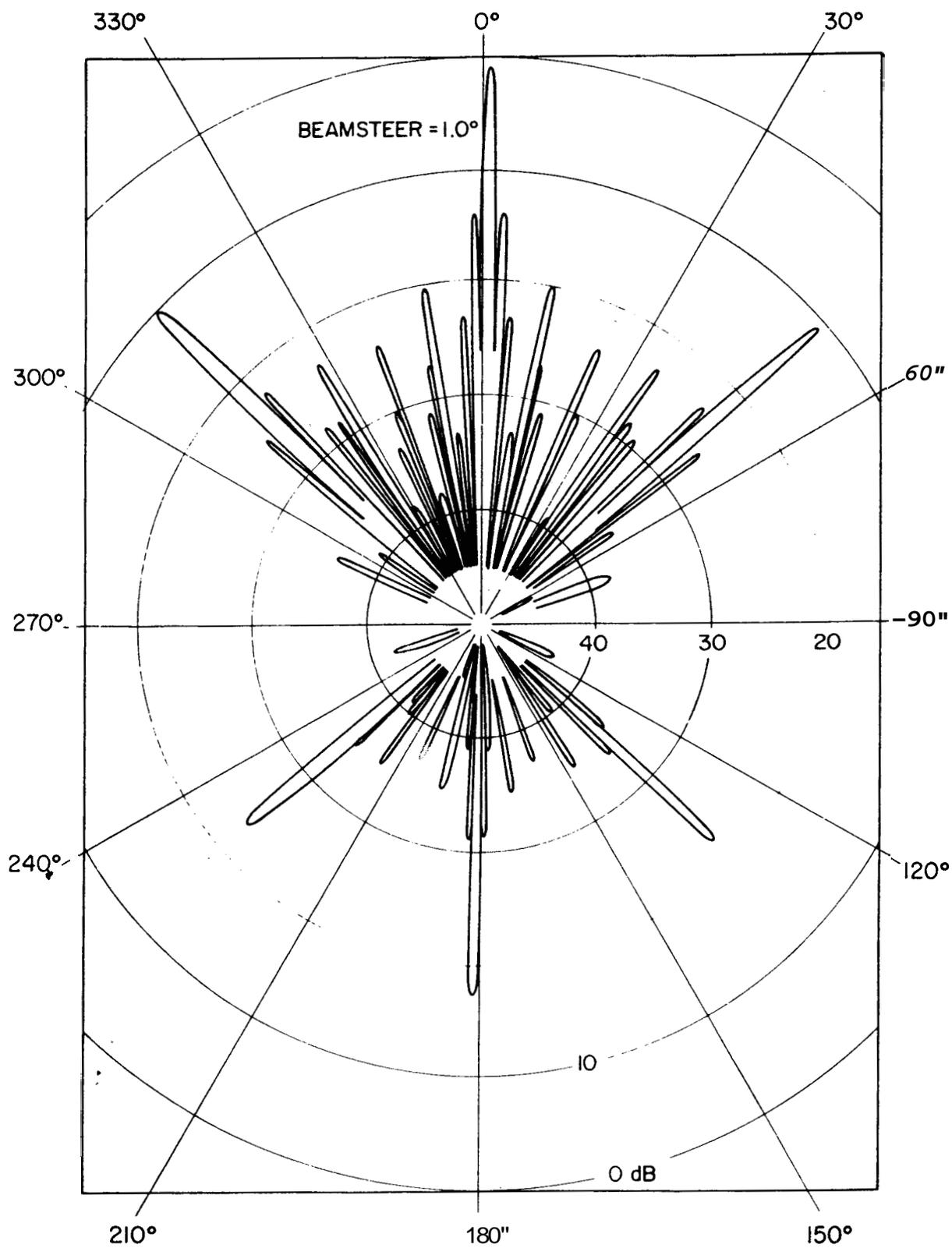
Figure *IV-9*. *Polar Plot* for *Beamsteer* = *1.0"*

156
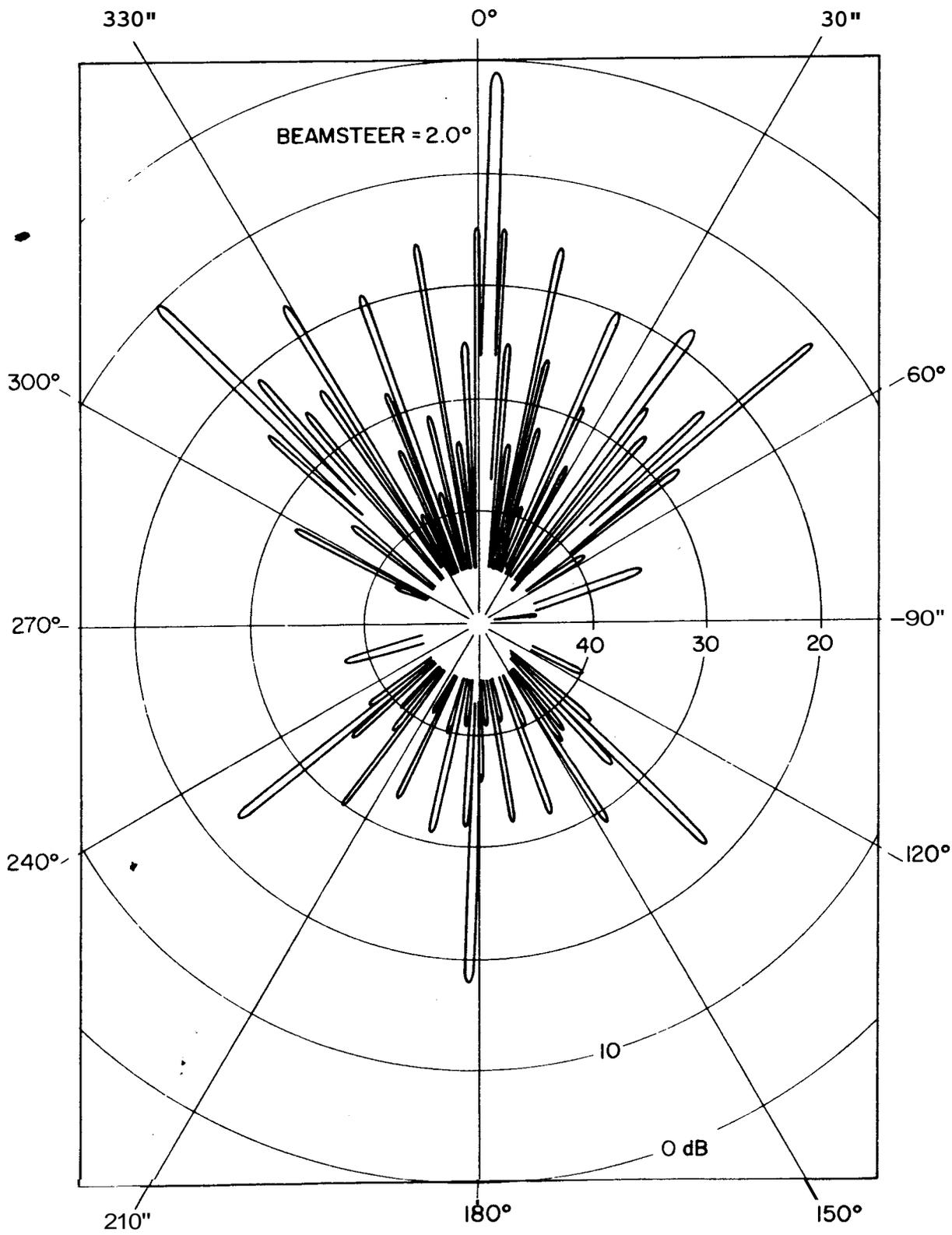
Figure IV-10. Polar Plot for Beamsteer = 2.0"
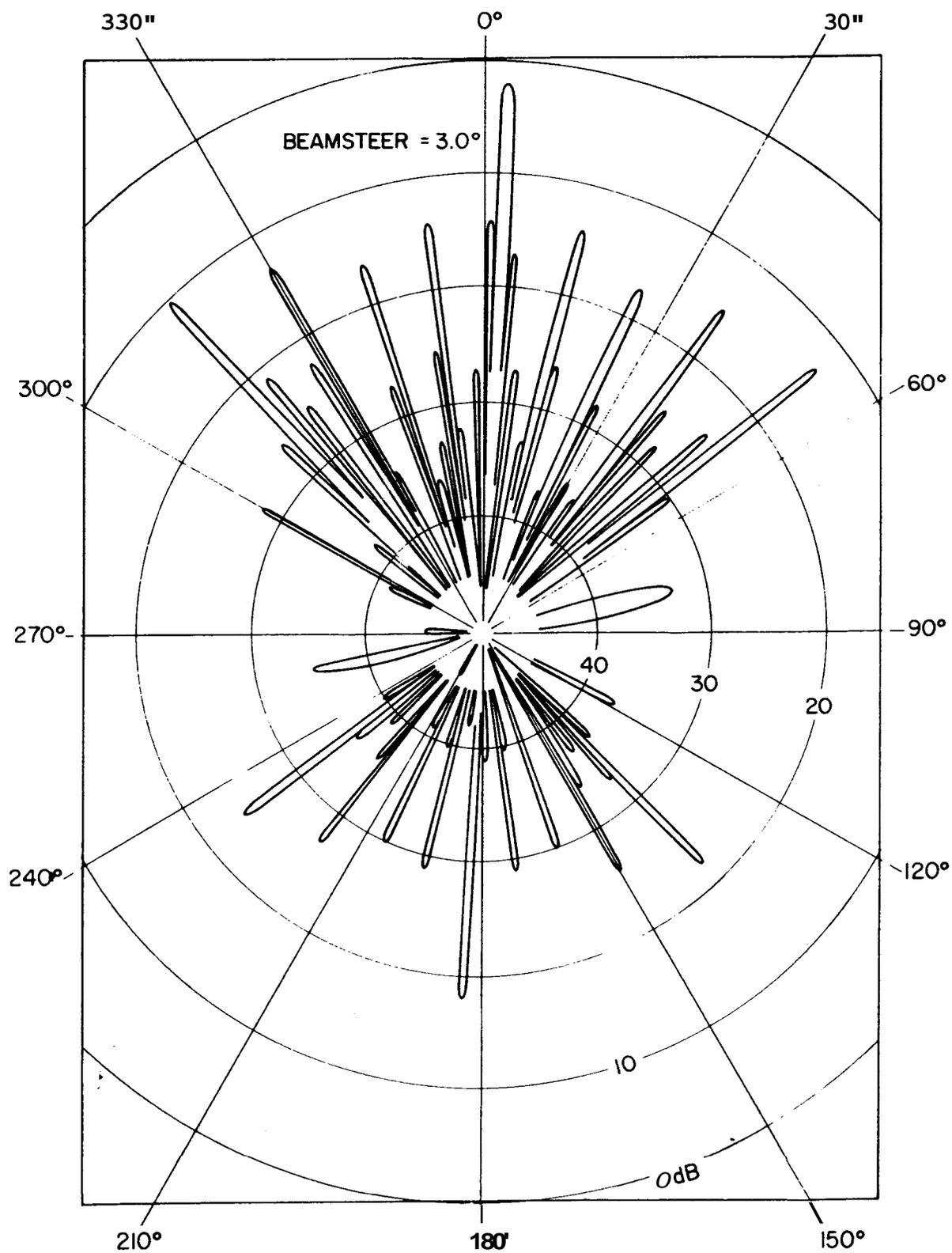
Figure IV-11. Polar Plot for Bearnsteer = 3.0"
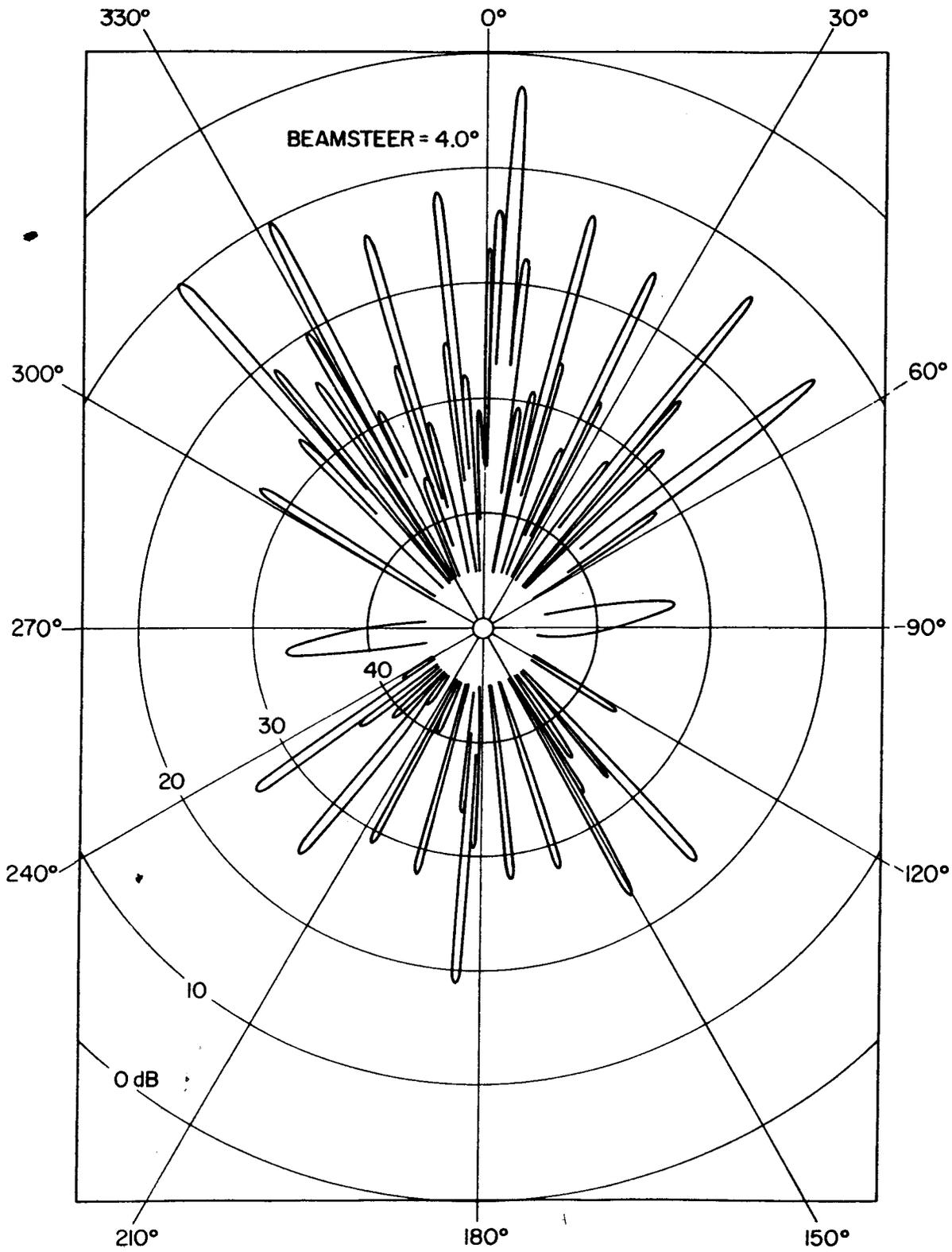
Figure IV-12. Polar Plot for Beamsteer = 4.0"
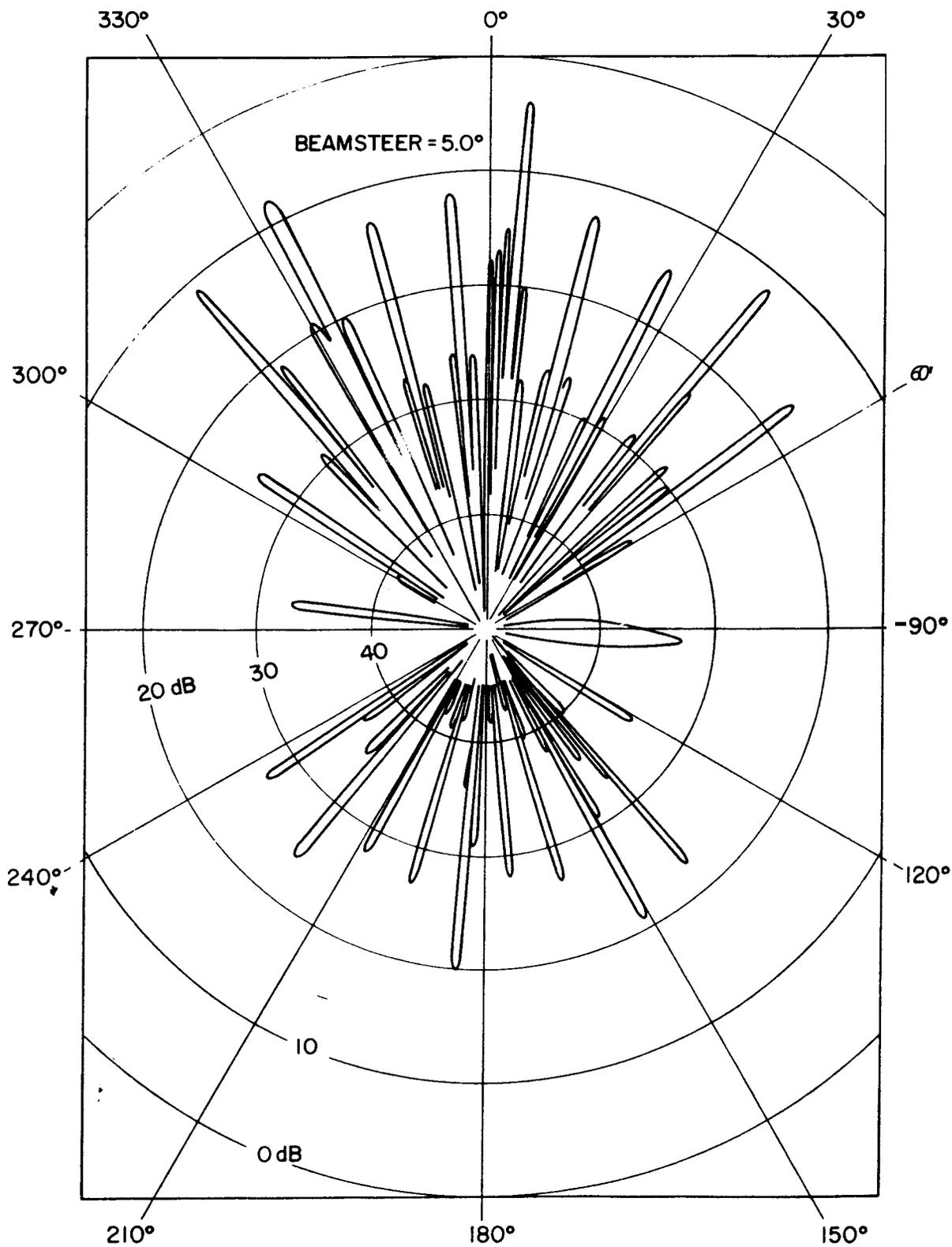
Figure *IV-13. Polar Plot for Beamsteer = 5.0"*

SECTION 7

Amplitude Weighting

Amplitude **weighting**[23] may be applied to the linear array in the form of

$$A(\ell) = 0.54 + 0.46 \cos \frac{2\pi\ell}{L} \tag{7:1}$$

Consider a continuous aperture of length L with a plane wave incident on the aperture at some angle θ. The wave field is given by,

$$E(\ell) = e^{j\frac{2\pi}{\lambda} \ell \sin \theta} \tag{7:2}$$

If amplitude weighting is applied in the form as shown in equation (7:1) then,

$$E(\ell) = \left(0.54 + 0.46 \cos \frac{2\pi}{L} \ell\right) e^{j\frac{2\pi}{\lambda} \ell \sin \theta} \tag{7:3}$$

The far field distribution is the Fourier Transform of equation (7:3) thus,

$$E = \int_{-\frac{L}{2}}^{\frac{L}{2}} \left\{0.54 + 0.46 \cos \frac{2\pi\ell}{L}\right\} e^{j\frac{2\pi}{\lambda} \ell \sin \theta} e^{-j\frac{2\pi}{L} \ell\mu} .d\ell \tag{7:4}$$

where $\frac{2\pi}{L}$ is thg space frequency of period L. The evaluation of equation (7:4) results in

$$E = \frac{L \sin x}{x} \left\{ 0.54 - 0.46 \left[\frac{1}{1 - \frac{\pi}{\cdots} 2} \right] \right. \tag{7:5}$$

where

$$x = \frac{\pi L}{\lambda} \left(\sin \theta - \frac{\lambda\mu}{L} \right) \tag{7:6}$$

If $\mathbf{x} = 0.0$ (i.e. $\sin \theta = \frac{\lambda\mu}{L}$), then E will attain its maximum value of

$$E_{max} = 0.54 \text{ L} \qquad (7:7)$$

At the half power point, E is 3 dB below E_{max}, or $\mathbf{E} = 0.38$ L and this gives rise to a value of $x = 2.047$ radians. Since $\mathbf{x} = \frac{\pi}{\lambda} \text{ L } (\sin \theta - \frac{\lambda\mu}{L})$ from equation (7:6), then at the half power points,

$$2.047 = \frac{\pi}{\lambda} \text{ L } \left(\sin \theta - \frac{\pi\mu}{L}\right) \qquad (7:8)$$

Thus,

$$\sin 8 - \frac{\lambda\mu}{L} = \frac{2.047\lambda}{\pi L} \qquad (7:9)$$

Let $\sin \theta - \frac{\lambda\mu}{L} = \sin \alpha$, then

$$\sin \alpha = \frac{2.047\lambda}{\pi L} \qquad (7:10)$$

Again if α is small then,

$$\alpha \simeq \frac{2.047}{\pi L} \text{ x } 57.29578 = \frac{37.332\lambda}{L} \text{ degrees} \qquad (7:11)$$

The beamwidth which is defined as 2α is then given by

$$\text{Beamwidth} = \frac{74.665\lambda}{L} \text{ degrees} \qquad (7:12)$$

Thus by the application of the weighting function as shown in equation (7:1) the beamwidth will increase by 32.2% to that with no weighting. However, the adjacent side lobes will be reduced to less than 1% of the main lobe. Successive side lobes, however, will tend to increase in amplitude and exceed 1%. It will also be noted that the main lobe will reduce in amplitude to 0.54 compared to that with no weighting. The value of 0.54, which may be defined as the normalising factor, is used to normalise the radiation pattern when weighting, of the form described above, is applied. The effects of the beam pattern when this form of weighting is applied are exemplified in the linear plot of Figure $(IV-14)$.

Figure IV-14. Illustration in Linear Form of the Radiation Pattern With the Application of Amplitude Weighting.

Reduction in Gain with Amplitude Weighting: Since the application of amplitude weighting reduces the amplitude of the radiation pattern, then the reduction in gain in decibels may be given as

$$W = 20 \log_{10} \left\{ \frac{L \sin x}{x} \left\{ 0.54 - 4.46 \left[\frac{1}{1 - \frac{\pi}{x}^2} \right] \right\} \right\} \qquad (7:13)$$

where **x** is defined in equation (7:6).

Taylor Weighting: Taylor[24] weighting is particularly useful in wide aperture, narrow beamwidth, linear array systems, where the main-lobe to side-lobe voltage ratio has been specified. This form of weighting also insures that the successive side lobes remain at the specified voltage ratio out to some integer number designated $\bar{n}$.

Let the radiation pattern resemble the following function in the central region

$$F(M) = \cos \pi \sqrt{\left(\frac{M}{\sigma} \right)^2 - A^2} \qquad (7:14)$$

where σ is a number somewhat greater than unity and is chosen such that $F(M)$ becomes zero at a corresponding integer designated $\bar{n}$.

σ is defined by:

$$\sigma = \frac{\overline{n}}{\sqrt{A^2 + (\overline{n} - \frac{1}{2})^2}} \qquad (7:15)$$

A has the properties such that $\cosh \pi A$ is the main-lobe to side-lobe voltage ratio. M is an integer ranging from $0 \leq M \leq \overline{n}$. To determine the Fourier coefficients or $F(M)$, one must evaluate the products

$$F(M) = C \prod_{n=1}^{\overline{n}-1} \left\{ 1 - \frac{M^2}{\sigma^2[A^2 + (n - \frac{1}{2})^2]} \right\} \left\{ \prod_{n=\overline{n}}^{\infty} \left(1 - \frac{M^2}{n^2} \right) \right\} \qquad (7:16)$$

where C is an arbitrary constant and may be taken to be $\cosh \pi A$.

In order to determine the weighting factors the inverse Fourier Transform must be performed on equation (7:16), and this is given generally as,

$$W(P) = \frac{1}{2\pi} \left\{ F(0) + 2 \sum_{M=1}^{\infty} F(M) \cos MP \right\} \qquad (7:17)$$

where $P^2 \leq \pi$

Since $F(M)$ is zero for $M \overset{>}{=} \overline{n}$, then the summation terminates at $M = \overline{n}$, thus simplifying the evaluation of equation (7:17).

Taylor has produced a table of values (Table IV-1) including the three parameters necessary in order to calculate the corresponding weights namely, A^2, σ, and $\overline{n}$. Another useful parameter, designated β_0, and found in column 3 of the table, may be used to determine the actual beamwidth of a linear array system when this form of weighting is applied. The actual beamwidth is given by,

$$\text{Actual beamwidth} = \frac{\beta_0 \cdot \sigma \cdot \lambda}{ND} \text{ degrees} \qquad (7:18)$$

For example, if a designed main-lobe to side-lobe voltage ratio is to be 100.00 (40dB), and $\overline{n}$ is chosen to be 6, then from the table,

$\sigma = 1.04298$ and $\beta_0 = 68.76"$. If a wave number of 42.21 is used, then the actual beamwidth will be,

$$\text{Actual beamwidth} = \frac{68.76 \text{ x } 1.04298}{42.21} \text{ degrees.} = 1.7^\circ \qquad (7:19)$$

TABLE IV-1

(1) Design side-lobe ratio (in dB)	(2) η (Side-lobe voltage ratio)	(3) $180\beta_0$ / π (in den.)	(4) A^2	(5) Values of the parameter .						
				$\bar{n}=2$	$\bar{n}=3$	$\bar{n}=4$	$\bar{n}=5$	$\bar{n}=b$	$\bar{n}=7$	$\bar{n}=8$
0	1.00000	28.65	0.00000	1.33333	1.20000	1.14286	1.11111	1.09091	1.07692	1.06667
5	1.77828	34.49	0.14067	1.29351	1.18672	1.13635	1.10727	1.08838	1.07514	1.06534
10	3.16228	40.33	0.33504	1.24393	1.16908	1.12754	1.10203	1.08492	1.07268	1.06350
15	5.62341	45.93	0.58950	1.18689	1.14712	1.11631	1.09528	1.08043	1.06949	1.06112
20	10.0000	51.17	0.90777	1.12549	1.12133	1.10273	1.08701	1.07490	1.06554	1.05816
25	17.7828	56.04	1.29177	---	1.09241	1.08698	1.07728	1.06834	1.06083	1.05463
30	31.6228	60.55	1.74229	---	---	1.06934	1.06619	1.06079	1.05538	1.05052
35	56.2341	64.78	2.25976	---	---	---	1.05386	1.05231	1.04923	1.04587
40	100.0000	68.76	2.84428	---	---		---	1.04298	1.04241	1.04068

Beamwidth Spread (Percent): The percentage spread in beamwidth when 40 dB Taylor weighting is applied may be determined, by first, determining the beamwidth of the $\sin x/x$ radiation pattern using the same wave number. For example, if the wave number of 42.21 is used the $\sin x/x$ beamwidth will be

$$\text{Beamwidth} = \frac{50.65}{42.21} = 1.2° \qquad (7:20)$$

The Beamwidth spread in percent will be

$$\text{Beamwidth spread} = \frac{1.7 - 1.2}{1.7} \; X \; 100 \qquad (7:21)$$

$$= 29\%$$

Thus, with the application of Taylor weighting, the beamwidth will increase by 29%.

It has been determined numerically that with the application of this form of weighting the main lobe will reduce in amplitude to 0.551 compared to that with no weighting. Thus, the beam pattern obtained with *40* dB Taylor weighting applied has been normalised to this value. The effects of 40 dB Taylor weighting on the beam pattern is exemplified in the linear plot of Figure IV-15.

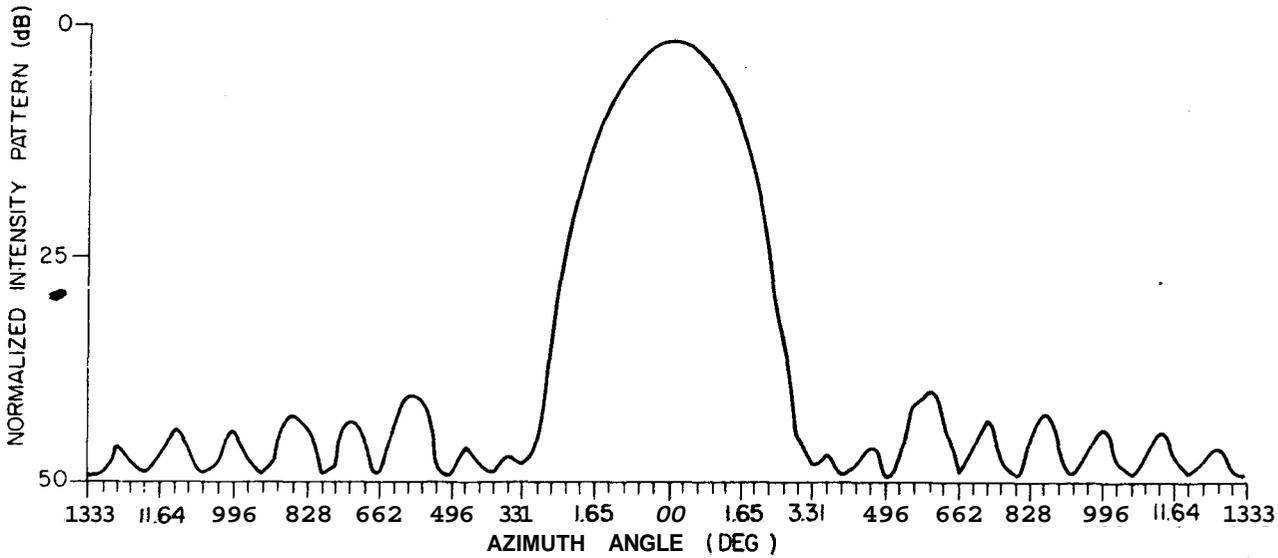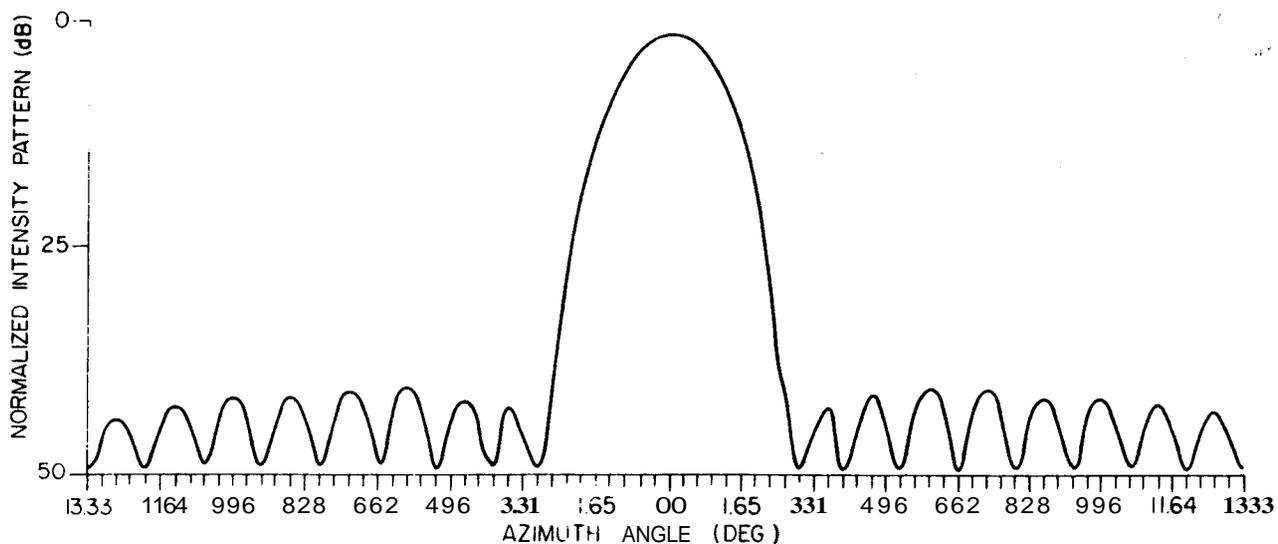*Figure IV-15. Illustration in Linear Form of the Radiation Pattern with Application of Taylor Weighting.*

Reduction in Gain With Taylor Weighting: **Since the application of Taylor weighting reduces the amplitude of the radiation pattern, then the reduction in gain in decibels may be given as**

$$W = 20 \log_{10} [F(M)] \tag{7 :21}$$

where F(M) is defined in equation (7:16).

SECTION 8

Azimuthal Bearing Errors Caused by Linear Array on Sloping Ground

Azimuthal bearing errors will result if the linear antenna array system is installed on sloping ground. The magnitude of this error will be dependant upon the true azimuthal bearing of the signal and its elevation angle. To illustrate this, consider the diagram of Figure IV-16.
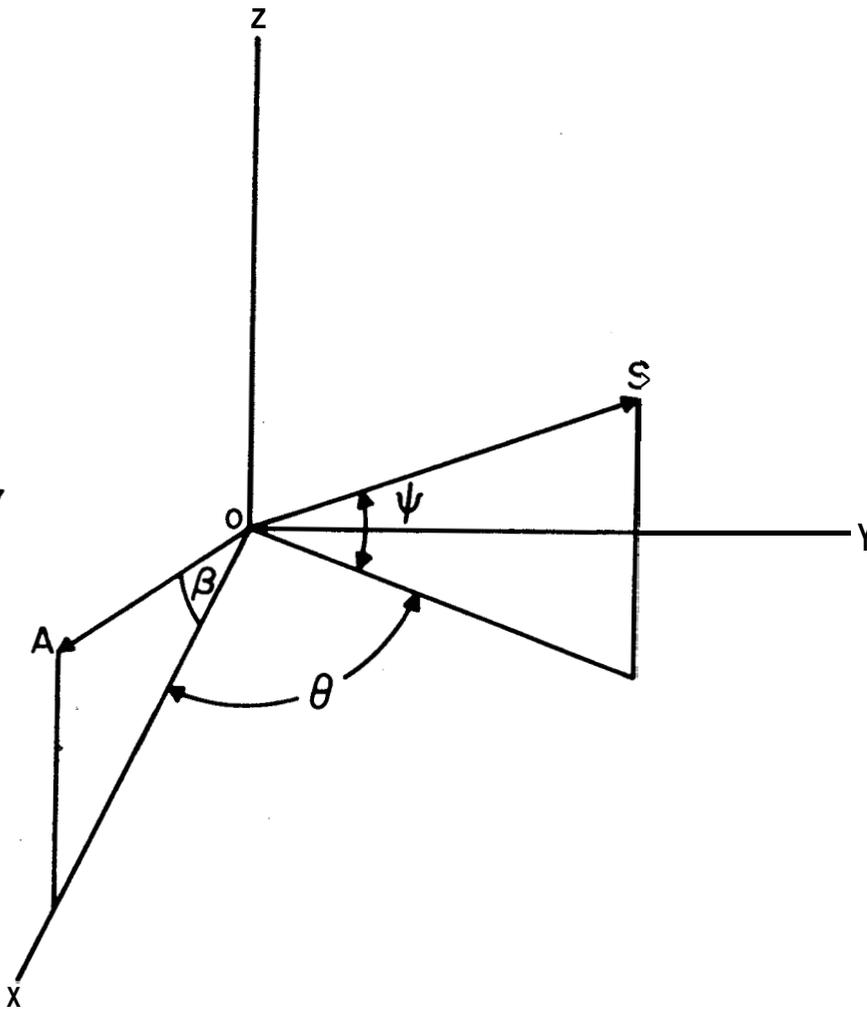
Figure IV- 16. Illustration of the linear Array on Sloping Ground

In this diagram, the unit vector $\mathbf{A}$, in the direction of the linear array, has an elevation angle β with respect to the $\mathbf{x}$, y plane. The unit vector S represents a signal vector having an elevation angle ψ and an azimuthal angle θ.

The projection of the S vector on the $\mathbf{x}$, y, $\mathbf{z}$, coordinates will give

$$S = \hat{x} \cos \alpha_1 + \hat{y} \cos \beta_1 + \hat{z} \sin \psi \qquad (8:1)$$

where β_1 is the angle between the S vector and the y coordinate, α_1 is the angle between the S vector and the x coordinate, and $\hat{x}$, $\hat{y}$, $\hat{z}$ are unit vectors in the $\mathbf{x}$, y, z directions respectively. Similarly for the $\mathbf{A}$ vector

$$A = \hat{x} \cos \beta + \hat{z} \sin \beta \qquad (8:2)$$

Since we are interested in the angle γ between the vectors $\mathbf{S}$ and $\mathbf{A}$, then the resultant cosine of the angle γ is simply the dot product of $\mathbf{S}$ and $\mathbf{A}$. Thus, $\cos(\gamma) = S \cdot \mathbf{A}$ therefore,

$$\cos(\gamma) = \cos \alpha_1 \cos \beta + \sin \psi \sin \beta \qquad (8:3)$$

From a knowledge of right spherical triangles $\cos \alpha_1$ may be deduced and is given by,

$$\cos \alpha_1 = \cos \psi \cos \theta \qquad (8:4)$$

Therefore

$$\cos(\gamma) = \cos \psi \cos \theta \cos \beta + \sin \psi \sin \beta \qquad (8:5)$$

To simplify matters, assume that the front **or** main lobe is broadside to the linear array system (i.e. $\theta = 90.0°$), then

$$\cos(\gamma) = \sin \psi \sin \beta \qquad (8:6)$$

Thus for an array having an elevation angle of β, the value of γ turns out to be a function of the elevation angle ψ of the signal. For example, if $\beta = 2.0°$ and $\psi = 20.0"$ then

$$y = \text{arc } \cos (\sin(20)\sin(2)) = 89.3" \qquad (8:7)$$

The bearing error $\Delta\gamma$ which results from the array being on sloping ground is

$$\Delta\gamma = \mathbf{90.0} - \text{arc cos } (\sin \psi \sin \beta) \qquad (8:8)$$

From the foregoing example, $\Delta\theta$ turns out to be $0.7°$. This bearing error is particularly important in wide aperture, narrow beamwidth, linear array systems. The result is that as the elevation angle of the signal increases, the array beam tends to steer away in azimuth from the direction of the signal source. Eventually, at some elevation angle, the beam will steer sufficiently away so that the direction of the signal is outside the beamwidth of the array. These variations in the elevation angle are articularly noticeable for radio waves that propagate via the ionosphere(25P.

SECTION 9

Radiation Pattern Format on as a Function of the Radial Distance R

For a performance evaluation of a linear array system, the test transmitter should be placed at some radial distance R from the system in order to minimize interference caused by the Fresnel effect.

Consider a linear array system of aperture length L, and also consider a point source at some radial distance R from the linear array as shown in Figure IV–17. Radio waves emanating from the point source will produce a curved wavefront with respect to the linear array. For some given length ℓ, the propagation length S may be given as

$$S = \{R_0^2 + (z + \ell)^2\}^{\frac{1}{2}} - R \qquad (9:1)$$

but $R_0 = R \sin \theta$ and $Z = R \cos \theta$ and therefore S may be given in terms of θ, ℓ and R to be

$$S = R^2 \sin^2 \theta + (\ell + R \cos \theta)^2\}^{\frac{1}{2}} - R \qquad (9:2)$$

For a given R and θ, $S(\ell)$ may be evaluated by use of the Maclaurin series to the second order term to be

$$S(\ell) = \ell \cos \theta - \frac{\ell^2 (1 - \cos 2\theta)}{2R} \qquad (9:3)$$

Thus the phase angle ϕ may be given as a function of ℓ to be

$$\phi(\ell) = \frac{2n}{\lambda} \ell \cos \theta - \frac{\pi \ell^2}{R\lambda} (1 - \cos 2\theta) \qquad (9:4)$$

The second term in Equation (9:4) represents the interfering–phase effect, or Fresnel effect for a given radial distance R. If we now assume orthogonal conditions (**I.E.** $\theta = 90°$), then

$$\phi(\ell) = \frac{2\pi \ell^2}{R\lambda} \quad \text{(excluding the minus sign)} \qquad (9:5)$$

Using the criteria that the interferring phase shall not exceed $\frac{\pi}{8}$ radians at $\frac{L}{2}$, then R may be given as

$$R = \frac{2L^2}{\lambda} \qquad\qquad (9:6)$$

With the criteria above, Equation (9:6) represents the boundary condition between the near field or Fresnel zone, and the far field or Fraunhofer region. The result obtained in Equation (9:6) also appears in Kraus[26]. From Equation (9:6) it will be noted that for a given aperture length L, the boundary condition is inversely proportional to the wavelength λ.
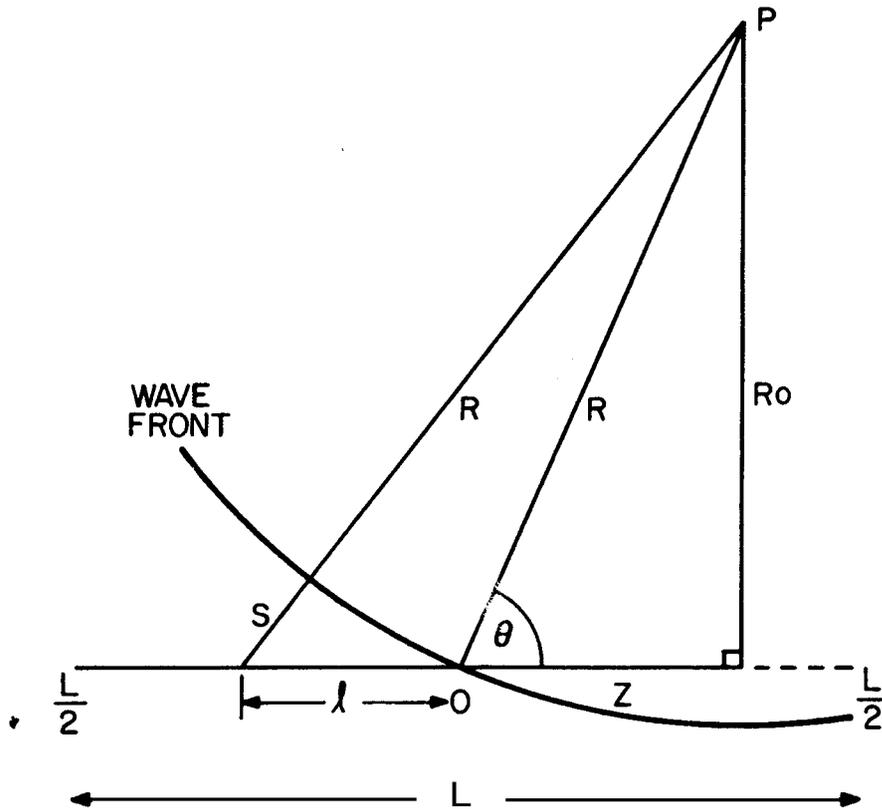
Figure IV-17. Illustration of a curved wave front emanating from the point P and which is arriving at some angle θ w.r.t. the linear array of length L.

```
0042:    ROOK,276900S      07/16/75       11:19
C        PROGRAM TO COMPUTE AND DISPLAY THE RADIATION PATTERN FOR
C        A LINEAR ARRAY OF BEVERAGE ANTENNAS.  THE NUMBER OF
C        ELEMENTS (NRX), USED IN THE ARRAY MUST BE AN INTEGER
C        POWER OF TWO ELEMENTS AND NOT TO EXCEED 64
C        THE ARRAY MAY BE
C        'SEGMENTED' PROVIDING THE TOTAL NUMBER OF ELEMENTS USED
C        IN THE SYSTEM ARE EXACTLY DIVISABLE BY THE NUMBER OF
C        ELEMENTS CHOSEN FOR THE SEGMENT. RADIATION PATTERNS ARE
C        ALSO COMPUTED FOR THE ARRAY SYSTEM ON LINEAR SLOPING GROUND
C        COSINE WEIGHTING OR 40DB TAYLOR WEIGHTING MAY BE APPLIED
C        TO THE ARRAY SYSTEM. IF THE ARRAY IS SEGMENTED, THE WEIGHTS
C        ARE APPLIED TO THE SEGMENTS ONLY.
C        THE INPUT PARAMETERS REQUIRED FOR THE PROGRAM AKE AS FOLLOWS:
C        D.......THE INTER-ELEMENT SPACING D IN METERS
C        NRX....NUMBER OF ELEMENTS
C        FAV.......THE FREQUENCY BF OPERATION IN MHZ
C        THETA.....BEAMSTEER ANGLE (DEGREES)
C        NPT.......THE NUMBER OF ELEMENTS PER SEGMENTS
C        (IF NPT=1, THE ARRAY IS NOT SEGMENTED)
C        ALPHA.......THE ELEVATION ANGLE OF THE SIGNAL IN DEGQEES
C        (IF ALPHA = 0.0, GROUND WAVE CONDITIONS ARE ASSUMED)
C        BETA.....GROUND ELEVATION ANGLE(DEGREES)
C        ISKIP.....PARAMETER FOR SELECTION OFAPPROPRIATE
C                  WEIGHTING FUNCTION
C                  ISKIP = 0...NO WEIGHTING
C                  ISKIP = 1...COSINE WEIGHTING
C                  ISKIP = 2...TAYLOR WEIGHTING
C        XLENGTH.....ANTENNA LENGTH (METERS)
C        EG..........RELATIVE DIALECTRIC CONSTANT
C        SIGMA.......GROUND CONDUCTIVITY (MHO/METER)
C        H...........ANTENNA HEIGHT (METERS)
C        RADIUS......WIRE RADIUS (METERS)
C         THE ABSOLUTE VALUE OF THE COMPLEX CHARACTERISTIC
C        IMPEDANCE ZO IS TAKEN AS THE TERMINATING IMPEDANCE ZL.
C        EXAMPLE OF PARAMETERS:-
C        7.,16,5.,0.,1,22.,0.,0,100.,12.,.003,1.,10.26E-4
C        DATA PARAMETERS START IN COL. 1 OF DATA CARD
C
C        B.J. ROOK MARCH 30 1975
C
         DIMENSION BRG(999),W(256),ITITLE(500),
        *IT(0:2000),LINE(100),RBUF(2000),ABUF(256)
        *,FT(2000),XLL(128),WF(128),XGAM(2)
         COMPLEX CWBUF(512),CMBUF(512),CBUF(64),CBUF2(64)
        *,XGAMMA,ZO,ZIN
         EQUIVALENCE (XGAMMA,XGAM(1))
         DATA ITITLE/' AZIMUTH ANGLE DFGREES '/,C/299.998/
        *,ILIM/128/
C        READ IN DATA PARAMETERS
         INPUT D,NRX,FAV,THETA,NPT,ALPHA,BETA,ISKIP,XLENGTH,
        *EG,SIGMA,H,RADIUS
         THETA = THETA/57.29578
```

```
      ALPHA1 = ALPHA/57.29578
      BETA = BETA/57.29578
      XLAMBDA = C/FAV
      DY 40 I = 1 , ILIM/2
      XLL(I) = 0.0
      WF(I) = 0.0
   40 CBUF(I) = CMPLX(1.,0.)
      CALL WISE(EG,SIGMA,H,RADIUS,XLENGTH,XGAM,Z0,FAV,
     *XGAMMA,XN,DB)
      ZLL = CABS(Z0)
      CALL DELAYCONST(NPT,D,THETA,XLAMBDA,CBUF,NRX ,XLL,NR)
      IF(ISKIP .EQ. 0)GO TO 43
      IF(ISKIP .EQ. 2)GO TO 200
      CALL WEIGHT(NRX,CBUF,NPT,WF)
      GO TO 43
  200 CALL TAYLOR(NRX,CBUF,D,WF,NPT)
   43 DO 30 I = 1 , ILIM
   30 CMBUF(I) = CMPLX(0.0,0.0)
      MCNTR = 1 + (ILIM/2)
      LCNTR = MCNTR - (NRX/2)
      DO 2 N = 1 , NRX
      CMBUF(LCNTR-1+N) =  CBUF(N)
    2 CONTINUE
      M = ALOG(FLOAT(ILIM))/ALOG(2.0) + 0.5
      CALL FAST4 (M , CMBUF , W , -1)
      DB 345 N = 1 o ILIM
  345 ABUF(N) = CABS(CMBUF(N))/FLOAT(NRX)
      AMPMX = ABUF(1)
      CONST = XLAMBDA/(D*FLOAT(ILIM))
      ID = 0
      DO 772 I = 2 , ILIM
      IF(AMPMX .GE. ABUF(I))GO TO 772
      AMPMX = ABUF(I)
      ID = I-1
  772 CONTINUE
  773 WRITE(108,12
      WRITE(108,13 NRX
      WRITE(108,14 D
      WRITE(108,23 FAV
      WRITE(108,29 XLENGTH
      WRITE(108,28 XN
      WRITE(108,38)DB
      WRITE(108,37)XGAM(2)
      WRITE(108,33)H
      WRITE(108,34)EG
      WRITE(108,35)SIGMA
      WRITE(108,36)RADIUS
      WRITE(108,39)Z0
      WRITE(108,31)ZLL
      IF(ALPHA .EQ. 0.0)GO TO 501
      WRITE(108,32)ALPHA
  501 IF(NPT .EQ. 1)GO TO 774
      WRITE(108,15)NPT
```

```
774    IF(THETA .EQ. 0. .AND. ISKIP .EQ. 0)GO  TO 566
       WRITE(108,16)
       IF(NPT .EQ. 1)GO TO 775
       WRITE(108,18)
       WRITE(108,20)
       WRITE(108,21)
       WRITE(108,22)I,XLL(I),WF(I),I=1,NR
       GO TO 566
775    WRITE(108,19)
       WRITE(108,20)
       WRITE(108,21)
       WRITE(108,22)I,XLL(I),WF(I),I=1,NR
566    CONTINUE
       DECODE(2000,93,ITITLE) IT(K) , K = 0 , 2000
       J = 0
       J2 = 0
       N = 1
432    I = 1
433    SINE = CONST*FLOAT(N-1)
       DSINE = CONST*FLOAT(N-1-ID)
       IF(SINE .GT. 2.0)GO TO 435
       SSINE = AMOD(SINE,1.0)
999    IF(SINE .GT. 1.0)GO TO 435
       IF(ISKIP .EQ.0)AMPMX=1.
       IF(ISKIP .EQ. 2)AMPMX=0.551
       IF(ISKIP .EQ. 1)AMPMX = 0.54
       BBUF(N) = ABUF(I)/AMPMX
       BRG(N) = 57.29578*ASIN(SINE)
       GO TO 44
435    IF(J .EQ. 1)GO TO 436
       NN = N
436    NN = NN - 1
       IF(NN .EQ. 0)GO TO 771
       J = 1
       BRG(N) = 180.0 - BRG(NN)
44     IF(DSINE .GT. 1.0)GO TO 770
       I = I + 1
       IF(SINE .LE. 1.0)GO TO 884
       IF(ISKIP .EQ. 0)AMPMX=1.
       IF(ISKIP .EQ. 2)AMPMX=0.551
       IF(ISKIP .EQ. 1)AMPMX=0.54
       BBUF(N) = ABUF(I)/AMPMX
884    N = N + 1
       IF(I - ILIM)433,433,432
770    IF(J2 .EQ. 1)GO TO 883
       N2 = N
883    N2 = N2 - 1
       BBUF(N) = BBUF(N2)
       N = N + 1
       J2 = 1
       IF(I - ILIM)433,433,432
```

```
771 L = 1
    CALL BEVERAGE(N,BRG,FT,FAV,ALPHA1,EG,H,SIGMA,ID,
   *XLENGTH,ZO,XGAMMA,XGAM,XN,ZLL,XGAIN)
    PER = ALOG10(NRX)/ALOG10(2.)
    IF(ISKIP .EQ. 0)XGAIN1 = 0.
    IF(ISKIP .EQ. 1)XGAIN1 = -5.35
    IF(ISKIP .EQ. 2)XGAIN1 = -5.16
    POWER =  (3.*PER) + XGAIN + XGAIN1 +20*ALOG10(BBUF(ID+1))
    WRITE(108,59)POWER
    WRITE(108,17)
    DO 403 J = 2 , N-1
    XL = FT(N-J)*BBUF(J)
    IF(XL.GT.0.0.AND.XL.LT.3.16E-3)GO TO 403
    IF(XL.EQ.0.0)GO TO 778
    LL = 50.0 + (20.*ALOG10(XL)) +.5
    GO TO 779
778 LL = 0
779 ENCODE(72,45,LINE)IT(L),BRG(N-J),LL
    WRITE(108,27)LINE(K),K=1,18
    L = L + 1
403 CONTINUE
    DO 404 J = 2 , N-1
    XL = FT(J)*BBUF(J)
    IF(XL.GT.0.0.AND.XL.LT.3.16E-3)GO TO 404
    IF(XL .EQ. 0.0)GO TO 776
    LL = 50.0 + (20.*ALOG10(XL)) + .5
    GO TO 777
776 LL = 0
777 ENCODE(72,45,LINE)IT(L),BRG(J),LL
    WRITE(108,27)LINE(K),K=1,18
    L = L + 1
404 CONTINUE
    WRITE (108,67)
    STOP
 17 FORMAT('1',29X,'NORMALISED INTENSITY PATTERN'/
   *37X,'1.0DB PER DIV'/
   *15X,'-50.0',20X,'-25.0',22X,'0.0'/
   *17X,26('-+'))
 45 FORMAT(4X,1A1,6X,F6.2,'+',NX,'*',T70,'+')
 27 FORMAT(18A4)
 67 FORMAT(17X,26('-+'))
 93 FORMAT(2000A1)
 12 FORMAT('1DISPLAY IN LINEAR FORM OF THE RADIATION PATTERN'
   *' FOR A LINEAR ARRAY OF BEVERAGE ANTENNAS',4X,'B. J. ROOK')
 13 FORMAT(/'THE NUMBER OF ELEMENTS USED = ',I2)
 14 FORMAT(/'INTER-ELEMENT SPACING (METERS) = ',F6.2)
 15 FORMAT(/'THE ARRAY IS IN THE SEGMENTED CONFIGURATION',
   *' WITH ',I2,' ELEMENTS PER SEGMENT')
 16 FORMAT('1','DELAY LINE LENGTHS AND WEIGHTING FACTORS ARE:')
 18 FORMAT(/,4X,'SEGMENT NO.',20X,'DELAY LINE',20X,'WEIGHTING')
 19 FORMAT(4X,'ELEMENT NO.',20X,'DELAY LINE',20X,'WEIGHTING')
 20 FORMAT(36X,'LENGTH',24X,'FACTORS')
 21 FORMAT(35X,'(METERS)',24X,'(DB)')
```

```
   22 FORMAT(8X,I2,27X,F6.2,25X,F5.2)
   23 FORMAT(/'FREQUENCY IN MHZ = ',F5.2)
   29 FORMAT(/'BEVERAGE ANTENNA WIRE LENGTH (METERS) = ',F6.2)
   28 FORMAT(/'VELOCITY OF PROPOGATION RATIO = ',F5.3)
   39 FORMAT(/'COMPLEX CHARACT. IMPED. Z0 = (',F7.2,',',
     *F7.2,') OHMS')
   31 FORMAT(/'TERMINATING IMPEDANCE. = ',F7.2,' OHMS')
   32 FORMAT(/'ELEVATION ANGLE OF SIGNAL (DEGREES) = ',F5.2)
   33 FORMAT(/'HEIGHT OF ANTENNA ABOVE GROUND (METERS) =',F5.2)
   34 FORMAT(/'RELATIVE DIALECTRIC CONSTANT OF GROUND = ',F4.1)
   35 FORMAT(/'GROUND CONDUCTIVITY (MHO/METER) = ',F8.6)
   36 FORMAT(/'WIRE RADIUS IN METERS (COPPER WIRE) = ',F8.7)
   37 FORMAT(/'PHASE CONSTANT (RADIANS/METER) = ',F8.6)
   38 FORMAT(/'ATTENUATION CONSTANT (DB/METER) = ',F8.6)
   59 FORMAT(/'POWER GAIN OF ANT. ARRAY REL. TO ISOTROPIC',
     *' RADIATOR =',F8.3, 'DB')
      END



      SUBROUTINE DELTA(W,EG,E0,SIGMA,ADELTA)
C     SUBROUTINE TO CALCULATE THE GROUND WAVE
C     TILT ANGLE
C     B. J. ROOK MARCH 30 1975
      S1 = EG - 1.
      s12 = S1*S1
      S2 = SIGMA/(E0*W)
      s22 = S2*S2
      s3 = s12 + s22
      S4 = EG*EG
      s5 = s4 + s22
      s55 = S5*S5
      DELTA = S3/S55
      DELTA = DELTA**.25
      ADELTA = ATAN(DELTA)
      RETURN
      END



      SUBROUTINE RHOV(XI1,W,E0,EG,SIGMA,RHO)
C     SUBRBUTINE TO CALCULATE THE VERTICAL
C     GROUND REFLECTION COEFFICIENT FBR A
C     GIVEN ELEVATION ANGLE(XI1).
C     B. J. ROOK MARCH 30 1975
      COMPLEX RHO,C2,Z,A,C
      Y = 0.-SIGMA/(W*E0)
      Z = CMPLX(EG,Y)
      B = COS(XI1)
      B = B*B
      A = Z*SIN(XI1)
      C = Z-B
      C2 = CSQRT(C)
      RHO = (A - C2)/(A + C2)
      RETURN
      END
```

```
      SUBROUTINE BEVERAGE(L,BRG,AMPP,FAV,XI1,EG,H,SIGMA,ID,
     *XLENGTH,Z0,XGAMMA,XGAM,XN,ZLL,XGAIN)
C     SUBROUTINE TO CALCULATE THE BEVERAGE ANTENNA
C     AZIMUTHAL RADIATION PATTERN AT A GIVEN ELEVATION
C     ANGLE(XI1). IF XI1=0.0, GROUND WAVE CONDITIONS
C     ARE ASSUMED.
C     B. J. ROOK MARCH 30 1975
      DIMENSION AMPP(1),XGAM(1),BRG(1),BX(1)
      COMPLEX Z(1),RHO,A(12),C(6),C4
     *,R(2),RHOO1,Z0,XGAMMA,RHOO
      DATA E0/8.85E-12/,PI/3.14159265/
     *CC/3.E8/
      ISK = 1
      IF(XI1 .EQ. 0.0)ISK=0
      F = FAV*1.E6
      ALPHA = XGAM(1)
      BETA = XGAM(2)
      RHOO = (ZLL-Z0)/(ZLL+Z0)
      RHOO1 =   XGAMMA*XLENGTH
      RHOO = RHOO*CEXP(-RHOO1)
      C4 = RHOO1/2.
      C4 = CEXP(-C4)
      W = 2.*PI*F
      IF(ISK .EQ. 1)GO TO 5
      CALL DELTA(W,EG,E0,SIGMA,XI1)
    5 X = W/CC
      XK = 2.*H*X
      XLAMBDA = CC/F
      AMPX = XLAMBDA**2/(377.*8.*PI)
      SIE = SIN(XI1)
      IF(ISK .EQ. 0)GO TO 6
      CALL RHOV(XI1,W,E0,EG,SIGMA,RHO)
      PHI = XK*SIE
      X = COS(PHI)
      Y = 0.0 - SIN(PHI)
      Z(1) = CMPLX(X,Y)
      A(2) = RHO*Z(1)
      A(3) = RHOH*Z(1)
      A(2) = 1. - A(2)
    6 DO 2 N = 1 , L-1
      XNN = BRG(N)/57.29578
      IF(ISK .EQ. 1)GO TO 7
      A(6) = SIE*COS(XNN)
      GO TO 8
    7 A(6) = SIE*COS(XNN)*A(2)
    8 A(7) = A(6)/(2.*Z0)
      RO = 1.-XN*COS(XI1)*COS(XNN)
      RO1 = 1.+XN*COS(XI1)*COS(XNN)
      S = RO*BETA*XLENGTH*.5
      S1 = RO1*BETA*XLENGTH*.5
      S3 = ALPHA*XLENGTH/2.
      C(1) = CMPLX(S3,S)
      C(2) = CMPLX(S3,S1)
```

```
      A(7) = A(7)*C4
      A(7) = A(7)*XLENGTH*(CSINH(C(1))/C(1)
    *+ RHOO*CSINH(C(2))/C(2))
      AMPP(N) = CABS(A(7))
      IF(N.NE.ID+1)GO TO 2
      A(8) = A(7)*A(7)*.5*REAL(ZO)
      POWER = CABS(A(8))/AMPX
      XGAIN = 10.*ALOG10(ABS(POWER))
    2 CONTINUE
      XNORM = 0.
      DO 4 K = 1 , L-1
      IF(AMPP(K) .GT. XNORM)XNORM = AMPP(K)
    4 CONTINUE
      DO 3 I = 1 , L-1
    3 AMPP(I) = AMPP(I)/XNORM
      XI1 = 57.29578*XI1
      IF(ISK .EQ. 0)WRITE(108,9)XI1
      RETURN
    9 FORMAT(/'GROUND WAVE TILT ANGLE (DEGREES) = ',F6.3)
      END




      SUBROUTINE WEIGHT(NRX,CBUF,NPT,WF)
C     SUBROUTINE TO COMPUT THE WEIGHTS
C     FOR COSINE WEIGHTING
C     B.J. ROOK MARCH 30 1975
      DIMENSION WF(1)
      COMPLEX CBUF(1)
      DATA PI/6.28318531/
      NM = NRX/2
      NR = NRX/NPT
      NR1 = NR/2
      CONST = PI/FLOAT(NR)
      DO 10 I = 1 , NR1
      XI = I
      X = CONST*XI
      W = 0.54 + 0.46*COS(X)
      N1 = ((I-1)*NPT) + 1
      N2 = I*NPT
      DO 20 N = N1 , N2
      CBUF(NM+N) = W*CBUF(NM+N)
      CBUF(NM+1-N) = W*CBUF(NM+1-N)
   20 CONTINUE
      WF(NR1+I) = ABS(20.*ALOG10(W))
      WF(NR1+1-I) = WF(NR1+I)
   10 CONTINUE
      RETURN
      END
```

```
      SUBROUTINE TAYLOR(NRX,CBUF,D,WF,NPT)
C     SUBROUTINE TO COMPUTE THE WEIGHTS FOR
C     40DB TAYLOR WEIGHTING
C     B.J. ROOK MARCH 30 1975
      COMPLEX CBUF(1)
      DIMENSION F(0:12),EL(0:40),WF(1)
      DATA PI/3.14159265/
     *,N/6/,A/2.84428/,S/1.04298/
      NM = NRX/2
      NR = NRX/NPT
      NR1 = NR/2
      DO 30 I = 0 , 12
   30 F(I) = 0.0
      L = 0
      XN = N - 1
      S = S*S
      REPEAT 10,FOR Z=(0.,XN,1.)
      C = 1.
      FF = 1.
      DO 11 K = N , 100000
      A1 = Z/FLOAT(K)
      A2 = A1*A1
      B = 1. - A2
      C = C*B
   11 CONTINUE
      DO 12 M = 1 , N-1
      D2 = FLOAT(M) - 0.5
      D1 = D2*D2
      E = S*(A+D1)
      EE = 1. - (Z**2/E)
      FF = FF*EE
   12 CONTINUE
      F(L) = FF*C
      L = L + 1
   10 CONTINUE
      XN1 = NR1
      XL = D*(XN1-0.5)
      DO 20 L = 0 , NR1
      AL = L
      AL = AL - 0.5
      P = D*AL*PI/XL
      IF(AL .EQ. -.5)P=0.0
      G= 0
      DO 31 M = 1 , N
      ARG = FLOAT(M)*P
      W = F(M)*COS(ARG)
      G = W + G
   31 CONTINUE
      G = 2.*G
      EL(L) = (F(0)+G)/(2.*PI)
   20 CONTINUE
      DO 40 I = 1 , NR1
      EL(I) = EL(I)/EL(0)
```

```
      N2 = ((I-1)*NPT)+1
      N3 = I*NPT
      DO 50 K = N2 , N3
      CBUF(NM+K) = EL(I)*CBUF(NM+K)
      CBUF(NM+1-K) = EL(I)*CBUF(NM+1-K)
   50 CONTINUE
      WF(NR1+I) = ABS(20.*ALOG10(EL(I)))
      WF(NR1+1-I) = WF(NR1+I)
   40 CONTINUE
      RETURN
      END


0008:   ROOK,276900S    07/16/75    12:40
      SUBROUTINE GRNDTILT(NRX,D,CBUF,THETA,ALPHA,BETA,XLAMBDA)
C     SUBROUTINE TO COMPUTE THE PHASE ERRORS
C     ACROSS THE ARRAY ASSOCIATED WITH A
C     GROUND TILT (BETA)
C     B.J. ROOK MARCH 30 1975
      COMPLEX CBUF(1)
      DATA PI/3.14159265/
      IF(ALPHA .EQ. .0 .AND. BETA .EQ. .0)RETURN
      SA = SIN(ALPHA)*SIN(BETA)
      EP = (PI/2.) - ACOS(SA)
      CONST = 2.*PI*SIN(EP)*D/XLAMBDA
      DO 10 N = 1 , NRX
      PHI = CONST*FLOAT(N-1)
      X = COS(PHI)
      Y = SIN(PHI)
      CBUF(N) = CBUF(N)*CMPLX(X,Y)
   10 CONTINUE
      RETURN
      END


      SUBROUTINE DELAYCONST(NPT,D,THETA, XLAMBDA,CBUF,NRX,XLL,NR)
C     SUBROUTINE TO  DETERMINE THE DELAY CONSTANCE PER
C     SEGMENT OF THE LINEAR ARRAY FOR A GIVEN STEER ANGLE
C     THETA.
C     B.J.ROOK MARCH 30 1975
      DIMENSION XLL(1)
      COMPLEX CBUF(1)
      DATA PI/6.28318531/
      NR = (NRX/NPT)
      IF(THETA .EQ. 0.0)RETURN
      D1 = FLOAT(NPT)*D*SIN(THETA)/XLAMBDA
      D2 = PI*D1
      DO 10 I = 1 , NR-1
      PHI = FLOAT(I)*D2
```

```fortran
      XLL(I+1) = FLOAT(I)*D1*XLAMBDA
      X = COS(PHI)
      Y = SIN(PHI)
      N1 = FLOAT(I)*NPT + 1
      N2 = N1 + NPT - 1
      DO 10 N = N1 , N2
      CBUF(N)   = CMPLX(X,Y)
   10 CONTINUE
      RETURN
      END


      SUBROUTINE CARSON (R,PQ,PI)
      COMPLEX RD1,RD2,RP,S2,S21,S4,S41,
     *SIG21,SIG2,SIG1,SIG3,SIG31,SIG4,SIG41,
     *P,Q,R,PQ
      IF(CABS(R) .GT. 10.)GO TO 22
      RD1 = 2.*CLOG(R/2.)
      RD2 = 2.*RD1
      RP = -RD1
      FAC2 = 0.
      S2 = CMPLX(0.,0.)
      SIGN = -1.
      DO 1 I = 1 , 50
      SIGN = -SIGN
      FAC1 = FAC2
      FAC1 = FAC1+ALOG(2*I-1)
      FAC2 = FAC1+ALOG(2*I)
      S21 = S2
      RP = RP + RD2
      S2 = S2 + SIGN*CEXP(RP-(FAC1+FAC2))
      IF(CABS((S21-S2)/S2) .LT. 1.E-5)GO TO 2
    1 CONTINUE
      STOP 1
    2 CONTINUE
      RD1 = 4.*CLOG(R/2.)
      RP = CMPLX(0.,0.)
      FAC2 = 0.
      S4 = CMPLX(0.,0.)
      SIGN = -1.
      DO 5 I = 1 , 50
      SIGN = -SIGN
      FAC1 = FAC2
      FAC1 = FAC1 + ALOG(2*I)
      FAC2 = FAC1 + ALOG(2*I+1)
      S41 = S4
      RP = RP + RD1
      S4 = S4 + SIGN*CEXP(RP-(FAC1+FAC2))
      IF(CABS((S41-S4)/S4) .LT. 1.E-5)GO TO 6
    5 CONTINUE
      STOP 2
    6 CONTINUE
      RD1 = 4.*CLOG(R)
      RP = CMPLX(0.,0.)
      XMULT1 = 0.
      SIGN = 1.
```

```fortran
      SIG1 = CMPLX(0.3333333,0.)
      DO 10 I = 3,100,4
      SIGN = -SIGN
      XI = ALOG(I+4)
      XMULT2 = XMULT1 + 2.*ALOG(I) + 2.*ALOG(I+2) + XI
      RP = RP + RD1
      SIG2 = SIG1
      SIG1 = SIG1 + SIGN*CEXP(RP-XMULT2)
      XMULT1 = XMULT2 - XI
      IF(CABS((SIG2-SIG1)/SIG1) .LT. 1.E-5)GO TO 15
   10 CONTINUE
      STOP 3
   15 SIG1 = R*SIG1
      RD1 = 2.*CLOG(R/2.)
      RD2 = 2.*RD1
      RP = -RD1
      FAC2 = 0.
      SIG2 = CMPLX(0.,0.)
      SIGN = -1.
      DO 20 I = 1 , 50
      SIGN = -SIGN
      FAC1 = FAC2
      ID = 2*I
      FAC1 = FAC1 + ALOG(ID-1)
      FAC2 = FAC1 + ALOG(ID)
      SUM = 0.
      DO 16 N = 1 , ID
      XN = N
   16 SUM = SUM + 1./XN
      SUM2 = SUM - 1./(2.*XN)
      A = ALOG(SUM2)
      A2 = A - (FAC1+FAC2)
      SIG21 = SIG2
      RP = RP + RD2
      SIG2 = SIG2 + SIGN*CEXP(A2+RP)
      IF(CABS((SIG21-SIG2)/SIG2) .LT. 1.E-5)GO TO 25
   20 CONTINUE
      STOP 4
   25 CONTINUE
      RD1 = 4.*CLOG(R)
      RP = 0.
      XMULT1 = 0.
      SIGN = 1.
      SIG3 = CMPLX(0.2,0.)
      DO 30 I = 5 , 100,4
      SIGN = -SIGN
      XI = ALOG(I+4)
      XMULT2 = XMULT1 + 2.*ALOG(I) +2.*ALOG(I+2) + XI
      RP = RP + RD1
      SIG31 = SIG3
      SIG3 = SIG3 + SIGN*CEXP(RP-XMULT2)
      XMULT1 = XMULT2 - XI
      IF(CABS((SIG31-SIG3)/SIG3) .LT. 1.E-5)GO TO 31
```

```
   30 CONTINUE
      STOP 5
   31 SIG3 = R*R*R*SIG3/9.
      RD1 = 4.*CLOG(R/2.)
      RP = CMPLX(0.,0.)
      FAC2 = 0.
      SIG4 = CMPLX(0.,0.)
      SIGN = -1.
      DO 40 I = 1 , 50
      SIGN = -SIGN
      FAC1 = FAC2
      ID = 2*I+1
      FAC1 = FAC1 + ALOG(ID-1)
      FAC2 = FAC1 + ALOG(ID)
      SUM = 0.
      DO 45 N = 1 , ID
      XN = N
   45 SUM = SUM + 1./XN
      SUM2 = SUM - 1./(2.*XN)
      A = ALOG(SUM2)
      A2 = A - (FAC1+FAC2)
      SIG41 = SIG4
      RP = RP + RD1
      SIG4 = SIG4 + SIGN*CEXP(A2+RP)
      IF(CABS((SIG41-SIG4)/SIG4) .LT. 1.E-5)GO TO 50
   40 CONTINUE
      STOP 6
   50 CONTINUE
      P = PI*(1.-S4)/8. + 0.5*(CLOG(2./(1.7811*R)))*S2
     *+ .707*(SIG3-SIG1) + .5*SIG2
      Q = 0.25 + .5*(CLOG(2./(1.7811*R)))*(1.-S4)
     *+ .707*(SIG3+SIG1) -PI*S2/8. - .5*SIG4
      Q = CMPLX(0.,1.)*Q
      PQ = P + Q
      GO TO 23
   22 PQ = ((CMPLX(1.,1.)*0.707)/R) - (1./(R*R))
   23 RETURN
      XGAMMA = CSQRT(XGAMMA)
      DB = 8.686*XGAM(1)
      BETA = XGAM(2)
      XN = 2.*PI/(XLAMBDA*BETA)
      RETURN
      END
```

equivalency

Dielectric constant Ground conductivity Height Wire radius Length?

```
      SUBROUTINE WISE(EG,SIGMA,H,RADIUS,XL,XGAM,Z0,
     *FAV,XGAMMA,XN,DB)
      DIMENSION XGAM(2),TAN(2)
      COMPLEX D,E,Z0,RCW,E2,PQ,XGAMMA
```

```
*,XK/41.6E-9/
   F = FAV*1.E6
   R = SIGMA*F
   XLAMBDA = C/F
   RC = 0.00317*H*SQRT(R)
   XIMAG = (EG - 1.)/(2.*C*XLAMBDA*SIGMA*1.E-7)
   RCW = CMPLX(1.,XIMAG)
   RCW = CSQRT(RCW)
   RRCW = CABS(RCW)
   RCW = RCW*RC
   IF(RC .LT. .25)GO TO 2
   CALL CARSON (RCW,PQ,PI)
   GO TO 3
 2 ANG = ATAN2(TAN(2),TAN(1))
   ANG2 = 2.*ANG
   R1 = RC*RRCW
   RES = COS(ANG) + SIN(ANG)
   RESDIF = COS(ANG) - SIN(ANG)
   ALG = ALOG(2./R1)
   A = COS(ANG2)*(0.6728 + ALG)
   B = A + (ANG*SIN(ANG2))
   P = 0.3927-(0.2357*R1*RES)+(R1*R1*0.0491*SIN(ANG2))
  *+R1*R1*0.0625*B + (ANG*.5)
   C1 = SIN(ANG2)*(0.6728+ALG)-(ANG*COS(ANG2))
   Q = -0.0386+(.5*ALG)+(.2357*R1*RESDIF)
  *+(.0625*R1*R1*C1)-(R1*R1*.0491*COS(ANG2))
   PQ = CMPLX(P,Q)
 3 CONTINUE
   RS = 2.*XK*SQRT(F)/RADIUS
   A = 4.E-7*PI*F*ALOG(2.*H/RADIUS)
   PQ = 8.*PI*F*PQ
   D = CMPLX(RS,A)
   E = D + PQ*1.E-7
   E1 = (4.*PI*PI*F*E0)/ALOG(2.*H/RADIUS)
   E2 = CMPLX(0.,E1)
   Z0 = E/E2
   Z0 = CSQRT(Z0)
   XGAMMA = E*E2
     END
```